

**Fatty acid-based Solid Lipid  
Nanoparticles and Their Effects on  
Metabolism and Permeability of  
Drugs**

**K1657774**

**RAHULKUMAR PATEL**

**BPharm, MSc**

**A thesis submitted in fulfilment of the requirements for the degree of  
Doctor of Philosophy**

**School of Life Sciences, Pharmacy and Chemistry  
Kingston University  
London**

**February 2023**

# Acknowledgments

To begin, I'd like to thank my supervisor, Dr. Amr Elshaer, for guiding me well throughout the research process, from title selection to finding the results. Their vast knowledge, motivation, and patience have given me the strength and motivation to excel in research writing. Conducting an academic study on such a difficult subject could not be as simple as he made it for me. He is my mentor and a better advisor for my doctorate studies than I could have imagined.

Aside from my Supervisor, I'd like to thank the rest of the team: Prof. James Barker and Dr. Elena Polycarpou for their encouragement and insightful suggestions. They have all played an important role in enhancing my research ideas and writing abilities.

I'd also like to thank Dr. Lauren Mulcahy-Ryan, Dr. Siamak Soltani-Khankahdani, Dr. Tara Brodie, Dr. Ali Al-kinani, and Dr Anna Caprifico for making it easier for me to access the research facilities and laboratory and for training me on different lab techniques. This research would not have been possible without their invaluable assistance. They are all very important to me.

I'll remember my fellow lab mates for the good times we had together, the sleepless nights that gave us the confidence to finish tasks on time, and for stimulating the discussions.

Finally, I want to thank my parents, siblings, friends, and acquaintances for remembering me in their prayers for my ultimate success. I would be nothing without them. They provided me with enough moral support, encouragement, and motivation to achieve my personal objectives. My two lifelines (parents) have always provided financial support for me, allowing me to focus solely on my studies and achieving my goals.

# Table of Contents

<b>List of Figures .....</b>	<b>6</b>
<b>List of Tables.....</b>	<b>9</b>
<b>List of Abbreviations .....</b>	<b>11</b>
<b>Publications.....</b>	<b>14</b>
<b>Abstract.....</b>	<b>15</b>
<b>Introduction.....</b>	<b>15</b>
<b>Aim.....</b>	<b>15</b>
<b>Methods .....</b>	<b>15</b>
<b>Results &amp; Discussion .....</b>	<b>16</b>
<b>Chapter 1: Pharmaceutical Excipients and Drug Metabolism .....</b>	<b>18</b>
<b>1.1 Introduction.....</b>	<b>19</b>
<b>1.2 Traditional Strategies to Overcome Pre-Systemic Metabolism .....</b>	<b>23</b>
1.2.1 Prodrug Approaches .....	23
1.2.2 Enzyme Inhibitors .....	23
1.2.3 Other Approaches.....	24
<b>1.3 Novel Approach to Overcome Pre-Systemic Metabolism.....</b>	<b>24</b>
1.3.1 Effect of Excipients.....	25
1.3.1.1 Surfactants .....	26
1.3.1.2 Polymers.....	34
1.3.1.3 Fatty acids .....	37
1.3.1.4 Co-solvents/Solvents.....	39
<b>1.4 Effect of excipients on CYP450 Expression.....</b>	<b>42</b>
<b>1.5 Conclusions .....</b>	<b>45</b>
<b>Chapter 2: Materials and Methods .....</b>	<b>48</b>
<b>2.1 Materials and methods .....</b>	<b>49</b>
2.2.1 Chemicals and reagents .....	49
2.2.2 Microsomal assay incubation conditions.....	49
2.2.3 LCMS instrumentation .....	50
2.2.4 Quantitative analysis of probe substrates by HPLC/UV .....	53
2.2.5 Screening of surfactants .....	54
2.2.6 Optimising surfactant/co-surfactant system .....	54
2.2.7 Pseudo-ternary phase diagram.....	55
2.2.8 Preparation of Solid lipid nanoparticles for testosterone and verapamil.....	55
2.2.9 Preparation of Solid lipid nanoparticles for dextromethorphan.....	57
2.2.10 Particle size determination and zeta potential of SLN .....	57
2.2.11 Morphology of SLN .....	58
2.2.12 Thermal analysis of SLN .....	58
2.2.13 Drug encapsulation and loading capacity .....	58
2.2.14 <i>In vitro</i> release study.....	59
2.2.15 <i>In vitro</i> metabolic assay .....	59
2.2.16 Caco-2 cell culture.....	60
2.2.17 Testosterone- and verapamil- loaded SLNs permeability study .....	60
2.2.18 Dextromethorphan permeability study .....	61
2.2.19 Cell toxicity study for testosterone- and verapamil-loaded SLN.....	61
2.2.20 Cell toxicity study for dextromethorphan-loaded SLN.....	62
<b>Chapter 3: Screening the Effect Of Fatty Acids On CYP450 Enzymes Using LCMS/MS....</b>	<b>63</b>
<b>3.1 Introduction.....</b>	<b>64</b>

3.1.1	Metabolic assay .....	64
3.1.2	Liquid chromatography- Mass spectrometry.....	65
3.1.3	Probe substrates .....	68
3.1.4	Fatty acids as pharmaceutical excipients.....	71
<b>3.2</b>	<b>Results and discussion.....</b>	<b>75</b>
3.2.1	LCMS/MS conditions.....	75
3.2.2	Validation of LCMS method .....	76
3.2.3	Optimisation of microsomal assay .....	79
3.2.4	Screening of Fatty acids using the cocktail-approach .....	84
3.2.5	Effect of Stearic acid and verapamil on Testosterone metabolism .....	87
<b>3.3</b>	<b>Conclusion .....</b>	<b>88</b>
<b>Chapter 4: Testosterone-loaded Solid Lipid Nanoparticles.....</b>		<b>89</b>
<b>4.1</b>	<b>Introduction .....</b>	<b>90</b>
<b>4.2</b>	<b>Results and Discussion .....</b>	<b>96</b>
4.2.1	Saturation solubility .....	96
4.2.2	Pseudo-ternary phase diagram.....	98
4.2.3	Preparation and characterization of SLN formulation .....	101
4.2.4	Size distribution and zeta potential of SLN .....	101
4.2.5	Scanning electron microscopy (SEM).....	103
4.2.6	Entrapment efficiency and loading capacity.....	103
4.2.7	Thermal analysis .....	104
4.2.8	<i>In vitro</i> release study.....	106
4.2.9	<i>In vitro</i> metabolic assay .....	107
4.2.10	Permeability study of testosterone-loaded SLN formulation.....	108
4.2.11	Cell toxicity study .....	110
<b>4.3</b>	<b>Conclusion .....</b>	<b>112</b>
<b>Chapter 5: Dextromethorphan-loaded solid lipid nanoparticles.....</b>		<b>113</b>
<b>5.1</b>	<b>Introduction.....</b>	<b>114</b>
5.1.1	Solid lipid nanoparticles for hydrophilic drugs.....	114
5.1.2	Double emulsification method .....	117
5.1.3	Microemulsion method .....	118
5.1.4	Other Conventional methods .....	118
<b>5.2</b>	<b>Results and Discussion .....</b>	<b>120</b>
5.2.1	Saturation solubility.....	120
5.2.2	Pseudo-ternary phase diagram.....	121
5.2.3	Preparation and characterization of SLN formulation .....	122
5.2.4	Permeability study of Dextromethorphan .....	126
5.2.5	Cell toxicity study .....	128
<b>5.3</b>	<b>Conclusion .....</b>	<b>130</b>
<b>Chapter 6: Verapamil-loaded Solid Lipid Nanoparticles.....</b>		<b>131</b>
<b>6.1</b>	<b>Introduction.....</b>	<b>132</b>
<b>6.2</b>	<b>Results and Discussion .....</b>	<b>136</b>
6.2.1	Saturation solubility .....	136
6.2.2	Pseudo-ternary phase diagram.....	138
6.2.4	Size distribution and zeta potential of SLN .....	139
6.2.5	Scanning electron microscopy (SEM).....	140
6.2.6	Entrapment efficiency and loading capacity.....	141
6.2.7	Thermal analysis .....	142
6.2.8	<i>In vitro</i> release study.....	143
6.2.9	<i>In vitro</i> metabolic assay .....	144
<u>6.2.10</u>	Permeability study of verapamil-loaded SLN formulation.....	145
6.2.11	Cell toxicity study .....	148

6.3 Conclusion .....	150
<b>Chapter 7: Conclusions and Future Direction .....</b>	<b>151</b>
7.1 Conclusions .....	152
7.2 Future directions .....	155
<b>References .....</b>	<b>156</b>
<b>Chapter 8: Appendices.....</b>	<b>194</b>

# List of Figures

<b>Figure 1.1</b> Schematic diagram presenting the route of poor bioavailability after oral administration of the drugs.....	22
<b>Figure 1.2</b> Illustrates the inhibition of CYP2C, CYP2D, CYP2E, and CYP3A by acetonitrile, methanol, ethanol, acetone and DMSO at 1% and 10% concentrations. ....	40
<b>Figure 1.3</b> Roadmap of various reported organic solvents based on their inhibitory effect on CYP450 system.....	42
<b>Figure 2.1</b> Illustrates different ratios of oil:S/CoS:water used for ternary phase diagram.....	55
<b>Figure 2.2</b> Demonstrates different steps for hot emulsion technique used to prepare testosterone-loaded solid lipid nanoparticles.....	56
<b>Figure 3.1</b> Illustrates the number of articles published with in vitro cocktail approach. ....	65
<b>Figure 3.2</b> The schematic diagram shows the main components of LC/MS.....	66
<b>Figure 3.3</b> Chemical structure of testosterone.....	69
<b>Figure 3.4</b> Chemical structure of omeprazole.....	69
<b>Figure 3.5</b> Chemical structure of dextromethorphan.....	70
<b>Figure 3.6</b> Chemical structure of verapamil.....	70
<b>Figure 3.7</b> MRM chromatogram for probe substrates and internal standard.....	76
<b>Figure 3.8</b> Calibration curve for individual analytes (n=3).....	77
<b>Figure 3.9</b> The metabolism of various probe drugs by CYP450 enzymes and their main metabolites.....	81
<b>Figure 3.10</b> Comparison of the microsomal assay (NADPH) to negative control (No NADPH).....	83
<b>Figure 3.11</b> Comparison of the microsomal assay with NADPH to negative control (No NADPH).....	83
<b>Figure 3.12</b> The effect of various fatty acids on metabolism of probe substrates.....	85
<b>Figure 3.13</b> The effect of stearic acid concentration on CYP450 inhibition.....	86
<b>Figure 3.14</b> The effect of stearic acid and verapamil on metabolism of testosterone.....	87
<b>Figure 4.1</b> Calibration curve for testosterone.....	97

<b>Figure 4.2</b> Saturation solubility of testosterone in different surfactants and co-surfactants.....	98
<b>Figure 4.3</b> Saturation solubility of testosterone in different ratios of brij 35 10%w/v and propylene glycol.....	98
<b>Figure 4.4</b> Differentiates two types of phases: A = two phase system (water and oil forms two separate layers) and B = single phase system (water and oil forms one layer).....	100
<b>Figure 4.5</b> Illustrates the pseudo-ternary phase diagram with different ratios of stearic acid:S/CoS:water.....	100
<b>Figure 4.6</b> Scanning electron microscope produced image for testosterone-loaded SLNs F1 (A) and F2 (B).....	103
<b>Figure 4.7</b> Illustrates DSC data for testosterone (A), stearic acid (B), and testosterone-loaded SLNs (C).....	105
<b>Figure 4.8</b> In vitro release of testosterone from SLNs using phosphate buffer pH6.8.....	106
<b>Figure 4.9</b> Shows effect of stearic acid-based SLNs on the metabolism of testosterone.....	107
<b>Figure 4.10</b> Confocal microscopic images of monolayers: A = Control, B = testosterone, and C = testosterone-loaded SLNs.....	109
<b>Figure 4.11</b> Permeability of testosterone in presence of stearic acid (testosterone SLNs) vs absence of stearic acid (on its own).....	109
<b>Figure 4.12</b> Cell viability study for three different time points (1.5, 3 and 24 hours).....	111
<b>Figure 5.1</b> Two primary approaches to prepare SLNs using solid lipids: a) melting solid lipids and b) dissolving in solvent.....	117
<b>Figure 5.2</b> Saturation solubility of dextromethorphan in different surfactants and co-surfactants.....	121
<b>Figure 5.3</b> Saturation solubility of dextromethorphan in different ratios of brij 35 and propylene glycol.....	121
<b>Figure 5.4</b> Pseudo-ternary phase diagram for stearic acid: S/CoS (1:3 v/v).....	122
<b>Figure 5.5</b> Calibration curve for dextromethorphan.....	123
<b>Figure 5.6</b> Images of successful and unsuccessful development of SLNs.....	125
<b>Figure 5.7</b> Effect of stearic acid on permeability of dextromethorphan, where M1 represents mixture of dextromethorphan and other components of SLNs formulation.....	127

<b>Figure 5.8</b> Confocal microscopic images of monolayers: A = Control, B = dextromethorphan, and C = M1 .....	127
<b>Figure 5.9</b> Cell viability data for various compounds at different time points (1.5, 3 and 24 hours).....	129
<b>Figure 6.1</b> Calibration curve for verapamil used for saturation solubility and in vitro release study.....	137
<b>Figure 6.2</b> Saturation solubility of verapamil in different surfactants and co-surfactants. ....	137
<b>Figure 6.3</b> Saturation solubility of verapamil in different ratios of brij 35 and propylene glycol. ....	138
<b>Figure 6.4</b> Pseudo-ternary phase diagram representing microemulsion (shaded region) and non-microemulsion (non-shaded region).....	139
<b>Figure 6.5</b> SEM image depicting spherical and smooth verapamil-loaded SLNs. ....	140
<b>Figure 6.6</b> DSC data for verapamil (black peak), stearic acid (red peak), and verapamil-SLN (blue peak). ....	143
<b>Figure 6.7</b> In vitro release study for verapamil from SLNs formulation using phosphate buffer pH6.8. ....	144
<b>Figure 6.8</b> metabolic assay of verapamil-SLNs.....	145
<b>Figure 6.9</b> Confocal microscopic image for monolayers used for control (A), verapamil (B), and verapamil-SLN (C).....	147
<b>Figure 6.10</b> Effect of stearic acid on permeability of verapamil.. ....	147
<b>Figure 6.11</b> Cell viability data for verapamil and other components at different time point (1, 3 and 24 hours).....	149
<b>Figure 8.1</b> Mass spectrometry parameters optimised for individual analytes. ....	182
<b>Figure 8.2</b> Mass spectrometry parameters optimised for testosterone.....	183



# List of Tables

<b>Table 1.1</b> Examples of drugs with very poor bioavailability with reported reasons. .....	20
<b>Table 1.2</b> Summary of the effect of surfactants on CYP activities. ....	31
<b>Table 1.3</b> Different types of polymers with some examples (85).....	35
<b>Table 1.4</b> Effect of different polymers on activities of CYP 2E1, 3A5, 2C9, 2C19, 1A2 and 2D6 (87).....	35
<b>Table 1.5</b> Effect of fatty acids on nine CYPs: 1A2, 2A6, 2B6, 2C8, 2C9, 2C19, 2E1 and 3A4 (97). ....	38
<b>Table 1.6</b> Effect of saturated and unsaturated fatty acids where, saturated fatty acids showed NI (no inhibition) and unsaturated inhibited all CYP isoforms (100). .....	39
<b>Table 1.7</b> Effect of excipients on PXR activation, CYP3A4 and MDR1.....	43
<b>Table 2.1</b> HPLC method optimisation parameters for cocktail drugs and testosterone. ....	51
<b>Table 3.1</b> List of fatty acids and their structures .....	72
<b>Table 3.2</b> MS optimised parameters for individual analyte.....	75
<b>Table 3.3</b> Shows the validation results for individual analytes. ....	78
<b>Table 3.4</b> Calculated intrinsic clearance, half-life and % depletion of each substrate. .....	82
<b>Table 3.5</b> IC50 values of stearic acid based on probe substrates.....	86
<b>Table 4.1</b> Different examples of solid lipid nanoparticles formulation (223). ....	94
<b>Table 4.2</b> Validation parameter for testosterone .....	97
<b>Table 4.3</b> Different compositions used to prepare two different testosterone-loaded SLNs: F1 and F2.....	101
<b>Table 4.4</b> Shows average particle size, PDI and zeta potential for F1 and F2 formulations. ....	102
<b>Table 4.5</b> Entrapment efficiency and Loading capacity for F1 and F2 formulations. .....	104
<b>Table 5.1</b> Different methods to incorporate water soluble drugs into SLNs. ....	115
<b>Table 5.2</b> Validation parameter for dextromethorphan .....	124

<b>Table 5.3</b> Different compositions for various formulations attempted to prepare dextromethorphan-loaded SLNs.....	124
<b>Table 6.1</b> Various nanotechnology-based approached for anti-hypertensive drugs. .....	133
<b>Table 6.2</b> Validation parameters for verapamil.....	137
<b>Table 6.3</b> Average particle size, PDI and zeta potential for verapamil-loaded SLNs. .....	140
<b>Table 6.4</b> Entrapment efficiency and loading capacity of verapamil-SLN .....	141

# List of Abbreviations

ACN	Acetonitrile
APCI	Atmospheric pressure chemical ionization
API	Active Pharmaceutical Ingredient
ATBC	Acetyl Tributyl Citrate
AUC	Area Under the Curve
BBB	Blood-brain barrier
BDDCS	Biopharmaceutic drug disposition classification system
CDC	Candesartan cilexetil
CE	Capillary electrophoresis
CL <sub>int</sub>	Intrinsic clearance
C <sub>max</sub>	Maximum plasma concentration
CMC	Critical Micellar Concentration
CTAB	Cetyltrimethylammonium Bromide
CYP450	Cytochrome P450
DHB	Dihydroxybergamottin
DMEM	Dublecco's modified Eagle's medium
DMPK	Drug metabolism and pharmacokinetics
DMSO	Dimethyl Sulfoxide
DSC	Differential scanning calorimeter
EMA	European medicines agency
ESI	Electrospray ionization
F <sub>1</sub>	Formulation 1
F <sub>2</sub>	Formulation 2
F68	Pluronic F68
FA	Fatty Acids
FBS	Fetal bovine serum
G6DPH	Glucose-6-phosphate dehydrogenase
G6P	D-glucose 6-phosphate dipotassium salt hydrate
GC	Gas chromatography
GIT	Gastrointestinal Tract
GRAS	Generally recognized as safe
HLB	Hydrophilic and lipophilic balance
HPC	Hydroxypropyl Cellulose
HPLC	High-pressure liquid chromatography

HPMC	Hydroxypropyl Methylcellulose
IC50	Inhibitory Concentration
ICH	International Council for Harmonisation of Technical Requirements for Registration of Pharmaceuticals for Human Use
IMS	Industrial methylated spirit
IS	Internal standard
K	Elimination rate constant
K <sub>2</sub> HPO <sub>4</sub>	Dibasic monohydrogen phosphate
KH <sub>2</sub> PO <sub>4</sub>	Monobasic dihydrogen phosphate
K <sub>i</sub>	Inhibitory Constant
K <sub>m</sub>	Michaelis-Menten kinetics
LC	Liquid chromatography
LCMS	Liquid chromatography/mass spectrometry
LOD	Limit of detection
LOQ	Limit of quantification
M <sub>1</sub>	Mixture
MALDI	Matrix-assister laser desorption/ionization
MDR1	Multi-drug Resistance Gene
MDZ	Midazolam
ME	Microemulsion
MgCl <sub>2</sub>	Magnesium chloride
mPEGx-PCLx	Methoxy Poly (ethylene glycol)-poly(ε-caprolactone)
MRM	Multiple reaction monitoring
mRNA	Messenger RNA
M <sub>w</sub>	Molecular weight
NaCMC	Sodium Carboxymethyl Cellulose
NADP	Nicotinamide adenine dinucleotide phosphate
NEAA	Nonessential amino acid
NI	No Inhibition
O/W	Oil-in-water
P <sub>app</sub>	Apparent permeability
PDI	Polydispersity index
PEG	Polyethylene Glycol
PG	Propylene glycol
PK	Pharmacokinetics

PVA	Polyvinyl alcohol
PVP	Polyvinyl pyrrolidone
PXR	Pregnane X receptor
S/CoS	Surfactant/co-surfactant
SA	Stearic acid
SDS	Sodium Dodecyl Sulfate
SEDDS	Self-emulsifying drug delivery system
SEM	Scanning electron microscope
siRNA	Small interfering RNAs
SLNs	Solid lipid nanoparticles
SMEDDS	Self-microemulsifying drug delivery system
SNEDDS	Self-nanoemulsifying drug delivery system
$T_{1/2}$	Half-life
TPGS	D - $\alpha$ -Tocopherol Polyethylene Glycol 1000 Succinate
TX-100	Triton X-100
USFDA	U.S. Food and drug administration
W/O	Water-in-oil
W/O/W	Water-oil-water

# Publications

Patel, R., Barker, J. and ElShaer, A. (2020) "Pharmaceutical excipients and drug metabolism: A mini-review," *International Journal of Molecular Sciences*, 21(21), p. 8224. Available at: <https://doi.org/10.3390/ijms21218224>.

## **Poster presentation**

Patel, R., Barker, J. and ElShaer, A. (2019) "LC/MS method development and optimisation for microsomal assay". Poster presentation at the Academy of Pharmaceutical Sciences 2019, London, UK.

Patel, R., Barker, J. and ElShaer, A. (2019) "LC/MS method development and optimisation for microsomal assay". Poster presentation at the Faculty of Science, Engineering and Computing 2019, London, UK.

# Abstract

## Introduction

Conclusions from previously reported studies have revealed that many commonly used pharmaceutical excipients, known to be pharmacologically inert, show effects on drug transporters and/or metabolic enzymes. Thus, the pharmacokinetics (absorption, distribution, metabolism, and elimination) of active pharmaceutical ingredients are possibly altered because of their transport and metabolism modulation from the incorporated excipients. Excipients such as surfactants, polymers, fatty acids, and solvents have been reported previously as CYP450 inhibitors. Based on all the stated outcomes, the most potent inhibitors were found to be surfactants and the least effective were organic solvents. However, there are many factors that can influence the inhibition of CYP450, for instance type of excipient, concentration of excipient, type of CYP450 isoenzyme, incubation condition, etc. Such evidence will be very useful in dosage form design, so that the right formulation can be designed to maximize drug availability, especially for poorly bioavailable drugs.

## Aim

The aim of this study is to identify the most potent fatty acids that can inhibit CYP450 enzymes and produce solid-lipid nanoparticles (SLNs) to minimize metabolism and increase drug permeability without harmful side effects.

## Methods

The high-performance Liquid Chromatography-Mass Spectrometric (LCMS) methods were developed for (i) simultaneous quantification of omeprazole, dextromethorphan, verapamil, and propranolol (IS) (ii) individual quantification of testosterone. The separation for both methods were achieved on Poroshell 120 EC-C18 (150 x 4.6 mm) using gradient and isocratic approaches. These analytical methods were successfully used for screening of fatty acids, pre-formulation, and formulation studies. Microsomal assay with rat-liver microsomes was used for screening of fatty acids based on their inhibitory effect on various CYP450s. The

most potent inhibitor (stearic acid) was then incorporated in three different solid-lipid nanoparticles formulations (SLNs). The pre-formulation and formulation studies were systematically optimized to produce SLNs. These SLNs were characterized by SEM, zetasizer, DSC, dialysis membrane, and HPLC. Moreover, metabolic assay, permeability assay and cytotoxicity were also studied to investigate the effect of stearic acid, present in SLNs, on CYP450s enzymes and caco-2 cell permeability.

## Results & Discussion

The results of the LCMS method validation revealed that the coefficient of determination ( $R^2$ ) values for all probe drugs were greater than 0.99. Furthermore, all the analytes showed highest recovery and lowest interday/intraday values. The effect of fatty acids on CYP450s activity was evaluated using rat-liver microsomes. The percentage of probe drugs recovered in the presence of heptadecanoic acid, myristic acid, pentadecanoic acid, and stearic acid were found to be higher than the control study. Stearic acid was the most potent inhibitor out of all the excipients with an  $IC_{50}$  value  $\geq 30 \mu\text{M}$  for CYP3A4, 3A5, 2C8, 2C19, and 2D6. At approximately  $200 \mu\text{M}$  of stearic acid, nearly 100% of the compounds were recovered. Based on the screening phase data, three solid-lipid nanoparticles formulations were produced using stearic acid as an oil phase.

Results indicated that testosterone loaded SLNs were spherical in shape with an average particle of 278.29 nm diameter with 55% entrapment efficiency. Moreover, microsomal and permeability assays revealed that the presence of stearic acid in testosterone decreased metabolism by CYP450s and increased permeability via caco-2 layer. Approximately, 54% of testosterone was recovered from the metabolic assay with  $CL_{\text{int}}$  of  $0.04 \mu\text{L}/\text{min}/\text{mg}$  and apparent permeability was successfully improved with  $P_{\text{app}}$  value of  $1.53 \times 10^{-6} \text{ cm}/\text{sec}$ .

On the other hand, verapamil loaded SLNs were spherical in shape with an average particle size of 300.30 nm but with a better entrapment efficiency of 77%. The formulation demonstrated burst release with nearly 20% drug release in under 0.5 hours, followed by sustained release for 23.5. In contrast to testosterone, metabolic assay revealed poor inhibition for CYPs with net recovery of 2.53% and  $CL_{\text{int}}$  of  $0.014 \mu\text{L}/\text{min}/\text{mg}$  for verapamil. However, there was significant



improvement in the apparent permeability of verapamil ( $P_{app} = 2.39 \times 10^{-6}$  cm/sec) when compared to control ( $P_{app} = 9.00 \times 10^{-6}$  cm/sec).

The third formulation, dextromethorphan loaded SLNs was unsuccessful because of its chemical nature and water solubility. Several strategies were used to prepare dextromethorphan-SLNs such as double emulsion, solvent evaporation, and convention hot emulsion method. The affinity of lipophilic drugs for lipids makes them simple to integrate into SLN. While hydrophilic drugs (such as dextromethorphan) are more readily partitioned in the water phase during the production process, they are more difficult to incorporate into the hydrophobic matrix and therefore, further investigation is required for this formulation.

The cell cytotoxicity study further confirms the safety of all the ingredients at different concentrations present in various formulations. Thus, stearic acid based SLNs are a potential formulation approach which can inhibit CYP450 enzymes and improve intestinal permeability of various drugs and therefore, requires further investigation to improve the formulation with various approaches.

**Keywords:** Fatty acids; cytochrome P450; metabolism; rat liver microsomes; inhibitor; solid lipid nanoparticles; permeability

# **Chapter 1: Pharmaceutical Excipients and Drug Metabolism**

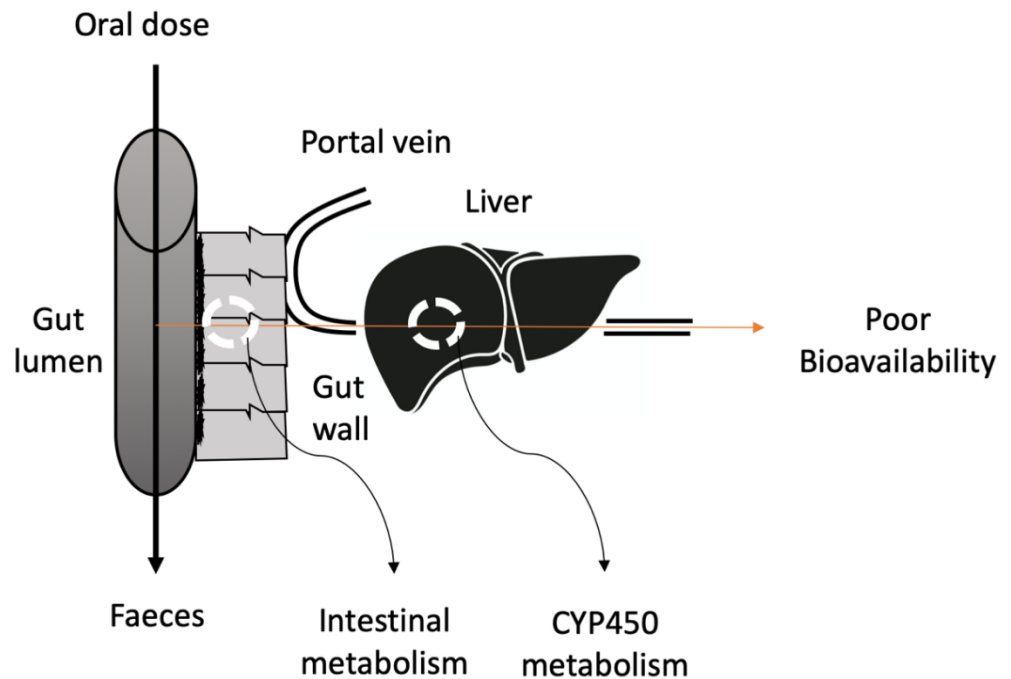
## **1.1 Introduction**

The most popular route for drug delivery is oral administration because of pain avoidance, ease of ingestion, patient compliance and versatility of drug candidates. Moreover, the manufacturing for oral drug delivery systems is less expensive as the production process is simple and there are no requirements for sterile conditions (1). Despite all the benefits of oral delivery, poor bioavailability of oral formulations is a limiting factor that can alter the efficacy and therapeutic effect (2). Various factors are contributing to low oral bioavailability including physiological factors, high gastric emptying time, the effect of food, intestinal barrier, and enzymatic degradation of drugs (2) (Table 1.1). First-pass metabolism is one of the key factors responsible for poor bioavailability. The extensive metabolism of drugs prior to reaching the systemic circulation is known as the first-pass metabolism. After oral administration, the drug is absorbed by the gastrointestinal tract (GIT) and transported to the liver through the portal veins. Then, the drug is metabolized in the liver by CYP450 enzymes before reaching the systemic circulation, resulting in a low available concentration at the intended target site (Figure 1.1). Due to insufficient plasma concentrations, the bioavailability of the drug is significantly reduced and therefore a high dose of the drug is required for better efficacy (3).

**Table 1.1** Examples of drugs with very poor bioavailability with reported reasons.

<b>DRUGS</b>	<b>PHARMACOLOGICAL CLASS</b>	<b>BIOAVAILABILITY (%)</b>	<b>REASONS</b>	<b>REFERENCES</b>
<b>ALENDRONATE</b>	Bisphosphonates	0.59-0.78	Poor solubility and absorption	(4-6)
<b>ATORVASTATIN</b>	Statins	14	P-gp and CYP450 activities	(7-9)
<b>BROMOCRIPTINE</b>	Dopamine receptor agonists	5-10	Extensive first-pass effect	(10,11)
<b>BUDESONIDE</b>	Corticosteroids	11	Hepatic first-pass effect	(12)
<b>CLODRONATE</b>	Bisphosphonates	1	Poor solubility and absorption	(4-6)
<b>CYTARABINE</b>	Antimetabolites	20	Intestinal and hepatic first-pass	(13)
<b>DOMPERIDONE</b>	D2 receptor antagonists	15	Gut and liver first-pass	(14)
<b>DOXORUBICIN</b>	Anthracycline antibiotics	5	Hepatic and intestinal metabolism	(15)
<b>ETIDRONATE</b>	Bisphosphonates	5	Poor solubility and absorption	(5)
<b>FELODIPINE</b>	Calcium channel blockers	15	P-gp and CYP450 activities	(12)
<b>FLUVASTATIN</b>	Statins	20	P-gp and CYP450 activities	(7-9)
<b>HYOSCINE</b>	Antispasmodics	20	Hepatic metabolism	(16)
<b>ISRADIPINE</b>	Calcium channel blockers	15	P-gp and CYP450 activities	(17)
<b>KETAMINE</b>	Dissociative anesthetics	20	Hepatic and intestinal metabolism	(18)
<b>LOVASTATIN</b>	Statins	<5	P-gp and CYP450 activities	(7-9)

<b>LIDOCAINE</b>	Local anesthetics	3	Hepatic first-pass effect	(19)
<b>MORPHINE</b>	Opioids	20-33	Gut and liver first-pass	(20)
<b>NIMODIPINE</b>	Calcium Channel blockers	13	P-gp and CYP450 activities	(21)
<b>NALOXONE</b>	Opioid antagonists	2-10	Extensive first-pass but 90% absorption	(22)
<b>PYRIDOSTIGMINE</b>	Acetylcholinesterase inhibitors	14	Poor absorption	(23)
<b>PAMIDRONATE</b>	Bisphosphonates	1	Poor solubility and absorption	(4-6)
<b>PRAVASTATIN</b>	Statins	17-34	P-gp and CYP450 activities	(7-9)
<b>PROCHLORPERAZINE</b>	Phenothiazines	20	Intestinal and hepatic first-pass	(24)
<b>RISEDRONATE</b>	Bisphosphonates	<1	Poor solubility and absorption	(4-6)
<b>SELEGILINE</b>	Monoamine oxidase type B inhibitors	20	Extensive first-pass	(25)
<b>SIMVASTATIN</b>	Statins	5-48	P-gp and CYP450 activities	(8-10)
<b>SUMATRIPTAN</b>	Serotonin receptor agonists	20	Hepatic first-pass	(26)
<b>TACRINE</b>	Cholinesterase inhibitors	10-30	Hepatic first-pass	(27)
<b>TERBUTALINE</b>	Adrenergic receptor agonists	9-21	Extensive first-pass and poor absorption	(28)
<b>TILUDRONATE</b>	Bisphosphonates	6	Poor solubility and absorption	(4-6)
<b>ZOLEDRONIC ACID</b>	Bisphosphonates	0.9-1.8	Poor solubility and absorption	(4-6)



**Figure 1.1** Schematic diagram presenting the route of poor bioavailability after oral administration of the drugs. The drug enters the gastrointestinal tract (GIT) and transports to the liver via the portal veins. Before reaching the systemic circulation, the drug is metabolised in the liver by CYP450 enzymes, which results in a low available concentration at the intended target site.

Liver is the primary site of metabolism for both xenobiotics and endogenous compounds. More than 90% of the liver's cells are hepatocytes, and they abundantly express a wide variety of phase I and II metabolic enzymes (29). Phase I metabolism, also known as functionalization, is the process of adding functional groups to the parent drug structure by oxidation, reduction, and hydrolysis. These functional groups include hydroxyl, carboxylic, amino, and thio groups. The process of conjugation in which a highly polar conjugate is generated by adding a polar molecule to either a phase I metabolite or the parent medication to promote further biliary or urine excretion is known as phase II metabolism (29). The principal enzymes responsible for first-pass metabolism or biotransformation of drug molecules are a family known as cytochromes P450 (CYP450). CYPs 450 includes a superfamily of heme proteins which is categorized into families and subfamilies based on amino acid sequence homology (29). They are allotted a family number (for instance, CYP1 or CYP2) followed by a subfamily letter (e.g., CYP1A or CYP2C) and are distinguished by a number for the individual enzyme or isoforms (e.g., CYP1A2 or CYP2C19) (30). According to Coller *et al.*, the most commonly prescribed drugs in the United States (USA) are reported to be metabolized by

CYP1, CYP2 and CYP3 families. The most common enzymes responsible for oxidation of approximately 79% of these drugs are CYP2C9, CYP2D6, CYP2C19 and CYP3A4/5 (31). Several *in vitro* and *in vivo* approaches have been developed and used to predict human intestine and hepatic first-pass metabolism. To assess hepatic metabolism, a variety of *in vitro* methods are available, with various degrees of efficacy (29). The most popular *in vitro* model is the microsomal preparation due to its ease of use, high concentration of metabolising enzymes, and ease of commercial availability. Recombinant human enzymes, precisely cut liver slices, and hepatocytes are further examples of *in vitro* models, whereas animal studies are frequently utilised in the preclinical stage to characterise the pharmacokinetic and systemic availability of substrates *in vivo* (29).

## **1.2 Traditional Strategies to Overcome Pre-Systemic Metabolism**

Several novel, as well as traditional, methods are being investigated to circumvent drug metabolism. Prodrugs, enzyme inhibitors, polymeric excipients, self-emulsifying drug delivery systems (SEDDS) and liposomes have been investigated over the years as inhibitors of metabolic enzymes.

### **1.2.1 Prodrug Approaches**

Prodrug is one of the common approaches investigated, according to the literature. Approximately 10% of the drugs in the pharmaceutical market are categorized as prodrugs and one third of small molecular weight (Mw) drugs are classified as prodrugs (32-37). Prodrugs are pharmacologically inert substances which undergo conversion, once inside the body, to release the active ingredient for its therapeutic effect (38,39). Prodrugs successfully overcome the drug physicochemical and biopharmaceutical obstacles, thus enhancing their pharmacokinetic properties such as oral absorption and metabolism (40,41).

### **1.2.2 Enzyme Inhibitors**

Another promising strategy to reduce the pre-systemic metabolism is the co-administration of CYP450 inhibitors with orally administered drugs (42). Probably, the best-known enzyme inhibitor is grapefruit juice, which significantly improves the oral bioavailability of many drugs (42,43). Food–drug interaction is a common occurrence and can be significant when the drug's pharmacokinetics are altered.

The classic example is the interaction between grapefruit juice and felodipine. Felodipine is known to undergo high pre-systemic metabolism resulting in very low absolute bioavailability with an average of 15%. A study showed the inhibitory effect of grapefruit juice flavonoids such as quercetin, naringenin and naringin on CYP3A4, using felodipine as a substrate (44). The concentration-dependent inhibition was examined when the flavonoids were co-incubated with felodipine (44). Moreover, many studies reported furanocoumarins, present in grapefruit juice, as an inhibitor for CYP450 (45-53). Bergamottin inhibits CYP1A2, CYP1B1, CYP 2A6, CYP2B6, CYP2C9, CYP2C19, CYP2D6, CYP2E1, CYP3A4 and CYP3A5. The dihydroxybergamottin (DHB) and paradisins inhibit CYP1A2, CYP1B1, CYP2C9, CYP2C19, CYP2D6 and CYP3A4 (54).

Besides grapefruit juice, many drugs in the market such as ketoconazole, torleandomycin, saquinavir, diltiazem and fluconazole exhibit an enzyme inhibitory effect resulting in improved bioavailability of many drugs (55). For instance, the oral bioavailability of alfentanil was increased 19-fold with troleandomycin (56). However, co-administration of enzyme inhibitors can lead to adverse drug effects which also includes fatal events. For example, when clarithromycin (inhibitor) is co-administered with astemizole, terfenadine or cisapride (substrates), a severe ventricular arrhythmia may occur (57).

### 1.2.3 Other Approaches

These include polymeric excipients, self-emulsifying drug delivery systems (SEDDS) and liposomes. Normally, polymers are used as enteric coatings for different types of drugs to overcome hydrolytic instability (58). Some polymers, such as polycarbophil and carbomer, demonstrate inhibitory effects on trypsin, which decrease pre-systemic metabolism in the intestine. That means drugs incorporated in such polymers can be protected from pre-systemic degradation by trypsin (59). Similarly, most of the studies on SEDDS and liposomes (such as Span 60, Span 80, Tween 60 and Tween 80) focus on increased solubility by these systems and their protective property towards pre-systemic metabolism is hardly examined (42).

## 1.3 Novel Approach to Overcome Pre-Systemic Metabolism

One method by which excipients may alter the drug metabolism is by inhibiting CYP450 enzymes present in cellular microsomes. The addition of commonly used pharmaceutical excipients can be a potential solution to these problems.



Pharmaceutical excipients are ingredients other than the active pharmaceutical ingredient (API) present in a finished pharmaceutical drug formulation. These are frequently used as lubricants, diluent, binders, flavorings, coating, and coloring agents for the formulation. These substances are often therapeutically inert (60).

The functional roles of pharmaceutical excipients include modulating bioavailability and solubility of APIs, increasing the stability of APIs in the dosage form, maintaining the osmolarity and/or pH of the liquid formulations, preventing dissociation and aggregation, etc. Recently, addition of pharmaceutical excipients in drug formulations have gained attention which can alter the pharmacokinetics of drugs, resulting in improved bioavailability (60). This chapter looks at the effect of surfactant, polymers, and other excipients on the expression of cytochrome P450 enzymes.

### 1.3.1 Effect of Excipients

Substances that can enhance or inhibit cytochrome P450 activity can alter the rate of drug metabolism, leading to an increase or decrease in drug bioavailability. There are many studies on new materials as drug delivery vehicles, including vesicles, block copolymer micelles, degradable polymer particles, dendrimers, polymer prodrugs and lipid nanoparticles; however, the effect of excipients used is often ignored. For instance, liquid acetaminophen, which contains propylene glycol, is less toxic than solid preparations with no propylene glycol. The main reason for acute hepatic failure in Europe and the United States is acetaminophen (61,62). Its toxicity is due to the reductive metabolism via CYP2E1 (63). Liquid formulation of acetaminophen contains a solubilizing agent called propylene glycol, which is used to dissolve the drug in aqueous solution (64). Since children ingest liquid formulations and are less vulnerable to its toxicity, a single-blinded cross-over study was conducted to compare the metabolism of solid and liquid acetaminophen 15 mg/kg dose by CYP2E1, using 15 healthy adults as volunteers. As a result, the measured Area under the curves (AUCs) for the metabolites were 16% lower than solid formulation. This is because propylene glycol is a competitive antagonist to CYP2E1; hence, it shows the protective effect in liquid formulation (64).

### 1.3.1.1 Surfactants

Surfactants, also known as surface-active agents, possess hydrophilic (polar) and hydrophobic (non-polar) characteristics. The hydrophobic (non-polar) part is referred to as the tail group and the hydrophilic (polar) part as the head group. Surfactants are normally used to increase the solubility of the drugs and to decrease the interfacial tension between the drug and the medium (65). Surfactants can be categorized into four different groups: anionic, cationic, zwitterionic and non-ionic surfactants. Anionic surfactants carry a negative charge, whereas cationic surfactants carry a positive charge on their hydrophilic head. Zwitterionic surfactants have the potential to carry both positive and negative charges (65).

Cremophor EL is a heterogeneous non-ionic surfactant made up of castor oil and ethylene oxide with a molar ratio of 1:35 (66). Cremophor EL helps in solubilizing many hydrophobic drugs which include photosensitizers, immunosuppressive agents, sedatives, anesthetics, and anticancer drugs (experimental) (66). Different *in vitro* studies have been reported for the impact of Cremophor EL on the metabolism of drugs (67)(68,69). In 2010, a study focused on the effect of Cremophor EL on CYP3A4 and CYP2C9 mediated metabolism of testosterone and diclofenac, respectively (67). Cremophor EL was tested at different concentrations (0.01–100 mM) using human liver microsomes *in vitro*. As a result, the inhibitory effect of Cremophor EL was found to be concentration dependent. The half-maximal inhibitory concentration (IC<sub>50</sub>) of the CYP3A4- and CYP2C9-mediated metabolism were determined as 0.60 and 0.03 mM, respectively.

Mudra *et al.* further showed that solubilizing agents inhibited verapamil-N-demethylase activity *in vitro* and *in situ*. The rate of verapamil-N-demethylation was reduced in the presence of Cremophor EL, suggesting moderate inhibition of CYP3A4: 20.7% and 21.8%, *in-situ* and *in-vitro* at 47.5 µg/mL, respectively (68). The inhibition of CYP450 by polyethoxylated solubilizing agents (e.g., Cremophor EL, Tween 80) can be attributed to the collective evidence that supports the following hypothesis: The drug absorption is altered in the presence of polyethoxylated solubilizing agents due to agent-produced membrane fluidization, causing in local environment perturbation required for protein to function (69-72). Similarly, the outcomes in this study are reliable with agent-induced fluidization of microsomal membrane resulting in perturbation of the enzyme micro-environment, thus decreasing CYP3A4 function.

To support this hypothesis, another study on Cremophor EL presented results consistent with the previous studies. *In vitro* metabolism of 7-ethoxycoumarin was studied at three different concentrations of the surfactant (0.03%, 0.06% and 0.1% w/v). Various enzymes are responsible for metabolism of ethoxycoumarin, but the major enzymes are CYP450 1A2, CYP450 1A1 and CYP450 2B. Increasing the concentration of Cremophor EL decreased the metabolic activity of these enzymes (73). The CYP450 activities were reduced from 97% to 93% when surfactant concentration was increased from 0.03% to 0.10%. This is because the surfactant concentration above its critical micellar concentration (CMC) value disrupts the CYP450 enzymes membrane, causing an inhibitory effect. In contrast, below its CMC value, there is less disruption (73).

In 2004, Gonzalez et al. investigated the effect surfactants have on the metabolism of the CYP3A2 substrate by Midazolam (MDZ) by determining the intrinsic clearance ( $CL_{int}$ ) of MDZ in rat hepatocytes and rat microsome systems (74). In the rat hepatocytic system, the  $CL_{int}$  of MDZ decreased significantly above its critical micellar concentration (CMC) at 0.03% ( $CL_{int}/0.03\% = 70.3\% \pm 2.1\%$ ) and 0.3% ( $CL_{int}/0.3\% = 54.9\% \pm 2.2\%$ ), whereas the  $CL_{int}$  of MDZ was not altered significantly below its CMC (at 0.0003% and 0.003%). Similar outcomes were observed with rat liver microsomes; significant decrease in  $CL_{int}$  of MDZ at 0.03% ( $CL_{int}/0.03\% = 89.5 \pm 3.7 \mu\text{L}/\text{min}/\text{mg protein}$ ) and 0.3% ( $CL_{int}/0.3\% = 35.0 \pm 0.8 \mu\text{L}/\text{min}/\text{mg protein}$ ) of the Cremophor EL. Thus, the addition of Cremophor EL reduced the intrinsic clearance of MDZ by inhibiting CYP450 in both systems (74).

Taxol is an active ingredient used for refractory ovarian cancer, lung cancer and breast cancer. It is readily metabolized by the CYP450 system in the liver. A study conducted by Carlos et al. (1994) illustrated that Cremophor EL had the most significant effect on taxol metabolism, by the CYP450 system, compared to other co-administered drugs (diphenhydramine, cimetidine, and dexamethasone) (75). In human and rat liver microsomes, the formation of 6 $\alpha$ -hydroxytaxol was completely prevented by Cremophor EL at 20  $\mu\text{g}/\text{mL}$ . In human liver slices, Cremophor EL reduced the formation of 6 $\alpha$ -hydroxytaxol as well as the ratio of metabolite to parent drug at 20  $\mu\text{g}/\text{mL}$  (75). However, at 2  $\mu\text{g}/\text{mL}$ , Cremophor EL showed very little effect. These results suggest that Cremophor EL indirectly reduces the taxol uptake by the liver. To conclude from all the studies, the inhibition of CYP450 enzymes by

Cremophor EL seems to be dependent on the concentration of surfactant, type of isoenzyme and type of microsomal assay.

Cremophor RH-40 is found in many oral drug formulations, which is mainly used to improve solubilization of the drugs, such as Tegretol, Anafranil and Sandimmun Neoral. Cremophor RH-40 has a different molar content of ethylene oxide (45 mol) than Cremophor EL (76). The inhibition of CYP450 enzymes by Cremophor RH-40 has been reported in many studies. Christiansen et al. examined the effect of non-ionic surfactants on CYP3A4 and CYP2C9 enzymes (67). The inhibitory action of Cremophor RH40 ( $IC_{50} = 0.80$  mM) was found to be less than Cremophor EL ( $IC_{50} = 0.60$  mM) for CYP3A4, whereas stronger inhibition was reported with a similar  $IC_{50}$  value (0.03 mM) for CYP2C9. To understand the action of Cremophor RH40 in biotransformation, it was examined for its inhibitory effect on CYP3A4 in-vitro as well as *in vivo* (60). According to the *in vitro* study conducted by Ren et al. (2008), the inhibition rate of CYP3A4 by Cremophor RH40 was 99.40%. Furthermore, single and multiple doses of Cremophor RH40 were examined in male Sprague-Dawley rats for its impact on MDZ metabolism. In comparison to control saline, Cremophor RH40 increased the area under curve ( $AUC_{0-\infty}$ ) of MDZ up to 1.1-fold and decreased the production of 1'-Hydroxymidazolam (1'-OH-MDZ) up to 0.44-fold in a single dose. The MDZ  $AUC_{0-\infty}$  was increased by 1.69-fold and 1'-OH-MDZ  $AUC_{0-\infty}$  was decreased by 0.9-fold in a multiple-dose regimen (60).

These results are consistent with the recent study on a Cremophor RH40-based self-micro emulsifying drug delivery system (SMEDDS) (77). A significant decrease in 1'-OH-MDZ production was observed ( $P < 0.05$ ), when the concentration of Cremophor RH40 was increased from 0.05% to 3% w/v. Studies have revealed that chemotherapeutic substances can downregulate the *CYP3A* gene expression (78,79). Therefore, Western blot analysis was performed to examine the effect of SMEDDS on the CYP3A activity. As a result, Cremophor RH40-based SMEDDS reduced the CYP3A protein expression levels at dilutions ranging from 1:50 to 1:100. Another study reported a similar significant inhibition of CYP3A4 and CYP2C19 enzymes *in vitro* by Cremophor RH40 when rabeprazole was used as a probe drug ( $P < 0.05$ ) (80). It was concluded that these inhibitory effects involved direct action or micelle formation to disrupt CYP activities.

Recently, Tween 80 has been reported to inhibit different isoenzymes of CYP450: 3A4, 2C9, 1A1, 1A2 and 2B. Tween 80 (polysorbate 80) is the most commonly used hydrophilic non-ionic surfactant with the ability to improve the solubility of compounds (67). Tween 80 is derived from oleic acid and polyethoxylated sorbitol and has been used in preclinical and clinical drug formulations (67). Moderate inhibition of CYP3A4 and CYP2C9 by Tween 80 was determined. The  $IC_{50}$  value for CYP3A4 and CYP2C9 was found to be 0.40 mM and 0.04 mM, respectively. Christiansen et al. and Rao et al. illustrated the inhibition of CYP450 to be a concentration-dependent manner. For example, when the concentration of Tween 80 in SMEDDS was increased from 0.05% to 3% (w/v), the 1'-OH-MDZ production was reduced from ~80% to 30% (77). The *in vitro* metabolism of 7-ethoxycoumarin was reduced from 85% to 65% when the concentration of Tween 80 was increased from 0.03% to 0.10% (73).

The incubation of Tween 80 with rat hepatocytes reduced  $CL_{int}$  of MDZ significantly, above its CMC ( $CL_{int}/0.03\% = 75.2\% \pm 1.6\%$ ;  $CL_{int}/0.3\% = 79.2\% \pm 1.5\%$ ,  $P < 0.05$ ), whereas the inhibitory effect of Tween 80 was reported below its CMC with rat liver microsomes ( $CL_{int}/0.003\% = 70\% \pm 5.7\%$ ,  $CL_{int}/0.03\% = 66.9\% \pm 1.0\%$ ,  $CL_{int}/0.3\% = 8.24\% \pm 0.28\%$ ,  $P < 0.05$ ) (74). Mudra et al. measured the impact of Tween 80 on intestinal verapamil-N-demethylation activity *in situ* and *in vitro*. The inhibition rate was found to be 56.3% (*in situ*) and 13.5% (*in vitro*) at 25  $\mu\text{g/mL}$ , reflecting the reduction of CYP3A activity (68).


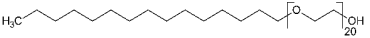
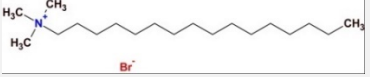
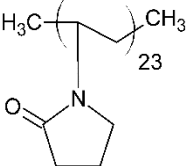
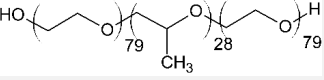
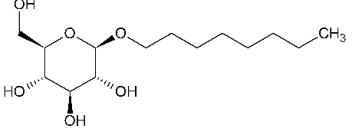
Tween 20 (Polysorbate 20) and Tween 80 are composed of the same hydrophilic group but different hydrophobic groups. Tween 20 has a mixture of palmitic, stearic, lauric and myristic acids, whereas Tween 80 contains oleic, linoleic and stearic acids (62). According to Ren et al. and Randall et al., Tween 20 is a more potent inhibitor than Tween 80. The production of 1'-OH-MDZ was inhibited by around 80% at 50 mM Tween 20. It also decreased the metabolism of 7-ethoxycoumarin from 66% to 56% at a concentration ranging from 0.03% to 0.10% v/v (60,73).

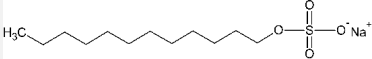

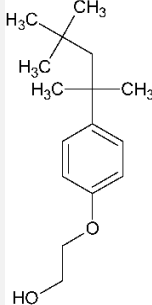
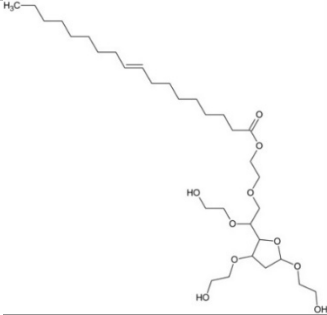
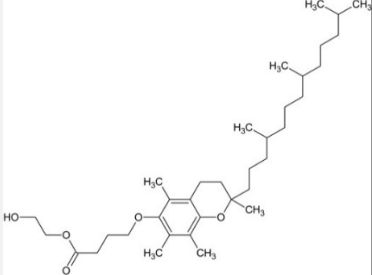
Triton X-100 (TX-100) is an octylphenol polyethoxylated non-ionic surfactant. Its structure consist of poly(ethylene glycol) with a 4-(1,1,3,3-tetramethylbutyl)phenyl group (81). TX-100 has been reported to act as a strong inhibitor for CYP450 enzymes. It reduced the metabolism of CYP3A4 substrates: 7-ethoxycoumarin by 54% and midazolam by 99.8% (60,73). The interaction of TX-100 with CYP450 in

*Prochilodus scrofa* was studied using the antioxidant and mono-oxygenase systems. The CYP content at 0.05 mM of TX-100 was found to be 0%, explaining the stronger inhibition of CYP450. Similarly, competitive inhibition of CYP1A1 by TX-100 was reported far below its CMC value (250  $\mu$ M) (82).

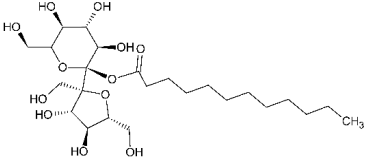

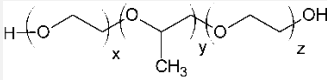
Furthermore, multiple studies pointed out the ability of other surfactants to interfere with CYP450, which can lead to improved bioavailability of drugs. The surfactants that were reported to show inhibitory actions are listed in Table 1.2. For instance, brij 35 showed concentration-dependent inhibition of CYP3A4. Three different concentrations of brij 35 (0.03%, 0.06%, and 0.10%) were incubated with hepatic microsomes in presence of 7-ethoxycoumarin, in which approximately 67% of CYP activity remained after the addition of 0.1% brij 35 as opposed to 100% activity with 0.03% brij 35 (73).

**Table 1.2** Summary of the effect of surfactants on CYP activities.

Surfactants	Substrates	Mechanism of action	Structures	Type	References
Brij 35	7-ethoxycoumarin	Increased CYP3A4 inhibition with increased surfactant concentration		Non-ionic	(73)
Brij 58	Rabeprazole	Significant inhibition of drug degradation by CYP enzymes		Non-ionic	(80)
CTAB	7-ethoxycoumarin	Increased CYP3A4 inhibition with increased surfactant concentration		Cationic	(73)
Kollidon 12 PF	7-ethoxycoumarin	Increased CYP3A4 inhibition with increased surfactant concentration		Non-ionic	(73)
Lutrol F68 NF	7-ethoxycoumarin	Increased CYP3A4 inhibition with increased surfactant concentration		Non-ionic	(73)
Octyl-B-D-glucopyranoside	7-ethoxycoumarin	Increased CYP3A4 inhibition with increased surfactant concentration		Non-ionic	(73)

SDS	7-ethoxycoumarin	Increased <i>CYP3A4</i> inhibition with increased surfactant concentration		Anionic	(73)
Solutol HS 15	7-ethoxycoumarin	Increased <i>CYP3A4</i> inhibition with increased surfactant concentration		Non-ionic	(73)
Triton X-100 reduced	7-ethoxycoumarin	Increased <i>CYP3A4</i> inhibition with increased surfactant concentration		Non-ionic	(73)
Polysorbate 80	Testosterone Diclofenac	Increased <i>CYP3A4</i> and <i>CYP2C9</i> inhibition in concentration-dependent manner		Non-ionic	(67)
TPGS	Testosterone Diclofenac	Increased <i>CYP3A4</i> and <i>CYP2C9</i> inhibition in concentration-dependent manner		Non-ionic	(67)



Sucrose laurate	Testosterone Diclofenac	Increased <i>CYP3A4</i> and <i>CYP2C9</i> inhibition in concentration-dependent manner		Non- ionic	(67)
Gelucire 44/14	Rabeprazole	Significant inhibition of drug degradation by CYP enzymes	Lauroyl polyoxyl-32 glycerides (C9H14N2)	Non- ionic	(80)
Polyoxyl 40 Stearate	Midazolam	Strong inhibition of <i>rCYP3A4</i>		Non- ionic	(60)
Pluronic F68	Midazolam	Strong inhibition of <i>rCYP3A4</i>		Non- ionic	(60)

### 1.3.1.2 Polymers

Polymers are macromolecular compounds and constitute a large and diverse group of substances, including synthetic polymers, semi-synthetic polymers, natural polymers and fermentation products (Table 1.3). These polymers are commonly used as excipients in pharmaceutical dosage forms; parenterally, orally, nasally, rectally, intravaginally, inhalationally and topically, on the oral mucosa and in ophthalmic preparations (83).

Lihui Qiu *et al.* evaluated the inhibition of six CYP isoforms by different mPEG<sub>x</sub>-PCL<sub>x</sub> (methoxy poly(ethylene glycol)-poly( $\epsilon$ -caprolactone)) amphiphilic copolymer micelles: mPEG2k-PCL2k, mPEG2k-PCL3.5k, mPEG2k-PCL5k and mPEG2k-PCL10k. The biodistribution of polymeric micelles were also studied on Sprague Dawley male rats with a near-infrared fluorescent dye after intravenous administration. The inhibitory effect was found to be concentration-dependent in manner (84). All CYP450 enzymes were significantly inhibited by mPEG2k-PCL<sub>x</sub> when the concentration was increased to 1000  $\mu$ g/mL. For example, the CYP activities were reduced to 68.7% for CYP2D2, 64.6% for CYP2C6, 40.4% and 33.5% for CYP3A2/1, 38.1% for 2B1, 26.2% for 2C11 and 9.4% for 1A2 by mPEG2k-PCL2k at 1000  $\mu$ g/mL. The extent of inhibition, ranked downwards, was as follows: mPEG2k-PCL2k > mPEG2k-PCL3.5k > mPEG2k-PCL5k > and mPEG2k-PCL10k (84). Moreover, the *ex vivo* fluorescence imaging results revealed that mPEG<sub>2k</sub>-PCL<sub>x</sub> micelles primarily accumulated in the liver following intravenous administration.

Similarly, Martin and co-workers investigated the effect of 10 commonly-used polymers on seven CYP isoforms (2E1, 3A4, 3A5, 2C9, 2C19, 1A2 and 2D6). As shown in Table 1.4, nine out of ten polymers inhibited CYP activities. Cytochromes 2E1, 3A5, 2C9, 2C19 and 2D6 were inhibited by polyethylene glycol (PEG), while 2E1, 3A4, 3A5 and 2C9 were downregulated by pluronic F68. Pluronic F127, polyvinyl acetate (PVA) and sodium carboxymethyl cellulose (NaCMC) inhibited 2E1, 2E1 and 1A2, respectively. Hydroxypropyl methylcellulose (HPMC) inhibited 2E1 and 3A5, whereas polyvinyl pyrrolidone (PVP) downregulated 3A4 and 1A2. Other polymers, such as Kollicoat, in this study also inhibited specific enzymes, apart from hydroxypropyl cellulose (HPC), which exhibited no effect on any of the enzymes (85).

**Table 1.3** Different types of polymers with some examples (83).

Polymers	Examples
Natural	Sodium alginate
	Gelatin
	Chitosan
Semi-synthetic	Cellulose derivatives
Synthetic	Polyethylene glycols
	Poloxamers
	Polyactides
	Polyamides
	Acrylic acid polymers
Fermentation products	Xanthan gum

**Table 1.4** Effect of different polymers on activities of CYP 2E1, 3A5, 2C9, 2C19, 1A2 and 2D6 (85).

Polymer	IC50 values ( $\mu\text{M}$ )						
	CYP2 E1	CYP3A 4	CYP3A 5	CYP2C 9	CYP2C 19	CYP1A 2	CYP2D 6
PEG	75.3 $\pm$ 2.1	-	78.0 $\pm$ 17.8	365.6 $\pm$ 32.8	139.0 $\pm$ 22.4	-	409.6 $\pm$ 34.5
F68	203.7 $\pm$ 48.3	59.1 $\pm$ 13.6	209.9 $\pm$ 29.7	244.8 $\pm$ 13.2	-	-	-
F127	218.9 $\pm$ 13.3	-	-	-	-	-	-
NaCMC	-	-	-	-	-	224.7 $\pm$ 14.8	-
HPC	-	-	-	-	-	-	-
HPMC	253.5 $\pm$ 17.9	-	19.4 $\pm$ 0.6	-	-	-	-
PVA	548.9 $\pm$ 30.4	-	-	-	-	-	-

Kollicoat	598.1	-	-	-	-	10.0 ±	89.9 ±
	± 26.1					3.9	2.9
HG	141.2	-	-	-	-	40.9 ±	-
	± 14.1					8.4	
PVP		107.3 ±	-	-	-	78.3 ±	-
		11.2				4.2	

Huang *et al.* used the Hill equation and Lineweaver–Burk plots to determine the inhibitory effect of pluronic F68 (F68) on *CYP3A4*. The dose-dependent inhibition was reported with the  $K_i$  and  $IC_{50}$  values for F68 averaged 0.16 and 0.11 mg/mL, respectively (86). The mechanism of action was based on the previously reported inhibitory effect study, which includes the direct interaction with CYP450 enzymes, cell membrane disruption and alteration of cell membrane (74).

Another study tested 22 commonly used excipients, which included sodium alginate, PEG4000, PEG1000, PEG6000 and PEG 2000. All the listed polymers inhibited 1'-OH-MDZ formation in the following order (from strong to weak): Sodium alginate > PEG4000 > PEG1000 > PEG6000 > PEG2000 (60). The physical and chemical nature of each excipient clearly play a major role in their inhibitory capacity. Thus, sodium alginate was the most effective inhibitor when compared to the other polymers due to its ability to disrupt *CYP3A4* activity strongly. On the other hand, the outcomes of this study were limited to *CYP3A4*. As previously mentioned, there are many families and subfamilies of CYP450. There is a possibility that the least effective polymer (PEG2000) could be the most effective on other CYP450 isoenzymes.

Pluronic P85 (P85) is a block co-polymer consisting of two equal polyoxyethylene chains joined by a polyoxypropylene chain. A study revealed that P85 strongly inhibited norverapamil formation by *CYP3A* in a concentration-dependent manner. The study included enterocyte-based metabolism, where the P85 concentrations used were 0.01% and 0.1% v/v. Compared to other polymers in the study, P85 reduced the formation of norverapamil by around 25% and 50% at 0.01% and 0.1% v/v, respectively (87).

### 1.3.1.3 Fatty acids

Fatty acids (FA) are the main components of phospholipids, triacylglycerols and many complex lipids. FAs are present in the majority of dietary fat in humans. Different foods provide a variety of fatty acids. In addition, the human body can synthesize them, either from other fatty acids or nonlipid precursors, e.g. glucose. In recent years, studies have revealed that various FAs have a wide range of microbicidal activity against several Gram-positive and Gram-negative bacteria, as well as enveloped viruses, including *Staphylococcus aureus* and *Neisseria gonorrhoeae* (88,89). For instance, lauric acid (LA) was found to be the most potent inhibitor for the growth of Gram-positive bacteria. These direct or indirect inhibitory effects are due to the destabilization of the bacterial cell membrane caused by fatty acids (90-94). Similar destabilization effect by fatty acids was reported by several researchers when saturated and unsaturated fatty acids were incubated with CYP450 enzymes.

Besides their potent microbicidal activity, FAs can also reduce pre-systemic metabolism of drugs by inhibiting CYP450 enzymes. The effect of saturated and unsaturated fatty acids on CYP3A4, 2E1, 2D6, 2C19, 2C9, 2C8, 2B6, 2A6 and 1A2 were studied using midazolam 1-hydroxylation, chlorzoxazone 6-hydroxylation, dextromethorphan O-demethylation, mephenytoin 4-hydroxylation, diclofenac 4-hydroxylation, amodiaquine N-deethylation, bupropion hydroxylation, coumarin 7-hydroxylation and phenacetin O-deethylation, respectively (95). As a result, out of all the saturated fatty acids, lauric acid showed potential inhibition of 2B6. Myristic acid inhibited 1A2 ( $IC_{50} = 15.8 \mu M$ ), 2B6 ( $IC_{50} = 10.7 \mu M$ ), 2C8 ( $IC_{50} = 13.3 \mu M$ ) and 2C9 ( $IC_{50} = 36.1 \mu M$ ). One of the mono-unsaturated fatty acids, oleic acid, inhibited all the CYP isoforms except for CYP2E1, CYP2C19 and CYP2A6. Similarly, arachidonic acid inhibited activities of CYP3A4, CYP2C19, CYP2C9, CYP2C8, CYP2B6 and CYP1A2. Other FAs also showed a distinct inhibitory effect on different isoforms: gondoic acid inhibited all except 2C8; linoleic acid inhibited CYP2B6, CYP2C8 and CYP2C9; linolenic acid inhibited CYP1A2, CYP2B6, CYP2C8 and 2C9; and timnodonic acid inhibited 2C8 (Table 1.5) (95). Amongst all the isoenzymes, most FAs inhibited CYP2C8 activity. This can be attributed to the large active site on CYP2C8, which allows different sized substrates to accommodate. It also has a peripheral FA binding site that can alter the dynamics of the main active site, affecting the reaction catalyzed by this enzyme. Moreover, it is responsible for

the transformation of polyunsaturated FAs to epoxide products (signaling agents). Hence, the unsaturated fatty acids are potent inhibitors for CYP enzymes than saturated fatty acids (90,96,97).

**Table 1.5** Effect of fatty acids on nine CYPs: 1A2, 2A6, 2B6, 2C8, 2C9, 2C19, 2E1 and 3A4 (95).

FATTY ACID	ABSOLUTE IC <sub>50</sub> (μM)								
	1A2	2A6	2B6	2C8	2C9	2C19	2D6	2E1	3A4
ARACHIDONIC ACID	9.7	21.4	4.6	1.3	3.3	23.2	18.3	61.7	11.7
BEHENIC ACID	>30	>30	>30	>30	>30	>30	>30	>30	>30
CERVONIC ACID	6.3	11.7	6.7	1.2	2.6	15.8	5.6	44.4	7.5
GONDOIC ACID	16.2	81.9	16.6	6.0	17	>100	>100	>100	>100
LAURIC ACID	>100	>100	21.5	42.9	>100	>100	>100	>100	>100
LINOLEIC ACID	13.3	28.9	7.1	1.0	7.4	55.8	17.5	58.9	18.5
A-LINOLENIC ACID	8.8	13.5	9.7	4.4	10.6	53.3	34.3	67.2	36.9
MYRISTIC ACID	15.8	>100	10.7	13.3	36.1	>100	>100	>100	>100
NERVONIC ACID	>11.1	>11.1	>11.1	>11.1	>11.1	>11.1	>11.1	>11.1	>11.1
OLEIC ACID	11.2	25	8.2	4.4	5.7	98.9	18.1	83.8	11.4
PALMITIC ACID	>100	>100	90.5	>100	>100	>100	>100	>100	>100
PALMITOLEIC ACID	7.8	36.2	8	9.7	11.9	58.1	30.3	72.1	26.5
STEARIC ACID	>33.3	>33.3	>33.3	>33.3	>33.3	>33.3	>33.3	>33.3	>33.3
TIMNODONIC ACID	8.2	17.4	5.9	1.5	3.8	13.8	5.7	77.4	16

The results are consistent with a published study on the inhibitory effect of saturated and poly-unsaturated fatty acids (98). Two saturated (palmitic acid and stearic acid) and five polyunsaturated fatty acids (linoleic acid, linolenic acid, arachidonic acid, eicosapentaenoic acid and docosahexaenoic acid) were examined for their effect on six isoforms of CYPs (1A2, 3A4, 2C9, 2C19, 2E1 and 2D6). As shown in Table

1.6, saturated fatty acids showed no inhibitory effect, while all polyunsaturated fatty acids inhibited all six isoforms (98). These polyunsaturated fatty acids had little inhibitory effect at low concentrations, whereas there was a complete inhibition of all isoforms at 200  $\mu\text{M}$ . One potential explanation based on the results is that, at high concentrations, polyunsaturated fatty acids disrupt the microsomal membrane, which prevents the binding of the drug to the active site of the CYP450 enzyme (98). However, other studies have reported that the CYP enzymes can also catalyze the metabolism of polyunsaturated fatty acids. Thus, fatty acids can act as a common substrate for the active site and compete with drugs to bind with CYP enzymes (99,100). Therefore, the mechanism of inhibition remains unknown.

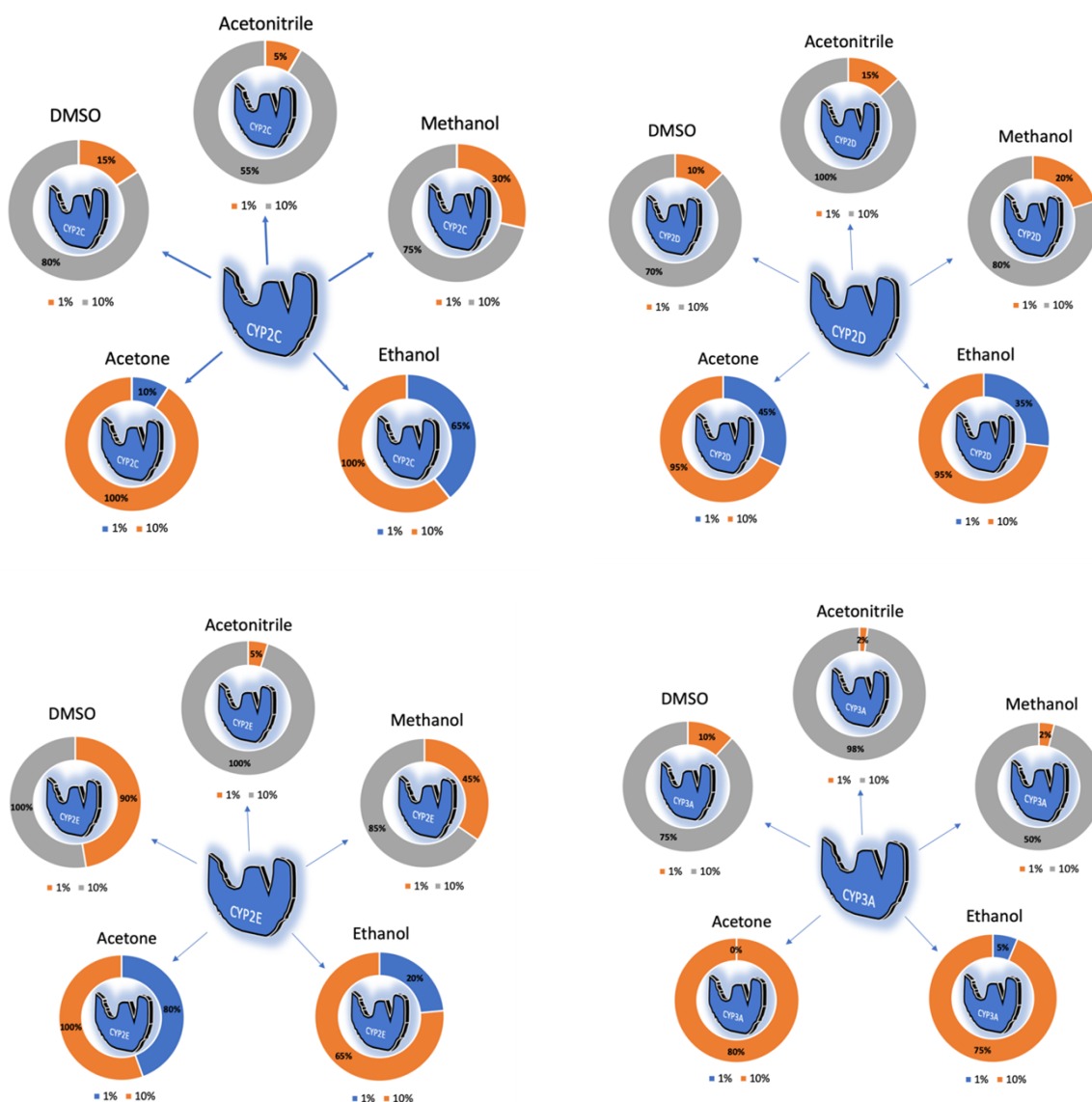
**Table 1.6** Effect of saturated and unsaturated fatty acids where, saturated fatty acids showed NI (no inhibition) and unsaturated inhibited all CYP isoforms (98).

Fatty acids	IC <sub>50</sub> ( $\mu\text{M}$ )					
	CYP1A2	CYP2C9	CYP2C19	CYP2D6	CYP2E1	CYP3A4
Palmitic acid	NI	NI	NI	NI	NI	NI
Stearic acid	NI	NI	NI	NI	NI	NI
Linoleic acid	74	4.1	15	192	113	49
Linolenic acid	52	8.1	9.3	151	82	61
Arachidonic acid	37	3.5	4.8	113	67	48
Eicosapentaenoic acid	41	4.4	4.4	127	53	54
Docosahexaenoic acid	41	2.9	6.7	122	65	34

#### 1.3.1.4 Co-solvents/Solvents

In the last few decades, the effect of organic solvents (such as acetonitrile) on CYP-mediated metabolism has been reported by many researchers (101-108). Most of the *in vitro* studies include organic solvents to dissolve the compounds and prepare the samples for analysis (109-113). The substrates of CYP450 must be present in dissolved form for enzymatic turnover in the *in vitro* drug metabolism experiments. However, due to the substrates' weak aqueous solubility, this is a challenging issue.

As a result, water miscible organic solvents are typically utilised at low concentrations to enhance the aqueous solubility. At higher concentrations, these organic solvents inhibit different isoforms of CYPs. Li et al. evaluated the inhibitory effect of five organic solvents (dimethyl sulfoxide (DMSO), acetonitrile, methanol, ethanol and acetone) on five CYP isoforms (114). All organic solvents at 10% v/v inhibited CYPs activities, whereas >10% inhibition of CYP2D and >40% inhibition of CYP2E (except acetonitrile) was reported at 1% v/v. Overall, the organic solvents showed concentration-dependent inhibition. The inhibitory effect of organic solvents is summarized in Figure 1.2. DMSO and ethanol showed the highest inhibitory effect amongst all organic solvents.



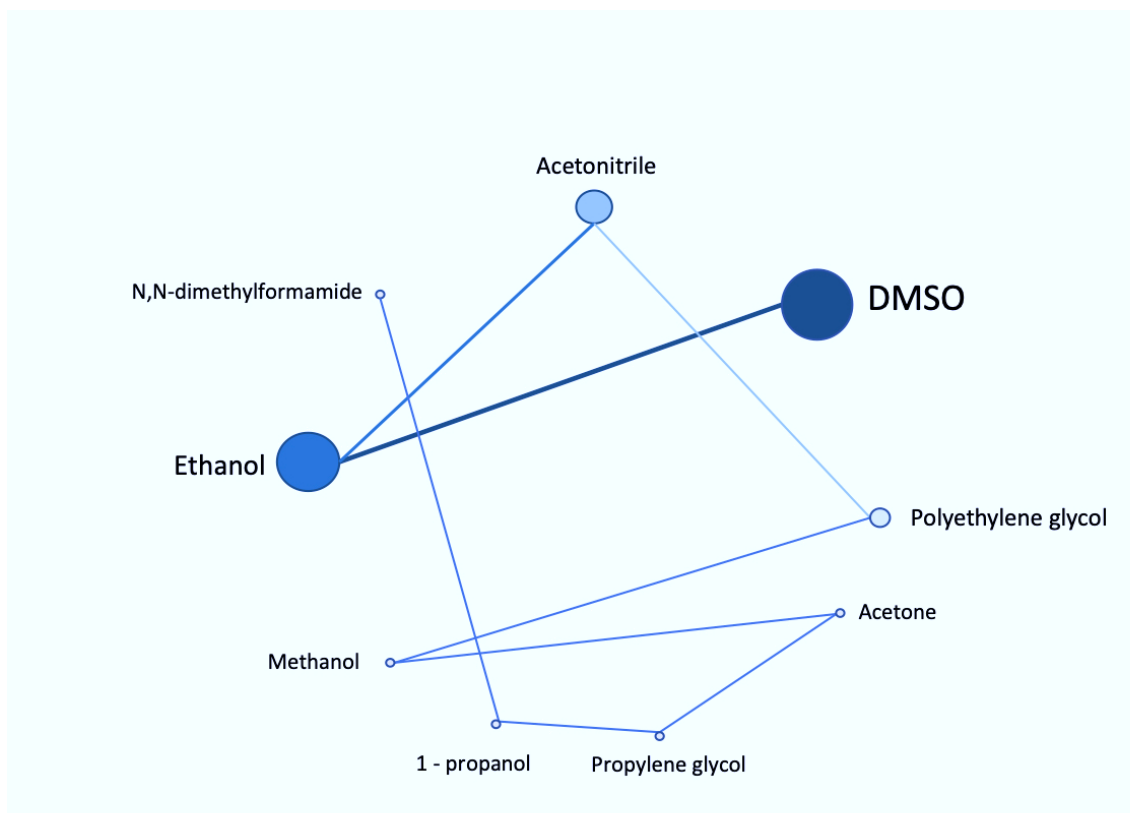
**Figure 1.2** Illustrates the inhibition of CYP2C, CYP2D, CYP2E, and CYP3A by acetonitrile, methanol, ethanol, acetone and DMSO at 1% and 10% concentrations.



Another study demonstrated similar results with DMSO. When diazepam was dissolved in DMSO, the CYP3A4 activity was inhibited in a mixed-type or competitive manner (115). The inhibition of CYP3A4 was concluded to be concentration- and time-dependent. The DMSO inhibitory constant ( $K_i$ ) value for the formation of temazepam and nordiazepam was found to be 24 and 6 mM, respectively.

In 2009, the effect of co-solvent on diclofenac and S-warfarin metabolism by CYP2C9 was studied using ethanol (116). The inhibitory effect was determined to be substrate dependent. Ethanol could inhibit S-warfarin metabolism at a low concentration of 17 mM, whereas it required high concentration of ethanol (510 mM) to competitively inhibit CYP2C9. Ethanol also presented concentration-dependent inhibition for both substrates: S-warfarin and diclofenac.

Eight organic solvents have been studied for their effects on CYP3A4 activity using pooled human microsomes (101). The hydrophilic organic solvents used for this study were DMSO, acetonitrile, methanol, 1-propanol, ethanol, polyethylene glycol, propylene glycol and N,N-dimethylformamide. All organic solvents, except methanol, had significantly decreased testosterone 6 $\beta$ -hydroxylation activity, which reflected the inhibition of CYP3A4. In contrast, only DMSO and polyethylene glycol showed potential inhibitory effect on midazolam 1'-hydroxylation activity. Similar to this study, DMSO showed the strongest inhibition for both metabolic activities. Moreover, the inhibition of testosterone 6 $\beta$ -hydroxylation activity by DMSO was in a concentration-dependent manner: from 10% to 50% inhibition at from 0.1% to 1% v/v. The summary of all the reported organic solvents is shown in Figure 1.3.



**Figure 1.3** Roadmap of various reported organic solvents based on their inhibitory effect on CYP450 system. The size of each circle represents the potency of various organic solvents and the lines depict the order of inhibition: from DMSO being the most potent to N,N-dimethylformamide being the least.

#### 1.4 Effect of excipients on CYP450 Expression

As discussed above, the alteration of CYP450 activities by excipients were mainly through direct inhibition. However, studies also revealed that some excipients can alter the metabolic mechanism via mRNA/ protein expression regulation (117), thus modulating absorption and metabolism of Class 3 drugs (high aqueous solubility and low intestinal permeability). Gene expression of the main metabolizing enzymes can be modulated by many environmental toxins or drugs, which can affect the toxicity and efficacy of co-medicated drugs and cause drug–drug interactions (118-121). Recently, Tompkins et al. investigated the effect of nineteen excipients on regulation of CYP3A4 expression in human liver and colon cells (117). CYP3A4 is a highly inducible isoenzyme and is mainly regulated by a xenobiotic receptor named Pregnane X receptor (PXR), at the transcription level (122,123). This study also included a PXR activation assay to predict the effect of excipients on CYP3A4 expression. As a result, all the excipients failed to activate the CYP2B6 promoter used for PXR activation assay. Instead, few excipients (HPMC, pregelatinized starch and polysorbate-80) showed a decrease in the multi-drug resistance gene

(MDR1) and CYP3A4 expression (Table 1.7). These results suggest that excipients stimulate their effect via an alternate route.

Based on a previous study, Takeshita et al. evaluated the effect of plasticizers on PXR-mediated transcription by the luciferase receptor, PXR-coactivator interaction, PXR knockdown, CYP3A4 activity assay and PCR analysis of CYP3A4 enzyme expression (124). Tompkins et al. (2010) used only two plasticizers which showed no effect on PXR or CYP3A4 induction. However, this study was focused on eight pharmaceutical plasticizers: acetyl tributyl citrate (ATBC), acetyl triethyl citrate, tributyl citrate, triethyl citrate, diethyl phthalate, dibutyl phthalate, triacetin and dibutyl sebacate. As a result, ATBC, dibutyl phthalate and acetyl triethyl citrate activated PXR. ATBC being the most potent transcription inducer showed dose-dependent activation. However, ATBC induced only intestinal CYP3A4 expression and not hepatic expression. This could be due to the PXR splice variants that vary in their gene targets, expression patterns, ligands, biological functions, subcellular localization, and protein interactions (124).

**Table 1. 7** Effect of excipients on PXR activation, CYP3A4 and MDR1. All the excipients failed to activate PXR but reduced expression of CYP3A4 and MDR1. ↑: increased expression, ↓: decreased expression, =: no change, x: not measured, and a: change not statistically significant (117).

EXCIPIENTS	FA2N4		HPH		LS174T	
	mRNA	Protein	mRNA	Protein	CYP3A4	MDR1
HPMC	↑	↓	=	x	↓	↓a
PREGELATINIZED STARCH	=	=	↓	x	↓	↓
CROSCARMELLOSE SODIUM	↑	=	↑	x	↓a	↓a
CROSPVIDONE	↑a	↓	=	x	↓	↓a
POLYSORBATE-80	↓	↓	↓	↓	=	=

### 1.5 Effect of excipients on drug permeability

Another limiting factor for oral drug delivery system is poor permeability. The small intestine is where most of the gastrointestinal absorption takes place (125). Enterocytes, or "absorptive cells," are just one type of the diverse population of cells

found in the intestinal epithelium. The majority of absorption in the small intestine is accounted for by enterocytes, which are the most prevalent cells there. Drugs taken orally are physically prevented from being absorbed by the intestinal epithelium's lipophilic nature and the tight junctions that exist between them (125). The term "apical efflux" (also known as "carrier-mediated efflux") refers to the mechanism by which many medications that reach the cytoplasm of mucosal cells are extruded to the intestinal epithelium. The multi-drug resistance<sup>1</sup> gene's product, P-Glycoprotein (P-gp), has been found to restrict the intestinal absorption of many different drugs. Recent research has shown that a variety of excipients can change permeability of incorporated drug and hence impact the therapeutic efficacy of the treatment (125). For examples, the effect of Cremophor EL on the absorption of rhodamine 123 (RHO 123) as a P-gp substrate was assessed in a study by Shono et al. (126). Cremophor EL concentrations ranging from 0.05 to 1% w/v were utilised in the investigation, which was carried out in rat jejunal intestine tissue. They observed that Cremophor EL increased RHO 123 uptake from the tissue's apical to basolateral side and decreased transport from the basolateral to apical side at concentrations as low as 0.05% w/v.

Cremophor® RH40 reduces P-gp activity, as demonstrated in a clinical experiment with digoxin (a P-gp substrate). Cremophor® RH40 was found to enhance digoxin absorption, resulting in an increase in bioavailability of up to 22% (127). Taking into account its inhibitory impact on P-gp, Cremophor® RH40 has been employed as a surfactant in the formulation of SMEDDS to boost the bioavailability of tacrolimus (a poorly water-soluble P-gp substrate).

Polysorbate 80 was observed to increase apical-to-basolateral permeability and decrease basolateral-to-apical permeability of RHO 123 in Caco-2 cell monolayers in a dose-dependent manner at doses ranging from 0.01 mM to 1 mM (128). In another investigation, Polysorbate 80 inhibited P-gp in Caco-2 cell monolayers for a model peptide drug (Acf (NMef)<sub>2</sub>NH<sub>2</sub>). The drug's basolateral-to-apical permeability was reduced to below the CMC of Polysorbate 80 (50 µM), indicating that monomers of this surfactant, rather than micellar forms, were responsible for its activity. When the concentration of Polysorbate 80 was increased to 30 µM, the apical-to-basolateral permeability increased (129).

## 1.5 Conclusions

Pharmaceutical excipients play an important role in pharmaceutical products and are often presumed to be pharmacologically inert. However, there is growing evidence that they can change the pharmacokinetics of APIs through various mechanisms, such as *P-gp* inhibition and CYP450 inhibition. In this chapter, the recent research concerning the effects of common pharmaceutical excipients on pre-systemic metabolism by phase I metabolic enzymes (CYP450) was discussed. According to our review, more than 40 commonly-used excipients were revealed to interfere with different isoforms of CYP450 *in vitro*, although very few have been assessed in humans. Based on the evidence, the mechanism of action was mainly found to be direct inhibition of the enzymes. Out of all the various excipients, surfactants were the most potent inhibitors due to their ability to cause perturbation of the enzyme's microenvironment. Despite many similarities in the results from different articles, there appears to be a need for a robust approach to integrate the *in vitro* data that can predict pharmacokinetic changes in humans. Further research investigations are warranted to shed light on this issue.

## 1.6 Aims and Objectives

Aim:

To investigate the effect of fatty acids on the metabolism of four probe substrates as well as the metabolism and permeability of different stearic acid-based SLNs using microsomal assays and Caco-2 monolayers.

Objectives:

- LCMS method will be developed and validated for probe substrates using 4-in-1 cocktail approach and conventional approach.
- Fatty acids will be screened in relation to inhibitory effect on CYP450 enzymes using microsomal assay and the best candidate will be used as formulation of choice.
- Solid lipid nanoparticles formulations with three model agents will be prepared, optimised, and characterized for physicochemical properties.
- The presence of fatty acid in SLNs will be studied for its effect on metabolic and permeability rates as well as cell cytotoxicity.

Novelty:

The formulation of drugs is performed with the primary goal of decreasing drug metabolism by CYP450 enzymes. Pre-systemic elimination, poor solubility, and poor permeability are major limiting factors for the oral bioavailability of drugs. Pharmaceutical excipients are substances, excluding the API, that are intentionally included in a drug product to meet regulatory body quality criteria and patient safety in terms of composition, appearance, and performance. Several studies have linked excipients to changes in transporter-mediated substrate absorption and modulations in cytochrome P450 (CYP) enzyme activity. However, fatty acids have not been studied extensively compared to other excipients such as surfactants and polymers. This study focuses on saturated and unsaturated fatty acids as they are commonly used excipients. Drug co-formulation or covalent attachment with fatty acids has been previously reported showing some promise in overcoming these issues by enhancing intestinal permeability, reducing clearance, and selective tissue uptake.

Stearic acid (SA) is a saturated fatty acid, frequently used in SLNs because it has benefits such as targeted release, controlled release, improved oral bioavailability,

improved drug/carrier stability, passive targeting ability, better brain permeability, improved biocompatibility, and a decreased rate of drug degradation. Lipids have received a lot of attention in the last decade as a carrier for drugs with low water solubility. The existence of novel lipid excipients with appropriate regulatory and safety profiles, as well as their ability to improve oral bioavailability, has aided in the development of lipid-based formulations as a drug delivery method.

Hence, studying the effect of stearic acid-based solid lipid nanoparticles on the metabolic activity of CYP450s and permeability of these formulations is the novelty of this research.

# **Chapter 2: Materials and Methods**



## 2.1 Materials and methods

### 2.2.1 Chemicals and reagents

Omeprazole, dextromethorphan hydrobromide, undecanoic acid, nonanoic acid, crotonic acid, and tridecanoic acid were purchased from Fluorochem (Glossop, UK). Verapamil HCL, propranolol (internal standard), stearic acid, pentadecanoic acid, heptadecanoic acid, transcucol, span 80, glycerol, and polyvinylpyrrolidone (PVP) MW 40,000 were procured from Tokyo Chemical Industry Ltd (Oxford, UK). Testosterone and brij 35 were purchased from Sigma-Aldrich Ltd (Gillingham, UK). Lauric acid, myristic acid, and propylene glycol were purchased from Acros Organic (Enderby, UK).

Rat (Sprague-dawley), male liver microsomes, Nicotinamide Adenine Dinucleotide Phosphate (NADP), D-Glucose 6-phosphate dipotassium salt hydrate (G6P), Glucose-6-phosphate dehydrogenase (G6PDH) and Magnesium chloride ( $MgCl_2$ ) were purchased from Sigma Aldrich (Haverhill, UK). Formic acid, LC-MS/MS graded Acetonitrile (ACN) and water were obtained from VWR (Lutterworth, UK). Distilled water and all other chemicals were of analytical grade and commercially available.

### 2.2.2 Microsomal assay incubation conditions

A microsomal assay was conducted using two different approaches: 1) Testosterone as an individual substrate 2) cocktail approach (4-in-1) using omeprazole, dextromethorphan, verapamil as probe substrates and propranolol as internal standard.

Incubation mixture consisted of 445 $\mu$ L microsomal protein (0.5mg/mL), 50 $\mu$ L NADPH system (1.3mM NADP, 3.3mM G6P, 0.4 units/mL G6PDH, and 3.3mM  $MgCl_2$ ), and 5 $\mu$ L of probe substrate cocktail (omeprazole, dextromethorphan and verapamil) or testosterone at a final volume of 500  $\mu$ L. 0.1 M Potassium phosphate buffer was prepared freshly every week by adding 0.414g of monobasic dihydrogen phosphate ( $KH_2PO_4$ ) and 1.212g of dibasic monohydrogen phosphate ( $K_2HPO_4$ ) in 100mL of distilled water and pH adjusted to 7.4. The concentrations used for individual substrates were based on their  $K_m$  values: 7.5 $\mu$ M of omeprazole, 5 $\mu$ M of dextromethorphan, and 2.3 $\mu$ M of verapamil or 3  $\mu$ M of testosterone (130) (131). The final concentration of ACN was below 1% v/v. Samples were preincubated with liver

microsomes for 5-10 min at +37 °C in the Thermomixer (Shenyang Yu Shuo Da Science and Technology, China). At the same time, 50µL NADPH was pre-warmed for 5 minutes. The reaction was then initiated by addition of NADPH. Incubation was carried out for 30 min and the reaction was terminated, at a specific time interval, by 100µL of ice-cold ACN containing 150ng/mL propranolol (IS). The procedure was also used to carry out negative controls (absence of NADPH). Samples were centrifuged for 1 hour at 500 x g and 100 µL of supernatants were collected, diluted, and analysed using LCMS (n=3) (111).

To study the effect of fatty acids on CYP450 activity, equal volumes of fatty acids (5 µL) were co-added to the substrate cocktail or testosterone in the incubation mixture (n=3). The procedure was then followed as described above for incubation without excipients (control). The concentration of tested fatty acids was 100 µM (98). The inhibition of CYP450 activity was expressed as % compound recovery based on the ratio of excipients incubation to control incubation. Moreover, the effect of verapamil on metabolism of testosterone was also tested using same procedure for microsomal assay.

To calculate the IC<sub>50</sub> value of the selected fatty acid, the inhibition of various CYP450 enzymes was conducted by preincubating with chosen fatty acid at various concentrations (2, 25, 50, 100, and 200 µM) at 37 °C for 5-10 min followed by the procedure described in the section 2.2.2.

### **2.2.3 LCMS instrumentation**

The samples were analysed on Thermo MS (TSQ Quantum Access, Thermo Electron corporation, UK) with an Electro Spray Ionisation (ESI) source in a positive mode. The quantification of probe substrate was performed using the multiple reaction monitoring (MRM) mode. The analysed compounds were optimised by the infusion method using an infusion pump. Data were acquired and quantified using Xcalibur™ software 2.0 (Thermo Scientific™, UK).

The Thermo HPLC system (UK), equipped with an Accela pump, Accela auto-sampler, and column oven was used to inject all samples. Poroshell 120 EC-C18 (150 x 4.6 mm) column was used to separate probe cocktail substrates with IS and testosterone. Gradient elution for cocktail and isocratic elution for testosterone were performed at a flow rate of 0.5 mL/min by using 0.1% formic acid in water (mobile

phase A) and 0.1% formic acid in ACN (mobile phase B). The injection volume for each sample was set to 10  $\mu$ L and the total run time for each cocktail and testosterone analysis was 10 min and 5 min, respectively (n=3) (Table 2.1).

**Table 2. 1 HPLC method optimisation parameters for cocktail drugs and testosterone.**

<b>GRADIENT FOR COCKTAIL</b>		
<b>Time (min)</b>	<b>0.1% formic acid in water (%)</b>	<b>0.1% formic acid in ACN (%)</b>
0.00	61	39
7.00	35.9	64.1
7.01	61	39
10.00	61	39
<b>Flow rate</b>	0.5 mL/min	
<b>Injection volume</b>	10 $\mu$ L	
<b>ISOCRATIC FOR TESTOSTERONE</b>		
<b>Time (min)</b>	<b>0.1% formic acid in water (%)</b>	<b>0.1% formic acid in ACN (%)</b>
0.00	20	80
5.00	20	80
<b>Flow rate</b>	0.5 mL/min	
<b>Injection volume</b>	10 $\mu$ L	

### **Validation study**

The optimised method was then validated for its intended use according to the International Council for Harmonisation of Technical Requirements for Registration of Pharmaceuticals for Human Use (ICH) guidelines (132). Various characteristics such as linearity, accuracy, precision, limit of detection (LOD) and limit of quantification (LOQ) were evaluated.

### **Linearity**

Five different concentration levels for individual compounds, ranging from 225 to 750ng/mL (omeprazole), 105 to 350ng/mL (dextromethorphan and verapamil), 105 to 350ng/mL (testosterone), and 150ng/mL (propranolol IS) were used. The slope of regression line, y-intercept, residual sum of the square, and correlation coefficient were calculated.

### **Accuracy**

Three different concentrations ranging within the calibration range were chosen and assessed in triplicates. The results were reported as percentage (%) recovery.

$$\% Recovery = \frac{(B)}{(A)} \times 100$$

**Equation 2.1** Percent recovery to determine the accuracy (132).

Where,

B = calculated concentration

A = original concentration

### **Precision**

Repeatability was assessed using three different concentrations in triplicates covering specific range: 337.5-637.5 ng/mL for omeprazole and 157.5-297.5 ng/mL for dextromethorphan, verapamil, and testosterone. The intermediate precision was evaluated by repeating the procedure on three consecutive days. The relative standard deviation was calculated.

### **Sensitivity**

LOQ and LOD were measured based on the standard deviation (SD) of the slope and the intercept/response.

LOQ was calculated using equation 2.2 and LOD was calculated using equation 2.3.

$$QL = \frac{10S}{M}$$

**Equation 2.2** to calculate limit of quantification (132).

Where,

S = the standard deviation of intercept

M = the slope of calibration curve

$$QD = \frac{3.3S}{M}$$

**Equation 2.3** to calculate limit of detection (132).

Where,

S = the standard deviation of intercept

M = the slope of calibration curve

### Data analysis

Results were collected and represented as mean  $\pm$  standard deviation with triplicates for linearity and CYP450 inhibition study. To evaluate the metabolism of individual probe substrate by CYP isoforms, IC<sub>50</sub> was calculated via GraphPad Prism 9, and intrinsic clearance (CL<sub>int</sub>), metabolic half-life (t<sub>1/2</sub>), and % compound remaining were determined using the equations below (133):

Elimination rate constant (*k*) = - slope of the regression line

$$t_{1/2} \text{ (min)} = \frac{\ln 2}{k} = \frac{0.693}{k} \quad \text{Equation (2.4)}$$

$$V \text{ (}\mu\text{L / mg)} = \frac{\text{Volume of incubation}(\mu\text{L})}{\text{Microsomal protein concentration in the incubation (mg)}} \quad \text{Equation (2.5)}$$

$$\text{CL}_{\text{int}} \text{ (}\mu\text{L / min/ mg protein)} = \frac{V \times 0.693}{t_{1/2}} \quad \text{Equation (2.6)}$$

$$\% \text{ Compound Remaining} = \frac{\text{Concentration at each time point (min)}}{\text{Concentration at 0 (min)}} \times 100 \quad \text{Equation (2.7)}$$

One way analysis of variance (ANOVA) against control (drug alone) at each time point were used for statistical analysis and probability value of p<0.05 was used to determine statistical difference.

### 2.2.4 Quantitative analysis of probe substrates by HPLC/UV

The amount of Testosterone dissolved in the solution was quantified by HPLC-UV using LC-2010AHT (Shimadzu, UK), UV detector and Poroshell 120 EC-C18 (150

x 4.6 mm) column. The analytical method that was developed using LCMS was adopted for quantification of testosterone. Testosterone was eluted using 80% acetonitrile + 0.1 formic acid and 20% of water + 0.1% formic acid as a mobile phase pumped at 0.5 mL/min. The UV-detector was set at a  $\lambda_{\text{max}}$  of 254 nm.

The amount of dextromethorphan and verapamil dissolved in the solution were also quantified using HPLC-UV and C18 column, individually. The method that was developed for cocktail approach using LCMS was used for quantification of dextromethorphan and verapamil. Dextromethorphan and verapamil were eluted using a gradient method (61% to 35.9% of mobile phase A, from 0.00 min to 7.01 min, followed by 61% of mobile phase A from 7.01 min to 10.00 min) pumped at 0.5 mL/min. Water + 0.1% FA was used as mobile phase A whereas, acetonitrile + 0.1% FA was used as mobile phase B. The UV-detector was set at 289 nm for dextromethorphan and 278  $\lambda_{\text{max}}$  for verapamil. The experiment Experiments were performed in triplicates and data are presented as mean  $\pm$ SD.

All the methods were re-validated using ICH guidelines (132), method explained in section 2.2.3.

### **2.2.5 Screening of surfactants**

The surfactants and co-surfactants (span 80, glycerol, propylene glycol, transcitol, brij 35, and PVP) were investigated for good solubilising capacity. Brij 35 is solid at room temperature and therefore, 10% w/v was prepared using distilled water. An excess amount of testosterone, dextromethorphan or verapamil was added to 2 mL of various surfactants placed on a magnetic stirrer and mixed at 100 rpm for 48 h at room temperature. After 48 h, the suspensions were centrifuged at 500 x *g* for 10 min. The supernatant was collected and diluted using ACN (1:10), followed by filtration prior to analysis by HPLC-UV. Experiments were performed in triplicates and data are presented as mean  $\pm$ SD.

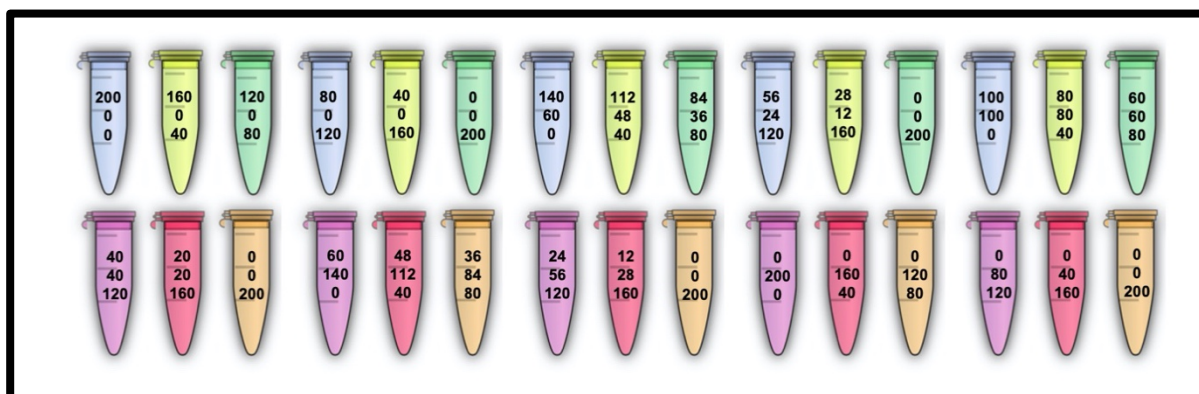
### **2.2.6 Optimising surfactant/co-surfactant system**

Brij 35 (10% w/v) and propylene glycol were chosen as the surfactant/co-surfactant system (S/CoS) based on the solubility of probe drugs (testosterone,

dextromethorphan, and verapamil) and HLB values of surfactant and co-surfactant. Different ratios of S/CoS (3:1, 2:2 and 1:3 w/w) were blended for solubility profile of S/CoS and the method was repeated as mentioned above.

### 2.2.7 Pseudo-ternary phase diagram

The quantitative ratio of oil (stearic acid), surfactant/co-surfactant, and aqueous phase required for oil-in-water (O/W) microemulsion was optimised by pseudo-ternary phase diagram and visual inspection. The pseudo-ternary phase diagram was constructed using different ratios of stearic acid: S/CoS: aqueous phase (%v/v) as shown in Figure 2.1. The S/CoS ratio for testosterone and verapamil formulation was 1:1 v/v whereas, for dextromethorphan was 1:3 v/v. The Eppendorf tubes were filled by micropipettes in accordance with the filling schemes with the total volume of the emulsion 200  $\mu$ L. The filling scheme was established using different percentage ratios of oil and S/CoS system (100:0, 75:25, 50:50, 25:75, and 0:100%) and water as remainder. For instance, the first eppendorf tube (200,0,0) represents 200 $\mu$ L of stearic acid, 0 $\mu$ L of S/CoS, and 0 $\mu$ L of water. The method was performed under high temperature (80°C) using water bath (ThermoFisher Scientific, UK) shaken at 200 rpm for 4 hours. The two different systems, homogenous and heterogenous, were evaluated by visual inspection.



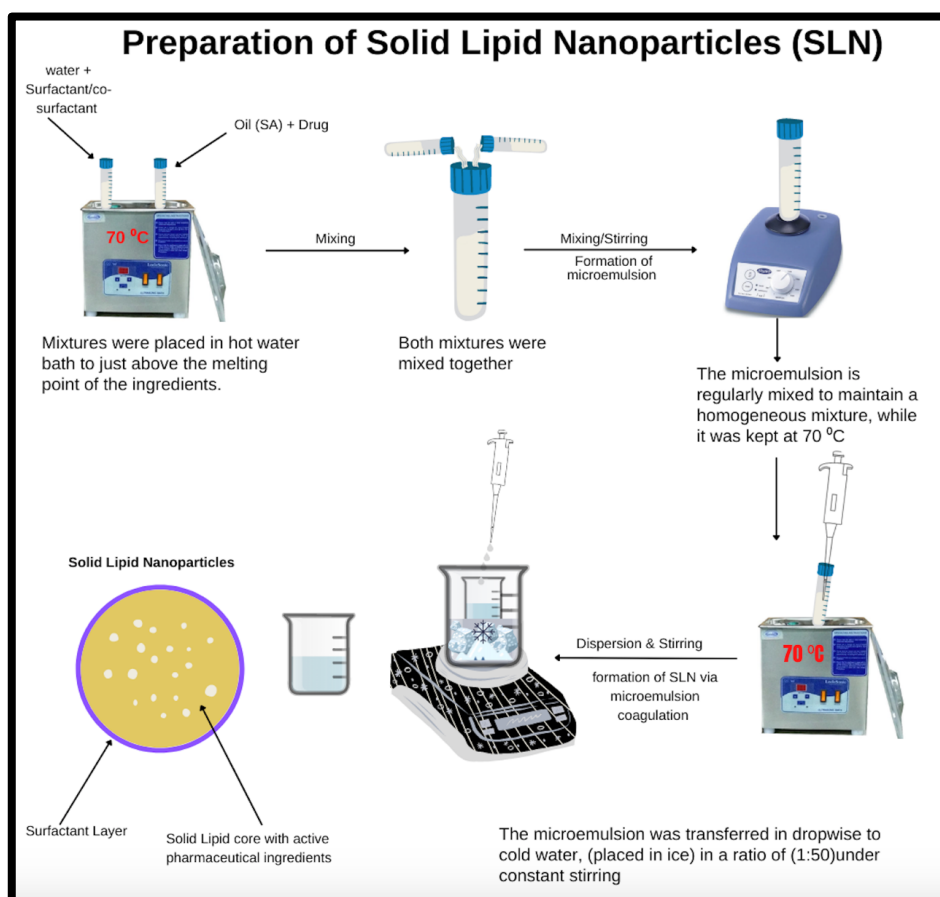
**Figure 2.1** Illustrates different ratios of oil:S/CoS:water used for ternary phase diagram. The system was established to include 0 to 100% of each component at various ratios. For example, the first tube (200,0,0) contains 200  $\mu$ L of oil, 0  $\mu$ L of S/CoS, and 0  $\mu$ L of water.

### 2.2.8 Preparation of Solid lipid nanoparticles for testosterone and verapamil

Solid lipid nanoparticles were prepared via a hot emulsion technique at a temperature above the melting point of stearic acid (Figure 2.2). Formulation includes stearic acid as the solid oil, brij 35 (10% w/v) as the surfactant, propylene

glycol as the co-surfactant and distilled water as the dispersion medium. Based on pseudo-ternary phase diagram, optimised quantities of all the components were measured. Two different formulations were prepared for testosterone whereas, one formulation was developed for verapamil.

Stearic acid (1 mL) was heated above its melting point along with 5mg of drug (testosterone or verapamil), using sonicator. Precisely, 8 mL of distilled water was mixed with 1 mL of S/CoS (1:1 ratio) and heated to the same temperature as stearic acid using sonicator for 10 min. The mixture was then added to stearic acid and sonicated for next 15 min to produce microemulsion. The microemulsion was dispersed into ice-cold distilled water (1:50) to form solid-lipid nanoparticles. The procedure was repeated with different ratios of stearic acid (1 mL): distilled water (7 mL), and S/CoS (2 mL) for testosterone.



**Figure 2.2** Demonstrates different steps for hot emulsion technique used to prepare testosterone-loaded solid lipid nanoparticles. The first step involved the preparation of microemulsion which was followed by SLNs formulation.



### **2.2.9 Preparation of Solid lipid nanoparticles for dextromethorphan**

Three different methods were used to prepare dextromethorphan-loaded SLNs: i) hot emulsion, ii) w/o/w double emulsion, and iii) solvent evaporation.

The hot emulsion technique was followed as described for testosterone-loaded SLNs in section 2.2.8.

The double emulsion method was adapted from the study by Peres *et al.* (134), where SLNs were prepared using w/o/w emulsion method. In this experiment, 0.6 g of stearic acid was melted above its melting point and mixed with an equivalent amount of propylene glycol. 0.2 mL of hot water containing 5mg of dextromethorphan was then transferred and sonicated for 15 seconds at 45% of amplitude to form pre-emulsion (W/O). The second emulsion (W/O/W) was prepared by adding 6.0 mL of warm Brij 35 aqueous solution and homogenized by ultrasonic at 45% amplitude for 60 seconds. This double emulsion (W/O/W) was dispensed into 90.0 mL of ice-cold water and stirred constantly using magnetic stirrer to solidify lipid nanoparticles.

The third method was solvent evaporation where three different surfactants were used (Brij 35 10%w/v, Tween 80, and poloxamer 188) to prepare three SLNs formulations. Firstly, 0.5 g of stearic acid and 0.7 g of propylene glycol were dissolved in chloroform (organic phase). Secondly, this organic phase was transferred to the 4 mL of aqueous phase containing 0.3 g of brij 35/tween 80/poloxamer 188 and homogenized to produce pre-emulsion. The pre-emulsion was sonicated for 60 seconds to achieve nano-emulsion and it was left overnight on magnetic stirrer to evaporate organic solvent, resulting in solid lipid nanoparticles.

### **2.2.10 Particle size determination and zeta potential of SLN**

Testosterone- and verapamil-loaded SLNs were analysed for the particle size, polydispersity index (PDI), and zeta potential by dynamic light scattering with a Zetasizer (Malvern Instruments, Malvern, UK). The SLN samples were dispersed in distilled water (1:10) to minimize interparticle interaction before analysis and refractive index was set to 1.43. The instrument was set to measure each sample in triplicates at 25°C.

### 2.2.11 Morphology of SLN

The morphology of wet and freeze-dried testosterone- and verapamil-loaded SLNs were examined via scanning electron microscope (SEM) (Model LEO 1455VP, LEO, Cambridge, UK) at an accelerate voltage of 10kV. Firstly, the SLNs samples were mounted on an aluminium stub which were then loaded onto a universal aluminium holder, followed by sputter coated (Polaron Equipment, Watford UK) with fine layer of gold-palladium to enable electricity conduction at low vacuum, 20 mA for 3 minutes in the presence of argon gas.

### 2.2.12 Thermal analysis of SLN

The thermal behaviour of testosterone- and verapamil-loaded SLN was analysed using a differential scanning calorimeter (DSC) (DSC25 Waters™, TA instruments, UK). Samples of stearic acid, testosterone and SLN containing testosterone were accurately weighed (7-9mg) into aluminium pans and crimped. The thermograms were recorded over a temperature range of 0 to 300°C at 10°C/min heating rate under constant nitrogen purge gas at a flow rate of 20mL/min.

### 2.2.13 Drug encapsulation and loading capacity

The indirect approach was chosen for measuring the entrapment efficiency and loading capacity of the testosterone- and verapamil-loaded SLNs. A defined amount of SLN sample was centrifuged in a Sigma 3-30KS (SciQuip, UK) at 12,298 x g for 60 min at 4°C temperature. The supernatant was collected and diluted for quantitative analysis by HPLC/UV, whereas the pellet was freeze dried and weighed using a weighing balance. The UV detection was carried out at 254nm and the calibration curve ( $y = 65128x + 4204.1$ ,  $R^2 = 0.9998$ ) obtained for testosterone with the concentration range of 1-125 µg/mL was used to calculate amount of testosterone in the SLN. The following equations 2.8 and 2.9 were used to calculate the entrapment efficiency with initial mass of 10 µg and loading capacity.

$$\text{Entrapment efficiency}(\%) = \frac{\text{mass of initial drug (Mi)} - \text{mass of free drug (Mf)}}{\text{mass of initial drug (Mi)}} \times 100$$

**Equation 2.8** Entrapment efficiency (134).

$$\text{Loading capacity(\%)} = \frac{\text{mass of initial drug (Mi)} - \text{mass of free drug (Mf)}}{\text{mass of lipids (Ml)}} \times 100$$

**Equation 2.9** Loading capacity (134).

#### **2.2.14 *In vitro* release study**

The release profile of testosterone as well as verapamil from the SLNs were measured by a dissolution test in 0.1M phosphate buffer solution (release medium, pH 6.8) using dialysis membrane (14,000 molecular weight cut-off, inflated, Scientific laboratory supplies, UK). The testosterone- and verapamil-loaded SLNs pellet were re-dissolved and washed with 5 mL of phosphate buffer solution and then all 5 mL was transferred to dialysis bag that immersed into 20 mL of phosphate buffer solution. The dissolution test was performed at 37°C temperature under magnetic stirrer maintained at 150 rpm for 24hr. At fixed time intervals (0, 5, 10, 15, 30 min, 1, 2, 3, 4, 5, 6, 12, 24, and 48 hrs), aliquots of the dissolution release medium (1 mL) were withdrawn and replaced by 1 mL of fresh medium. The fraction of drug lost due to sampling at various time intervals is accounted by including volume of dissolution media (20mL) and the amount of sample withdrawn and replace (1mL) at each time point in the final drug release calculation. The withdrawn samples were analysed by HPLC-UV at 254nm in triplicates (n=3), and the cumulative release of testosterone was calculated as mean  $\pm$ SD.

#### **2.2.15 *In vitro* metabolic assay**

The CYP inhibition profile of 65  $\mu$ M stearic acid from testosterone- and verapamil-loaded SLN were performed by metabolic assay. The SLN pellet was resuspended in 0.1M phosphate buffer (pH 7.4) and specific volume (3  $\mu$ L) of the suspension was transferred to incubation system (497  $\mu$ L). The metabolic reaction of testosterone- and verapamil- loaded SLNs was compared with positive control (testosterone/verapamil with no stearic acid). The procedure mentioned in chapter 2 for microsomal assay was repeated to measure the inhibitory effect. At definite time intervals (0, 5, 15, and 30min), the microsomal reaction was terminated by transferring 100  $\mu$ L of incubated sample to 100  $\mu$ L of ice-cold ACN, followed by centrifugation at 3000 x g for 50 min at 20°C. The supernatants were collected and

diluted (1:2) for LC/MS analysis. The experiment was conducted in triplicates (n=3) and data calculated as mean  $\pm$ SD.

#### **2.2.16 Caco-2 cell culture**

Caco-2 cells at passage 38 were gifted by Kingston University and used at passages 40-48. The cells were freeze thawed and seeded in a 75 cm<sup>2</sup> T-flask containing 10 mL of Duplecco's modified Eagle's medium (DMEM) and other supplements: 10% foetal bovine serum (FBS), 1% penicillin-streptomycin, 1% nonessential amino acid (NEAA), and 1% sodium pyruvate. 5 mL of culture media were replaced every 2-3 days and cells were grown at 37°C and 5% CO<sub>2</sub>. At 90% confluence, the cells were passaged by 5mL trypsin. To carry out transepithelial transport assay, 2 x 10<sup>5</sup> cells/cm<sup>2</sup> were seeded on 0.4  $\mu$ m pore polycarbonate-coated membranes (24-well transwell plates, 6.5mm, 1.9cm<sup>2</sup>) and were grown for 21 days. The media was replaced in both apical (0.3 mL) and basolateral layer (0.5 mL) every 2-3 days.

#### **2.2.17 Testosterone- and verapamil- loaded SLNs permeability study**

The permeability of testosterone- and verapamil-loaded SLN was assessed after 21 days of seeding. The basolateral compartments were replaced with fresh media (0.5 mL) whereas, the apical compartments were replaced with 0.3 mL of medium containing 1.4mg testosterone- or verapamil-loaded SLN, testosterone/verapamil on its own (positive control), and fresh media (negative control). At different time intervals (0, 10, 20, 30, 40, 50, 60, and 90 minutes), sample aliquots (100  $\mu$ L) were collected from the basolateral compartment followed by addition of an equal volume of fresh medium pre-warmed at 37°C. The cells were incubated at 37°C and 5% CO<sub>2</sub> during the experiment. The samples were diluted (dilution factor = 2) and analysed by LC/MS. At the final time point, the samples were collected from both layers to confirm the mass balance. The testosterone- and verapamil-loaded SLNs permeability was compared with testosterone (control) and verapamil (control) permeability, respectively. All experiments were performed in triplicates (n=3) and data presented as mean  $\pm$ SD. The cell integrity and formation of monolayer was observed using confocal microscope.

After permeability studies, Caco-2 cell monolayers were washed three times with phosphate buffer saline (PBS) pH 7.4 and fixed at room temperature for 15-20 minutes using freshly prepared paraformaldehyde solution. Cells were washed in PBS before being permeabilized at room temperature for 30 minutes with 0.2%

Triton-X-100 in PBS. Cells were rewashed with PBS and incubated with rabbit anti-ZO-1 monoclonal antibody for 3 hours at room temperature. Following three washes, the cells were co-incubated for one hour at room temperature with another antibodies Alexa Fluor 488 goat anti-rabbit and Alexa Fluor Phalloidin 546. After this, the cells were washed twice with 5% normal goat serum in PBS and once with PBS before being mounted with Gel Mount media (Fisher scientific, UK) (135). Slides were prepared and visualised by confocal laser scanning microscopy (Zeiss LSM510) equipped with helium and argon neon lasers.

### **2.2.18 Dextromethorphan permeability study**

The permeability study was conducted using mixture ( $M_1$ ) of 5 mg dextromethorphan, 1 mL stearic acid, 0.3 mL brij 35 10% w/v, 0.7 mL propylene glycol, and 8 mL water. The permeability of  $M_1$  was evaluated after 21 days of seeding. The basolateral compartments were replenished with fresh media, while the apical compartments were replaced with medium containing  $M_1$ , dextromethorphan, and fresh media (positive control). The method for permeability study and confocal microscopy was followed as described in Section 2.2.17. All experiments were carried out in triplicates ( $n=3$ ).

### **2.2.19 Cell toxicity study for testosterone- and verapamil-loaded SLN**

Caco-2 cells were passaged on 96-well plates for MTT cell viability assay and were allowed to confluent for 7-days. Prior to MTT assay, the cells were treated with 100 $\mu$ L of different chemicals ( $n=6$ ): 2, 20, 40 and 80  $\mu$ g/mL of testosterone/verapamil, SLNs, stearic acid, propylene glycol, brij 35, dimethyl sulfoxide (DMSO), water, 70% industrial methylated spirit (IMS) as positive control, and media as negative control. All treated and control groups were incubated simultaneously at 37°C and 5% CO<sub>2</sub>. After 2 hours, 100  $\mu$ L of incubated medium in each well were replaced with 100  $\mu$ L MTT solution (1mg/mL) followed by incubation for 1, 2, and 24 hours. 50  $\mu$ L of DMSO was then added to each well and agitated for 10 min at room temperature. The absorbance was read at 554 nm on the infinite M200 PRO (Tecan, UK) plate reader.

One way analysis of variance (ANOVA) for permeability study against control (drug alone) at each time point were used for statistical analysis and probability value of  $p<0.05$  was used to determine statistical difference.

### **2.2.20 Cell toxicity study for dextromethorphan-loaded SLN**

MTT cell viability assay was carried out on 96-well plates using Caco-2 cells. The method used for MTT cell viability assay is described in Section 2.2.19.

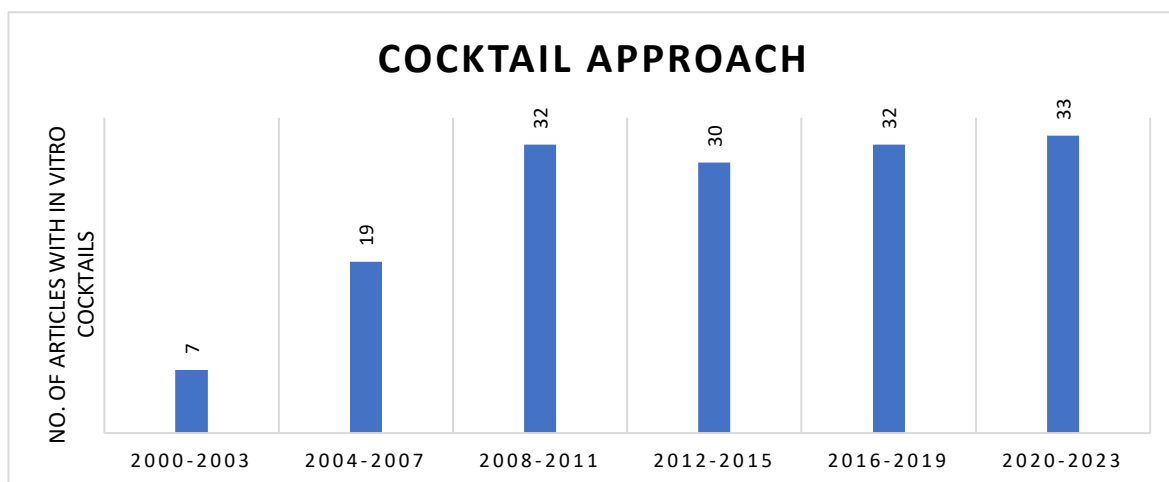
# **Chapter 3: Screening the Effect Of Fatty Acids On CYP450 Enzymes Using LCMS/MS**

## 3.1 Introduction

### 3.1.1 Metabolic assay

Pharmaceutical properties play important roles in the success of new drug candidates (136). Studies have reported that more than 40% of new drug candidates failed in the development stage because of insignificant biopharmaceutical properties (137) (138). This led to a major initiative of a high throughput ADME/TOX assays in the pharmaceutical industries and condensed pharmacokinetic (PK) studies in early drug discovery to address PK related issues (138). The high throughput method for *in vitro* drug metabolic studies provides many advantages: 1. Early metabolic profile determination provides important information and ranking capabilities for drug metabolism and pharmacokinetics (DMPK) teams which helps in further modifications to improve metabolic properties; 2. In addition to pre-clinical species, human enzymes can be utilized to predict human clearance *in vivo*; 3. The ease of preparation from different species, flexible availability and long term storage makes *in vitro* method time- and cost-effective (139). High throughput methods for microsomal assay consist of two main procedures: 1. Sample preparation and microsomal incubation 2. Rapid quantification with liquid chromatography/mass spectrometry (LCMS) for number of samples (140). Over the years, three different approaches have been performed to assess the *in vitro* metabolism activity of CYP450: (i) the classic strategy, with distinct incubations and analyses, (ii) the sample pooling strategy, collecting various incubation mixtures for Liquid chromatography-mass spectrometry (LCMS) analysis, and (iii) the cocktail strategy (141). Recently, the combination of the cocktail approach with LCMS, where multiple CYP isoforms are studied in a single microsomal incubation of substrate mixture, have become more popular as shown in Figure 3.1 (142) (143) (144). This approach is both, time- and cost-effective as it consumes less metabolic reagents and samples.



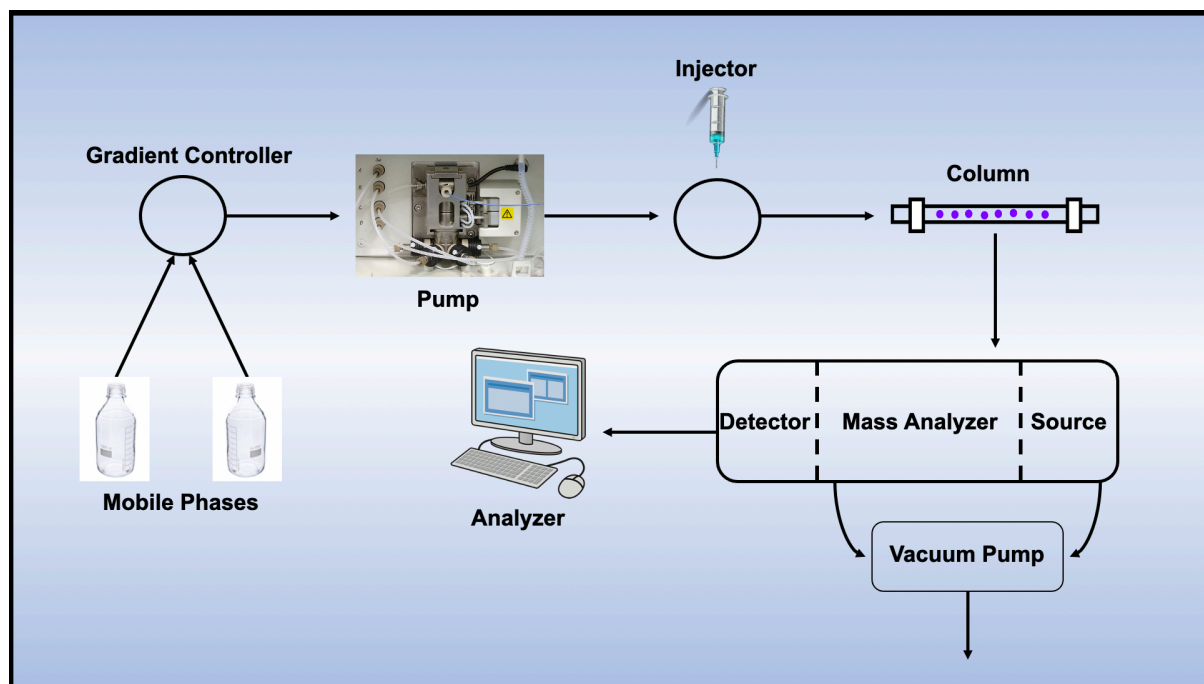


**Figure 3.1** Illustrates the number of articles published with in vitro cocktail approach (extracted from google scholar) where the numbers on the bar represents number of articles between years.

### 3.1.2 Liquid chromatography- Mass spectrometry

To evaluate the metabolic assay parameters, LCMS was used as a high throughput analytical method. Liquid chromatography (LC) is one of the key techniques for dealing with drug metabolism profiling in the field of drug development. Besides liquid chromatography, other techniques such as capillary electrophoresis (CE) and gas chromatography (GC) have been used occasionally. However, CE exhibits poor sensitivity and incompatibility of many compounds, whereas GC is limited to volatile drugs and metabolites. The continuous development of LC as a separation technique which provides high sensitivity and specificity, enhanced resolution, and high speed makes it an ideal analytical technique for metabolic assay (145) (146) (147).

In general, LCMS is a combination of High-Pressure Liquid Chromatography (HPLC) with MS linked via an interface containing an ionization source (Figure 3.2). LC separates all the analytes which are sprayed into pressurised ion source and converted into ions in presence of a desolvation gas. The mass analyser then categorises ions according to their mass-to-charge ratio ( $m/z$ ), and the detector counts and amplifies signals from ions emerging from the mass analyser. As an outcome, mass spectrum (a plot of the ion current vs  $m/z$ ) is generated, which is used for qualitative and quantitative analysis (148) (149).



**Figure 3.2** The schematic diagram shows the main components of LC/MS: LC unit (pump, autosampler and column), ion source, mass analyzer, and detector.

The most commonly used ionization sources for LCMS are Atmospheric pressure chemical ionization (APCI), Electrospray ionization (ESI), and Matrix-assisted laser desorption/ionization (MALDI) (150). The leading method of choice out of all the ionisation techniques, as per the data is ESI. Sample solution, using electrical energy, is passed through a small capillary (<250  $\mu\text{M}$  internal diameter) at an atmospheric pressure to produce ions. The small capillary is at potential difference to a counter electrode (between +500 and +4500 V) and the voltage requirement depends on the solvents and the needle's inner diameter (151). An aerosol of charged droplets are initially generated by electrostatic spraying of analytes and sometimes flow of gas, for example  $\text{N}_2$ , is utilised for this process. These droplets contain both analyte and solvent particles with net positive/negative charge, which depends on the applied voltage polarity. These ions eventually become solvent free

and transfer into the mass analyser (151). One of the major benefits of using ESI is molecules with larger size can also be ionised, as reported for the Coliphage T4 DNA ionization with a molecular weight of  $1.1 \times 10^8$  Da (152) (153). Coupled with HPLC, HPLC/ESI-MS becomes a powerful technique for analysing small and large molecules with different polarities in complexed biological samples. (154)

Recently, Busch and co-workers studied six different substrates of UGT and CYP enzymes and quantified the metabolites simultaneously using LCMS (155). The LCMS method was validated according to European Medicines Agency (EMA) and U.S. Food and Drug Administration (FDA) guidelines. To assess the applicability of assay, six different concentrations of each substrate were used (0, 5, 10, 15, 20 and 25  $\mu$ M) and the Michaelis-Menten kinetics ( $K_m$ ) were observed. As a result,  $K_m$  values were within the range for all the substrate concentrations (155). Similarly, Otten *et al.* developed a high throughput CYP450 cocktail inhibition assay using LCMS as a quantitative method. Seven specific substrates for CYP isoforms were used as cocktail (7-in-1): Phenacetin (CYP1A2), midazolam (CYP3A4/5), bupropion (CYP2B6), tolbutamide (CYP2C9), amodiaquine (CYP2C8), dextromethorphan (CYP2D6), and S-mephenytoin (CYP2C19). Moreover, the cocktail assay conditions were validated against the classic assay (single probe substrate method). Based on the result, there was a good correlation ( $r^2$  value) between the cocktail assay and single probe assay with  $r^2$  values of 0.83, 0.99, 0.78, 0.80, 0.93, 0.82, and 0.85 observed for CYP 1A2, 3A4/5, 2B6, 2C9, 2C8, 2D6, and 2C19, respectively (156)

Similarly, another study established a method for simultaneous quantification of a cocktail containing seven substrate-derived metabolites for evaluating the *in vitro* inhibition of CYP450 enzymes (157). The metabolites used were 1'-hydroxy-midazolam (CYP3A4/5), dextrophan (CYP2D6), 4'-hydroxy-mephenytoin (CYP2C19), 4'-hydroxy-diclofenac (CYP2C9), n-desethyl-amodiaquine (CYP2C8), hydroxy-bupropion (CYP2B6), and acetaminophen (CYP1A2). The calculated  $IC_{50}$  values for cocktail was greatly correlated with those on single probe assay ( $r^2 > 0.99$ ). For instance, the CYP1A2 enzyme activity was found to be  $157.6 \pm 3$  pmol/min/mg as single substrate and  $162 \pm 3$  pmol/min/mg as cocktail (157).

Wang *et al.* developed an efficient method for the simultaneous evaluation of six major CYP enzymes' inhibition using a cocktail approach. The inhibitors used for CYP3A4, 2D6, 2C19, 2C9, 2C8, and 1A2 were ketoconazole, quinidine, nootkatone,

sulfaphenazole, quercetin, and  $\alpha$ -naphthoflavone, respectively. The results obtained from this study corresponds to other studies in the literature: the cocktail half-maximal inhibitory concentration  $IC_{50}$  values of inhibitors were found to be like a single probe assay (158). The use of a cocktail approach in *in vitro* metabolic studies has successfully shortened the evaluation time for the assay and provides quick and reliable data with minimum use of reagents.

Furthermore, the cocktail approach has also been used *in vivo*. Shinya and co-worker analysed multiple CYP450 isoform activities by using specific CYP substrates in rats. The effect of inducers and inhibitors was also studied. The plasma concentrations of various drugs and their metabolites were quantified by LCMS. Fluconazole and fluvoxamine increased the area under the curve (AUC) and maximum plasma concentration ( $C_{max}$ ) of caffeine, and the AUC of midazolam and omeprazole. On the other hand, dexamethasone increased the AUC and  $C_{max}$  of losartan, and reduced the  $C_{max}$  of midazolam (159).

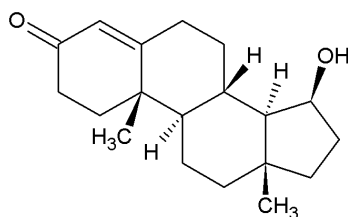
The 7-in-1 drug cocktail has recently been studied to determine the activity of seven major CYP enzymes *in vivo*. The urine and plasma samples were collected and analysed by highly sensitive LCMS over an 8 h period. All the results were in correlation with previously reported studies and the method met all the requirements of sensitivity, specificity, precision, accuracy, sensitivity, and stability (160).

### 3.1.3 Probe substrates

#### a) Testosterone

Testosterone is a C19 steroid used for its androgenic and anabolic effects with a ketone group in position 3, a double bond in position 4, and hydroxy group in position 17. Testosterone is classified as class II drug by Biopharmaceutic drug disposition classification system (BDDCS) with poor solubility, high permeability and extensive metabolism. The log P value of testosterone is 3.37. Its basic molecular structure consists of one cyclopentane ring, three cyclohexane rings and methyl groups at position 10 and 13 (Figure 3.3). Although evidence shows that oral administration of nano milled testosterone or testosterone in oil might deliver therapeutic level of testosterone, it is readily metabolized by CYP450 resulting in short half-life and poor bioavailability of testosterone (161). Testosterone is a probe drug predominantly

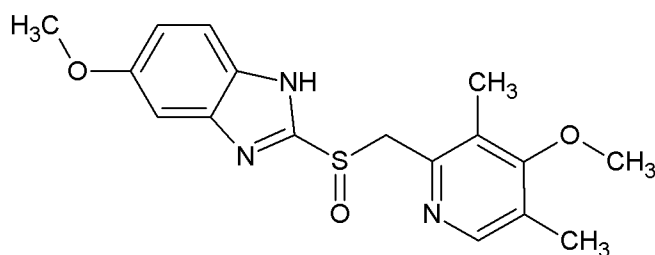
metabolised by the CYP3A4 to 6 $\beta$  hydroxy testosterone and therefore, is often a choice of drug used to study CYP3A4 activity.



**Figure 3.3** Chemical structure of testosterone.

#### b) Omeprazole

Omeprazole is a proton pump inhibitor, chemical name 6-methoxy-2-((4-methoxy-3,5-dimethylpyridin-2-yl) methylsulfinyl)-1 H-benzo[d]imidazole (Figure 3.4), used for diseases like peptic ulcer, dyspepsia, laryngopharyngeal reflux, gastroesophageal reflux, and Zollinger-Ellison syndrome (162). The BDDCS classifies omeprazole as a class II medication because of its poor solubility, high permeability, and extensive metabolism. Omeprazole is mainly metabolised by CYP2C19 to 5-hydroxyomeprazole and therefore, has been used as a probe substrate to assess CYP2C19 activity. Omeprazole is also substrate to CYP3A4 and is metabolised to omeprazole sulphone (163).

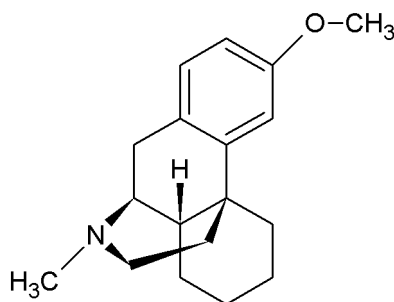


**Figure 3.4** Chemical structure of omeprazole.

#### c) Dextromethorphan

Dextromethorphan is an over-the-counter medication (Figure 3.5) used as cough suppressant. But the mechanism of action to suppress cough is not well recognised. Due to its poor solubility, high permeability, and extensive metabolism, dextromethorphan is categorised as a class II drug by the BDDCS. The rapid first pass metabolism and elimination of dextromethorphan after oral administration

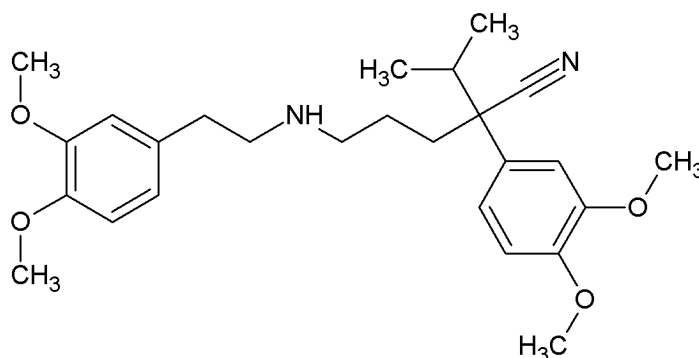
causes lack of therapeutic response and poor bioavailability (164). In liver, dextromethorphan is primarily metabolised through N-demethylation and O-demethylation. The O-demethylation of dextromethorphan to dextrorphan is mediated by CYP2D6 and N-demethylation to 3-methoxymorphinan is mediated by CYP3A4. Dextromethorphan is commonly used as a probe substrate to study the activity of CYP2D6 enzyme (165).



**Figure 3.5** Chemical structure of dextromethorphan.

#### d) Verapamil

Verapamil is a cardiovascular drug which is classified as class I drug by BDDCS (high solubility and permeability with extensive metabolism). Verapamil is extensively metabolised by various CYP enzymes: 3A4, 3A5 and 2C8. The chemical structure of verapamil is illustrated in Fig. 3.6. Verapamil undergoes N-dealkylation and N-demethylation, mediated mainly by CYP3A4, to produce its major metabolites D-617 and norverapamil, respectively (166).



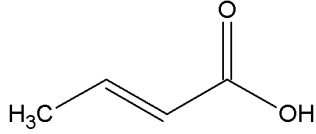
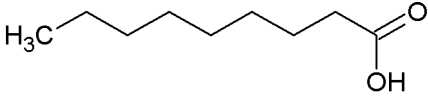
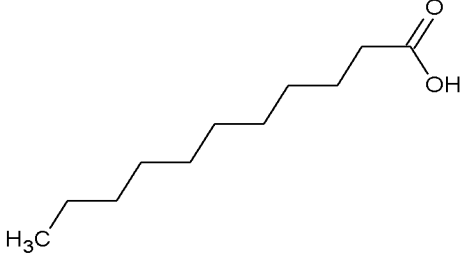
**Figure 3.6** Chemical structure of verapamil.

#### 3.1.4 Fatty acids as pharmaceutical excipients

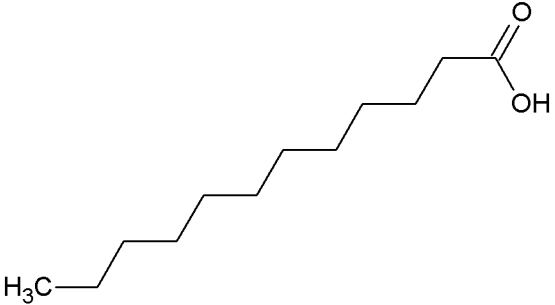
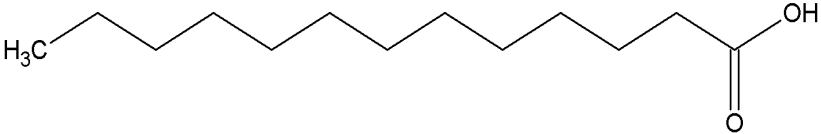
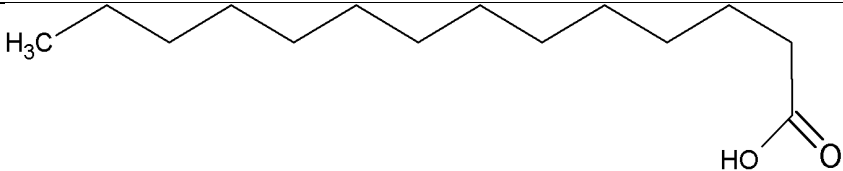
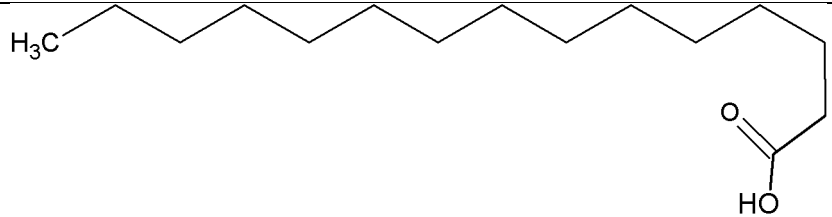
Fatty acids are monocarboxylic acid derived from saturated or unsaturated aliphatic hydrocarbons. The fatty acids can be short chain (C4-C6), medium chain (C6-C12), long chain (C14-C20), unsaturated or branched. Because of this diverse chemical nature, there are a wide range of lipids or lipid-like excipients commercially available which are called “lipids” in pharmaceuticals (167). The primary application of fatty acids in the pharmaceutical field are as solubilizing agents for poorly water-soluble drugs while the semi-synthetic PEG fatty acid esters are used as solubilizers as well as surfactants and emulsifiers (167). It has been proven that fatty acids can inhibit UGT and CYP enzymes when tested with liver microsomes. The polyunsaturated fatty acids such as linolenic acid, linoleic acid, eicosapentaenoic acid, docosahexaenoic acid, and arachidonic acid are known inhibitors for CYP 2C9 and 2C19 (168). Arachidonic acid and linoleic acid are also potent inhibitors of recombinant UGT 1A9 and 2B7 (169). The majority of the studies are focusing on the effect of unsaturated fatty acids on different CYP enzymes; however, this study mainly focused on the inhibition potential of saturated fatty acids.

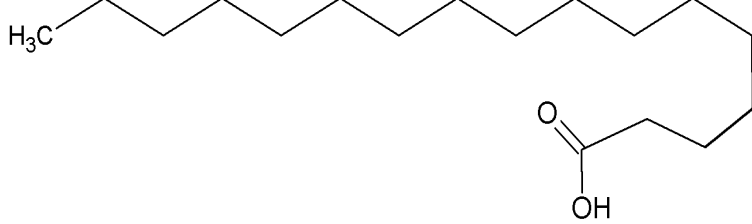
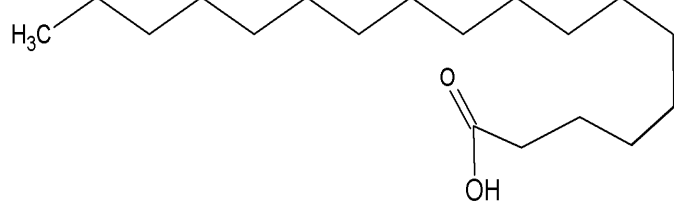
The purpose of the present study was to evaluate the effect of nine fatty acids (Table 3.1) on the activity of five major CYP enzymes in rat liver microsomes, using LCMS.

**Table 3.1** List of fatty acids and their structures

<b>Fatty acids</b>	<b>Saturated/unsaturated</b>	<b>Lipid numbers</b>	<b>Structure</b>
Crotonic acid	Unsaturated	C4:1	 <chem>CC=CC(=O)O</chem>
Nonanoic acid	Saturated	C9:0	 <chem>CCCCCCCCC(=O)O</chem>
Undecanoic acid	Saturated	C11:0	 <chem>CCCCCCCCCCC(=O)O</chem>



Lauric acid	Saturated	C12:0	
Tridecanoic acid	Saturated	C13:0	
Myristic acid	Saturated	C14:0	
Pentadecanoic acid	Saturated	C15:0	

Heptadecanoic acid	Saturated	C17:0	 <p>The diagram shows the skeletal structure of heptadecanoic acid. It consists of a long, zigzag hydrocarbon chain representing 17 carbon atoms. The left end of the chain is labeled with H<sub>3</sub>C. The right end of the chain is connected to a carboxyl group, which is drawn as a carbon atom double-bonded to an oxygen atom (O) and single-bonded to a hydroxyl group (OH).</p>
Stearic acid	Saturated	C18:0	 <p>The diagram shows the skeletal structure of stearic acid. It consists of a long, zigzag hydrocarbon chain representing 18 carbon atoms. The left end of the chain is labeled with H<sub>3</sub>C. The right end of the chain is connected to a carboxyl group, which is drawn as a carbon atom double-bonded to an oxygen atom (O) and single-bonded to a hydroxyl group (OH).</p>

### 3.2 Results and discussion

The 4-probe substrates to study various CYP450 isoforms were chosen based on previously reported studies, USFDA recommendations, and sensitivity for analytical detection (170) (171) (172) (173) .

#### 3.2.1 LCMS/MS conditions

The compounds and IS were optimised using a Thermo mass spectrometer with ESI source. ESI is the most used technique in the drug discovery field due to its suitability with the physicochemical properties of the drugs. The ions from solution are discharged into the gas phase in absence of heat and  $[M+H]^+/[M-H]^-$  ions are produced from labile compounds with zero thermal degradation (174). Different compound and source parameters were optimised by infusing pure solutions using an infusion pump. All the compounds were stable with good intensity when ionised in positive polarity mode. The compound and source dependent parameters were optimised to obtain reproducible results (Table 3.2) (See Appendix A and B).

**Table 3. 2 MS optimised parameters for individual analyte.**

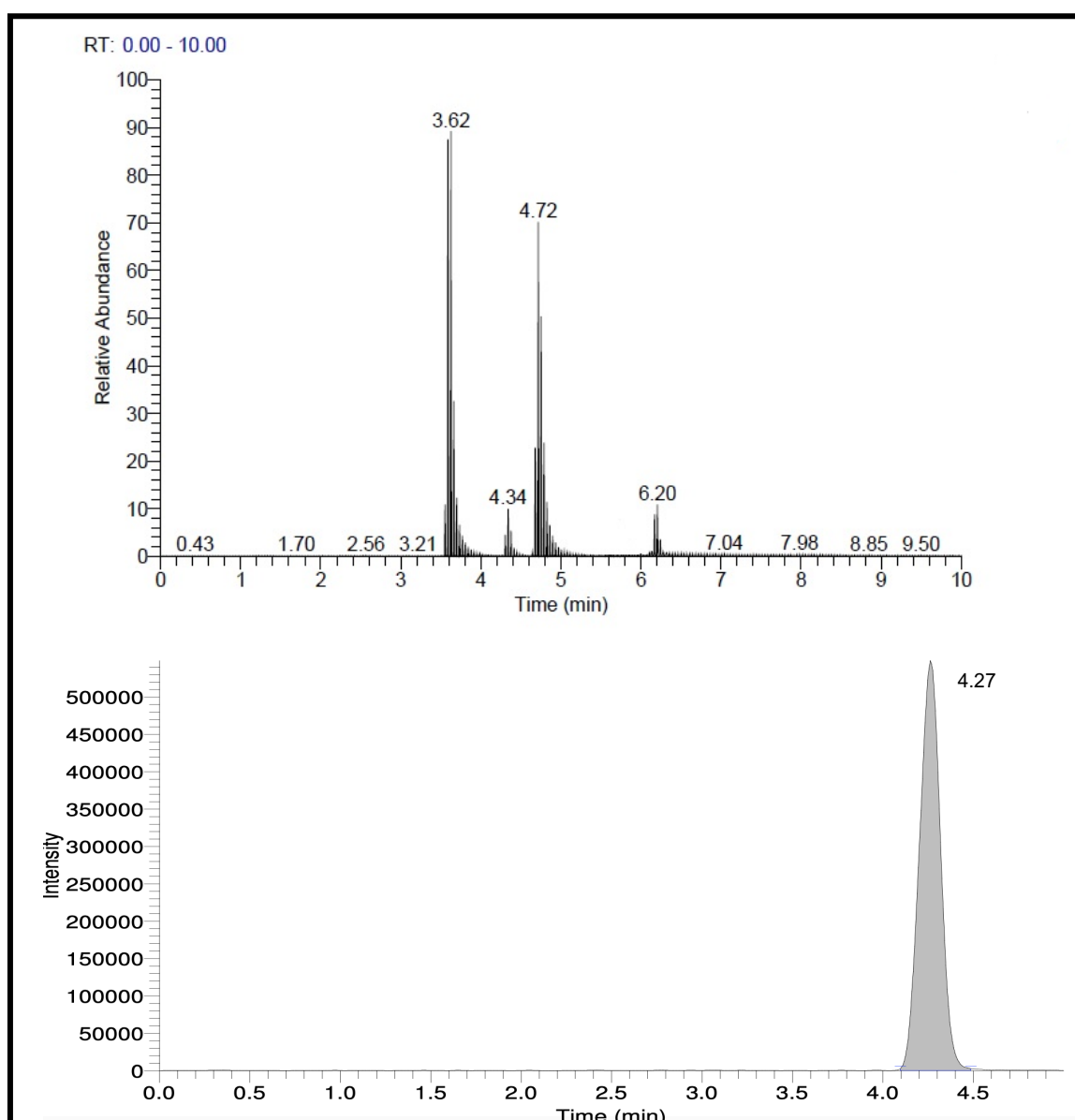
<b>ANALYTE</b>	<b>PRECURSOR ION (M/Z) M+1</b>	<b>PRODUCT ION (M/Z)</b>	<b>COLLISION ENERGY (V)</b>
<b>OMEPRAZOLE</b>	346.00	136.10, 180.04	32, 27
<b>DEXTROMETHORPHAN</b>	272.09	147.08, 171.04	29, 38
<b>VERAPAMIL</b>	455.20	149.97, 165.04	33, 27
<b>PROPRANOLOL (IS)</b>	260.08	116.16, 155.10	19, 26
<b>TESTOSTERONE</b>	289.00	97.15, 109.12	26, 24

Following the optimisation of compound and source dependant parameters, different LC conditions such as flow rate, mobile phase composition, and selection of column were optimised to achieve maximum overall sensitivity and specificity with minimum run time. Like the recent study by Li *et al.* 2021, where ACN and methanol with various proportion of formic acid (0.02%, 0.1% and 0.2%) were tested, ACN resulted in lower column pressure and narrow peak shapes than methanol. Moreover, 0.1% formic acid improved the peak shape and increased the MS response. Adding more than 0.1% formic acid had no obvious effect (175) (176). In this study, gradient elution with increasing ACN with 0.1% formic acid (mobile phase B) always had a better separation of the cocktail analytes. Likewise, isocratic

method (which eliminates the requirement for column equilibration periods) for testosterone with 80% of ACN delivered intense narrow peak with minimal run time. Appropriate peak symmetry and sensitivity were acquired by adding 0.1% formic acid in both mobile phases (177).

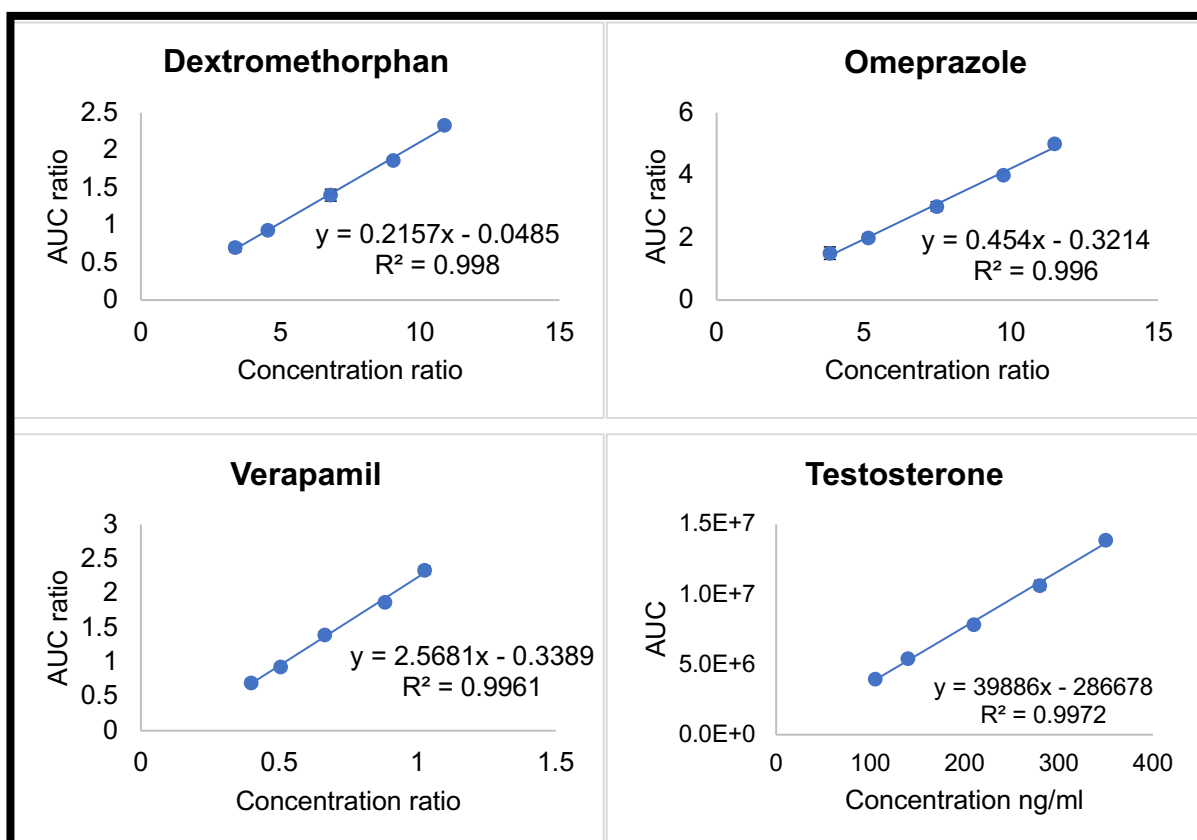
### 3.2.2 Validation of LCMS method

Figure 3.7 represents the multiple reaction monitoring (MRM) chromatogram of all the analytes with internal standard dissolved in water (70%) and acetonitrile (30%). The retention times for omeprazole, propranolol, dextromethorphan, and verapamil were approximately 3.62, 4.34, 4.72, 6.20 min, respectively. The retention time for testosterone was 4.27 min.



**Figure 3.7** MRM chromatogram for probe substrates and internal standard: omeprazole (3.62 min), propranolol (4.34 min), dextromethorphan (4.72 min), verapamil (6.20 min), and testosterone (4.27 min).

The method was validated for its linearity, accuracy, precision, LOQ and LOD for each analyte. A calibration curve was drawn using at least five different concentrations (n=3) (Figure 3.8), whereas three different concentrations were used to prepare the quality control samples. As summarised in Table 3.3, the method provided high sensitivity and linearity for each analyte, and the accuracy and precision were within the recommended limits  $\pm 20\%$ . Additionally, the effectiveness of the LCMS was confirmed by performing three-day validations. The percentage recovery for omeprazole, dextromethorphan, verapamil, and testosterone was found to be within range for all analytes at different concentration (Table 3.3). The precision of the optimised method presented  $<10\%$  variation coefficient at different concentrations. The LOD value for omeprazole, dextromethorphan, verapamil, testosterone was 61.80, 19.82, 27.88, 23.50 ng/ml, whereas the LOQ value was found to be 187.27, 60.0, 84.5, and 71.20 ng/mL, respectively.



**Figure 3. 8** Calibration curve for individual analytes (n=3). The axis represents ratios of analyte to IS concentration and analyte to IS AUC for dextromethorphan, omeprazole, verapamil, and concentration to AUC for testosterone. The concentration range for each substrate are as followed: 225-750 ng/mL for omeprazole and 105-350 ng/mL for verapamil, dextromethorphan, and testosterone.

**Table 3. 3** Shows the validation results for individual analytes.

Analyte	Linearity (R <sup>2</sup> value)	Concentration (ng/mL)	Accuracy (%)	Precision (%)	LOQ (ng/mL)	LOD (ng/mL)
Dextromethorphan	0.998	157.50	102.87 ±1.57	3.05 ±2.99	60.07	19.82
		227.50	101.66 ±0.51	2.95 ±2.88		
		297.50	103.49 ±2.00	3.08 ±3.01		
Omeprazole	0.996	337.50	108.00 ±2.07	1.36 ±1.23	187.27	61.80
		487.50	101.00±1.61	1.25 ±1.22		
		637.50	108.00±1.39	1.34 ±1.25		
Verapamil	0.996	157.50	106.12 ±2.38	1.03 ± 1.12	84.51	27.88
		227.50	101.96 ±3.48	1.11 ±1.32		
		297.50	107.05 ±1.86	1.08 ±1.44		
Testosterone	0.997	157.50	101.21 ±2.53	1.25 ± 1.13	71.20	23.50
		227.50	102.45 ±1.55	1.55 ±1.20		
		297.50	101.66 ±2.10	1.45 ±1.32		

### 3.2.3 Optimisation of microsomal assay

The activities of CYP enzyme can be evaluated via two techniques: the individual probe substrate technique or the cocktail probe substrate technique. Due to the rising number of new chemical entities, rapid methods for CYP activity assessment are highly desirable. In fact, it is strongly recommended that CYP activity screening should be completed as early as possible to continue projects more efficiently. Cocktail approach allows simultaneous determination of several CYP isoforms activities with high efficiency, consequently saving significant number of resources and time (178). *In vitro* drug metabolism investigations, which are inexpensive and simple to perform, provide an adequate screening tool for characterising drug metabolites, elucidating their routes, and making recommendations for additional *in vivo* testing. A subcellular fraction of tissue called microsomes is obtained using differential high-speed centrifugation. The microsomal fraction contains all CYP enzymes. The primary co-factor required for CYP-mediated processes is a redox-sustaining system like NADPH, and these needs are well understood. Furthermore, CYP kinetic measurements are not confounded with other metabolic processes or cellular uptakes, making microsomes and recombinant CYPs the preferable testing platforms over hepatocytes (179).

However, it has been demonstrated that the activity of the commercial microsomes varied considerably between batches and vendors. For example, the rat liver microsomes from two vendors demonstrated excellent activity in the metabolization of the drugs buspirone and loperamide, whereas those from the third vendor showed no activity at all. Additionally, three different batches of rat liver microsomes from the same vendor produced varying levels of activity in the metabolization of buspirone and loperamide. The variations in microsomal activity may result from natural animal-to-animal variance and variations in the methods used by the suppliers to prepare their products (179).

The non-specific substrates were chosen for cocktail approach to study different CYP isoforms whereas, CYP3A4-specific substrate testosterone was chosen for individual probe substrate technique. All the substrates were based on a recommended list by the US FDA guidance for preferable/acceptable *in vitro* probe substrates (180). These probe drugs omeprazole, dextromethorphan, verapamil,

and testosterone (Figure 3.9) are substrate to various CYP isoforms (3A4, 3A5, 2D6, 2C19, and 2C8). The CYP2 family, which includes 2D6 and 2C19, together metabolise more than 50% of prescribed drugs, whereas the CYP3A4/5 metabolise more than 120 prescribed drugs (181). Thus, the study focused mainly on these CYP isoforms.

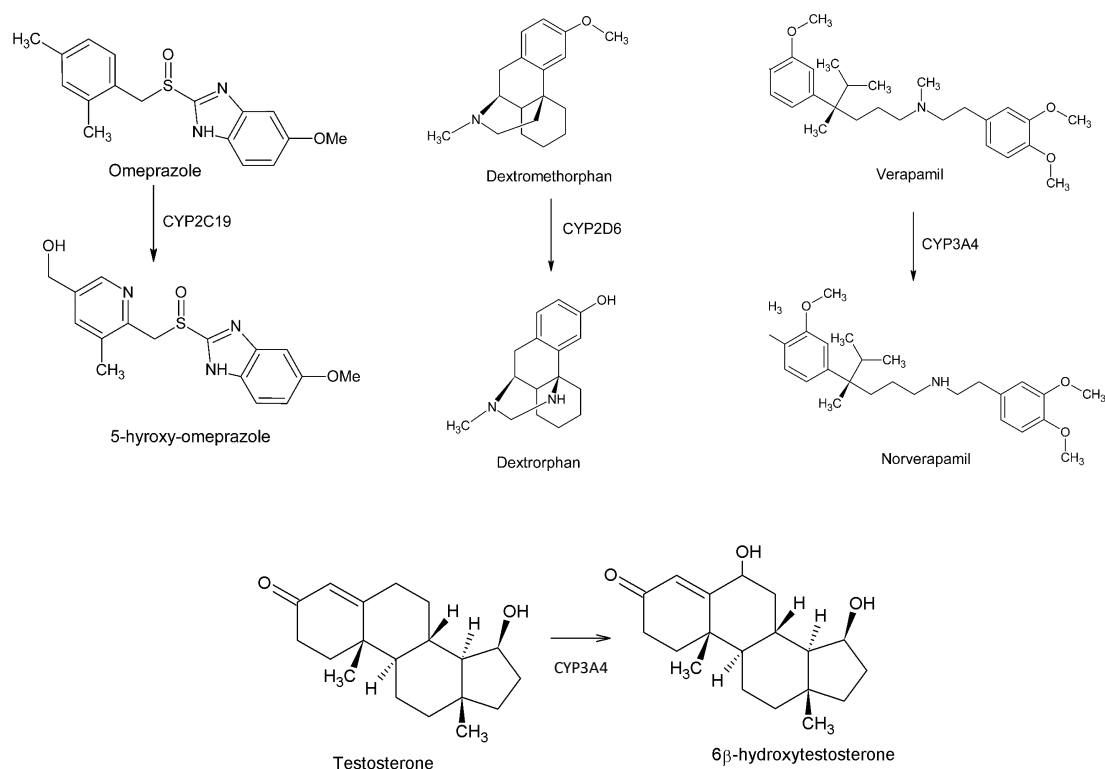
The incubation concentration for substrates was chosen based on the Michaelis-Menten constant ( $K_m$ ) values reported in the literatures (130) (131).  $K_m$  value is the substrate concentration at which the substrate has taken up half of the enzyme's active sites. The reported values for probe substrates were as followed: 18  $\mu\text{M}$  for omeprazole, 0.4-8.5  $\mu\text{M}$  for dextromethorphan, 4.24-52.8  $\mu\text{M}$  for verapamil, and 36-94  $\mu\text{M}$  for testosterone. To maintain high selectivity and activate specific CYP pathways, the concentration of substrates was kept at or below the  $K_m$  values (130).

Besides the choice of probe substrate, various factors such as the incubation conditions, choice of organic solvents, buffer solutions, and concentration of liver microsomes were also considered for method optimisation.

The organic solvents chosen for this study were based on the solubility of probe substrates. The microsomal assay can tolerate a very small quantity of organic solvents for instance, ACN  $\leq 1\%$ , dimethyl sulfoxide (DMSO)  $\leq 0.2\%$ . Exceeding these limits can result in inhibition of CYP450 activity (182) (183) (184). Hence, the probe substrates were dissolved in ACN ( $\leq 1\%$ ) and water. The combination of ACN and water (30:70) provided good solubility with minimal use of organic solvent.

Another important element to consider in microsomal assays is protein concentration. The minimal use of protein concentration (0.25-1 mg/mL) will avoid non-linear kinetics and/or non-specific binding that produces artefacts (185). In this experiment, two microsomal assay containing different protein concentrations (0.2 and 0.5mg/mL) were also studied. The higher probe substrate conversion rate was achieved with 0.5mg/mL when compared to 0.2mg/mL (186).





**Figure 3.9** The metabolism of various probe drugs by CYP450 enzymes and their main metabolites.

The results were compared with the metabolic assay containing no NADPH (negative control). The depletion of each probe substrate was found to be more than 50% after a 30-min incubation (Figure 3.10). The intrinsic clearance ( $CL_{int}$ ) was found to be higher for dextromethorphan ( $CL_{int} = 31.40 \mu\text{L}/\text{min}/\text{mg}$ ) and verapamil ( $CL_{int} = 28.10 \mu\text{L}/\text{min}/\text{mg}$ ), compared to omeprazole ( $CL_{int} = 15.20 \mu\text{L}/\text{min}/\text{mg}$ ). This signifies that omeprazole was cleared more slowly than dextromethorphan and verapamil (Table 3.4). Abelo *et al.*, 2000 studied the metabolism of omeprazole by CYP2C19 where the  $CL_{int}$  for S-omeprazole was found to be  $14.6 \mu\text{L}/\text{min}/\text{mg}$  (187). The metabolism of the S-omeprazole is mostly mediated by CYP2C19, as shown by studies by means of cDNA-expressed enzymes. The  $CL_{int}$  value for omeprazole was in high correlation with the study reported by Abelo *et al.*, 2000 (187). *In vivo*, omeprazole metabolism to hydroxyomeprazole co-segregates with S-mephenytoin 4-hydroxylation, clearly indicating a role for CYP2C19 in the metabolism (163). Birkett and co-workers studied the major metabolic pathways for omeprazole *in vitro* where, microsomal assay with metabolites was performed using human liver microsomes. Data confirmed that hydroxyomeprazole formation was compromised in CYP2C19-deficient individuals which is quantitatively the major metabolic route

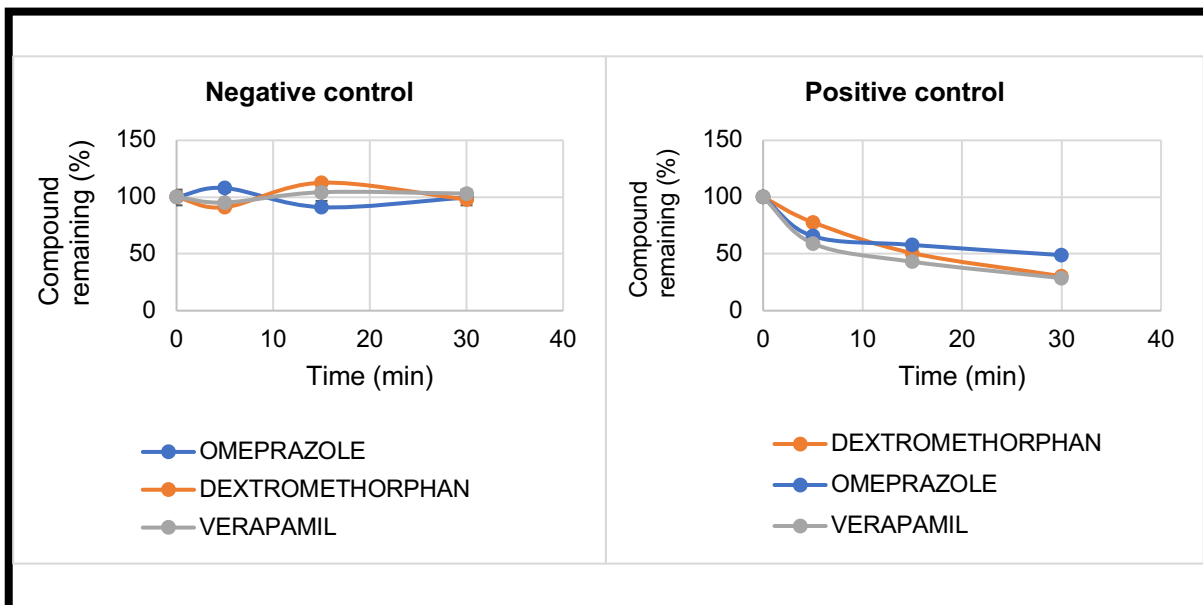
for omeprazole (163). Accumulation of all the data suggests that CYP2C19 is primarily responsible for the CL<sub>int</sub> of omeprazole.

**Table 3.4** Calculated intrinsic clearance, half-life and % depletion of each substrate.

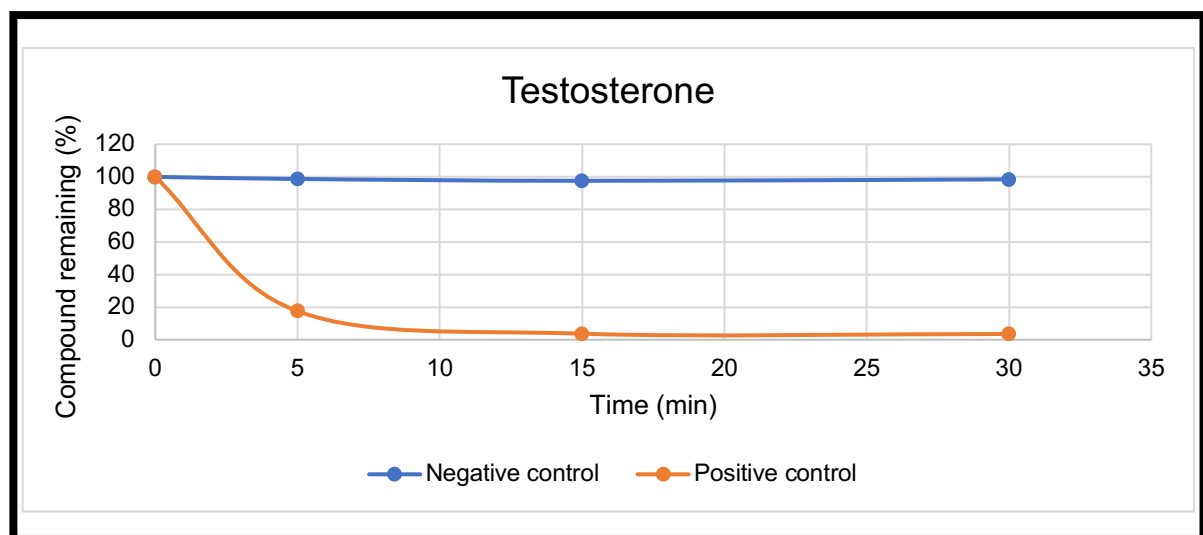
	<b>K<sub>m</sub></b> <b>(μM)</b>	<b>Cl<sub>int</sub></b> <b>(μL/min/mg)</b>	<b>T1/2</b> <b>(min)</b>	<b>Compound</b> <b>remaining</b> <b>(%)</b>	<b>R<sup>2</sup></b> <b>value</b>
<b>Omeprazole</b>	7.5	15.20	45.59	48.93	0.78
<b>Dextromethorphan</b>	5	31.40	22.07	30.36	0.99
<b>Verapamil</b>	2.3	28.10	28.63	28.63	0.92
<b>Testosterone</b>	3	145.55	4.76	3.55	0.62

Additionally, the CL<sub>int</sub> determined for dextromethorphan and verapamil agreed with a previously reported study where the metabolism of dextromethorphan and verapamil was found to be rapid and extensive with higher CL<sub>int</sub> value, in-vitro. Axelsson *et al.* determined the intrinsic clearance of various compounds using rat liver microsomes and slices of rat liver affected by cryopreservation procedure and compared the CL<sub>int</sub> between these two systems. According to data, CL<sub>int</sub> values for dextromethorphan (21±2.1 μL/min/mg) was similar to our outcome whereas, freshly prepared rat liver microsomes showed poor CL<sub>int</sub> for dextromethorphan (10.2 ±1.1 μL/min/mg) and verapamil (7.6 ±3.2 1 μL/min/mg) (188). The CL<sub>int</sub> values differ from species to species. For instance, Abelo *et al.*, 2000 study demonstrated that the CL<sub>int</sub> value for dextromethorphan was 10-fold higher in pig live microsomes than human liver microsomes. This is because, in pig liver microsomes, CYP2B contributes significantly to the metabolism of dextromethorphan (187).

On the other hand, testosterone data reveals highest intrinsic clearance (145.55 μL/min/mg) amongst all the substrates with shortest half-life (Figure 3.11). The substrate binding cavity of CYP3A is larger (~1,386 Å<sup>3</sup>) than other CYP isoenzymes and therefore, it is capable of metabolizing bulky substrates such as macrolide antibiotics, statins, cyclosporine, and other structurally different substrates (189). Furthermore, more than 2 substrates can occupy the active site of this enzyme, simultaneously (189). Hence, testosterone is extensively metabolised by CYP3A4 and the larger binding cavity of CYP3A4 can be responsible for higher intrinsic clearance value.



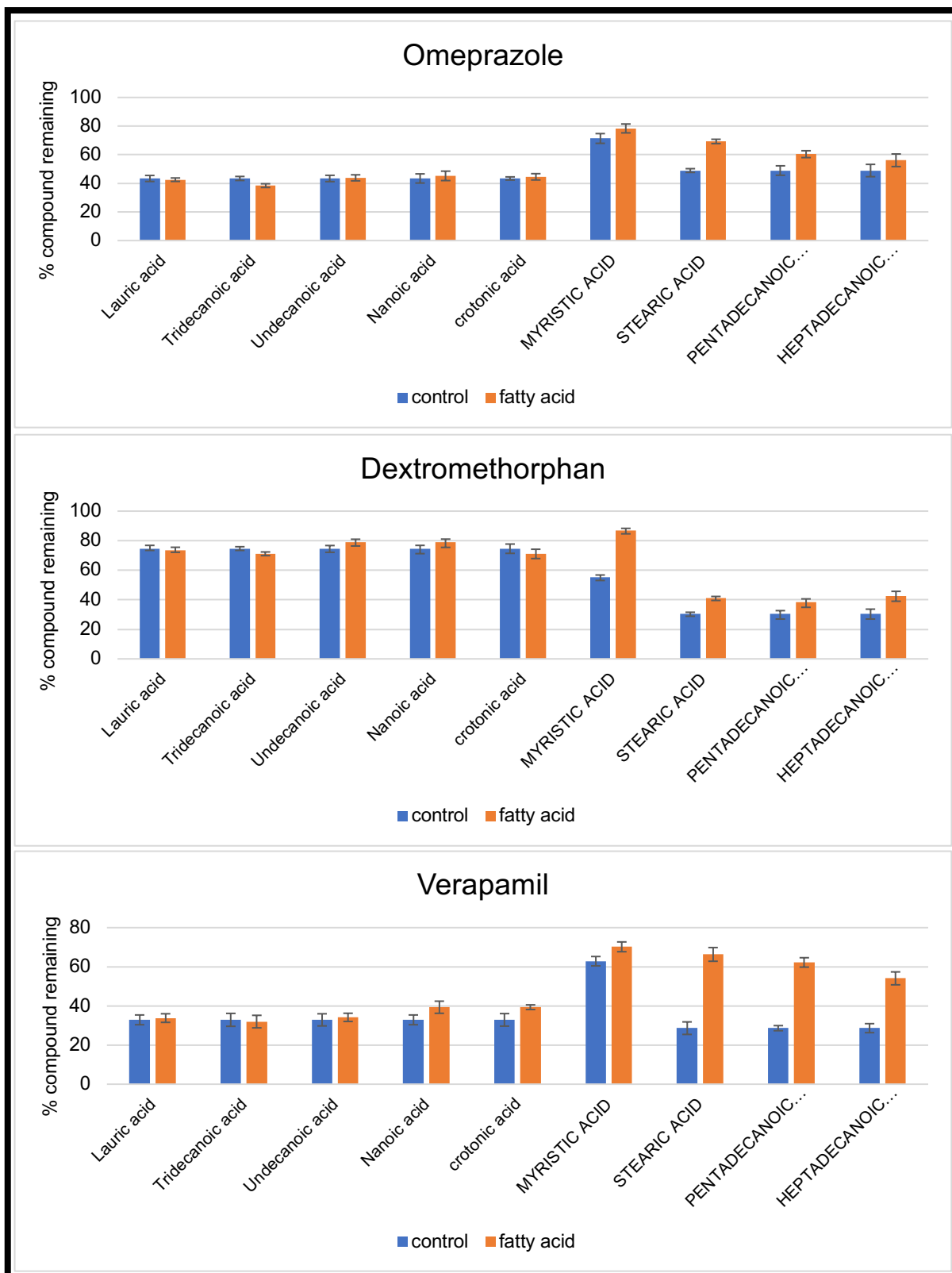
**Figure 3.10** Comparison of the microsomal assay (NADPH) to negative control (No NADPH). The data are presented as percentage compound remaining after various time intervals.



**Figure 3.11** Comparison of the microsomal assay with NADPH to negative control (No NADPH). The presence of NADPH triggered the microsomal reaction, which can be seen in the positive control with a % compound remaining after depletion.

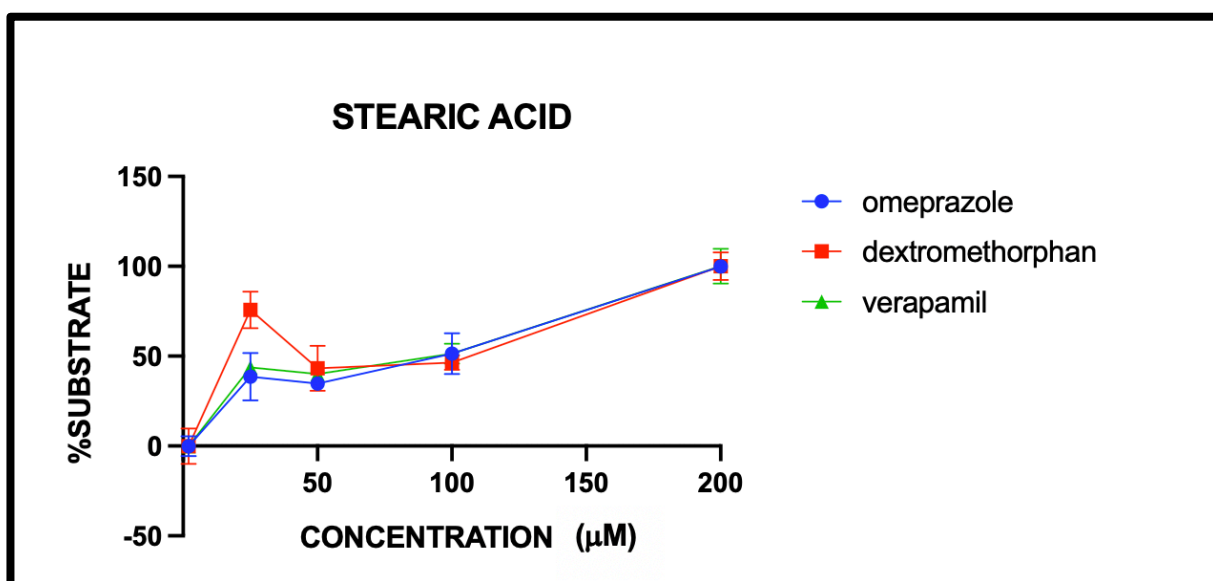
### 3.2.4 Screening of Fatty acids using the cocktail-approach

The current study demonstrated the effect of saturated and unsaturated fatty acids on CYP450 activities using cocktail probe substrates. The majority of the fatty acids, such as lauric acid, tridecanoic acid, undecanoic acid, nonanoic acid, and crotonic acid, had no effect on activities of CYP 3A4, 3A5, 2C8, 2C19, and 2D6. In the presence of myristic acid, stearic acid, pentadecanoic acid and heptadecanoic acid, the percentage of compounds recovered were found to be higher than the control (Figure 3.12). This could be attributed to the chain length, short and medium-chain carbons, crotonic acid (C4), nonanoic acid (C9), undecanoic acid (C11), lauric acid (C12), and tridecanoic acid (C13) had no inhibitory effect, whereas long-chain carbon, myristic acid (C14), pentadecanoic acid (C15), heptadecanoic acid (C17), and stearic acid (C18) showed moderate to high inhibitory effect, except heptadecanoic acid which showed stronger inhibition only with verapamil as probe drug. Overall, stearic acid showed the highest inhibition amongst all the fatty acids. Around 20% of omeprazole, 10% of dextromethorphan and 38% of verapamil was recovered in presence of stearic acid. The significant difference was observed with all three probe drugs ( $p < 0.05$ ). The mechanism of inhibition remains unclear however based on the evidence, competing with probe drugs as the common substrate or disrupting the CYP450 enzymes membrane that prevents drug from binding to the active site are possible explanations for the outcomes (190) (191). Several FAs could potentially bind to CYP450 enzymes and cause a type I spectral change, inhibiting the metabolism of many drugs that also induce type I spectral change after binding to CYP450 enzymes. According to Yao *et al.* some FAs are substrates for CYP450 enzymes. The study included the effect of several unsaturated fatty acids on the activity of CYP2C9 and 2C19 using microsomal assay. As a result, NADPH-dependant depletion in the concentration of unsaturated fatty acids were observed. Unsaturated fatty acids thus appear to inhibit CYP450 enzymes by competing with drugs as the common substrate (190).



**Figure 3. 12** The effect of various fatty acids on metabolism of probe substrates. Data are represented as compound remaining (%) with or without 100  $\mu$ M fatty acids ( $n=3$ ). The control study represents metabolic reaction in absence of 100  $\mu$ M fatty acids. The procedure used to test FAs is similar to control study where, FAs and probe substrates were incubated with rat liver microsomes under specified conditions.

According to Figure 3.13 the inhibitory effect of stearic acid was concentration dependant. Increasing the concentration of stearic acid leads to higher recovery of individual substrates. However, stearic acid presented comparatively less inhibitory effect ( $IC_{50} \geq 30 \mu M$ ) on the activities of CYP3A4, 3A5, 2C8, 2C19, and 2D6 (Table 3.5). Nearly 100% of the compounds were recovered at approximately 200  $\mu M$  of stearic acid. The higher  $IC_{50}$  value of stearic acid might reflect a poor binding affinity of stearic acid with CYP450 enzyme. Yao et. al., 2006, studied the inhibitory effect of 5 polyunsaturated fatty acids on 6 CYP450 enzymes (1A2, 3A4, 2C9, 2C19, 2D6, and 2E1). These unsaturated fatty acids showed higher binding affinity towards CYP2C9 and 2C19 with  $IC_{50}$  value lower than 10  $\mu M$  (190). The main difference between saturated and unsaturated fatty acids is the presence of double bonds. Since saturated fatty acids have no double bonds present in their structure, the binding affinity of stearic acid was found comparatively poor, leading to higher  $IC_{50}$  value.



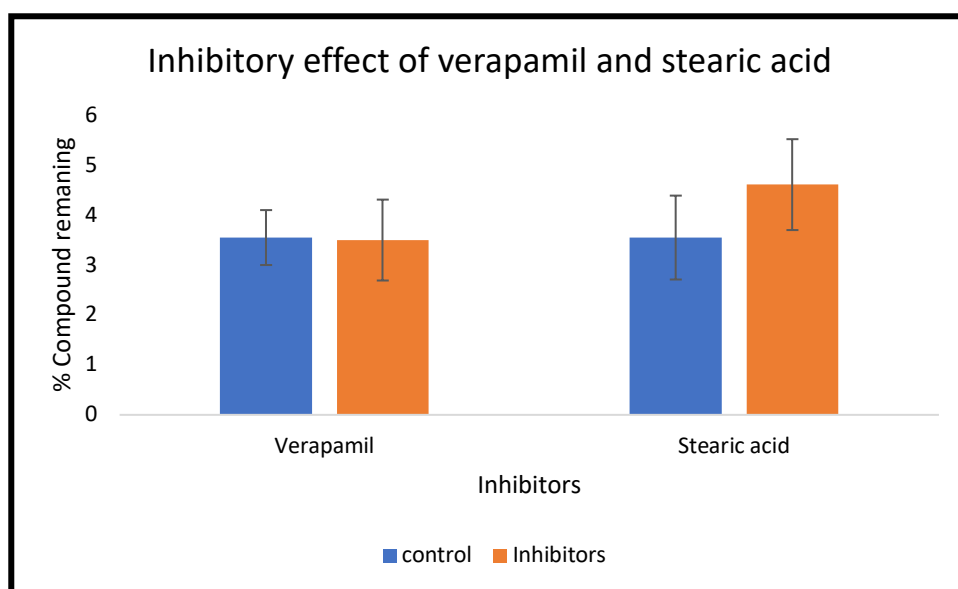
**Figure 3.13** The effect of stearic acid concentration on CYP450 inhibition: y-axis represents % substrate recovery and x-axis represents stearic acid concentration. The percentage recovery of substrates was found to be directly proportional to the concentration of stearic acid (mM).

**Table 3.5**  $IC_{50}$  values of stearic acid based on probe substrates.

Fatty acid	$IC_{50}$ ( $\mu M$ )		
	Omeprazole	Dextromethorphan	Verapamil
Stearic acid	60.94 $\pm$ 2.13	29.55 $\pm$ 3.22	52.40 $\pm$ 2.45

### 3.2.5 Effect of Stearic acid and verapamil on Testosterone metabolism

Testosterone was not included in the cocktail approach because recent studies have revealed that verapamil can act as a CYP3A4 inhibitor which can change the pharmacokinetics of any co-administered substrate of CYP3A4 (192). From our outcomes, stearic acid showed a moderate inhibitory effect against CYP isoforms and therefore, testosterone was used as a probe substrate to study the effect of verapamil as well as stearic acid on CYP3A4 activity. According to the data in Figure 3.14, verapamil as well as stearic acid showed no inhibitory effect. In presence of testosterone, <5 % compound was recovered with stearic acid ( $P > 0.05$ ) compared to the control. Therefore, it can be stated that stearic acid is a strong inhibitor for CYP 3A5, 2D6, 2C19, and 2C8 and a substrate-dependent inhibitor for CYP 3A4, as it showed strong inhibition in the presence of verapamil and no inhibition in the presence of testosterone.



**Figure 3.14** The effect of 100 $\mu$ M stearic acid and 100 $\mu$ M verapamil on metabolism of testosterone. Verapamil showed no inhibitory effect whereas, stearic acid had weak inhibitory effect.

Overall, the data merely show non-specific stearic acid CYP450 inhibition. The metabolic assay with quantification of metabolite production is recommended in order to understand the particular inhibition of CYP450 isoforms. Therefore, further investigation is required to understand specific inhibition and mechanism of inhibition at cellular level.

## **Conclusion**

A method was developed successfully to establish the activity of 3 CYP isoforms using a cocktail of 3 substrates. The outcomes from a compound depletion approach were comparable to previously reported metabolite formation approach. This robust and high-throughput cocktail method can provide rapid and reliable data compared to the single probe substrate method, in conjunction with LC-MS/MS offering reproducible results without compromising analyte resolution or sensitivity. The method is very cost effective since it only requires probe substrates, no metabolites, and a small amount of reagents. However, further investigation on inhibition studies is required for evaluating the drug-drug interactions of the 3 CYPs using this method. Stearic acid was chosen for further studies as it showed significant inhibition with the majority of CYP450 enzymes and studies have reported benefits of using stearic acid as an excipient (such as controlled release, targeted release, improved oral bioavailability, and many more) for lipid formulations.



# **Chapter 4: Testosterone- loaded Solid Lipid Nanoparticles**

## 4.1 Introduction

The human cytochrome P450 enzymes which fall under the family of CYP3A (CYP3A4, CYP3A5, and CYP3A7) are mainly responsible for the metabolism of many drugs, toxicants, and steroids, including testosterone, estradiol, cholesterol, dehydroepiandrosterone, and sulphate derivate (193). Testosterone is an androgenic/anabolic hormone (193). Testosterone, commonly used for hypogonadism treatment, is a substrate to CYP3A4 which undergoes extensive first-pass metabolism with bioavailability of ~1% after oral administration. The vascular and metabolic hormone testosterone has numerous physiological impacts on various target tissues. Testosterone is critical for maintaining body composition, bone mass, muscle mass and function. Therefore, testosterone deficiency leads to the onset of obesity and frailty (194). To improve the level of testosterone in the body with high bioavailability, there are various types of dosage forms that have been developed and clinically utilized, such as alkylated esterified testosterone for oral formulation, testosterone esters for intra-muscular and testosterone pellets for subcutaneous implant. These formulations or delivery system are uncomfortable to administer, hepatotoxic, and produce varied testosterone levels (195).

Recently, testosterone transdermal systems have become popular and marketed internationally. Clinical studies of testosterone loaded transdermal systems show good efficacy in delivering adequate replacement therapy for testosterone. However, the main drawbacks of using transdermal approach are the skin irritation, limited dosing flexibility, adhesion problems, and high manufacturing cost (195).

Historically, there have been two main approaches used to deliver oral testosterone: alkylation of testosterone at C-12 position to produce testosterone analogues that are resistant to hepatic first-pass metabolism; or esterification of testosterone using fatty acids to produce testosterone undecanoate that avoids the portal circulation by absorbing via the intestinal lymphatic system (196). Oral methyltestosterone has been linked to serious hepatotoxicity, including peliosis hepatis, hepatic adenocarcinoma, and cholestasis, and thus rarely used in the clinical management for hypogonadism. On the other hand, testosterone undecanoate showed inter- and intra-patient variability in testosterone response which was influenced by dietary fat. As a result, neither of these oral formulations has seen widespread clinical use in the treatment of testosterone deficiency (196).

To address the lack of an oral testosterone product that meets the rigours of current U.S. regulatory standards for efficacy and safety, testosterone was developed in a novel self-emulsifying drug delivery system that was initially investigated in short-term clinical trials (197). The drug delivery systems that improve bioavailability for BCS class 2 drugs (low solubility, high permeability) are lipid-based oral drug delivery systems. The application of lipid-based systems such as self-nanoemulsifying (SNEDDS)/ self-micro emulsifying (SMEDDS)/ self-emulsifying (SEDDS) drug delivery systems, nano emulsion, microemulsion, and solid lipid nanoparticles (SLNs) have been successful for improving oral bioavailability of poorly soluble drugs (198). The increase in residence time, dissolution, and lymphatic uptake of drug are main factors that increase the bioavailability of drug. SLNs are colloidal carriers (50-1000nm) discovered in the early 1990s, which are produced by dispersing hot lipid microparticles in aqueous surfactant solution or water (199) (200). SLNs are used as an alternate transport system to traditional colloidal carriers, such as liposomes, emulsions, and polymeric nano and microparticles. The main benefits of using SLNs over traditional and innovative carrier systems are controlled release, physical stability which protects the incorporated drugs from degradation, and being cost-effective (201)(202)(203). Besides oral application, SLNs are also formulated for various routes of administration such as dermal, parenteral, pulmonary, rectal, and ocular and characterised by *in vitro/in vivo* studies (204)(205)(206). SLNs consist of lipids which are solid at room/human body temperature, stabilisers (surfactants/co-surfactant system), active ingredients (usually drugs), and water (207) (208). The solid lipids commonly used for SLNs are partial glycerides (Imwitor), triglycerides (tri-stearin), fatty acids (palmitic acid, stearic acid, waxes (cetyl palmitate), and steroids (cholesterol) (209) (210). SLNs can provide higher drug entrapment efficiency with stable drug in their lipid matrix and deliver a controlled release from 24 hours to several weeks. These lipids are physiologically well endured and generally recognised as safe (GRAS) except cetyl palmitate (211) (212). SLNs formulations containing  $\leq 2.5\%$  of lipids do not demonstrate any cytotoxicity *in vitro* (210). The co-administration of drugs with lipids can also alter drug absorption pathway although majority of orally administered drugs reach systemic circulation via the portal vein, few lipophilic drugs are transported via intestinal lymphatic's which increases the oral bioavailability of drug (212). The gastrointestinal tract (GI) acts as a chemical and physiological barrier executing many challenges for oral drug

delivery systems. Therefore, all these beneficial properties of SLNs make them the preferred transport system for ineffective hydrophobic drugs.

Faghihi *et al.*, 2020 designed and prepared diazepam loaded solid lipid nanoparticles to overcome different side effects associated with repetitive administration of diazepam (213). SLNs were prepared using stearic acid (SA), cholesterol, and glycerol monostearate and the technique used was high shear homogenization coupled with sonication. Amongst various surfactants, Tween 80 (nonionic) was chosen with concentration range of 0.5-1% w/w. Diazepam concentrations were 0.12 or 0.24% w/w in various formulations. Overall, the average particle size of SLNs was 150 nm in spherical shape with 79.06% entrapment efficiency and more than 85% of drug release in 24 hours was achieved. It can be concluded from the study that diazepam loaded SLNs could be a better option for drug delivery with less side effects due to reduced administration intervals (213).

Dimethyl fumarate, fumaric acid ester, is a frequently prescribed drug for various neurological disorders because of its anti-inflammatory and cytoprotective actions of neurons (214). Despite the advancement in numerous drug delivery approaches, drug delivery to the brain is still considered as a challenge because of the blood-brain barrier (BBB). Amongst all the nanocarriers, SLNs are recognised to offer many advantages including enhanced drug stability, controlled drug release, better brain permeability, and passive targeting ability (215) (216) (217). Kumar and co-workers formulated dimethyl fumarate-loaded SLNs using stearic acid and Compritol 888 ATO as lipids for different formulations and the method used for SLNs was hot micro emulsification. Tween 80 and Phospholipid 90g were chosen as surfactants. As a result, successful SLNs were produced with an average particle size of 258 nm and an entrapment efficiency of >90% and sustained drug release was confirmed from *in vitro* release study. Moreover, the SLNs successfully demonstrated significant Caco-2 cellular uptake, enhanced brain bioavailability, and offer promising outcome for safe, scalable as well as effective nanotechnology-based product (218).

Another study showed successful preparation of candesartan cilexetil (CDC)-loaded SLN using a different method called the modified emulsification-ultrasonic technique. CDC is a prodrug that undergoes hydrolysis to form candesartan (219). Prodrugs are normally used to increase bioavailability of the drugs. Despite this,

absolute bioavailability of candesartan is poor (15% as tablets and 40% as solution). Mahajan and Kaur, 2018 prepared CDC-loaded SLN using stearic acid as lipid and poloxamer188 as a surfactant (219). The entrapment efficiency of 78.28%, average particle size of 197.9 nm, zeta potential -21.3 mV were reported. Moreover, 60.43% of the drug was released in 24h and the pharmacokinetic study in rats depicted a 3-fold increase in  $AUC_{0-t}$  of CDC-SLN compared to free drug suspension. Hence, CDC-loaded SLN successfully improved the oral bioavailability of poorly soluble candesartan cilexetil.

In 2014, Shah *et. al.* compared two different techniques, conventional vs novel microwave-based microemulsion, to produce SLNs (220). Tetracycline was chosen as a probe drug since it is one of the common antibiotics with poor water solubility. SLN formulation was made using two different techniques consisting of stearic acid (lipid), tween 20 (surfactant), water, and tetracycline. The particle sizes and polydispersity were found to be better (~200 nm, ~0.15) with microwave-produced SLNs compared to conventional technique (~450 nm, ~0.3) indicating improved stability with microwave-based method. Moreover, true stability test (visual inspection with time) revealed higher stability with microwave-based SLN, especially when refrigerated. Improved entrapment efficiency, lower crystallinity was also reported with microwave-based SLN (220).

Despite all the benefits and successful research with SLNs, a pharmaceutical product with SLN has not yet hit the market. A list of examples, but not limited to, of various drug formulations developed using SLN technology are summarised in Table 4.1 (221).

**Table 4.1** Different examples of solid lipid nanoparticles formulation (221).

<b>Drugs</b>	<b>Lipids</b>	<b>Biopharmaceutical application</b>
<i>5-Fluorouracil</i>	Dynasan 118 and dynasan 114	Sustained release in simulated colonic media
<i>Apomorphine</i>	Polyethylene glycolpalmitostearate and glycerylmonostearate	Improved bioavailability in rats
<i>Calcitonin</i>	Trimyristin	Improved efficacy of proteins
<i>Clozapine</i>	Tripalmitin, tristearin and trimyristin	Improved bioavailability
<i>Cyclosporin A</i>	Glycerylpalmitostearate and glycerylmonostearate	Controlled release
<i>Gonadotropin release hormone</i>	Monostearin	Prolonged release
<i>Ibuprofen</i>	Tripalmitin, triluarin and stearic acid	Stable formulation and low toxicity
<i>Idarubicin</i>	Emulsifying wax	Oral protein delivery
<i>Insulin</i>	Glycerylmonostearate, glycerylbehenate, glyceryltripalmitate, glycerylpalmitostearate, cetylpalmitate, octadecyl alcohol and stearic acid	Potential for oral protein delivery
<i>Lopinavir</i>	Campritol 888 ATO	Enhanced bioavailability
<i>Nimusulide</i>	Glyceryl tristearate, palmitostearate and glycerylbehanate	Sustained release
<i>Progesterone</i>	Oleic acid, stearic acid and monostearin	Improved oral drug delivery
<i>Repaglinide</i>	Tristearin and glycerylmonostearate	Reduced toxicity
<i>Tetracycline</i>	Stearic acid and glycerylmonostearate	Sustained release

The aim of this chapter was to prepare and characterize testosterone-loaded SLN as well as determine the effect of prepared SLNs on CYP3A4 activity. After oral administration, the bioavailability of testosterone is ~1% and testosterone undecanoate is 7% in human and therefore, there is a certain need for an improved oral testosterone formulation that can also provide controlled release of drug. Nanoparticle delivery systems with lipids as excipients are known to increase the bioavailability and promote the oral absorption of various drugs (222). Hence, SLNs were the choice of delivery system for this study which has many advantages over conventional formulation for testosterone (for instance, improved bioavailability, target drug delivery, controlled release, protection from degradation, and ease of scale up). The lipid excipient that will be used is stearic acid. According to the previous chapter, stearic acid was found to be a good inhibitor for CYP450 enzymes and is a commonly used lipid in SLNs formulation. Incorporating stearic acid in SLNs should reduce the drug metabolism by CYPs and increase permeability hence, enabling the oral administration of testosterone.

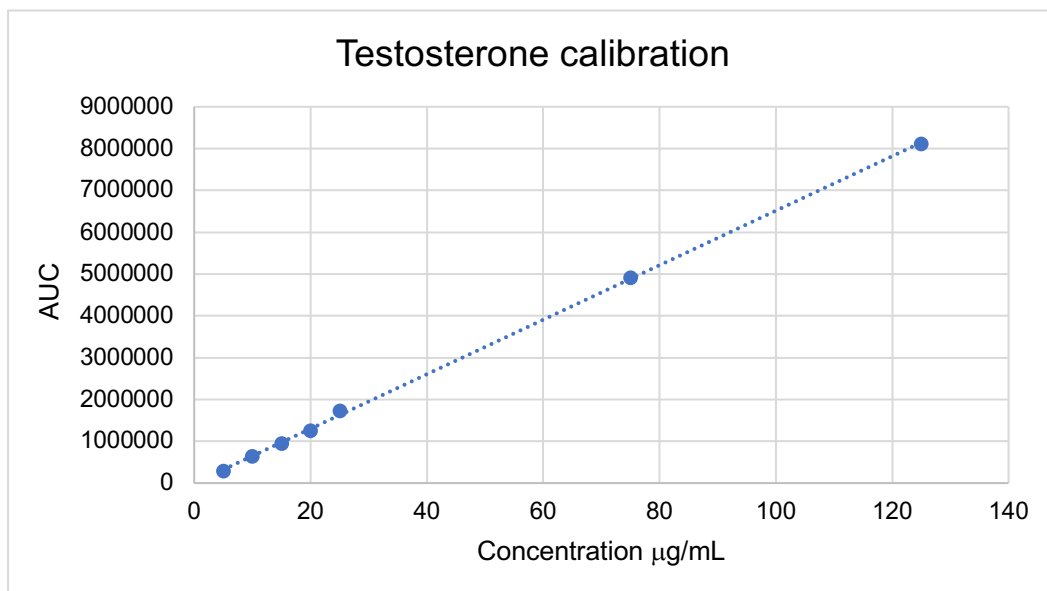
## 4.2 Results and Discussion

### 4.2.1 Saturation solubility

The traditional saturation solubility test was performed to measure the solubility of testosterone in different surfactants. Surfactants play a vital role in the preparation of microemulsion they reduce the interfacial tension between two phases (oil and water) which allows the dispersion of all the components. However, single chain surfactants alone are not sufficient to reduce interfacial tension between oil and water to produce microemulsion. Therefore, introducing co-surfactants/co-solvents allow interfacial films adequate flexibility to form different curvatures necessary to produce microemulsion (223).

The equation from calibration curve ( $y = 65128x + 4204.1$ ,  $R^2 = 0.9998$ ) was used to determine the unknown concentration of drug (Figure 4.1) and HPLC/UV method was validated using ICH guidelines (Table 4.2). The correlation between soluble concentration of testosterone (mg/mL) versus surfactants was plotted to determine the saturation point of testosterone. It was found that testosterone dissolved diversely in different surfactants. Solubility of testosterone in different surfactants is shown in Figure 4.2. As a result, testosterone had the highest solubility in brij 35 10%w/v ( $87.52 \pm 0.13$  mg/mL) and propylene glycol ( $43.60 \pm 0.16$  mg/mL) compared to transcutol, span 80, PVP, and glycerol (least soluble). Hydrophilic and lipophilic balance (HLB) values of the designated components is one of the most important characteristics while developing a microemulsion system. The behaviour of surfactants is dependent on the HLB, so surfactants with HLB values between 4-6 are preferred for water-in-oil (W/O) microemulsion whereas HLB values between 8-18 are preferred for oil-in-water (O/W) microemulsion (224). For this study, Brij 35 with HLB value of 15 was chosen as a surfactant (225). Propylene glycol was selected as a co-surfactant as it contains small polar heads with an appropriate length of alkyl chain to fill the gaps which brij 35 alone cannot achieve, thus lowering the interfacial tension and forming strong microemulsion (224). Beside this, testosterone showed the highest solubility in brij 35 and propylene glycol which makes them ideal candidate for SLN formulation.



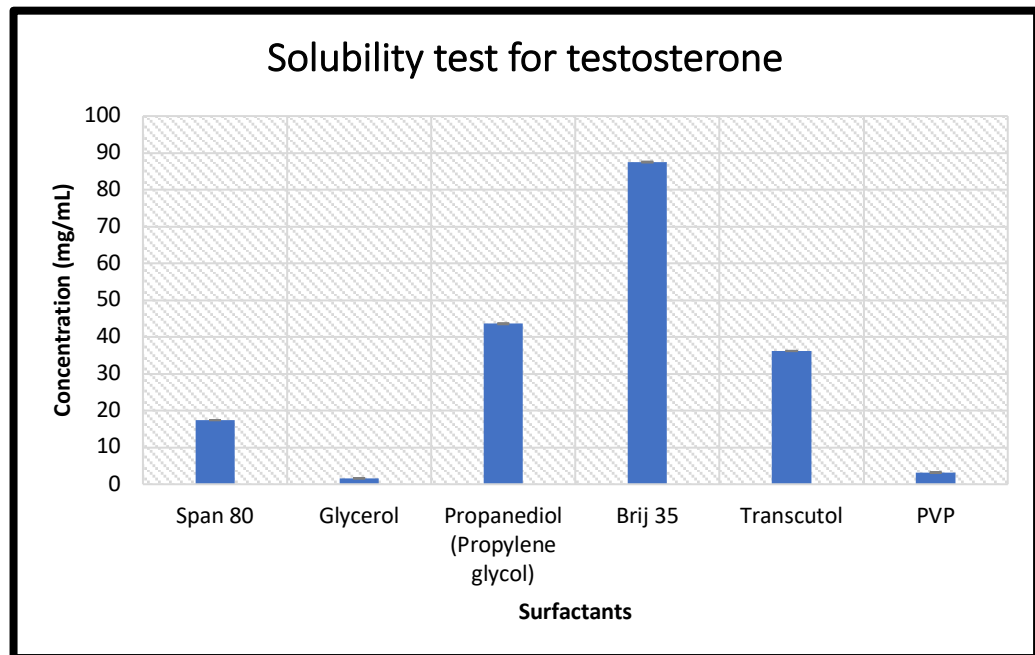


**Figure 4. 1** Calibration curve for testosterone. The data is presented as  $n=3 \pm SD$ . The axis represents testosterone concentration (x-axis) and AUC (y-axis). The concentration range for testosterone was 1-125  $\mu\text{g/mL}$

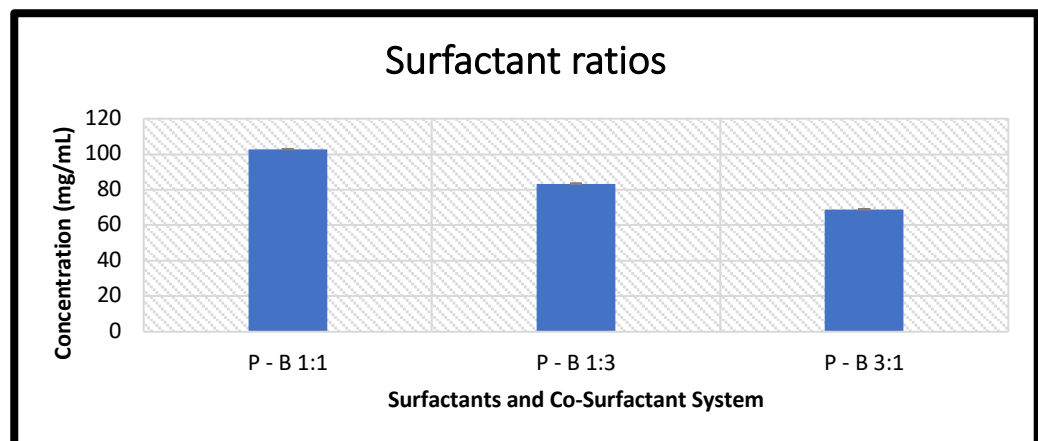
**Table 4. 2** Validation parameter for testosterone

Analyte	Linearity (R <sup>2</sup> value)	Concentration ( $\mu\text{g/mL}$ )	Accuracy (%)	Precision (%)	LOQ ( $\mu\text{g/mL}$ )	LOD ( $\mu\text{g/mL}$ )
Testosterone	0.999	8	102.10 $\pm 1.34$	1.34 $\pm 1.02$	2.23	1.50
		22	101.21 $\pm 2.11$	1.25 $\pm 1.10$		
		100	102.77 $\pm 1.27$	1.55 $\pm 1.03$		

The solubility of testosterone was further tested in different ratios of S/CoS (1:1, 1:3, and 3:1). As shown in Figure 4.3, testosterone was highly soluble in 1:1 ratio of propylene glycol/brij 35 (~100 mg/mL) compared to 1:3 and 3:1. Based on solubility studies, 1:1 ratio of brij 35 and propylene glycol were selected as the surfactant/co-surfactant system as they showed high solubility profile for testosterone compared to other surfactants and ratios.



**Figure 4.2** Saturation solubility of testosterone in different surfactants and co-surfactants (span 80, glycerol, propylene glycol, brij 35, transcutool, and PVP). The solubility test was conducted in triplicates ( $n=3$ ) and data are presented as mean concentration  $\pm$ SD.



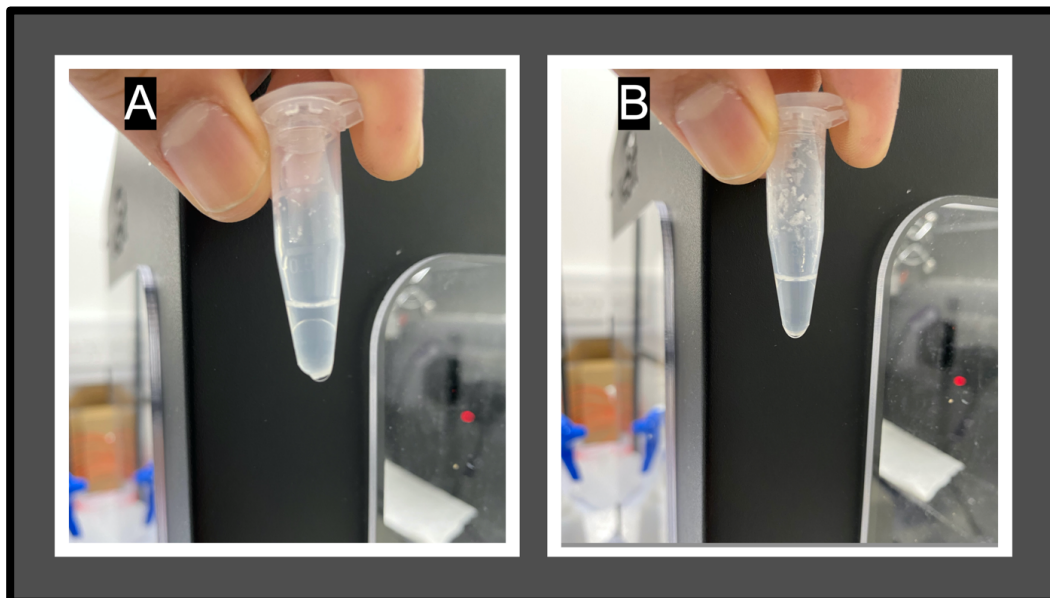
**Figure 4.3** Saturation solubility of testosterone in different ratios of brij 35 10%w/v and propylene glycol, where P=propylene glycol and B=brij 35 (10% w/v). The solubility test with S/CoS system was performed in triplicates  $n=3$  and data are shown as mean concentration  $\pm$ SD.

#### 4.2.2 Pseudo-ternary phase diagram

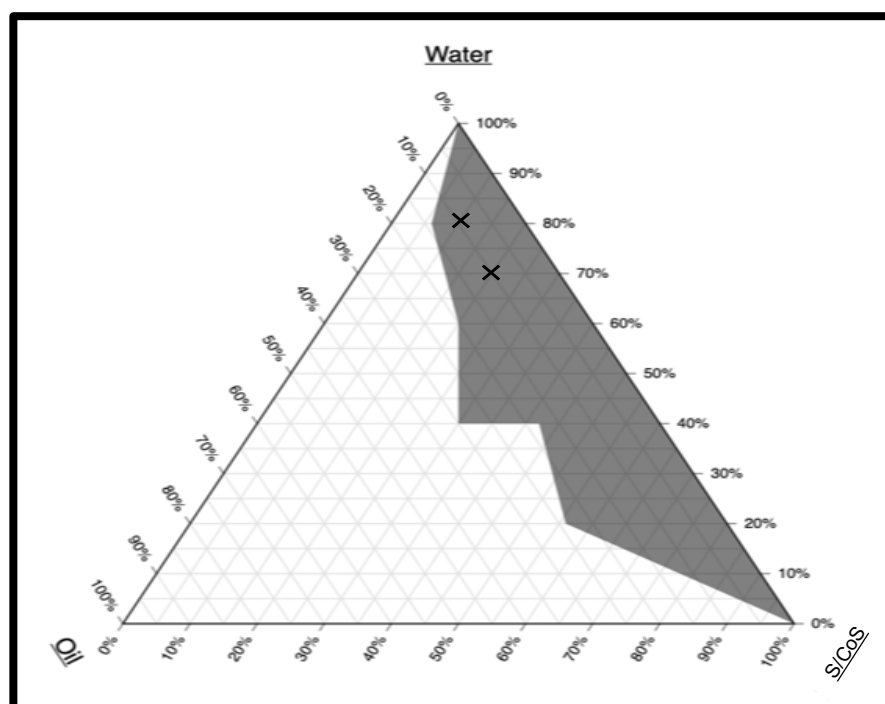
The pseudo-ternary phase diagram was constructed using hot emulsion method. Figure 4.4 shows (a) non-microemulsion and (b) microemulsion in the Eppendorf tubes. Ternary phase diagram was constructed using various ratios of stearic acid (oil), water, and S/CoS system (Figure 4.5). The droplet size and rheological properties of the microemulsion system depend mainly on the type of surfactant used. If the HLB values of surfactant, co-surfactant, and oil match, then it provides

minimal interfacial tension and better stability between the oil and water phases (226).

A highly structured microemulsion can be built with a mixture of lipophilic and hydrophilic non-ionic surfactants. Brij 35 is a dodecyl-poly-ethylene-oxide-ether with a poly-ethylene-oxide chain (hydrophilic part) and n-alkyl chain (hydrophobic part) (227). Propylene glycol has proven to increase interfacial fluidity and decrease the polarity of water (228). When different combinations of oil, water and S/CoS are mixed it produces microemulsion. The shaded area in the phase diagram represents ME region whereas, the non-shaded region represents no emulsion. The phase study revealed that a good ratio of the three phases can result in a good ME, increasing the amount of S/CoS system can reduce the interface tension, so on. ME region was formed with higher ratio of water compared to oil and S/CoS. This can be attributed to the incorporation of propylene glycol (PG). PG allows maximum incorporation of water into an oil-surfactant system leading to increase in ME region (226). Based on the outcome and visual inspection, two different ratios were chosen for SLN formulation F1 and F2: 1:1:8 and 1:2:7 (SA:S/CoS:water). These two ratios showed good ME with minimal volumes of oil and S/CoS. Moreover, increasing S/CoS concentrations reduces initial SLNs particle size until sufficient surface coverage has been achieved and increasing concentration further will not lead to smaller particle sizes (227).



**Figure 4.4** Differentiates two types of phases: A = two phase system (water and oil forms two separate layers) and B = single phase system (water and oil forms one layer in presence of optimised amount of oil/S/CoS/water system).



**Figure 4.5** Illustrates the pseudo-ternary phase diagram with different ratios of stearic acid:S/CoS:water, where shaded region represents microemulsion and non-shaded region represents no emulsion. The two crosses on diagrams indicates two distinct ratios chosen for SLNs formulation study.

#### 4.2.3 Preparation and characterization of SLN formulation

Two formulations were developed based on the ternary phase diagram. The composition of testosterone-loaded SLN is given in Table 4.3. Hot emulsion method is one of the cost-effective and easiest techniques to produce SLNs. Firstly, drug-loaded hot microemulsion is prepared at high temperature (5-10 °C above the melting point of solid lipids), followed by cooling these dispersions in ice-cold water and then performing ultra-sonication to produce SLNs. Ultra-sonication is a useful tool to break droplets based on growth, formation, and implosive collapse (229). The amount of testosterone in each formulation was kept constant and minimal to avoid its interaction and variability caused by higher concentration.

**Table 4.3** Different compositions used to prepare two different testosterone-loaded SLNs: F1 and F2.

Function	Composition	F1	F2
<b>Microemulsion</b>			
<b>Active ingredient</b>	testosterone	5 mg	5 mg
<b>Solid lipid</b>	Stearic acid	10%	10%
<b>S/CoS</b>	Brij 35 10%w/v/PG	10%	20%
<b>Water phase</b>	Water	80%	70%
<b>Solid lipid nanoparticles</b>			
<b>SLNs</b>	Microemulsion: ice water	1:50	1:50

#### 4.2.4 Size distribution and zeta potential of SLN

Particle size and PDI (size distribution) are important characteristics for the production and stability of SLNs which largely depends on the preparation technique and the particle composition (230). As shown in Table 4.4, the droplet size of both formulations falls under the acceptable range for nanoparticles where, F2 had a smaller particle size ( $278.29 \pm 33.19$  nm) compared to F1 ( $316.53 \pm 42.62$  nm). The decrease in particle size at high S/CoS concentration was due to the reduction in

interfacial tension between lipid and aqueous phases, leading to the formation of smaller size droplets of emulsion. Moreover, higher concentration of surfactants stabilizes the particles formed by steric barriers on the particle's surface, thus protecting nanoparticles from coagulation (231) (232) (233).

**Table 4.4** Shows average particle size, PDI and zeta potential for F1 and F2 formulations.

	Surfactant	Size (nm)	SD	PDI	SD	Zeta Potential (mV)	SD
<b>F1</b>	10%	316.53	±42.62	0.44	±0.03	-21.93	±0.38
<b>F2</b>	20%	278.20	±33.19	0.27	±0.03	-36.10	±0.92

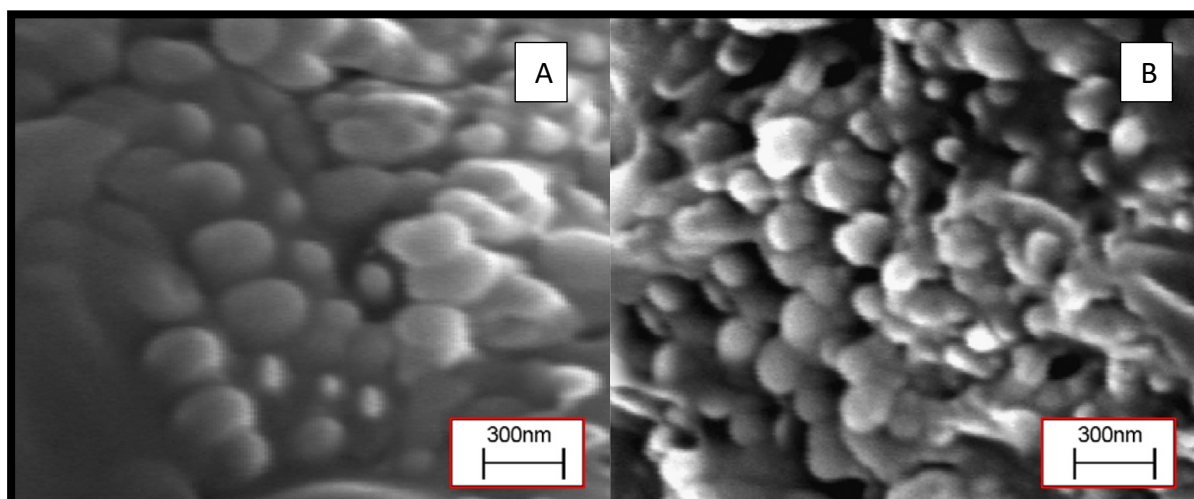
PDI indicates the width of the particle size distribution, and the PDI value shows the quality of dispersion which ranges from 0 to 1. The PDI values  $\leq 0.5$  are acceptable however, most researcher distinguish PDI values  $\leq 0.3$  as optimum and  $\leq 0.1$  as highest quality of dispersion (234). The PDI value for F2 ( $0.27 \pm 0.03$ ) was found to optimum whereas, F1 depicted PDI value under 0.5 which is acceptable.

Zeta potential, depending on the chemistry of the particles, can be either positive or negative in polarity. Zeta potential is an electric potential produced by the charge present on the particle surface. Zeta potential indicates the degree of repulsion between the charged particles in the formulation. Repulsive forces improve physical stability of the formulation by preventing aggregation of particles during storage (235).

Zeta potential for F1 and F2 were found to be  $-21.93 \pm 0.38$  mV and  $-36.10 \pm 0.92$  mV, respectively. The negative charge comes from ionization of hydrophilic carboxyl group from stearic acid (236). Dispersions with zeta potential more than  $\pm 20$  mV are stated as physically stable (220). The results in Table 4.4, thus, suggests that both SLNs produced in this study are physically stable dispersions. Moreover, higher zeta potential value in F2 formulation can be attributed to higher concentration of brij 35 10% w/v which contains hydrophilic hydroxyl group, resulting in  $-36.10 \pm 0.92$  mV.

#### 4.2.5 Scanning electron microscopy (SEM)

SEM was used to complete the information about morphology as well as particle size of testosterone-loaded SLNs. As shown in Figure 4.6, the nanoparticles remained spherical in shape with smooth surfaces. The data from dynamic light scattering agreed with the size shown by SEM images. Hence, it can be confirmed that the method used to produce SLNs in this experiment was successful.



**Figure 4.6** Scanning electron microscope produced image for testosterone-loaded SLNs F1 (A) and F2 (B).

#### 4.2.6 Entrapment efficiency and loading capacity

Entrapment efficiency is one of the important parameters for characterizing SLNs. According to a literature, indirect approach is frequently used to assess the entrapment efficiency of a drug in SLNs where, % drug content in aqueous phase after separation from the lipid particles is determined (237). To obtain optimal entrapment efficiency, the concentration of S/CoS was varied. As shown in Table 4.5, the entrapment efficiency and loading capacity of the formulation was very different. F1 had poor entrapment efficiency and loading capacity (32.37%, 2.9%) compared to F2 (55.44%, 6.3%). F2 contains higher percentage of S/CoS compared to F1 formulation, which increased the solubility of the drug in the lipid leading to the higher entrapment efficiency. Similar results were reported by Abdelbary *et al.* and Ekambaram *et al.* (238) (239) where, the entrapment efficiency showed similar response to surfactant concentration. Beside concentration of surfactant, another factor that influences entrapment efficiency is the chemical nature of lipids. According to Western *et al.* lipids with perfect lattice (such as monoacid triglycerides) causes drug expulsion whereas, hard fats of distinct chain length

(stearic acid) and complex glycerides such as mono-, di- and triglycerides form imperfect crystals providing space for drugs to accommodate (240).

**Table 4.5** Entrapment efficiency and Loading capacity for F1 and F2 formulations.

Formulation	Surfactant	EE (%)	LC (%)
F1	10%	32.37 ±1.50	2.9 ±0.35
F2	20%	55.44 ±3.43	6.3 ±0.96

#### 4.2.7 Thermal analysis

Thermal analysis of solid lipid nanoparticles was performed by DSC analysis to determine physical transformation (such as phase transitions) of the nanoparticle's components in response to heat flow to the samples. Figure 4.7 demonstrates DSC curves for stearic acid, testosterone, and testosterone-loaded SLN. Stearic acid and testosterone showed endothermic peaks at 72.32°C and 155.95°C, respectively. The lower intensity peak at 118.35°C in testosterone thermogram can be attributed to the dehydration and the second one at 155.95°C corresponds to the melting point of the crystal (241). This finding was similar to the previously reported study by Kalkura *et al.* where, DSC analysis was performed on testosterone using a Mettler TA 3000 system. The DSC curve indicated two endothermic transitions at 116°C (dehydration) and 154°C (crystal) (241). The impurity in the sample can often show several peaks. Substances with eutectic impurities show two peaks (Figure 4.7b): first peak represents eutectic impurity, whose peak size is proportional to the amount of impurity (242), second peak represents the main melting peak for stearic acid.

Testosterone-loaded SLN showed only one endothermic peak at 71.91°C which can be attributed to the melting point of stearic acid. Figure 4.7 shows that the thermogram of SLNs had lower enthalpy value and melting point (117.62 J/g, 71.91°C) than stearic acid (268.25 J/g, 72.32°C). Lower enthalpy values can be attributed to less orderly formed crystalline lattices as well as defects in the crystalline lattice caused by the presence of liquid lipid (stearic acid) (243). This disruption in the formation of the crystalline lattice can prevent drug expulsion during storage (244). Another reason for a lower melting enthalpy is the small particle size of SLNs with increased surface area, which causes heat to flow slowly through the



substances than in larger crystals (245). The decrease in the melting point of SLNs is due to the liquid lipid content in SLNs compared to stearic acid crystals. DSC thermogram of SLNs exhibited small broadening of the stearic acid endothermic peak which can be due to small particle size with large surface area, excipients in SLNs undergoing a heating and cooling cycles, or the presence of impurities in liquid lipid (246). The thermogram of SLNs formulation presented no peak at the melting point of testosterone. The fact that the endothermic peak of testosterone disappeared shows that the drug is uniformly dispersed in an amorphous state and that no drug crystallised from the dispersion (247). Thus, it could be concluded that testosterone was molecularly dispersed within the lipid matrix which can be justified considering the dissolution of testosterone in the molten lipid (stearic acid) during loading (248). Additionally, the stearic acid peak in formulation shifts to the lower temperature. This can be attributed to the increase in surface area due to reduction in particle size, thus, decreasing the melting enthalpy compared to heat flow through large crystals (249).

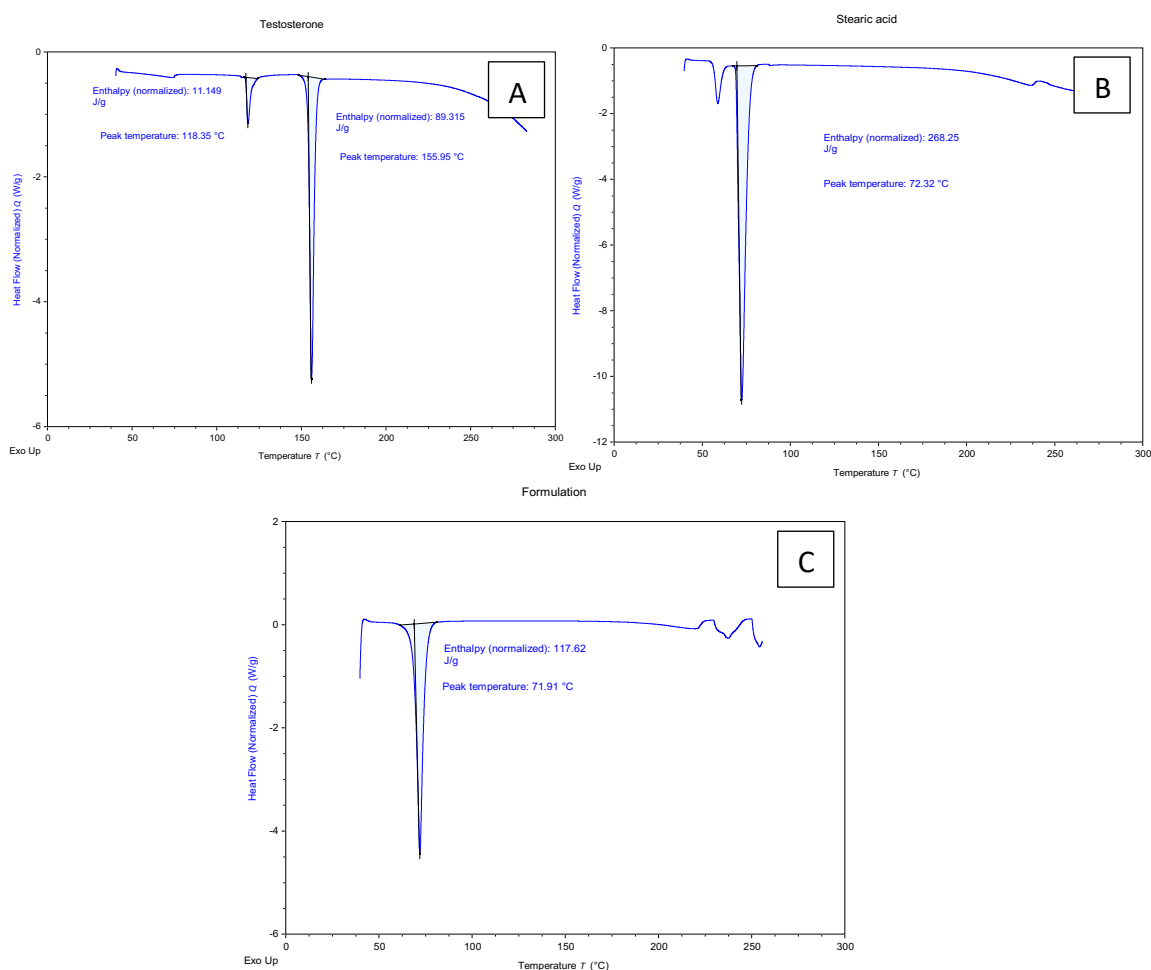
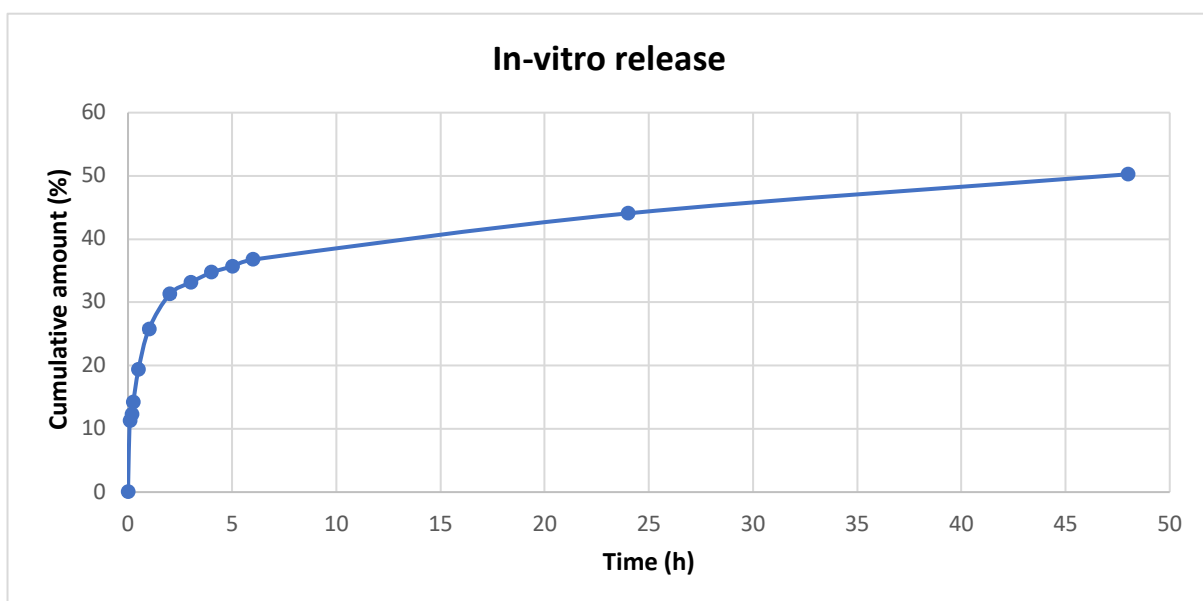


Figure 4.7 illustrates DSC data for testosterone (A), stearic acid (B), and testosterone-loaded SLNs (C) which includes melting enthalpy and temperature for each compound. The absence of a drug peak in SLNs thermogram confirm even dispersion of drug inside SLNs.

#### 4.2.8 *In vitro* release study

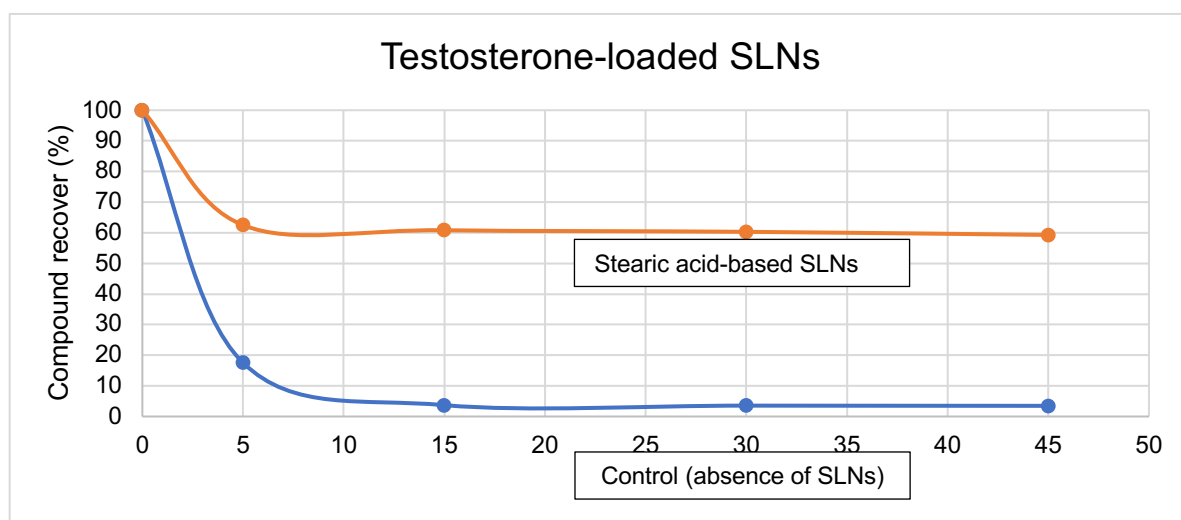
The method chosen for cumulative drug release study was dialysis membrane method. F2 was selected for *in vitro* release study because of higher entrapment and loading capacity compared to F1. Figure 4.8 represents the cumulative percentage release of testosterone from SLN at given time intervals. Testosterone is poorly soluble drug, so the release of testosterone from SLN was expected to be slow and controlled. Overall, around 50% of the drug was released in 48h from which 30-40% was released in 5 h and 10-20% was released in next 43 hr. This can be attributed to the higher surfactant content which stabilizes the SLNs and restricts the release of the drug outside the SLN (250). The data can be supported by Ghada Abdelbary *et al.* 2009 study where, different diazepam-loaded SLNs were designed and characterised. According to their study, increasing the surfactant concentration causes high viscosity of the lipid-solvent phase which leads to slower release of the drug from SLNs (251). On the other hand, the fast release of drug in first 5 hr is because of high diffusion coefficient, large surface area and a short diffusion distance for testosterone from outer region of the nanoparticles (252).



**Figure 4.8** *In vitro* release of testosterone from SLNs using phosphate buffer pH6.8. The slow and controlled release of testosterone was confirmed over 48 hours of time frame. The experiment was performed in triplicates ( $n=3$ ) and the data are depicted as mean  $\pm$ SD.

#### 4.2.9 *In vitro* metabolic assay

Testosterone-loaded SLN (F2) was tested for CYP450 inhibition to decrease metabolism of testosterone. The method used for metabolic assay was same as *in vitro* metabolic assay for screening of excipients. The compound remaining v/s time graph was plotted for better comparison of SLN data with control data. As a result, around 60% of the compound was recovered from testosterone-loaded SLN whereas, around 4% of the compound was recovered from the control sample (Figure 4.9). In other words, stearic acid as well as surfactants present in testosterone-loaded SLN strongly reduced the metabolism of testosterone. This might be as a result of stearic acid's direct or indirect inhibition, as demonstrated in Chapter 2, or SLNs' ability to mask the embedded drug and protect it from CYP3A4 metabolism. Moreover, the intrinsic clearance ( $CL_{int} = 0.04 \mu\text{L}/\text{min}/\text{mg}$ ) and half-life ( $T_{1/2} = 38.94 \text{ min}$ ) for testosterone-loaded SLNs were improved significantly when compared to control ( $CL_{int} = 0.29 \mu\text{L}/\text{min}/\text{mg}$ ,  $T_{1/2} = 4.76 \text{ min}$ ). The inhibitory effect of stearic acid reported in previous chapter and the lipid protection provided by the SLN from enzymatic degradation makes this formulation potential candidate for oral drug delivery of testosterone. Luo *et al.* prepared SLNs for enhancing oral bioavailability of vinpocetine. The outcomes were like our report where, vinpocetine's bioavailability was increased by incorporating it into SLNs hence reducing the exposure of drug to enzymatic degradation (253). Testosterone is a substrate to CYP3A4 enzyme and embedding it into solid lipid matrix reduced its exposure to enzymatic degradation.

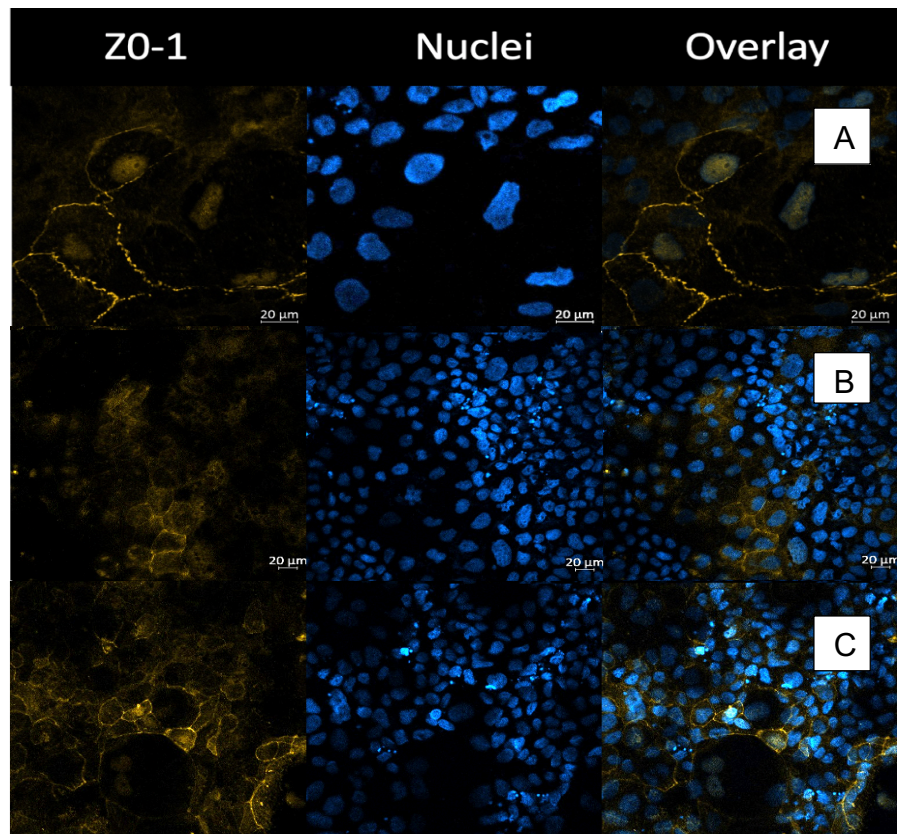


**Figure 4.9** Shows effect of stearic acid-based SLNs on the metabolism of testosterone. The results were compared with control (absence of SLNs) showed potent inhibition of CYP450 enzymes. Data is represented as % compound recovered/remaining ( $n=3$ ), mean  $\pm$ SD

#### 4.2.10 Permeability study of testosterone-loaded SLN formulation

For testosterone to be effective as therapeutic agents, they must have efficient cellular absorption from the gut membrane. Confocal microscopy was conducted to compare the cellular uptake of testosterone-loaded SLNs (F2) with testosterone solution. The formation of monolayer membrane was confirmed by confocal microscopic images (Figure 4.10) and the apical to basolateral permeabilities of testosterone was studied in the presence and absence of stearic acid. The results show that SLNs and testosterone solution uptake was time dependent. At the end of 90 minutes, very little fluorescence was observed in the dye solution, indicating poor internalisation into cell monolayers. However, testosterone-loaded SLNs had higher fluorescence intensity in both the cell cytoplasm and the nucleus, indicating that the SLNs were internalised into the Caco-2 cells.

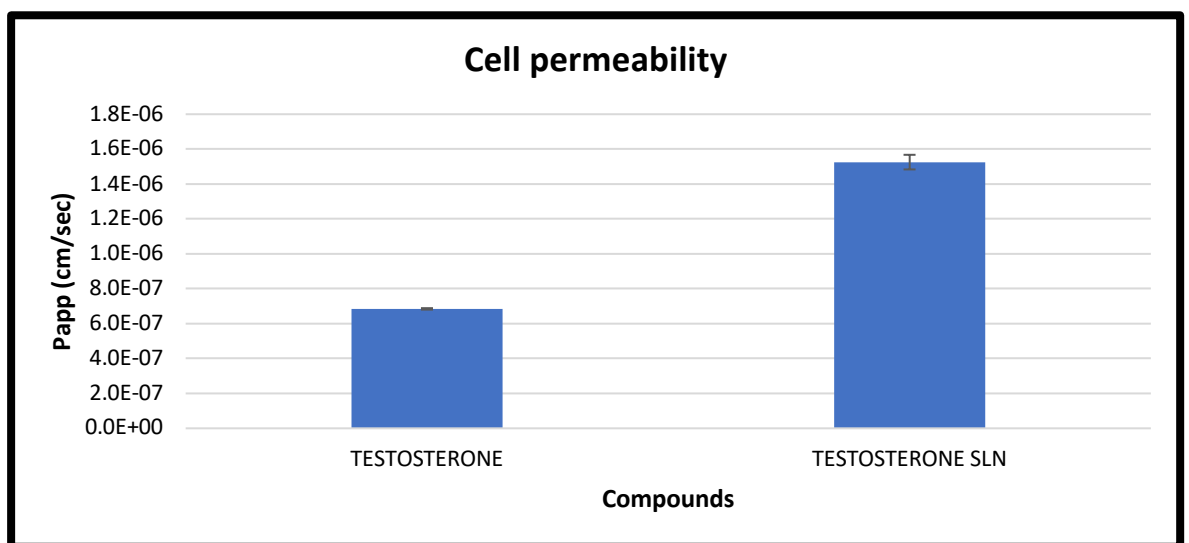
Prior to permeability experiments, Caco-2 cells were incubated with the buffer for 15 min. The apparent permeability ( $P_{app}$ ) of testosterone in presence and absence (control) of stearic acid was calculated using the equation 4.1. As a result (Figure 4.11), the permeability of testosterone had significant effect ( $P < 0.05$ ) in presence of stearic acid ( $P_{app} = 1.53 \times 10^{-6}$  cm/sec) when compared to control ( $P_{app} = 6.84 \times 10^{-7}$  cm/sec). The increase in permeability can be due to the disordering effect of stearic acid on membranes. Gori et. al. studied the effect of palmitic acid on permeability and intestinal epithelial barrier integrity. Palmitic acid is a saturated long-chain fatty acid (16:0) just like stearic acid (18:0). According to their study, palmitic acid significantly increased the permeability across the epithelial barrier without causing any cytotoxicity. The presence of palmitic acid altered the integrity of the gut epithelium causing functional changes to the barriers through a putative effect on the tight junction and adherent junction proteins (paracellular gap openings) (254). Hence, the stearic acid outcomes can be justified as it demonstrates similar data to palmitic acid which can increase the permeability via paracellular gaps. Another possible explanation for higher cellular uptake could be an increase in the hydrophobic interaction between nanoparticles and Caco-2 cell membrane, or the presence of propylene glycol which is a potential absorption enhancer that can alter the epithelial barrier property (255).



**Figure 4. 10** Confocal microscopic images of monolayers: A = Control, B = testosterone, and C = testosterone-loaded SLNs

$$P_{app} = \left( \frac{dQ}{dt} \right) / (A \times C) \quad (254)$$

**Equation 4.1** Apparent permeability ( $P_{app}$ ) where  $dQ/dt$  represents rate of drug transport;  $A$  is the surface area of cell monolayer, and  $C$  is the drug concentration.

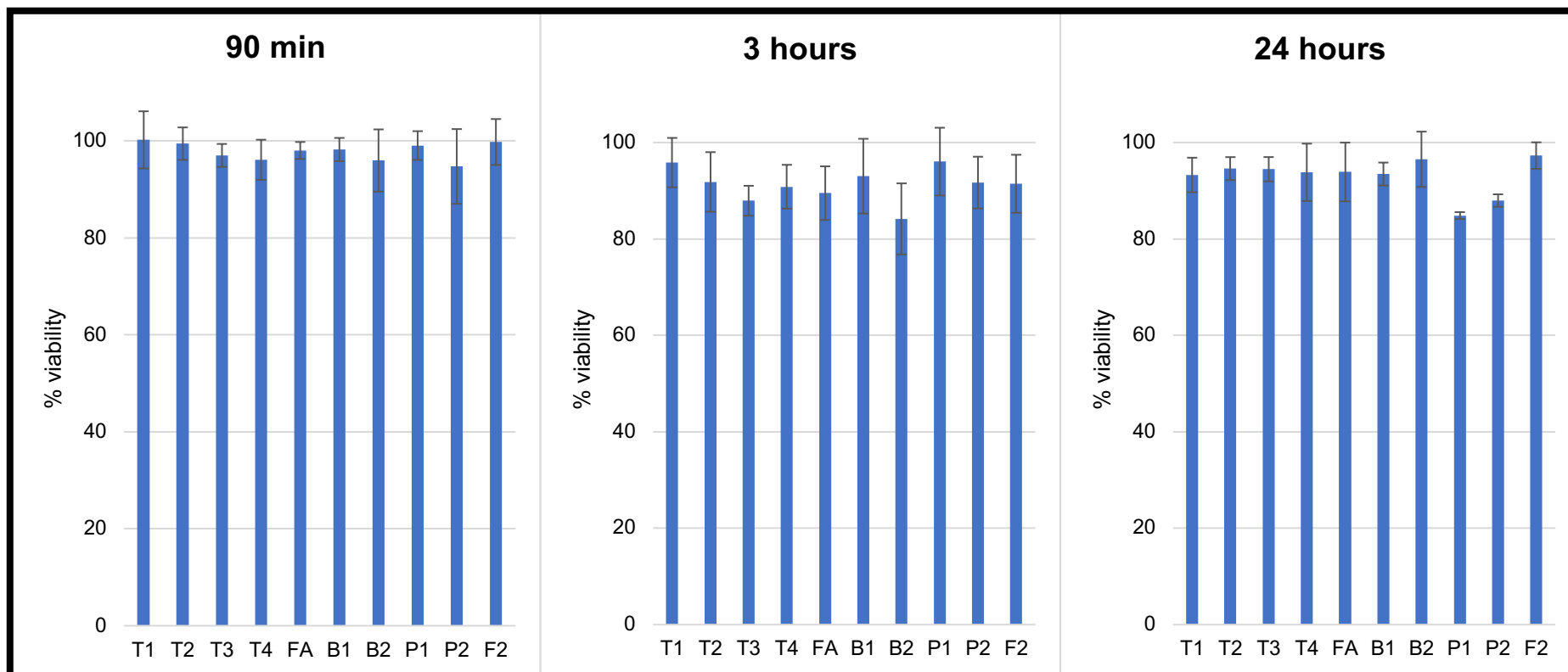


**Figure 4. 11** Permeability of testosterone in presence of stearic acid (testosterone SLNs) vs absence of stearic acid (on its own).

#### 4.2.11 Cell toxicity study

The MTT assay is a simple assay that can be used to estimate the number of viable cells in the microtitre tray wells to determine the cellular toxicity of the developed nanoparticles. The principle of this assay is that living cells have potential to reduce the MTT solution (tetrazolium salt 3-(4,5-dimethylthiazol-2-yl)-2,5-diphenyltetrazolium bromide)) to a blue formazan dye which is quantified using spectrophotometry (256).

Cell viability study was conducted via the MTT assay to estimate the toxicity of testosterone at different concentrations, excipients and testosterone-loaded SLNs (Fig 4.12). All compounds were tested at three different time intervals 1.5, 3, and 24 hours. From figure 4.12 it can be concluded that cell viability for all compounds at different concentration remain more than 80%. However, the cell toxicity was time dependent. The cell viability for the first 90 min remained above 90% for all the compounds and SLNs but it gradually started depleting to ~90% after 3 hours and below 90% after 24 hours. Amongst all the compounds, propylene glycol (P1 and P2) showed the highest depletion after 24 hours whereas, the formulation (F2) displayed least toxicity. This suggests that testosterone-loaded SLNs does not impose any toxic effects on Caco-2 cells.



**Figure 4. 12** Cell viability study for three different time points (1.5, 3 and 24 hours). Various compounds were tested for cell toxicity where T1(2  $\mu\text{g}/\text{mL}$ ), T2 (20  $\mu\text{g}/\text{mL}$ ), T3 (40  $\mu\text{g}/\text{mL}$ ), and T4 (80  $\mu\text{g}/\text{mL}$ ), are four different concentrations of testosterone; FA represents fatty acid (stearic acid); B1(10% v/v), B2 (20% v/v) and P1 (10% v/v), P2 (20%v/v)are two different concentrations for brij 35 10%w/v and propylene glycol, respectively; Lastly, F2 represents SLNs formulation.

### **4.3 Conclusion**

Herein, testosterone-loaded SLNs formulation was systematically optimised and their physical chemical properties were also characterised. Different variables such as concentration of surfactants, type of surfactants, solubility of testosterone, and composition of water: S/CoS: oil significantly affects the particle size, entrapment efficiency and PDI of nanoparticles. The *in vitro* release study revealed controlled release of drug from SLNs, and microsomal assay demonstrated significant inhibition of CYP450 enzymes, leading to reduced metabolism of testosterone. Moreover, the testosterone-loaded SLNs and different compounds present in SLNs showed no cytotoxicity even at higher concentrations. The permeability of testosterone across Caco-2 cells was increased significantly in presence of stearic acid. Thus, solid lipid nanoparticles can be potential formulation for delivering testosterone with improved permeability and reduced metabolism by CYP450 enzymes.



# **Chapter 5:**

## **Dextromethorphan-loaded solid lipid nanoparticles**

## 5.1 Introduction

### 5.1.1 Solid lipid nanoparticles for hydrophilic drugs

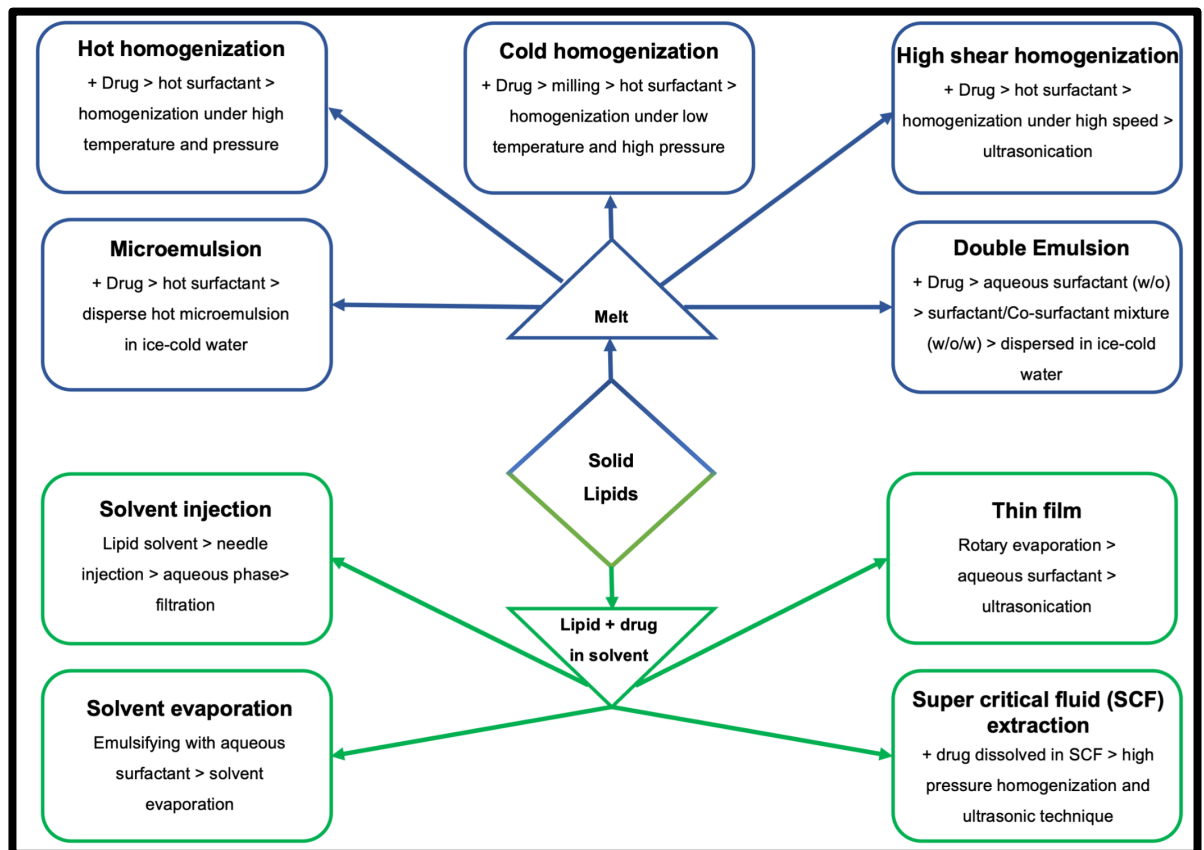
The main hypothesis behind the development and preparation of solid lipid nanoparticles (SLNs) was to offer the potential carrier system for controlled or sustained drug release by incorporating the drug within a solid matrix. The presence of a solid particle core might increase the physical and chemical stability of such nanoparticles (257). The most promising carrier system for hydrophobic drugs is found to be SLN because of its incorporation efficiency, high compatibility, and presence of solid lipid. However, the development of SLN for hydrophilic or water-soluble drugs is an elusive goal and remained a subject of a research due to the incompatibility between SLN and hydrophilic molecule (258). During the fabrication process of SLN, the hydrophilic drug migrates rapidly into the external aqueous phase due to weak interaction between drug and lipid. Hence, different methods and approaches have been employed and shown potential towards delivering water-soluble drugs using SLN as a carrier system, as discussed below and summarized in Table 5.1 (259).

Commonly used methods for preparation of SLNs are displayed in Figure 5.1 which describes two primary approaches. The first common approach includes dispersion of the drug into melted solid lipid (5-10°C above its melting point), followed by different techniques such as microemulsion, high-pressure homogenization, and double emulsion to produce SLN. The second approach includes dissolving drug as well as solid lipid into an appropriate solvent and finally made into SLN by using surfactant(s) and solvent evaporation technique. The commonly used method for loading hydrophilic drugs into SLN are microemulsion and double emulsion-based method (259).

**Table 5. 1** Different methods to incorporate water soluble drugs into SLNs.

<b>Hydrophilic drug</b>	<b>Methods</b>	<b>Purpose of study or route of administration</b>	<b>Entrapment efficiency (%)</b>	<b>Reference</b>
<i>Ampicillin</i>	Solvent evaporation	Improved antibacterial activity	77	(260)
<i>Amikacin</i>	Hot homogenization	Increased efficacy	60-86	(261)
<i>Ascorbic acid</i>	Hot homogenization	Better cellular uptake	90	(262)
<i>Azidothymidine</i>	Solvent emulsion homogenization	Intravenous (IV)	72	(263)
<i>Calcitonin</i>	Solvent emulsification	Oral	90	(264)
<i>Catalase</i>	Double emulsion and solvent evaporation	Oral	78	(265)
<i>Cisplatin</i>	Microemulsion	Intravenous (IV)	82.3	(266)
	Hot homogenization	Sustained drug release	90	(267)
	HIP-Coacervation			
<i>Ciprofloxacin</i>	HIP-solvent diffusion	Prolonged drug release and therapeutic effect	73-85	(268) (269)
	Ultrasonic melt-emulsification			
<i>Chloroquine</i>	Double emulsion	Increased cellular uptake	78-90	(270)
<i>Diclofenac sodium</i>	W/O/W solvent evaporation	Transdermal delivery	99	(271)
<i>Doxycyclin</i>	Double emulsion	Sustained drug release	94	(272)
<i>Doxorubicin</i>	HIP-Coacervation	Increased permeation	79	(273) (274)
	Solvent emulsification	Enhanced loading capacity	85	

	Lipophilic prodrug	Intravenous (IV)		
	Drug-polymer conjugate			
<i>Floxuridine</i>	Lipophilic prodrug	Oral	70-82	(275)
<i>Isoniazid</i>	Micro-emulsification	Oral	69	(276)
<i>Insulin</i>	Double emulsion	Oral; subcutaneous	40-52	(277)
	HIP-Coacervation	Sustained drug release	90	(278)
<i>Leuprolide acetate</i>	HIP-Coacervation	Sustained drug release	48-85	(278)
<i>Lysozyme</i>	Cold homogenization	Improved activity of enzymes	60	(279)
<i>Methotrexate</i>	HIP-Coacervation	Intravenous (IV)	70	(280)
	Microemulsion	Intravenous (IV)	67.3	(281)
	Solvent-free method			
<i>Nicotinamide</i>	Microemulsion	Parenteral	36	(282)
<i>Nisin</i>	High-pressure homogenization	Sustained anti-microbial activity	69-72	(283)
<i>Polymyxin B</i>	Double emulsion	Enhanced micro	90	(284)
<i>Tetracycline</i>	Microwave-assisted microemulsion	Prolonged drug release	40-50	(285)
<i>Tobramycin</i>	HIP-microemulsion	Occular	2.5	(286)
<i>Vinoreblin bitartrate</i>	Cold homogenization	Increased cellular toxicity against cancer	72	(287)



**Figure 5.1** Two primary approaches to prepare SLNs using solid lipids: a) melting solid lipids and b) dissolving in solvent. Former approach can be produced using five different techniques which includes microemulsion, hot/cold homogenization, high shear homogenisation, and double emulsion. Later approach can be prepared using solvent injection, thin film, SCF, and solvent evaporation technique (259).

### 5.1.2 Double emulsification method

Generally, to incorporate lipophilic drugs in SLN, oil-in-water (o/w) emulsions are preferred. Whereas, for hydrophilic drugs, double emulsion method such as water-oil-water (w/o/w) emulsions are reported (288) (289). Gallarate *et al.* produced insulin-loaded SLN by first dissolving the drug into acidic aqueous phase, then emulsifying it with a lipid called glyceryl monostearate (w/o pre-emulsion). This w/o system was then emulsified to w/o/w emulsion by introducing second aqueous phase containing Pluronic F68 (surfactant) and soy lecithin (co-surfactant). This produced SLNs with entrapment efficiency of 40% (290). Another study used double emulsion technique to encapsulate hydrophilic drugs for transporting small interfering RNAs (siRNAs). These water-soluble siRNAs are promising therapeutics, but they face challenges crossing lipid barriers because of their low affinity. To produce siRNA RVG-9R/BACE-1-loaded SLNs for a nose to brain

delivery, witepsol E-85 was used as solid lipid, dichloromethane as organic solvent, polyvinyl alcohol (PVA) as surfactant, and water as aqueous phase. Briefly, solid lipid and drug were dissolved in organic solvent to form primary emulsion. This primary emulsion was sonicated and poured into 2% PVA aqueous solution and homogenised to produce w/o/w double emulsion. The organic solvent was then allowed to evaporate by stirring on a magnetic stirrer overnight at room temperature. The formulation showed good entrapment efficiency and enhanced Caco-2 cell permeability (291).

### 5.1.3 Microemulsion method

Microemulsions are thermodynamically stable dispersions which upon dilution in ice-cold water with constant stirring produce nanoparticles (SLNs). This method can be used for lipophilic as well as hydrophilic drugs. Bhandari and Kaur prepared isoniazid loaded SLNs with minor modification to the method. Microemulsion is composed of combination of lipids (stearic acid and Compritol 888 ATO, 1:4 ratio), surfactant (Tween 80), and co-surfactant (soy lecithin). This microemulsion was then further transferred to ice-cold water under constant stirring to produce well dispersed SLNs. These nanoparticles showed good entrapment efficiency of 69% with good stability at 4°C (276). Likewise, another study prepared doxorubicin-loaded SLNs using stearyl amine, palmitic acid, and beeswax as the solid lipids. Tween 80, taurocholate, and cholesteryl hemisuccinate were used as surfactants, whereas ethanol and DSPE-PEG (2000) as co-surfactants. These combinations of various components entrapped 78% of drug in SLNs (292).

### 5.1.4 Other Conventional methods

Besides double emulsion and microemulsion methods, several studies have reported the use of different conventional methods that can produce SLNs with suitable entrapment efficiency. These are hot homogenization, cold homogenization, and ultrasonic melt-emulsification methods.

Hot homogenization technique is like homogenization of emulsion, where a lipid emulsifier phase (hot lipid and drug) is melted above the melting point of lipid and aqueous emulsifier phase (heated to same temperature) is achieved by high shear mixing device (homogenizer). High-pressure homogenization of the emulsion is

prepared above the melting of lipid carrier. High temperature of this emulsion lowers the viscosity of lipid phase, resulting in lower particle size. However, increasing the number of homogenization cycles can also lead to larger particle size due to coalescence. The drawbacks of using hot homogenization technique are degradation of drug payload due to elevated temperature, Partitioning of the drug into an aqueous phase, and indeterminate polymorphic transitions of various lipids (293).

To overcome these limitations, a cold homogenization technique was introduced. Like the hot homogenization technique, the drug is first dispersed into lipid melts, however this melted phase is cooled rapidly using liquid nitrogen or dry ice to allow the even distribution of the drug in lipid matrix. The ball/mortar milling is then used to pulverized drug-loaded solid lipid to microparticles (50-100 microns). The dispersion is further introduced to high pressure homogenization at or below ambient temperature to produce SLNs. However, the SLNs made by this method tend to have larger particle size with broader size distribution (294).

The advantage of using the third conventional technique (ultrasonic melt-emulsification) for producing SLN is the availability of the equipment in every lab. This method uses high speed sonication to produce smaller particles. However, it comes with many limitations such as, broader particle size distribution, physical instability upon storage, and metal contamination from ultrasonication (294).

Thus, it is evident that two best methods to prepare hydrophilic drug-loaded SLNs are double emulsion and the microemulsion. This is because both the methods are cost effective and easy to employ. However, these methods come with certain drawbacks, such as use of organic solvents, drug leakage upon storage, and stability issues. Therefore, further research is required to incorporate hydrophilic drugs in SLNs with minimal limitations.

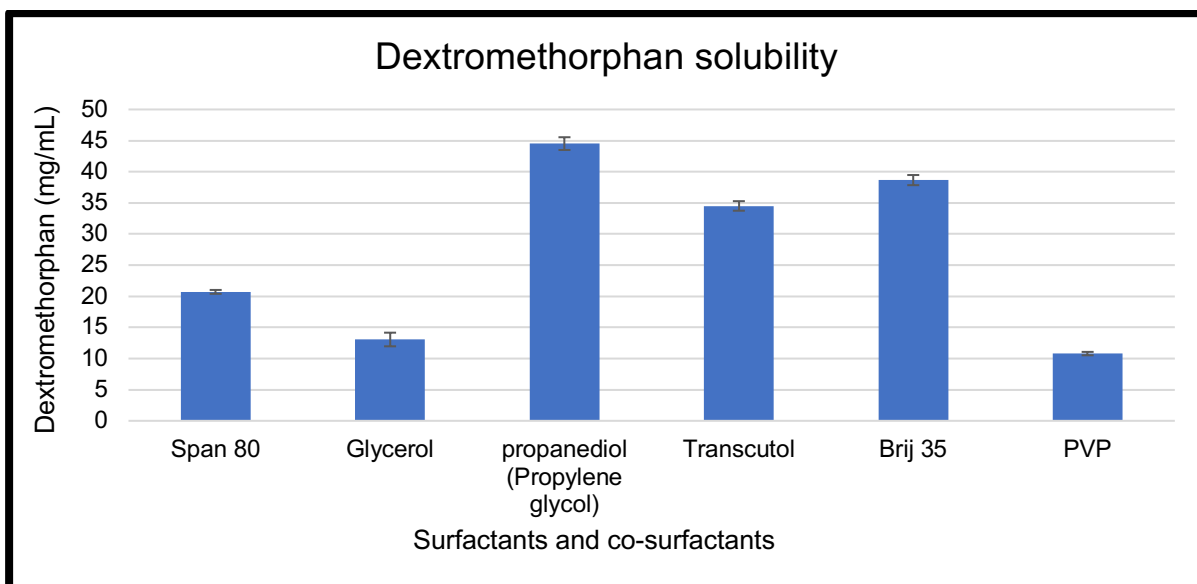
The aim of this study is to prepare dextromethorphan-loaded SLNs using different techniques mentioned above and to evaluate the effect of these SLNs on activity of CYP450 and Caco-2 cell permeability.

## 5.2 Results and Discussion

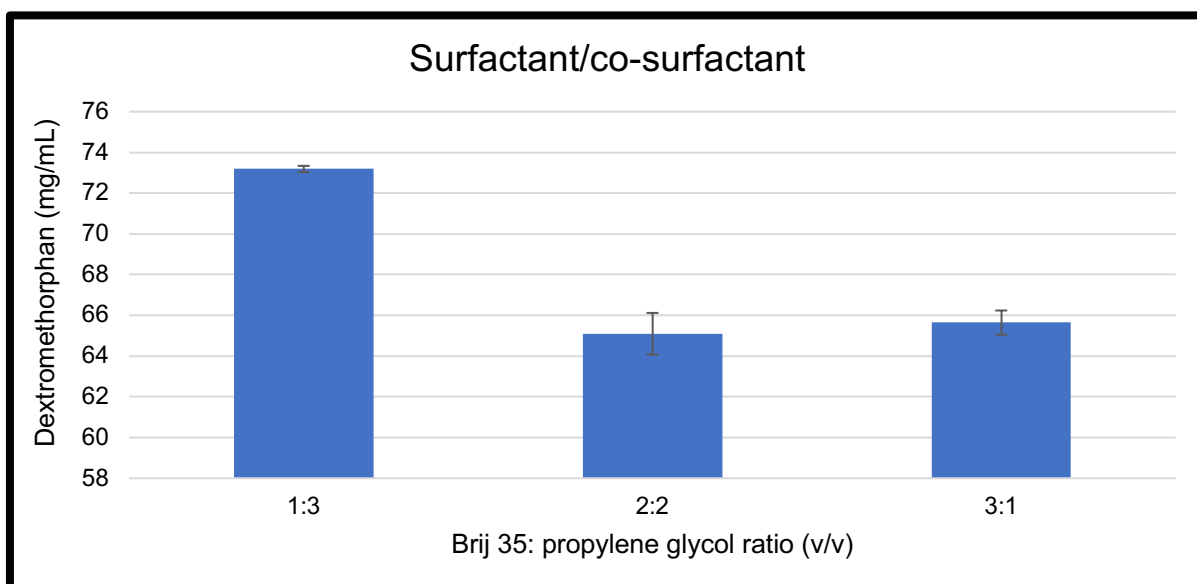
### 5.2.1 Saturation solubility

Surfactants and co-surfactants play important role in the preparation of stable SLN. In the immiscible system of oil-water, they are found at the interface of the oil and water. Surfactants lower the surface tension and interface free energy which stabilizes the oil droplets in SLNs. Moreover, they can increase the dissolution of hydrophilic/lipophilic drugs in the aqueous medium (295). The HLB value of the surfactant plays a crucial role for the selection of surfactants in SLNs. Research has recommended that surfactants with  $HLB > 12$  can spontaneously produce SLNs with smaller particle size (296). Therefore, solubility of dextromethorphan in various surfactants and co-surfactants was conducted prior to formulation of SLNs. Based on the data (Figure 5.2) dextromethorphan was highly soluble in propylene glycol ( $44.51 \pm 1.02$  mg/mL) and Brij 35 ( $38.66 \pm 0.81$  mg/mL). Propylene glycol is commonly used as co-surfactant. Co-surfactants are used to increase the solubility of hydrophilic/lipophilic drugs and improve the dispersibility of hydrophilic surfactant (Brij 35) in the oil phase. Thus, enhancing stability and formulation homogeneity (297). To understand the effect of different proportions of surfactant and co-surfactant on solubility of drug, different ratios of brij 35 and propylene glycol were studied. According to Figure 5.3, dextromethorphan was highly soluble with 1:3 ratio v/v of surfactant/cosurfactant ( $73.18 \pm 0.15$  mg/mL). Hence, it can be confirmed that increasing the amount co-surfactant improves the solubility of the drug.





**Figure 5.2** Saturation solubility of dextromethorphan in different surfactants and co-surfactants. The experiment was performed in triplicates and the data is represented as mg/mL  $\pm$  SD.

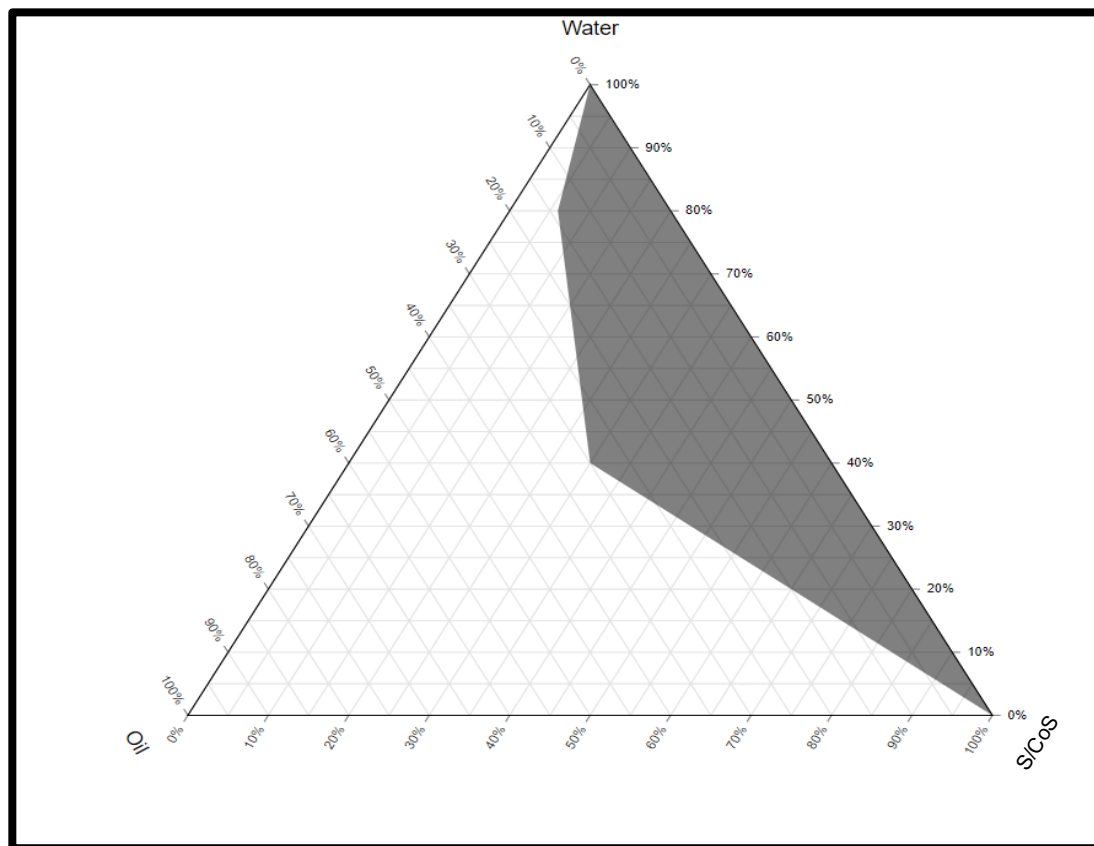


**Figure 5.3** Saturation solubility of dextromethorphan in different ratios of brij 35 and propylene glycol. The experiment was performed three times  $n=3$  and the data are represented as mg/mL  $\pm$  SD.

### 5.2.2 Pseudo-ternary phase diagram

The concentrations of oil (stearic acid), surfactant (brij 35), and co-surfactant (propylene glycol) and their ratios are key parameters in formulating stable SLNs for drug delivery. Ternary phase diagrams have commonly been used to recognise the microemulsion region for given compounds (298). Figure 5.4 shows the ternary phase diagram using different ratios of oil, S/CoS (1:3 v/v), and water. The ternary phase diagram for SLNs with solid lipids has not been extensively examined before. The shaded area in the ternary phase diagram signifies ME region, while the non-

shaded region represents no emulsion. The phase diagram obtained from this study shows narrow microemulsion on that aqueous rich area. This can be attributed to the presence of hydrophilic surfactant (brij 35) and hydrophilic part of co-surfactant (propylene glycol). Additionally, Propylene glycol allows maximum incorporation of water into oil-surfactant system leading to increase in ME region.



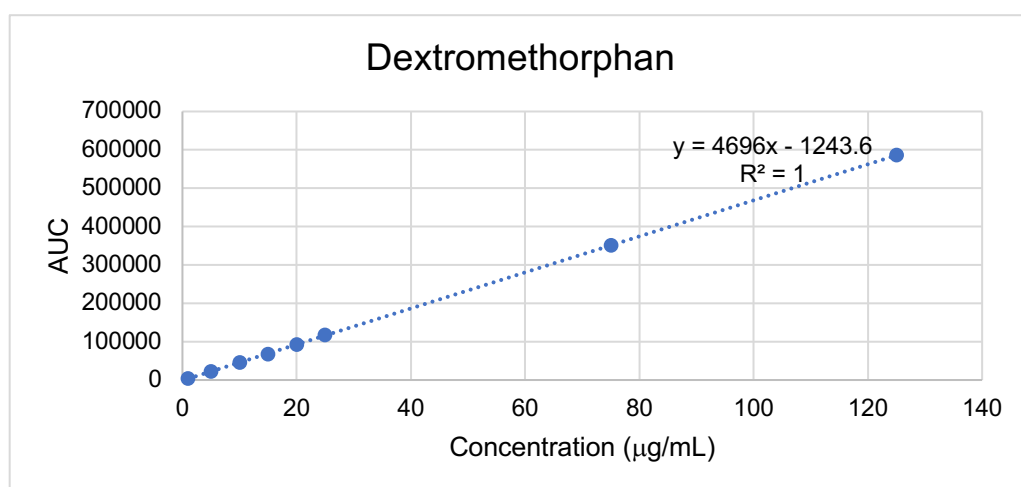
**Figure 5.4** Pseudo-ternary phase diagram for stearic acid: S/CoS (1:3 v/v) :water, where shaded region represents microemulsion and non-shaded region represent no microemulsion.

### 5.2.3 Preparation and characterization of SLN formulation

SLNs formulations are potential delivery system for lipophilic drugs where solubility of the drug in aqueous phase is a limiting factor. Lipophilic drugs are easily incorporated in SLN due to their affinity for lipids. Whereas hydrophilic drugs are difficult to incorporate inside the hydrophobic matrix as the drug has maximum affinity to partition in the water phase through fabrication process (299). Hence, this study included seven different formulations to incorporate maximum amount of dextromethorphan. The concentration of drug in each formulation was calculated using calibration curve Fig 5.5 with  $R^2$  value of 1 and the method was validated for its intended use (Table 5.2). F3, F4, and F5 were prepared using same approach as testosterone-loaded SLN. F6 was formulated using double emulsion method and

F7, F8, F9 were formulated using solvent evaporation method with different type of surfactants (Table 5.3). Based on visual inspection, formulation F3, F4, and F5 failed to produce dextromethorphan-loaded SLNs (Figure 5.6). The conventional method, which is generally used for hydrophobic drugs, failed to incorporate hydrophilic drug (dextromethorphan). Blank formulation produced milky SLNs with good particle size of  $278.2 \pm 33.19$  nm, while F3, F4, F5 produce unstable formulation with solid precipitates. Since the method remains like testosterone-loaded SLN and the blank produced fine SLNs, this result can be attributed to the expulsion of dextromethorphan upon addition of hot emulsion in ice-cold water. The outcome was confirmed by calculating entrapment efficiency and it was found that 0% dextromethorphan was entrapped inside SLNs.

The second method that was considered was the double emulsion (F6). Since dextromethorphan escaped from O/W microemulsion approach, double emulsion W/O/W was potential method to overcome the problem. Compared to O/W approached SLNs, F6 produced fine SLNs (Figure 4.7C) with average particle size of  $142 \pm 3.00$  nm, PDI  $0.06 \pm 0.001$ . However, the entrapment efficiency was 0% which confirms the expulsion of dextromethorphan to the external aqueous phase. Similar outcomes were reported with F7, F8, F9 where solvent evaporation technique with different surfactants were studied. All three approaches failed to incorporate dextromethorphan (hydrophilic drug). All the outcomes confirm that dextromethorphan has higher affinity towards aqueous and therefore, further investigation is required to understand the behaviour of hydrophilic drugs within lipid-based formulations.



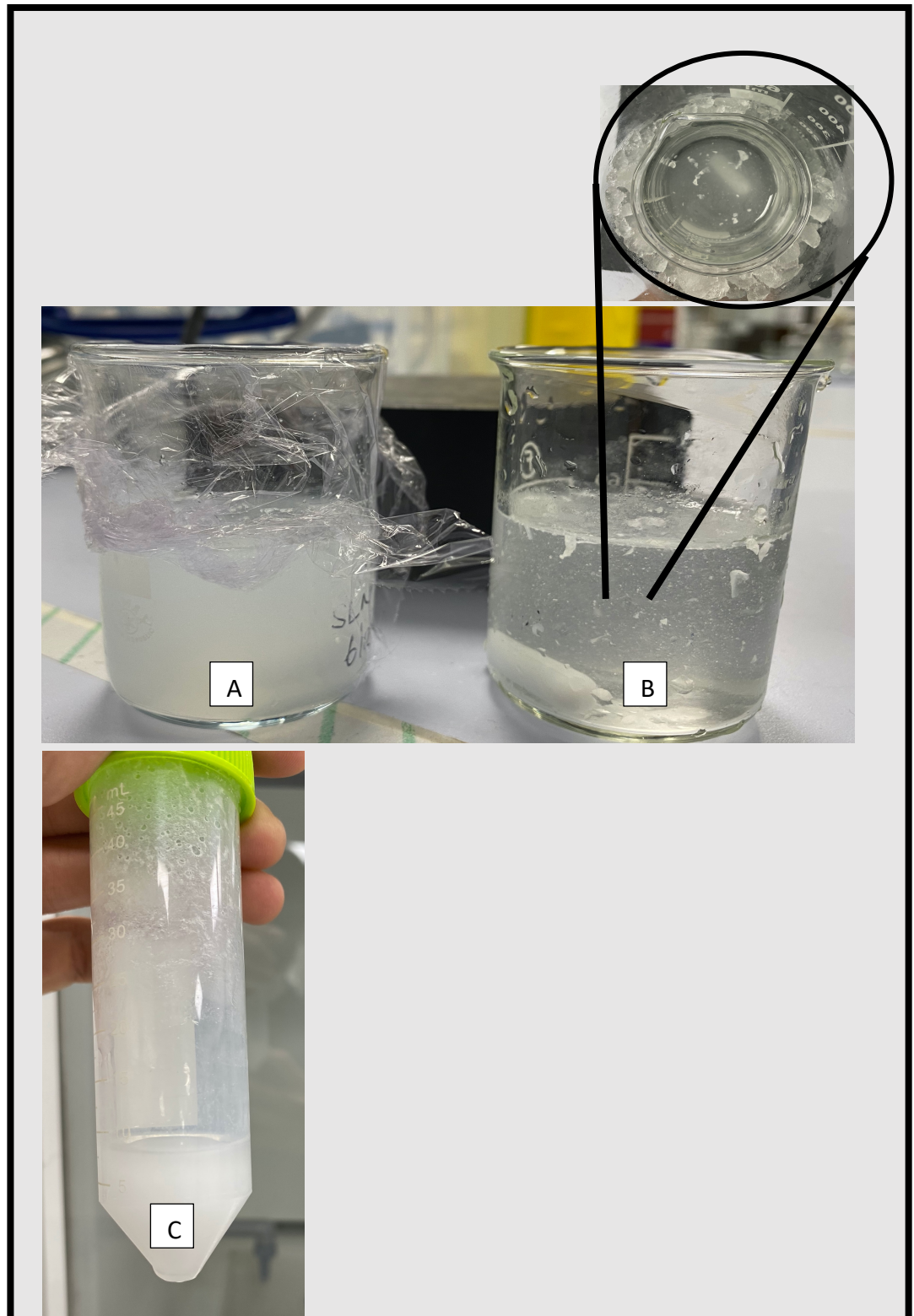
**Figure 5.5** Calibration curve for dextromethorphan where, x-axis represents concentration of dextromethorphan and y-axis shows AUC response.

**Table 5.2** Validation parameter for dextromethorphan

Linearity (R <sup>2</sup> value)	Concentration (µg/mL)	Accuracy (%)	Precision (%)	LOQ (µg/mL)	LOD (µg/mL)
1	8	104.21 ±1.55	1.05 ±1.11	1.88	1.05
	22	100.10 ±1.11	1.30 ±1.52		
	100	101.05 ±2.02	1.26 ±1.86		

**Table 5.3** Different compositions for various formulations attempted to prepare dextromethorphan-loaded SLNs.

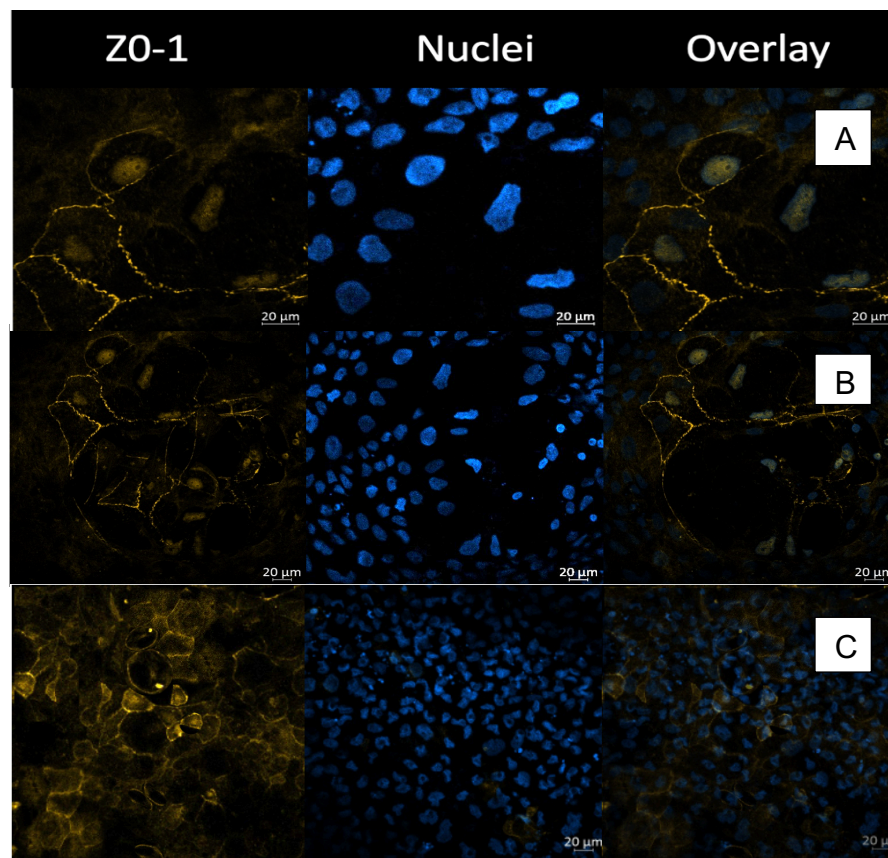
Function	Composition	F3	F4	F5	F6	F7	F8	F9
<b>Active ingredient</b>	Dextro-methorphan	5.0 mg						
<b>Solid lipid</b>	Stearic acid	1.0 mL	1.0 mL	1.0 mL	0.6 g	0.5 g	0.5 g	0.5 g
<b>Surfactant/ Co-surfactant</b>	Brij 35	0.3 mL	0.7 mL	1.3 mL		0.3 g	-	-
	Propylene glycol	0.7 mL	1.3 mL	2.7 mL	0.6 g	0.7 g	0.7 g	0.7 g
	Tween 80	-	-	-		-	0.3 g	-
	Poloxamer 188	-	-	-		-	-	0.3 g
<b>Water phase (W1)</b>	Water	8.0 mL	7.0 mL	6.0 mL	0.2 mL	4.0 mL	4.0 mL	4.0 mL
<b>Water phase (W2)</b>	Water	-	-	-	6.0 mL	-	-	-
<b>SLN</b>	Cold/hot water	49.0 mL	49.0 mL	49.0 mL	90.0 mL	-	-	-



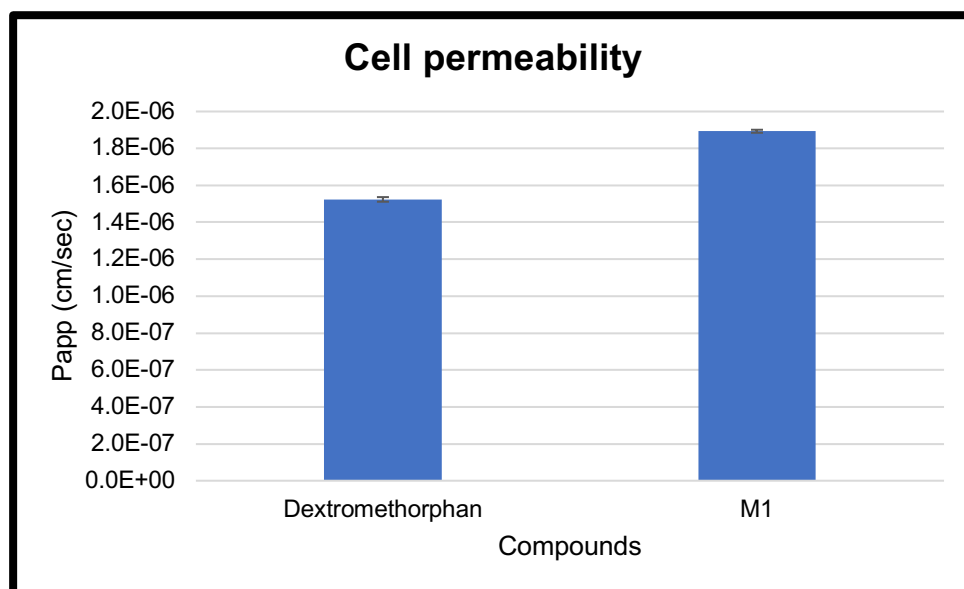
**Figure 5. 6** Images of successful and unsuccessful development of SLNs: (A) represents SLNs without dextromethorphan and (B) represents failure to produce SLNs with different approaches F3, F4, F5, F7, F8, and F9. (C) F6 produce milky SLNs.

#### 5.2.4 Permeability study of Dextromethorphan

The formation of the monolayer membrane was established by confocal microscopic images (Figure 5.7) and the apical to basolateral permeabilities of dextromethorphan and dextromethorphan mixture ( $M_1$ ) were studied in presence and absence of stearic acid.  $M_1$  was used as a replacement solution to dextromethorphan-loaded SLNs which consisted of oil, water, S/CoS and drug mixture. The apparent permeability ( $P_{app}$ ) of dextromethorphan in presence and absence of stearic acid was calculated using the equation 4.1. As a result (Figure 5.8), the permeability of dextromethorphan was improved significantly in presence of stearic acid ( $P_{app} = 1.89 \times 10^{-6}$  cm/sec) when compared to control ( $P_{app} = 1.52 \times 10^{-6}$  cm/sec) with  $P < 0.05$ . The increase in permeability can be because of the disordering effect by stearic acid on cell membranes. As noted in the permeability study of testosterone-loaded SLNs, the integrity of the gut epithelium may have been affected, resulting in functional changes to the barriers similar to those caused by palmitic acid (254).



**Figure 5. 7** Confocal microscopic images of monolayers: A = Control, B = dextromethorphan, and C = M1



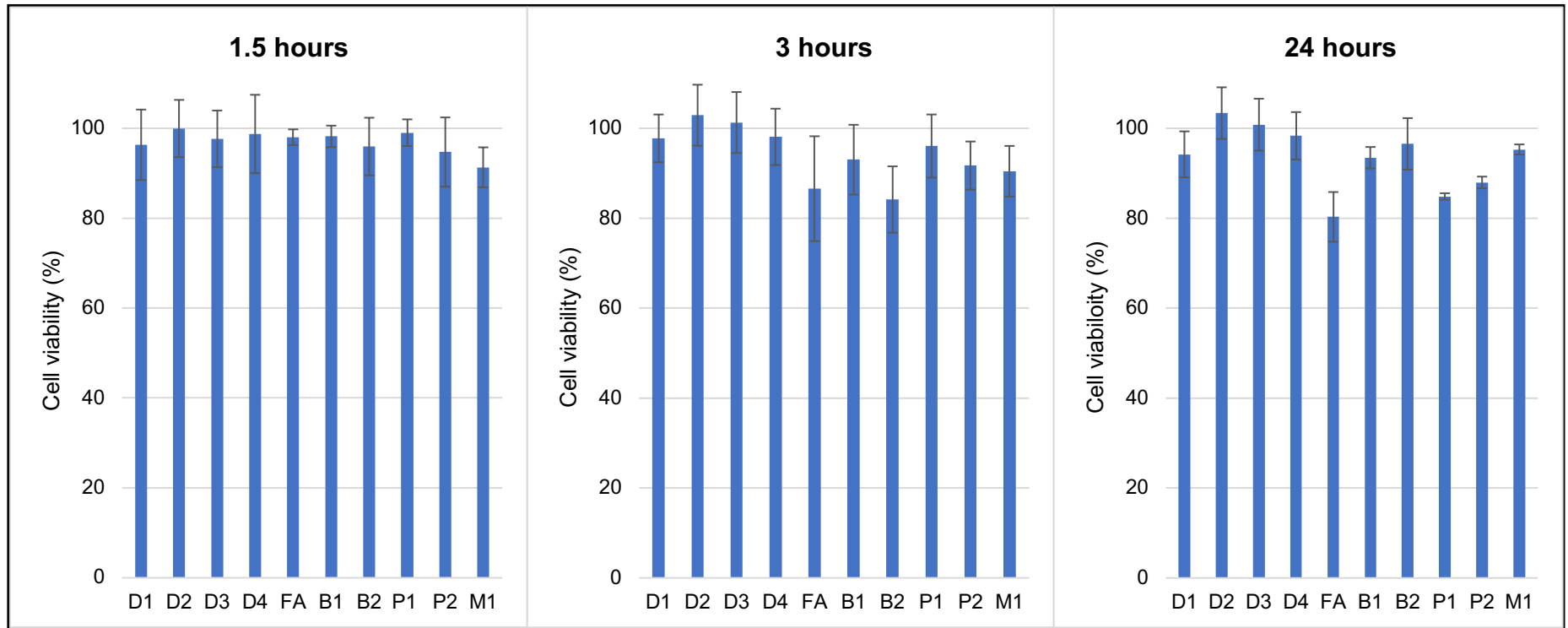
**Figure 5. 8** Effect of stearic acid on permeability of dextromethorphan, where M1 represents mixture of dextromethorphan and other components of SLNs formulation. The experiment was performed in triplicates  $n=3$  and the data is represented as  $cm/sec \pm SD$ .

### 5.2.5 Cell toxicity study

To determine the toxicity of dextromethorphan at various doses, excipients, and M<sub>1</sub>, cell viability research using the MTT assay was carried out. (Fig 5.9). Three separate time points 1.5, 3, and 24 hours were used to examine every compound. From figure 5.9 it is evident that cell viability is greater than 80% for all substances at all concentrations. This confirms that all substances used for preparation of M<sub>1</sub> are safe to use.

Figure 5.9 shows that cell viability for all compounds at different concentrations remains greater than 80%, but cell toxicity is time dependent. For all compounds and SLNs, cell viability remains above 90% for the first 90 minutes, but it gradually depletes to ~90% after 3 hours and below 90% after 24 hours. Among all the compounds, propylene glycol (P1), Brij 35 10% w/v (B2) and fatty acid (FA) had the greatest depletion after 24 hours, while the mixture (M<sub>1</sub>) had low toxicity.





**Figure 5.9** Cell viability data for various compounds at different time points (1.5, 3 and 24 hours). Various compounds were tested for cell toxicity where D1(2  $\mu\text{g}/\text{mL}$ ), D2 (20  $\mu\text{g}/\text{mL}$ ), D3 (40 $\mu\text{g}/\text{mL}$ ), and D4 (80  $\mu\text{g}/\text{mL}$ ) are four different concentrations of testosterone; FA signifies fatty acid (stearic acid); B1 (10%v/v), B2 (20%v/v) and P1(10% v/v), P2 (20% v/v) represents two different concentrations for brij 35 and propylene glycol, respectively; M1 is a physical mixture of testosterone, stearic acid, water, and S/CoS.

## **Conclusion**

Herein, different approaches were used to prepare dextromethorphan-loaded SLNs. Based on the data, dextromethorphan showed higher affinity towards external aqueous phase and thus all the approaches failed to incorporate dextromethorphan. However, the mixture of all excipients with dextromethorphan was used for permeability and cell toxicity studies. Permeability of dextromethorphan was increased in presence of stearic acid. Moreover, the  $M_1$  and different compounds present in mixture or dextromethorphan showed no cytotoxicity even at higher concentrations. The inhibitory effect of stearic acid on CYP450 and Caco-2 cell permeability studies makes stearic acid potential candidate for lipid formulations. However, further studies are required to explore different approaches to incorporate stearic acid and dextromethorphan in a formulation.

# **Chapter 6: Verapamil- loaded Solid Lipid Nanoparticles**

## 6.1 Introduction

The most convenient and widely used route of administration is oral drug delivery as it offers several advantages such as patient compliance, painless administration, and no assistance. Nevertheless, the vast majority compounds fail in the research and development stage owing to their poor absorption and bioavailability upon oral route of administration. The drugs with low oral bioavailability fail to reach their minimum effective concentration to exert their therapeutic action (300). Factors that influence bioavailability of drugs are as follows: (a) drug solubility as it should be available as a solution at the absorption site; (b) poor partition coefficient as it affects the permeation of drugs via lipid membrane; (c) first-pass metabolism of drugs resulting in poor bioavailability; (d) P-glycoprotein (P-gp) influences the absorption of drugs from gastrointestinal tract (GIT) and increases drug elimination; (e) degradation of drugs in the GIT due to low pH in stomach or by chemical reactions also reduces oral bioavailability (301).

Presently, novel drug delivery systems have been investigated to overcome these limitations while improving sustained drug release properties and therapeutic efficacy of various classes of drugs, such as antihypertensive drugs. Antihypertensive class of drugs are used to treat hypertension and are categorised into the following: ACE inhibitors, angiotensin antagonists, calcium channel blockers, diuretics, central sympathomimetics, vasodilators,  $\alpha$ -adrenergic blockers, and  $\beta$ -adrenergic blockers. The majority of these drugs show significant drawbacks like poor bioavailability, low permeability, short half-life, and adverse side effects. To deliver such antihypertensive drugs effectively, drug delivery systems which can provide low dosing frequency, improved bioavailability, enhanced selectivity, and reduced side effects are required (302) (303). Nanotechnology is an alternative strategy to administer antihypertensive drugs with enhanced bioavailability and therapeutic effect (304). Table 6.1 depicts an insight of numerous nanotechnology-based approaches to incorporate poorly soluble antihypertensive drugs.

**Table 6. 1** Various nanotechnology-based approaches for anti-hypertensive drugs.

<b>Antihypertensive drugs</b>	<b>Nanotechnology-based approaches</b>	<b>Application</b>	<b>References</b>
<b>Candesartan cilexetil</b>	Nanosuspensions	Enhanced bioavailability	(305)
	Polymeric micelles	Improved loading capacity and % drug release	(306)
<b>Carvediol</b>	Nanosuspensions	Enhanced bioavailability	(307)
	Solid lipid nanoparticles	Increased bioavailability	(308)
<b>Felodipine</b>	Nanosuspensions	Increase solubility and oral bioavailability	(309)
	Polymeric nanoparticles	Controlled drug release	(310)
<b>Nebivolol</b>	Polymeric nanoparticles	Prolonged drug release	(311)
<b>Nifedipine</b>	Polymeric nanoparticles	Increased bioavailability	(312)
	Nanocrystals	Improved dissolution rate	(313)
<b>Nitrendipine</b>	Nano emulsion	Enhanced bioavailability and therapeutic efficacy	(314)
	Nanocrystals	Improved bioavailability and physical stability	(315)
	Solid lipid nanoparticles	Enhanced bioavailability	(316)
<b>Valsartan</b>	Polymeric nanoparticles	Prolonged release of drug	(317)
	Nanosuspensions	Enhanced drug release	(318)

	Self-nanoemulsifying drug delivery system	Improved dissolution rate	(319)
	Solid lipid nanoparticles	Improved bioavailability	(318)
<b>Verapamil</b>	Solid lipid nanoparticles	Increased oral bioavailability	(320)

Verapamil is an L-type calcium channel blocker with well-known effects such as antiarrhythmic, anti-hypertension, and anti-anginal properties (312). Verapamil inhibits calcium influx which stops the contraction of smooth muscles, resulting in lower blood vessel resistance and reduced blood pressure in the peripheral circulation. Verapamil belongs to BCS class I family with decent absorption of  $\leq 90\%$  from GI membrane, nevertheless the systemic bioavailability after oral administration is only 20-35% (321). The poor and variable systemic bioavailability is due to extensive first-pass metabolism via portal circulation. 90% of the drug is bound to plasma proteins with a volume of distribution 3-5 L/kg. It is metabolised into at least 12 inactive metabolites, however one of them, norverapamil, still has 20% of the parent drug's vasodilating effects. Seventy percent of its metabolites are excreted in the urine, 16% are eliminated in the faeces, whereas 3 to 4% are eliminated unchanged via urine (320). Thus, it is essential to develop a formulation to enhance its bioavailability by preventing the first-pass effect. Solid lipid nanoparticles are promising lipid nanoparticulate drug delivery systems with many advantages over other colloidal carriers: a) easy scale up, b) sustained or controlled release, c) effectively target specific tissues, and d) improve stability. Numerous SLNs formulations are developed for distinct antihypertensive drugs (321).

Agrawal *et al.* prepared, optimized, and characterized verapamil-loaded SLNs. The method used to prepare SLNs was high shear homogenization and ultrasonication. The entrapment efficiency of 80.32% with smaller particle size of 218 nm was successfully achieved (321). Havanoor *et al.* produced isradipine-loaded SLNs to improve hypertension treatment. Hot homogenization and ultrasonic techniques were used for this study. These SLNs exhibited maximum drug entrapment (91 to 97%) because of its lipophilic nature. *In vivo* study showed prolonged release of Isradipine from SLNs compared to conventional suspension. The burst release was observed for first two hours with both SLNs and suspension. However, the decrease

in blood pressure after 2 hours was found to be greater with SLNs compared to conventional suspension (322). Another study attempted to improve oral bioavailability and target lymphatic transport system by developing nimodipine-loaded SLNs. The oral bioavailability of nimodipine is around 13%. The pharmacokinetic study conducted in male Albino Wistar rats revealed 2.08-fold rise in relative bioavailability compared to nimodipine solution (323). Similar data were reported with candesartan cilexetil loaded SLNs. Candesartan cilexetil is used for heart failure and hypertension. The entrapment efficiency was between 91 to 96 % with improved oral bioavailability, 2.75-fold times more than conventional solution (324).

The main objective of this research was to formulate verapamil-loaded SLNs using stearic acid to decrease its metabolism by inhibiting CYP450 enzymes and improve its permeability. The solid lipid nanoparticles prevent the degradation of various drugs by luminal enzymes. Initially, the selection of appropriate surfactants was carried out and the SLNs formulation was then prepared using hot water bath coupled with ultrasonication technique.

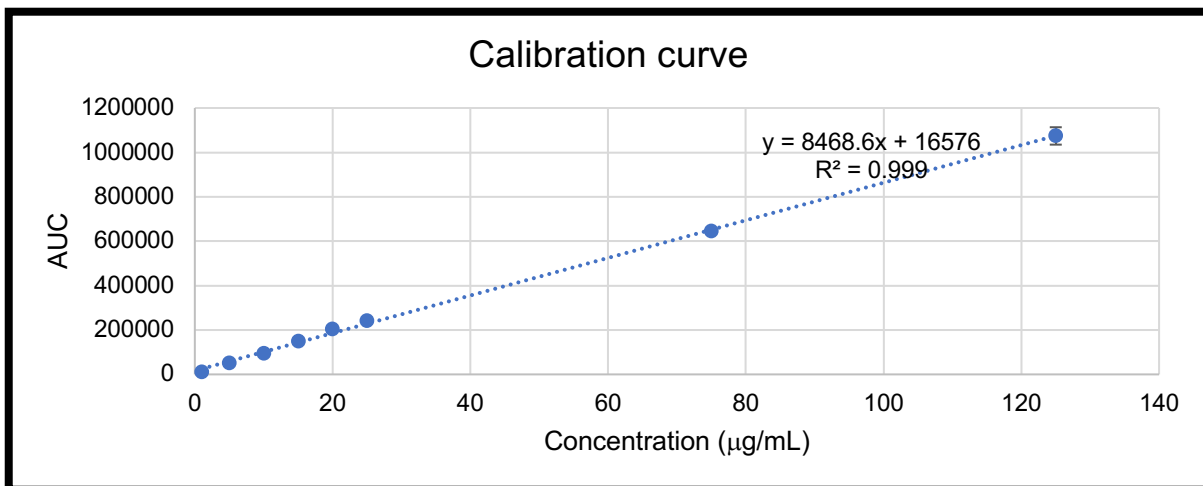
## 6.2 Results and Discussion

### 6.2.1 Saturation solubility

The calibration curve equation ( $y = 8468.6x + 16576$ ,  $R^2 = 0.999$ ) was used to calculate the unknown drug concentration (Figure 6.1) and the method was validated using ICH guidelines (Table 6.2). The saturation point of verapamil was determined by plotting the correlation between the soluble concentration of verapamil (mg/ml) v/s surfactants and co-surfactants. As a result, when compared to transcitol, span 80, PVP, and glycerol, verapamil had the highest solubility in brij 35 ( $53.19 \pm 0.80$  mg/mL) and propylene glycol ( $62.21 \pm 1.48$  mg/mL) (Figure 6.2). Bhalekar *et al.* formulated darunavir-loaded SLNs using Tween 80 and Span 80 (325). The combination of Tween 80 and Span 80 produced particles of smaller size. Tween, a long-chain surfactant, stabilises the aqueous phase of the emulsions while Span, a short-chain surfactant, stabilises the lipidic phase into the continuous aqueous phase. As a result, an emulsion system with low particle size and PDI is formed. Similarly, Brij 35 (long chain surfactant) with an HLB value of 15 was chosen as a surfactant for this study and propylene glycol (short chain) was chosen as a co-surfactant.

The solubility of verapamil was further tested in different ratios of S/CoS (1:1, 1:3, and 3:1). As shown in Figure 6.3, verapamil was highly soluble in 1:1 ratio of brij 35/propylene glycol ( $\sim 110$  mg/mL) compared to 1:3 and 3:1. Based on solubility studies, 1:1 ratio of brij 35 and propylene glycol were selected as surfactant/co-surfactant system as they showed good solubility profile for verapamil compared to other S/CoS ratios.

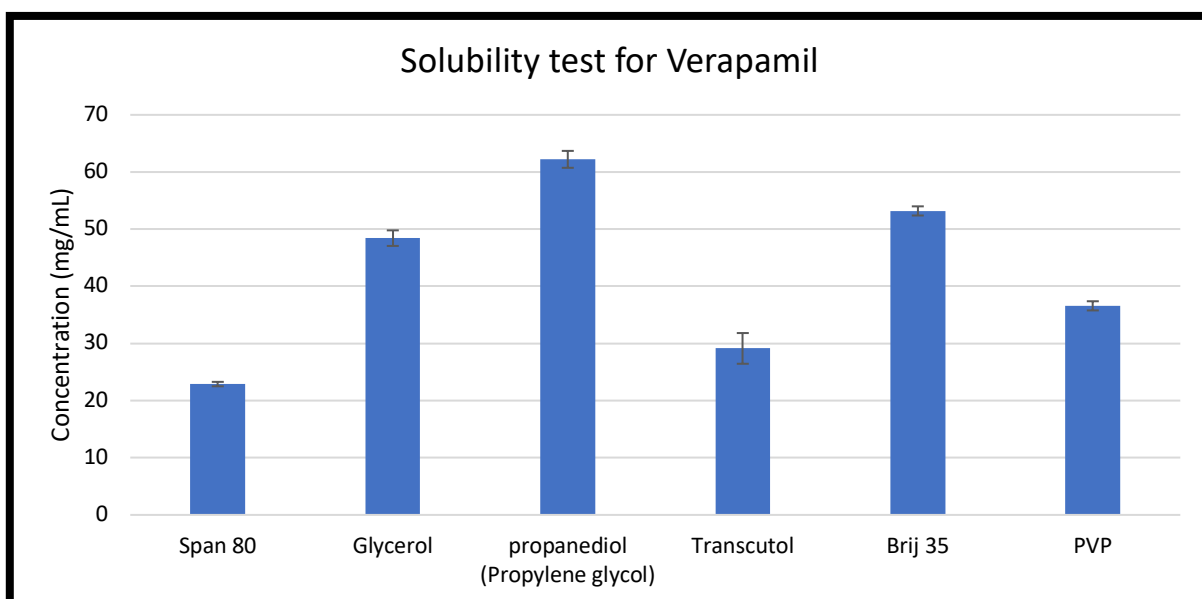




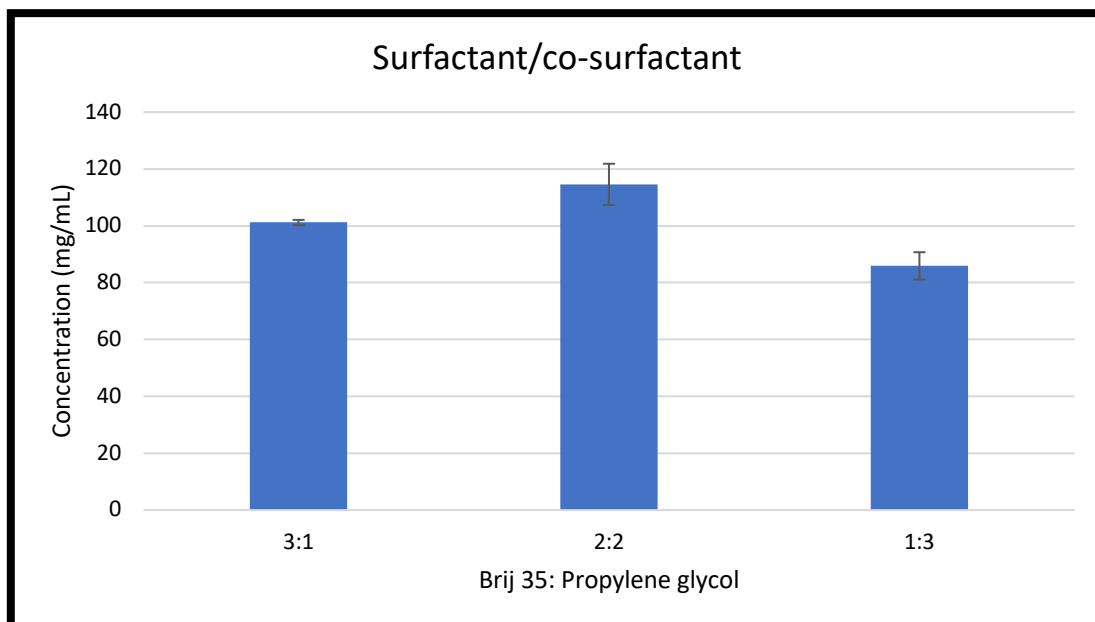
**Figure 6.1** Calibration curve for verapamil used for saturation solubility and in vitro release study. The x-axis represents concentration of verapamil and y-axis is the AUC response to specific concentration.

**Table 6.2** Validation parameters for verapamil

Linearity (R <sup>2</sup> value)	Concentration (µg/mL)	Accuracy (%)	Precision (%)	LOQ (µg/mL)	LOD (µg/mL)
0.999	8	103.98 ±2.87	1.57 ±1.00	2.51	1.98
	22	99.57 ±2.56	1.96 ±1.78		
	100	102.39 ±1.33	1.33 ±1.02		



**Figure 6.2** Saturation solubility of verapamil in different surfactants and co-surfactants.



**Figure 6. 3** Saturation solubility of verapamil in different ratios of brij 35 and propylene glycol.

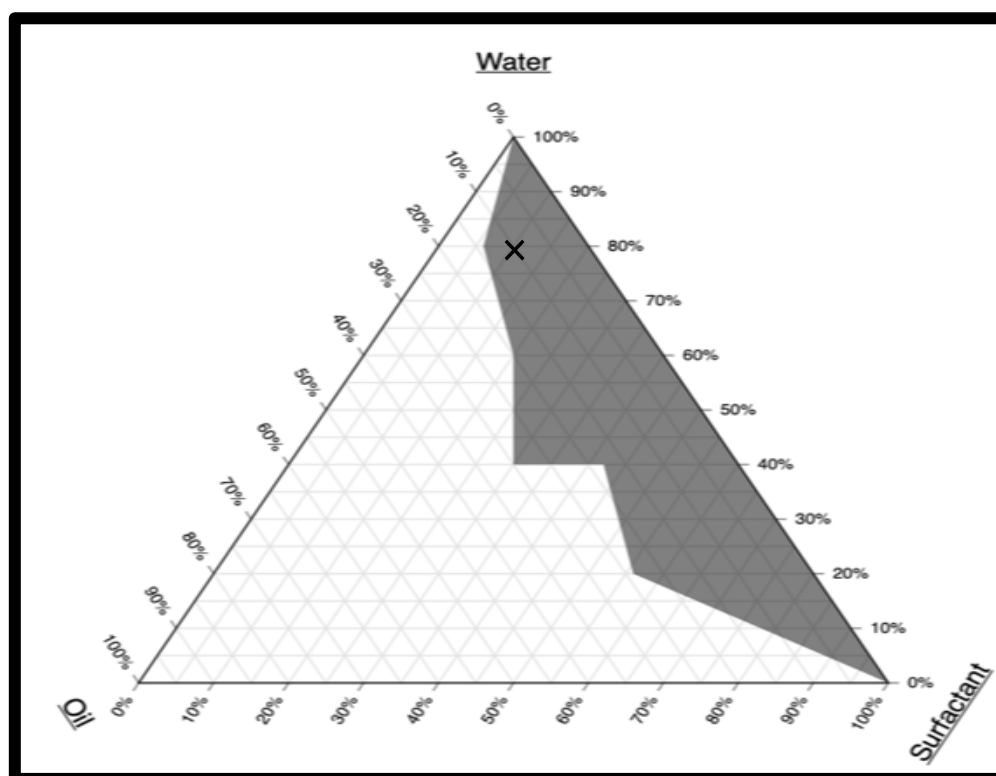
### 6.2.2 Pseudo-ternary phase diagram

The pseudo-ternary phase diagram for microemulsion was constructed using hot emulsion technique. The ternary phase diagram was created by varying the ratios of stearic acid (oil), water, and the S/CoS (1:1 v/v ratio) system (Figure 6.4).

As mentioned in section 4.2.2, when different combinations of oil, water, and S/CoS are combined, microemulsion is formed.

The shaded region in the phase diagram represents the ME region, while the non-shaded area represents no emulsion. ME region was formed with a higher water-to-oil and S/CoS ratio. Brij 35 is hydrophilic in nature which makes it more soluble in water, hence it tends to form oil-in-water emulsions. Short-chain alcohols and polyols like propylene glycol (PG) are known to function as co-surfactants. Since PG is primarily soluble in water (226), it is assumed that a significant amount of it gets incorporated into the surfactant layer and will increase interfacial fluidity while the remaining portion of it will lower the polarity of the water. One of the least hydrophilic simple polyols, PG is essentially insoluble in oil phase yet soluble in water. The maximum amount of incorporated water in the oil-surfactant system increased with the incorporation of co-surfactants like PG, with the microemulsion zone increasing in comparison to the surfactant system (226).

Based on the results and visual inspection 1:1:8 (SA:S/CoS:water) ratio was chosen for developing verapamil-loaded SLNs.



**Figure 6.4** Pseudo-ternary phase diagram representing microemulsion (shaded region) and non-microemulsion (non-shaded region). The cross on diagram represents the ratio of selected SLNs formulation.

#### 6.2.4 Size distribution and zeta potential of SLN

The size of the nanoparticles is an important factor since it affects how quickly and how much medication is distributed, as well as how much of it is absorbed. The greater interfacial surface area available for drugs absorption due to the lower particle size promotes bioavailability (321). As shown in Table 6.3, the droplet size of SLNs falls under the acceptable range for nanoparticles ( $300.30 \pm 80.46$  nm). This is due to a decrease in interfacial tension between the lipid and aqueous phases, which results in the formation of smaller emulsion droplets. The particle size was found to be in agreement with Bhalekar *et al.* study. The combination of long chain surfactant (Tween 80) and short chain co-surfactant (Span 80) resulted in particles of diameter 346 nm (325).

The mean size of the particles, the solvent's refractive index, the measuring angle, and the variance of the distribution are all considered when calculating the polydispersity index. High polydispersity index values signify a wide size dispersion,

whilst low polydispersity index readings may imply better particle population homogeneity (321). The PDI value for SLNs was found to be in acceptable range ( $0.49 \pm 0.08$ ).

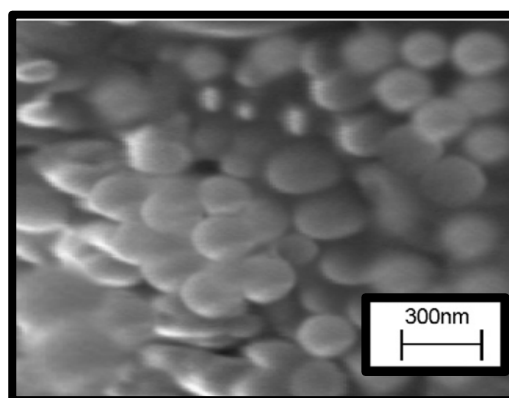
Zeta potential this formulation was found to be  $-19.1 \pm 3.64$  mV. The negative charge is caused by the ionisation of the hydrophilic carboxyl group in stearic acid as explained in section 4.2.4 (236). Additionally, the negative charge on the surface of the nanoparticle is thought to facilitate uptake from the intestine by the Payers patch, leading to the lymphatic circulation, and it is also thought to prevent entanglement of the nanoparticles in the negatively charged mucous because like charges repel one another (325). Results in Table 6.3, suggests that SLNs produced in this study are predicted as physically stable dispersions.

**Table 6.3** Average particle size, PDI and zeta potential for verapamil-loaded SLNs.

	<b>Average particle size (nm)</b>	<b>PDI</b>	<b>Zeta potential (mV)</b>
<b>Verapamil based SLN</b>	$300.30 \pm 80.46$	$0.49 \pm 0.08$	$-19.1 \pm 3.64$

#### 6.2.5 Scanning electron microscopy (SEM)

SEM was used to complete the morphology and particle size information of verapamil-loaded SLNs. According to SEM images, most of the particles in the verapamil-loaded SLNs were spherical in shape with smooth surface (Figure 6.5). As a result, it is possible to confirm that the method used to produce SLNs in this experiment was well-established.



**Figure 6. 5** SEM image depicting spherical and smooth verapamil-loaded SLNs.

### 6.2.6 Entrapment efficiency and loading capacity

Entrapment efficiency is one of the important parameters for characterizing SLNs. According to a literature, indirect approach is frequently used to assess the entrapment efficiency of a drug in SLNs where, % drug content in aqueous phase after separation from the lipid particles is determined (237). As shown in Table 6.4, the entrapment efficiency of the formulation was found to be 77.34%. The amount of surfactant can have significant effect on entrapment efficiency. Hongyu Ji *et al.* optimised curcumin-loaded SLNs using Plackett–Burman screening design and Box–Behnken experiment design. The data revealed that increasing surfactant amount in the formulation can also have negative effect. The drug can dissolve more into surfactant than in the solid lipids resulting in poor entrapment efficiency (326). On the other hand the lower surfactant concentration may result in less stabilisation of the particle due to insufficient surfactant covering of the nanoparticles (327). The higher entrapment efficiency of 77.34 may be attributed to increased surface covering of nanoparticles by a suitable surfactant concentration, which stops drug leakage from the lipid matrix. Thus, verapamil-loaded SLNs were formulated using ternary phase diagram to incorporate maximum amount of verapamil.

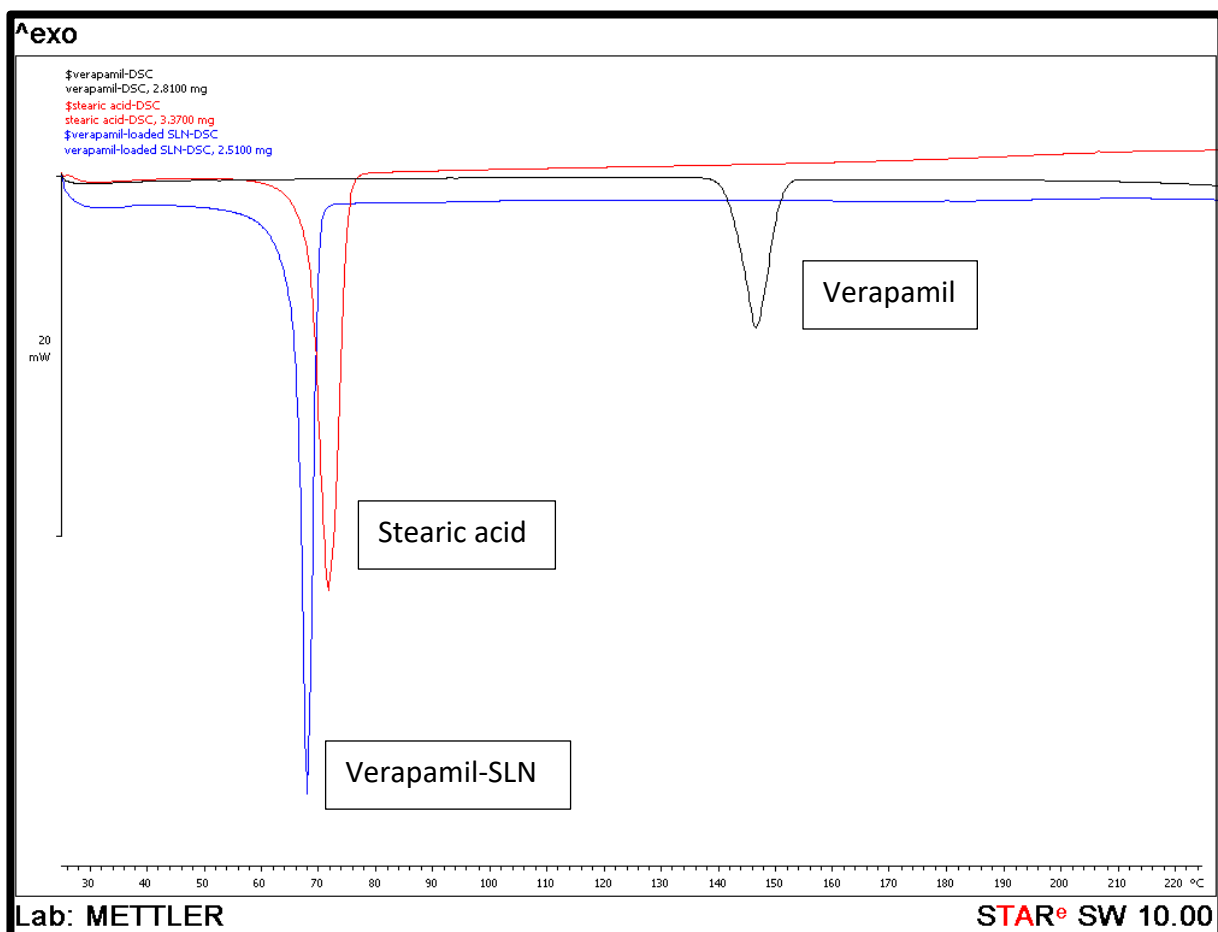
Verapamil-loaded SLNs were fabricated using techniques identical to those used to create testosterone-loaded SLNs (F1 and F2) in Chapter 4. The F1 and verapamil-loaded SLNs had the same composition but had a varied entrapment efficiency for the loaded agents. This can be explained by hydrophilic nature of surfactant as well as solubility of verapamil. Brij 35 as well as verapamil are water soluble resulting in entrapment profile with right balance of S/CoS system. Hence, according to testosterone- and verapamil-loaded SLNs, the entrapment efficiency was affected by the concentration of S/CoS system and type of drug.

**Table 6.4** Entrapment efficiency and loading capacity of verapamil-SLN

Formulation	EE (%)	LC (%)
Verapamil-loaded SLNs	77.35 ±2.67	1.13 ±0.34

### 6.2.7 Thermal analysis

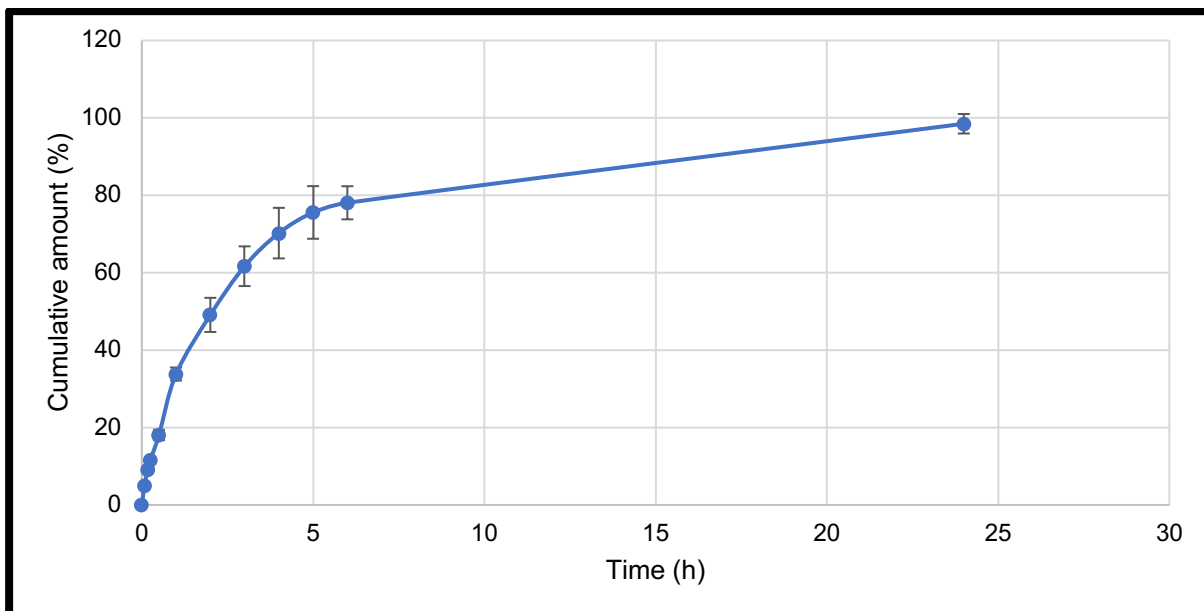
DSC analysis was used to perform thermal analysis of solid lipid nanoparticles to determine physical transformations (such as phase transitions) of the nanoparticle's components in response to heat flow to the samples. DSC data provides evidence as to whether a given sample is crystalline or amorphous. DSC curves for stearic acid, verapamil, and verapamil-loaded SLN are shown in Figure 6.6. Endothermic peaks were observed for stearic acid and verapamil at 71.64°C and 146.46°C, respectively. Whereas verapamil-loaded SLN showed only one endothermic peak at 68.00°C, which can be attributed to stearic acid's melting point. According to reports, when the drug does not show its endothermic peak in nanosized formulations, it is considered to be amorphous (328) (329) (321). The thermogram of this formulation showed no peak at the melting point of verapamil, it was possible to conclude that verapamil was molecularly dispersed within the lipid matrix, which is supported by verapamil dissolution in the molten lipid (stearic acid) during loading (248). The data can be supported by previously reported study where, DSC thermogram of verapamil-loaded SLNs showed no peak for verapamil in SLNs (321). Furthermore, the stearic acid peak in the formulation shifted to a lower temperature. This is due to an increase in surface area in regard to particle size reduction, which lowers the melting enthalpy when compared to heat flow through large crystals. (249).



**Figure 6.6** DSC data for verapamil (black peak), stearic acid (red peak), and verapamil-SLN (blue peak).

### 6.2.8 *In vitro* release study

The drug release behaviour *in vitro* of verapamil-SLNs was investigated using a dialysis membrane in phosphate buffer pH 6.8. The release of verapamil from the SLNs was found to be sustained with zero lag time (Figure 6.7). The formulation showed burst release with almost 20% drug release with in first 0.5 h followed by the sustained release from the SLNs. This burst release could be caused by the presence of free verapamil in the external phase and on the surface of the nanoparticles. The slow release following burst release is attributed to the entrapped verapamil inside lipid core. Thus, by using verapamil-loaded SLNs, it is possible to achieve the loading dose of the drug via initial burst release, followed by the maintenance dose via sustained release. This will, in fact, prevent fluctuations in the drug plasma level (323).

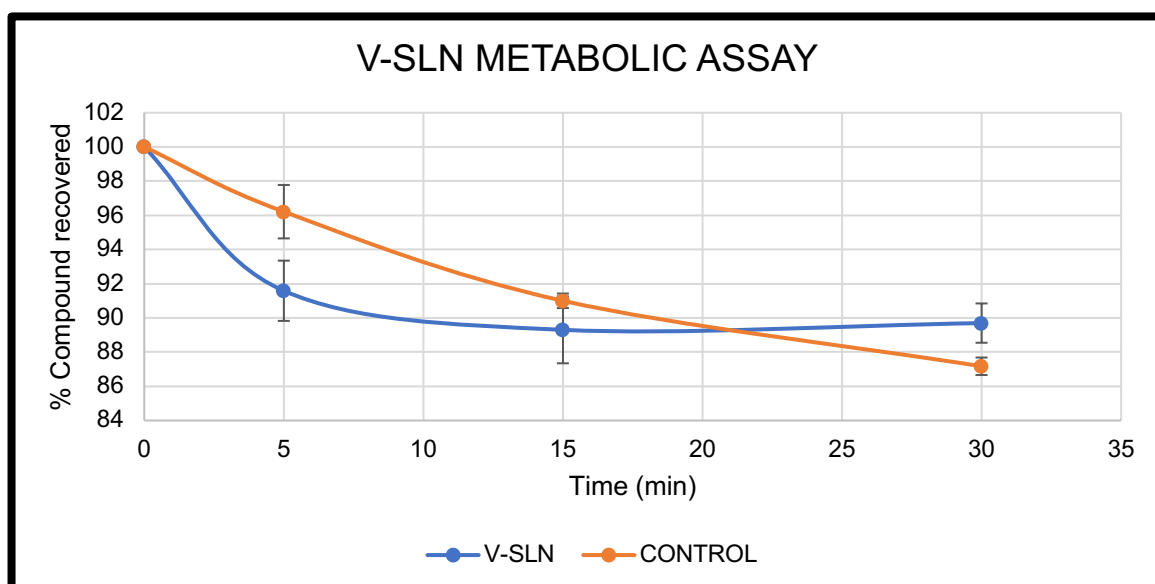


**Figure 6. 7** *In vitro* release study for verapamil from SLNs formulation using phosphate buffer pH6.8. The experiment was performed in triplicates ( $n=3$ ) and the data are presented as mean cumulative amount (%)  $\pm$ SD

#### 6.2.9 *In vitro* metabolic assay

Verapamil-loaded SLN was tested for CYP450 inhibition in order to decrease metabolism of verapamil. The metabolic assay method was the same as the *in vitro* metabolic assay method used for excipient screening. For a better comparison of SLN data with control data, a compound remaining v/s time graph was plotted (Figure 6.8). As a result, approximately 89.70% of the compound was recovered from verapamil-loaded SLN, while approximately 87.17% was recovered from the control sample. In other words, stearic acid present in verapamil-loaded SLN weakly inhibited CYP450 and hence, the metabolism of verapamil was reduced to some extent. One possible explanation is the initial burst release of verapamil from SLNs which makes them readily available for CYP450 enzymes, causing poor inhibition by stearic acid. Furthermore, verapamil-loaded SLNs had better intrinsic clearance ( $CL_{int} = 0.014$  L/min/mg) and half-life ( $T_{1/2} = 100$ min) when compared to controls ( $CL_{int} = 0.019$  L/min/mg,  $T_{1/2} = 73.39$  min). The inhibitory effect of stearic acid reported in the previous chapter, combined with the lipid protection provided by the SLN from enzymatic degradation, makes this formulation a viable candidate for oral verapamil drug delivery. YiFan Luo *et al* created SLNs to improve vinpocetine oral bioavailability. The results were like our report, in which vinpocetine's bioavailability was increased by incorporating it into SLNs, thereby reducing drug exposure to enzymatic degradation (253).





**Figure 6.8** metabolic assay of verapamil-SLNs, where = stearic acid and other excipients showed weak inhibition towards CYP450 isoforms.

#### 6.2.10 Permeability study of verapamil-loaded SLN formulation

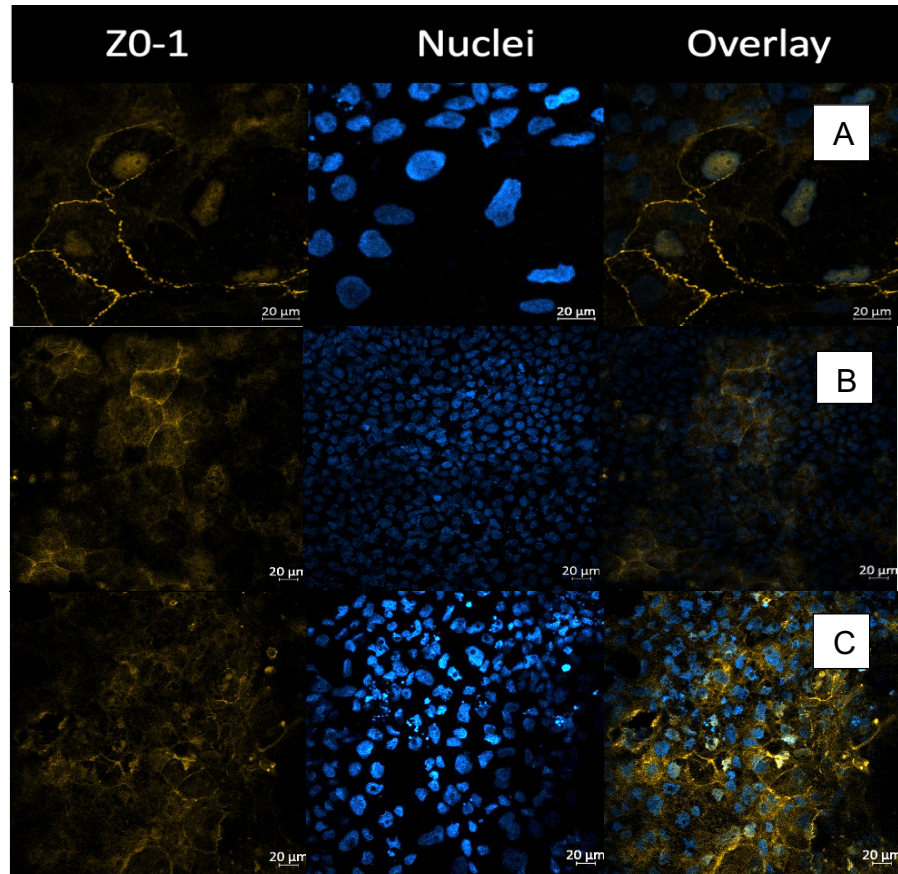
Caco-2 cells are the most commonly used as a model of the intestinal cell barrier. Caco-2 cells, a human epithelial colorectal adenocarcinoma, spontaneously develop into a polarised epithelial cell monolayer with morphological and biochemical similarities to intestinal epithelium. Caco-2 cells express TJs between adjacent cells, microvillar transporter, and efflux proteins when they reach a confluent monolayer on a cell culture filter (330). A significant amount of P-glycoprotein is also established, which is usually considered as an additional component influencing drug absorption and pharmacokinetics (331). This makes these cells an ideal tool for predicting and understanding the underlying carrier-mediated mechanisms of nanoparticles, therapeutically important protein, peptide, and chemical compound absorption across human intestinal tissue.

To compare the cellular uptake of verapamil-loaded SLNs with verapamil, Caco-2 cell monolayers was selected as model. Confocal microscopic images (Figure 6.9) confirmed the formation of a monolayer membrane, and the apical to basolateral permeabilities of verapamil were investigated in the presence and absence of lipid. The results show that the uptake of SLNs and verapamil was time dependent. After 90 minutes, there was very little fluorescence in the dye solution, indicating poor internalisation into cell monolayers. However, the fluorescence intensity of

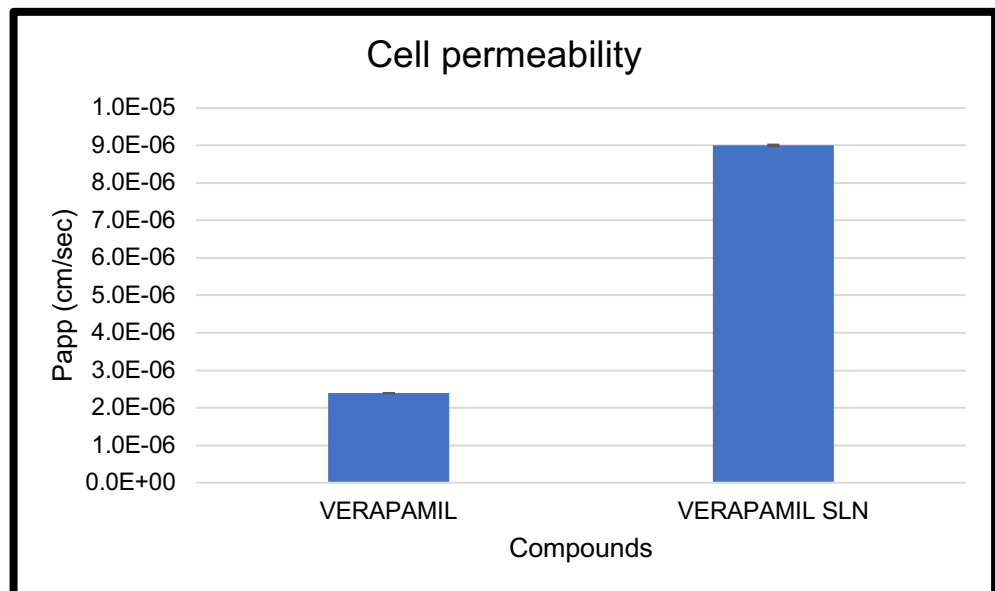
verapamil-loaded SLNs was higher in both the cell cytoplasm and the nucleus, indicating that the SLNs were internalised into the Caco-2 cells.

The equation 4.1 was used to calculate the apparent permeability ( $P_{app}$ ) of verapamil in the presence and absence (control) of stearic acid. As a result (Figure 6.10), the permeability of verapamil was significantly increased ( $P < 0.05$ ) in the presence of stearic acid ( $P_{app} = 2.39 \times 10^{-6}$  cm/sec) vs. control ( $P_{app} = 9.00 \times 10^{-6}$  cm/sec). Similar outcome was reported in Chapter 4 for testosterone-loaded SLNs. As explained in section 4.2.10, the disordering effect of stearic acid on membranes could be via a putative effect on tight junction and adherent junction proteins (paracellular gap openings) causing functional changes to the barriers (254).

Despite the fact that the Caco-2 cell monolayer model is widely used and acknowledged as a standard for assessing intestinal transport, it has some disadvantages, including a lack of mucus, which is the fundamental characteristic of the intestinal mucosa and variation between gene expression profiles (332). Therefore, further study involving a co-culture model of human HT29-MTX (goblet-like cells) with Caco-2 cell type can be developed. The co-culture model offers a transport environment that is comparable to that of the human intestinal epithelium.



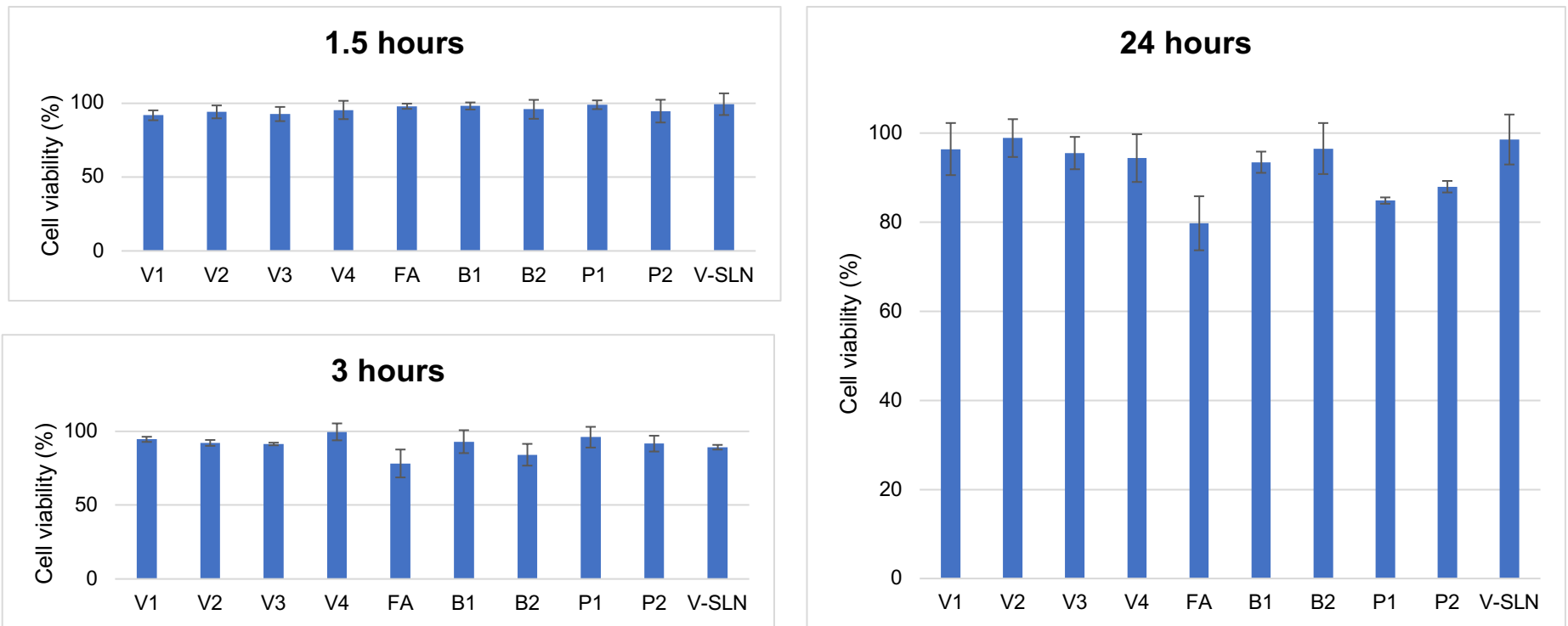
**Figure 6. 9** Confocal microscopic image for monolayers used for control (A), verapamil (B), and verapamil-SLN (C).



**Figure 6. 10** Effect of stearic acid on permeability of verapamil. The data shows significant increase ( $P < 0.05$ ) in presence of SLN formulation compared to verapamil on its own.

### 6.2.11 Cell toxicity study

The MTT assay is an easy technique that can be used to determine the cellular toxicity of developed nanoparticles by estimating the number of viable cells in microtitre tray wells. MTT assay was used to determine the toxicity of verapamil at various concentrations, excipients, and verapamil-loaded SLNs (Fig 6.11). All compounds were evaluated at three-time intervals of 1.5, 3, and 24 hours. Figure 5.14 shows that cell viability for all compounds at different concentrations remains more than or equal to 80%; however, cell toxicity was time dependent. Cell viability remains above 90% for the first 90 minutes for all compounds and SLNs, but it gradually depletes to 80-90% after 3 hours and 24 hours. Propylene glycol (P1 and P2) and stearic acid (FA) demonstrated the greatest depletion after 24 hours, while the formulation (F1) demonstrated very low toxicity. This implies that verapamil-loaded SLNs have no toxic effects on caco-2 cells and therefore, is ideal candidate as formulation for delivery of verapamil.



**Figure 6. 11** Cell viability data for verapamil and other components at different time point (1, 3 and 24 hours). Different compounds were tested for cell toxicity where V1 (2  $\mu\text{g/mL}$ ), V2 (20  $\mu\text{g/mL}$ ), V3 (40  $\mu\text{g/mL}$ ), and V4 (80  $\mu\text{g/mL}$ ) are four different concentrations of verapamil; FA represents stearic acid; B1 (10%v/v), B2 (20%v/v) and P1 (10%v/v), P2 (20%v/v) are different concentrations for brij 35 and propylene glycol, respectively; V-SLN represents verapamil-loaded SLNs formulation.

### **6.3 Conclusion**

In this study, the formulation of verapamil-loaded SLNs was systematically optimised, and their physical and chemical properties were also investigated. Variables such as surfactant concentration, surfactant type, verapamil solubility, and water: S/CoS: oil composition has a significant impact on nanoparticle particle size, entrapment efficiency, and PDI. The *in vitro* release study revealed sustained drug release from SLNs, and the microsomal assay revealed weak inhibition on CYP450 enzymes. Furthermore, even at higher concentrations, the verapamil-loaded SLNs and other compounds found in SLNs showed no cytotoxicity. Verapamil permeability across Caco-2 cells was significantly increased in the presence of stearic acid. Thus, solid lipid nanoparticles may be a promising formulation for improving the permeability of verapamil or CYP3A4/3A5 substrates as well as provide sustained drug release with higher entrapment efficiency.

# **Chapter 7: Conclusions and Future Direction**

## 7.1 Conclusions

Oral administration is the common route of drug delivery because of its convenience, high patient compliance, and cost effectiveness. Therefore, oral bioavailability is a crucial factor in the discovery and development of many novel drugs for successful oral drug therapy. The proportion of the dose absorbed from the GI lumen to the enterocytes and the fraction of the dose that avoids first-pass elimination are two factors that, in general, influence oral bioavailability. First-pass metabolism refers to the extensive metabolism of drugs before they enter the systemic circulation. CYP450 enzymes are the primary enzymes responsible for first-pass metabolism and biotransformation of therapeutic agents whereas, one of the most influencing efflux and uptake transporters, P-glycoprotein, are responsible for intestinal absorption of various drug substances. Pharmaceutical excipients play a significant role in the formulation of a dosage form by ensuring the homogeneity and safety of pharmaceutical products, facilitating disintegration, or improving API solubilization. The evidence also suggests that many excipients can alter the absorption and disposition properties of an encapsulated drug, altering its therapeutic efficacy. Surfactants, polymers, fatty acids, and solvents have previously been identified as CYP450 inhibitors. So, it has been proposed that fatty acid-based formulations can inhibit CYP450 enzymes as well as improve permeability of probe drugs.

The basis of Chapter 2 was to develop and optimise two analytical methods to quantify using cocktail approach (4-in-1) for omeprazole, dextromethorphan, verapamil, propranolol (IS), and standard approach for testosterone. LC parameters such as mobile phase composition, flow rate, injection volume, and selection of column were optimised to obtain maximum specificity and sensitivity with minimal run time. The response measured was the normalised peak area of the analytes using LCMS. The LCMS method was validated in accordance with the ICH guidelines. In this context, sensitivity, linearity, accuracy, and precision were all determined. The results were found to be linear across the concentration range investigated, with all analytes exhibiting the highest recovery values and the lowest intraday or interday variation values. The developed LCMS methods were rapid, specific, sensitive, and reproducible for quantification of all probe substrates. These methods were successfully used for screening of fatty acids, pre-formulation, and formulation studies. For screening of fatty acids, the combination of microsomal assay and LCMS were used to quantify the effect of fatty acids on CYP450



enzymes. Based on the outcome, stearic acid was found to be the most potent inhibitor for CYP450 enzymes and chosen for further pre-formulation and formulation studies.

SLNs are colloidal systems which consist of a lipid with high melting point as a solid core coated with aqueous S/CoS and the drug. The use of solid lipid rather than liquid lipid is advantageous because it has been demonstrated to improve control over the release kinetics of entrapped compounds and the stability of embedded chemically-sensitive lipophilic ingredients. Several physicochemical properties associated with the physical state of the lipid phase contribute to these potentially beneficial effects. In Chapter 3, testosterone-loaded SLNs were produced and optimised to achieve desired physicochemical properties. The concentration of S/CoS system was one of the most crucial factors that influenced the size of the particle, PDI, and entrapment efficiency of the drug. The entrapment of the drug inside SLNs was confirmed by DSC analysis and the *in vitro* dissolution study showed controlled release of testosterone from the formulation. Furthermore, the *in vitro* metabolic and permeability assays confirmed the inhibition of CYP450 enzymes and increased permeability via caco-2 cell layer. Hence, the formulation was successfully developed which reduced the metabolism of testosterone and increased its permeability in presence of stearic acid.

Hydrophilic drugs are effective therapeutic agents; however, they are difficult to deliver via SLNs as they have higher affinity towards water phase and will expel out during fabrication. As a result, developing an effective drug delivery system may involve a diverse approach. Dextromethorphan is commonly used to relief cough and its salt form is sparingly soluble in water. In Chapter 4, different strategies were used to incorporate dextromethorphan in SLNs which includes hot emulsion technique, double emulsion technique, and solvent evaporation technique. Although SLNs have been extensively studied as hydrophobic drug carriers, delivery of hydrophilic molecules remains a challenge. Hence, due to its higher affinity for aqueous phase, different strategies failed to incorporate dextromethorphan into SLNs. The mixture of dextromethorphan and other excipients (stearic acid, S/CoS, and water) were prepared to evaluate the effect of stearic acid on the permeability of the drug. According to the data, permeability was significantly improved in the presence of stearic acid compared to the control study and therefore further

research is required to improve its entrapment efficiency and different strategies to load dextromethorphan into SLNs.

Verapamil is metabolised to two main metabolites, norverapamil and D-617, which are then broken down further by the CYP450 system to form at least three additional metabolites. In Chapter 5, verapamil-loaded SLNs were prepared using hot emulsion technique. The saturation solubility test for verapamil in different surfactants and their ratios were carried out to optimise highest solubility of verapamil in S/CoS system. The ternary phase diagram was then constructed to determine microemulsion region. These microemulsion were dispersed into ice-cold water to produce SLNs and were characterized for its particle size, PDI, zeta potential and morphology. As a result, verapamil-loaded SLNs were spherical in shape with high entrapment efficiency of 77%. *In vitro* dissolution study showed burst release due to free verapamil in the external phase, followed by sustained release. However, the metabolic assay revealed weaker inhibition of CYP450 enzymes and increased permeability in presence of stearic acid-based SLNs.

To conclude, these results indicate that SLNs formulations developed with stearic acid are potential colloidal system for reducing drug metabolism and increase permeability of various lipophilic drugs. Stearic acid successfully showed inhibition effect for different CYP450 enzyme and are safe to use at distinct concentration range. However, further investigation is required to improve its encapsulation for hydrophilic drugs and must be further tested in animal models.

## 7.2 Future directions

Despite the fact that the current study effectively fabricated many SLNs, it has a number of drawbacks, which includes non-specific CYP450 enzyme inhibition studies, the use of rat liver microsomes, and stearic acid as the sole lipid for all probe drugs. The enzyme-specific inhibition strategy will provide more particular information about the inhibitor and its effect on CYP450 isoforms. Furthermore, comparing human liver microsomes and hepatocytes to rat liver microsomes will reveal qualitative similarities and differences between the two species.

There are many possibilities for the optimal approach to continue this investigation, but the outline that is provided below may be of some help.

It would be interesting to incorporate a combination of two oils which can improve the entrapment efficiency of drugs or solubility of hydrophilic and lipophilic drugs.

Another important step would be, to study the effect of all the excipients used in the preparation of SLNs on CYP450 enzymes. In this case, brij 35 and propylene glycol.

Lastly, modification of dextromethorphan to less soluble form can potentially improve its encapsulation in to SLNs. Some additional studies are also required to understand the mechanism of action of stearic acid on CYP450s and P-gp.

# References

- (1) Sastry SV, Nyshadham JR, Fix JA. Recent technological advances in oral drug delivery – a review. *Pharmaceutical Science & Technology Today* 2000;3(4):138-145.
- (2) Zhang W, Li Y, Zou P, Wu M, Zhang Z, Zhang T. The Effects of Pharmaceutical Excipients on Gastrointestinal Tract Metabolic Enzymes and Transporters—an Update. *AAPS J* 2016;18(4):830-843.
- (3) Pathak K, Raghuvanshi S. Oral Bioavailability: Issues and Solutions via Nanoformulations. *Clin Pharmacokinet* 2015;54(4):325-357.
- (4) Ezra A, Golomb G. Administration routes and delivery systems of bisphosphonates for the treatment of bone resorption. *Advanced drug delivery reviews* 2000;42(3):175-195.
- (5) Cremers SCLM, Van Hogezaand R, Banffer D, Hartigh J, Vermeij P, PAPAPOULOS SE, et al. Absorption of the oral bisphosphonate alendronate in osteoporotic patients with Crohn's disease. *Osteoporosis international* 2005;16(12):1727-1730.
- (6) Niemi R, Turhanen P, Vepsäläinen J, Taipale H, Järvinen T. Bisphosphonate prodrugs: synthesis and in vitro evaluation of alkyl and acyloxymethyl esters of etidronic acid as bioreversible prodrugs of etidronate. *European journal of pharmaceutical sciences* 2000;11(2):173-180.
- (7) Reinoso RF, Sanchez Navarro A, Garcia MJ, Prous JR. Preclinical pharmacokinetics of statins. *Methods and findings in experimental and clinical pharmacology* 2002;24(9):593-613.
- (8) Garcia MJ, Reinoso RF, Sanchez Navarro A, Prous JR. Clinical pharmacokinetics of statins. *Methods and findings in experimental and clinical pharmacology* 2003;25(6):457-481.
- (9) Buse J. Statin Treatment in Diabetes Mellitus. *Clinical Diabetes* 2003;21:168-172.
- (10) Degim IT, Acartürk F, Erdogan D, Lortlar ND. Transdermal Administration of Bromocriptine. *Biological & pharmaceutical bulletin* 2003;26(4):501-505.
- (11) Turner JV, Glass BD, Agatonovic-Kustrin S. Prediction of drug bioavailability based on molecular structure. *Analytica chimica acta* 2003;485(1):89-102.
- (12) Dorne JLCM, Walton K, Renwick AG. Human variability in CYP3A4 metabolism and CYP3A4-related uncertainty factors for risk assessment. *Food and chemical toxicology* 2003;41(2):201-224.
- (13) Mary N, J, Kumar P, S. Cross-linked nanoparticles of cytarabine: Encapsulation, storage and in-vitro release. *International Journal of Pharmacy and Pharmacology* ;1(1):1.

- (14) Ahmad N, Keith-Ferris J, Gooden E, Abell T. Making a case for domperidone in the treatment of gastrointestinal motility disorders. *Current opinion in pharmacology* 2006;6(6):571-576.
- (15) Sturgill MG, August DA, Brenner DE. Hepatic Enzyme Induction with Phenobarbital and Doxorubicin Metabolism and Myelotoxicity in the Rabbit. *Cancer investigation* 2000;18(3):197-205.
- (16) Bennett M, Lucas V, Brennan M, Hughes A, O'Donnell V, Wee B. Using anti-muscarinic drugs in the management of death rattle: evidence-based guidelines for palliative care. *Palliative medicine* 2002 Jul;16(5):369-374.
- (17) Tse FLS, Jaffe JM. Pharmacokinetics of PN 200-110 (isradipine), a new calcium antagonist, after oral administration in man. *European journal of clinical pharmacology* 1987;32(4):361-365.
- (18) Kharasch ED, Labroo R. Metabolism of Ketamine Stereoisomers by Human Liver Microsomes. *Anesthesiology (Philadelphia)* 1992;77(6):1201-1207.
- (19) Isohanni MH, Neuvonen PJ, Olkkola KT. Effect of Fluvoxamine and Erythromycin on the Pharmacokinetics of Oral Lidocaine. *Basic & clinical pharmacology & toxicology* 2006 Aug;99(2):168-172.
- (20) Manoir BD, Bourget P, Langlois M, Szekely B, Fischler M, Chauvin M, et al. Evaluation of the pharmacokinetic profile and analgesic efficacy of oral morphine after total hip arthroplasty. *European journal of anaesthesiology* 2006 Sep;23(9):748-754.
- (21) Choi Jun-Shik, Burm Jin-Pil. Enhanced Nimodipine Bioavailability After Oral Administration of Nimodipine with Morin, a Flavonoid, in Rabbits. *Archives of pharmacal research* 2006;29(4):333-338.
- (22) Kleiman-Wexler RL, Adair CG, Ephgrave KS. Pharmacokinetics of naloxone: an insight into the locus of effect on stress-ulceration. *The Journal of pharmacology and experimental therapeutics* 1989 Nov 1;;251(2):435-438.
- (23) Aquilonius SM, Eckernäs SA, Hartvig P, Lindström B, Osterman PO. Pharmacokinetics and oral bioavailability of pyridostigmine in man. *European journal of clinical pharmacology* 1980 Nov;18(5):423-428.
- (24) Finn A, Collins J, Voyksner R, Lindley C. Bioavailability and Metabolism of Prochlorperazine Administered via the Buccal and Oral Delivery Route. *Journal of clinical pharmacology* 2005 Dec;45(12):1383-1390.
- (25) Clarke A, Jankovic J. Selegiline orally disintegrating tablet in the treatment of Parkinson's disease. *Therapy* 2006 May 1;;3(3):349-356.
- (26) Cosson VF, Fuseau E. Mixed effect modeling of sumatriptan pharmacokinetics during drug development : II. From healthy subjects to phase 2 dose ranging in patients. *Journal of pharmacokinetics and biopharmaceutics* 1999;27(2):149-171.
- (27) Jann MW, Shirley KL, Small GW. Clinical Pharmacokinetics and Pharmacodynamics of Cholinesterase Inhibitors. *Clinical Pharmacokinetics* 2002;41(10):719-739.

- (28) Nakhat P, Kondawar A, Babla I, Rathi L, Yeole P. Studies on buccoadhesive tablets of terbutaline sulphate. *Indian journal of pharmaceutical sciences* 2007 Jul 1,;69(4):505.
- (29) Wang Q, Li M. Presystemic and First-Pass Metabolism. *Drug Delivery*; 2016. p. 164-185.
- (30) Nelson DR. The Cytochrome P450 Homepage. *Human Genomics* 2009 Oct;4(1):59-65.
- (31) Zanger UM, Turpeinen M, Klein K, Schwab M. Functional pharmacogenetics/genomics of human cytochromes P450 involved in drug biotransformation. *Anal Bioanal Chem* 2008;392(6):1093-1108.
- (32) Markovic M, Ben-Shabat S, Keinan S, Aponick A, Zimmermann EM, Dahan A. Lipidic prodrug approach for improved oral drug delivery and therapy. *Medicinal research reviews* 2019 Mar;39(2):579-607.
- (33) Huttunen KM, Raunio H, Rautio J. Prodrugs—from Serendipity to Rational Design. *Pharmacological reviews* 2011 Sep;63(3):750-771.
- (34) Wolk O, Agbaria R, Dahan A. Provisional in-silico biopharmaceutics classification (BCS) to guide oral drug product development. *Drug Design, Development and Therapy* 2014;8:1563-1575.
- (35) Rautio J, Kumpulainen H, Heimbach T, Oliyai R, Oh D, Järvinen T, et al. Prodrugs: design and clinical applications. *Nature reviews. Drug discovery* 2008 Mar;7(3):255-270.
- (36) Clas S, Sanchez RI, Nofsinger R. Chemistry-enabled drug delivery (prodrugs): recent progress and challenges. *Drug discovery today* 2014 Jan;19(1):79-87.
- (37) Zawilska JB, Wojcieszak J, Olejniczak AB. Prodrugs: A challenge for the drug development. *Pharmacol Rep* 2013 Jan;65(1):1-14.
- (38) Dahan A, Zimmermann EM, Ben-Shabat S. Modern Prodrug Design for Targeted Oral Drug Delivery. *Molecules* 2014 Oct 14,;19(10):16489-16505.
- (39) Han HK, Amidon GL. Targeted prodrug design to optimize drug delivery. *AAPS PharmSci* 2000;2(1):6.
- (40) Amidon GL, Leesman GD, Elliott RL. Improving intestinal absorption of water-insoluble compounds: A membrane metabolism strategy. *Journal of pharmaceutical sciences* 1980 Dec;69(12):1363-1368.
- (41) Stella VJ. Prodrugs: Some Thoughts and Current Issues. *Journal of pharmaceutical sciences* 2010 Dec;99(12):4755-4765.
- (42) Pereira de Sousa I, Bernkop-Schnürch A. Pre-systemic metabolism of orally administered drugs and strategies to overcome it. *Journal of controlled release* 2014 Oct 28,;192:301-309.
- (43) Bailey DG, Malcolm J, Arnold O, David Spence J. Grapefruit juice—drug interactions. *British journal of clinical pharmacology* 1998 Aug;46(2):101-110.

- (44) Fasinu P, Choonara YE, Khan RA, Du Toit LC, Kumar P, K. Ndesendo VM, et al. Flavonoids and Polymer Derivatives as CYP3A4 Inhibitors for Improved Oral Drug Bioavailability. *Journal of pharmaceutical sciences* 2013 Feb;102(2):541-555.
- (45) Lin H, Kent UM, Hollenberg PF. The Grapefruit Juice Effect Is Not Limited to Cytochrome P450 (P450) 3A4: Evidence for Bergamottin-Dependent Inactivation, Heme Destruction, and Covalent Binding to Protein in P450s 2B6 and 3A5. *The Journal of pharmacology and experimental therapeutics* 2005 Apr 1;313(1):154-164.
- (46) Tassaneeyakul W, Guo L, Fukuda K, Ohta T, Yamazoe Y. Inhibition Selectivity of Grapefruit Juice Components on Human Cytochromes P450. *Archives of biochemistry and biophysics* 2000 Jun 15;378(2):356-363.
- (47) Girenavar B, Poulouse SM, Jayaprakasha GK, Bhat NG, Patil BS. Furocoumarins from grapefruit juice and their effect on human CYP 3A4 and CYP 1B1 isoenzymes. *Bioorganic & medicinal chemistry* 2006;14(8):2606-2612.
- (48) Paine MF, Criss AB, Watkins PB. Two Major Grapefruit Juice Components Differ in Intestinal CYP3A4 Inhibition Kinetic and Binding Properties. *Drug metabolism and disposition* 2004 Oct 1;32(10):1146-1153.
- (49) Paine MF, Criss AB, Watkins PB. Two Major Grapefruit Juice Components Differ in Time to Onset of Intestinal CYP3A4 Inhibition. *The Journal of pharmacology and experimental therapeutics* 2005 Mar 1;312(3):1151-1160.
- (50) Greenblatt DJ, Moltke LL, Harmatz JS, Chen G, Weemhoff JL, Jen C, et al. Time course of recovery of cytochrome p450 3A function after single doses of grapefruit juice. *Clinical pharmacology and therapeutics* 2003 Aug;74(2):121-129.
- (51) Ohnishi A, Matsuo H, Yamada S, Takanaga H, Morimoto S, Shoyama Y, et al. Effect of furanocoumarin derivatives in grapefruit juice on the uptake of vinblastine by Caco-2 cells and on the activity of cytochrome P450 3A4. *British journal of pharmacology* 2000 Jul;130(6):1369-1377.
- (52) Eagling, Profit, Back. Inhibition of the CYP3A4-mediated metabolism and P-glycoprotein-mediated transport of the HIV-1 protease inhibitor saquinavir by grapefruit juice components. *British journal of clinical pharmacology* 1999 Oct;48(4):543-552.
- (53) Fukuda K, Ohta T, Yamazoe Y. Grapefruit Component Interacting with Rat and Human P450 CYP3A : Possible Involvement of Non-Flavonoid Components in Drug Interaction. *Biological & pharmaceutical bulletin* 1997 May 15;20(5):560-564.
- (54) Hanley MJ, Cancalon P, Widmer WW, Greenblatt DJ. The effect of grapefruit juice on drug disposition. *Expert opinion on drug metabolism & toxicology* 2011 Mar;7(3):267-286.
- (55) Galetin A, Gertz M, Brian Houston J. Contribution of Intestinal Cytochrome P450-Mediated Metabolism to Drug-Drug Inhibition and Induction Interactions. *Drug metabolism and pharmacokinetics* 2010;25(1):28-47.

- (56) Bylund J, Bueters T. Presystemic Metabolism of AZ'0908, A Novel mPGES-1 Inhibitor: An In Vitro and In Vivo Cross-Species Comparison. *Journal of pharmaceutical sciences* 2013 Mar;102(3):1106-1115.
- (57) Zhou S, Yung Chan S, Cher Goh B, Chan E, Duan W, Huang M, et al. Mechanism-Based Inhibition of Cytochrome P450 3A4 by Therapeutic Drugs. *Clinical Pharmacokinetics* 2005;44(3):279-304.
- (58) Horn JR, Howden CW. Review article: similarities and differences among delayed-release proton-pump inhibitor formulations. *Alimentary pharmacology & therapeutics* 2005 Dec;22(s3):20-24.
- (59) Lueßen HL, Rentel C-, Kotzé AF, Lehr C-, de Boer AG, Verhoef JC, et al. Mucoadhesive polymers in peroral peptide drug delivery. IV. Polycarbophil and chitosan are potent enhancers of peptide transport across intestinal mucosae in vitro. *Journal of controlled release* 1997;45(1):15-23.
- (60) Ren X, Mao X, Si L, Cao L, Xiong H, Qiu J, et al. Pharmaceutical excipients inhibit cytochrome P450 activity in cell free systems and after systemic administration. *European journal of pharmaceutics and biopharmaceutics* 2008;70(1):279-288.
- (61) Holubek WJ, Kalman S, Hoffman RS. Acetaminophen-induced acute liver failure: results of a United States multicenter, prospective study. *Hepatology (Baltimore, Md.)* 2006 Apr;43(4):880; author reply 882-880.
- (62) Marx J. Protecting Liver from Painkiller's Lethal Dose. *Science (American Association for the Advancement of Science)* 2002 Oct 11,;298(5592):341-342.
- (63) Zaher H, Buters JTM, Ward JM, Bruno MK, Lucas AM, Stern ST, et al. Protection against Acetaminophen Toxicity in CYP1A2 and CYP2E1 Double-Null Mice. *Toxicology and applied pharmacology* 1998 Sep;152(1):193-199.
- (64) Ganetsky M, Böhlke M, Pereira L, Williams D, LeDuc B, Guatam S, et al. Effect of Excipients on Acetaminophen Metabolism and Its Implications for Prevention of Liver Injury. *Journal of clinical pharmacology* 2013 Apr;53(4):413-420.
- (65) Sekhon BS. Surfactants: Pharmaceutical and Medicinal Aspects. *Journal of Pharmaceutical Technology, Research and Management* 2013 May 2,;1(1):43-68.
- (66) Gelderblom H, Verweij J, Nooter K, Sparreboom A. Cremophor EL: the drawbacks and advantages of vehicle selection for drug formulation. *European journal of cancer (1990)* 2001 Sep;37(13):1590-1598.
- (67) Christiansen A, Backensfeld T, Denner K, Weitschies W. Effects of non-ionic surfactants on cytochrome P450-mediated metabolism in vitro. *European journal of pharmaceutics and biopharmaceutics* 2011;78(1):166-172.
- (68) Mudra DR, Borchardt RT. Absorption Barriers in the Rat Intestinal Mucosa. 3: Effects of Polyethoxylated Solubilizing Agents on Drug Permeation and Metabolism. *Journal of pharmaceutical sciences* 2010 Feb;99(2):1016-1027.
- (69) Hugger ED, Novak BL, Burton PS, Audus KL, Borchardt RT. A comparison of commonly used polyethoxylated pharmaceutical excipients on their ability to inhibit



- P-glycoprotein activity in vitro. *Journal of pharmaceutical sciences* 2002 Sep;91(9):1991-2002.
- (70) Hugger ED, Audus KL, Borchardt RT. Effects of Poly(ethylene glycol) on Efflux Transporter Activity in Caco-2 Cell Monolayers. *Journal of pharmaceutical sciences* 2002 Sep;91(9):1980-1990.
- (71) Regev R, Assaraf, Yehuda G., Eytan GD. Membrane fluidization by ether, other anesthetics, and certain agents abolishes P-glycoprotein ATPase activity and modulates efflux from multidrug-resistant cells. *European journal of biochemistry* 1999 Jan;259(1-2):18-24.
- (72) Rege BD, Kao JPY, Polli JE. Effects of nonionic surfactants on membrane transporters in Caco-2 cell monolayers. *European journal of pharmaceutical sciences* 2002;16(4):237-246.
- (73) Randall K, Cheng SW, Kotchevar AT. Evaluation of surfactants as solubilizing agents in microsomal metabolism reactions with lipophilic substrates. *In Vitro Cell Dev Biol -Animal* 2011;47(9):631-639.
- (74) Bravo González RC, Huwyler J, Boess F, Walter I, Bittner B. In vitro investigation on the impact of the surface-active excipients Cremophor EL, Tween 80 and Solutol HS 15 on the metabolism of midazolam. *Biopharmaceutics & drug disposition* 2004 Jan;25(1):37-49.
- (75) Jamis-dow CA, Klecker RW, Katki AG, Collins JM. Metabolism of taxol by human and rat liver in vitro: A screen for drug interactions and interspecies differences. *Cancer chemotherapy and pharmacology* 1995;36(2):107-114.
- (76) Tayrouz Y, Ding R, Burhenne J, Riedel K, Weiss J, Hoppe-Tichy T, et al. Pharmacokinetic and pharmaceutic interaction between digoxin and Cremophor RH40. *Clinical pharmacology and therapeutics* 2003 May;73(5):397-405.
- (77) Rao Z, Si L, Guan Y, Pan H, Qiu J, Li G. Inhibitive effect of cremophor RH40 or tween 80-based self-microemulsifying drug delivery system on cytochrome P450 3A enzymes in murine hepatocytes. *J Huazhong Univ Sci Technol [Med Sci]* 2010;30(5):562-568.
- (78) Lim Y, Kuo S, Lai M, Huang J. Inhibition of CYP3A4 expression by ketoconazole is mediated by the disruption of pregnane X receptor, steroid receptor coactivator-1, and hepatocyte nuclear factor 4alpha interaction. *Pharmacogenetics and genomics* 2009 Jan;19(1):11-24.
- (79) Fujita T, Yasuda S, Kamata Y, Fujita K, Ohtani Y, Kumagai Y, et al. Contribution of Down-Regulation of Intestinal and Hepatic Cytochrome P450 3A to Increased Absorption of Cyclosporine A in a Rat Nephrosis Model. *The Journal of pharmacology and experimental therapeutics* 2008 Nov 1;327(2):592-599.
- (80) Ren S, Park M, Kim A, Lee B. In vitro metabolic stability of moisture-sensitive rabeprazole in human liver microsomes and its modulation by pharmaceutical excipients. *Arch Pharm Res* 2008;31(3):406-413.

- (81) Farsang E, Gaál V, Horváth O, Bárdos E, Horváth K. Analysis of Non-Ionic Surfactant Triton X-100 Using Hydrophilic Interaction Liquid Chromatography and Mass Spectrometry. *Molecules* 2019 Mar 28;24(7):1223.
- (82) Da Silva MEF, Meirelles NC. Interaction of non-ionic surfactants with hepatic CYP in *Prochilodus scrofa*. *Toxicology in vitro* 2004;18(6):859-867.
- (83) Karolewicz B. A review of polymers as multifunctional excipients in drug dosage form technology. *Saudi Pharmaceutical Journal* 2016 Sep;24(5):525-536.
- (84) Qiu L, Li Q, Huang J, Wu Q, Tu K, Wu Y, et al. In vitro effect of mPEG2k-PCLx micelles on rat liver cytochrome P450 enzymes. *International journal of pharmaceutics* 2018 Dec 1;552(1-2):99-110.
- (85) Martin P, Giardiello M, McDonald TO, Rannard SP, Owen A. Mediation of in Vitro Cytochrome P450 Activity by Common Pharmaceutical Excipients. *Molecular pharmaceutics* 2013 Jul 1;10(7):2739-2748.
- (86) Huang J, Si L, Jiang L, Fan Z, Qiu J, Li G. Effect of pluronic F68 block copolymer on P-glycoprotein transport and CYP3A4 metabolism. *International journal of pharmaceutics* 2008;356(1):351-353.
- (87) Johnson BM, Charman WN, Porter CJH. An in vitro examination of the impact of polyethylene glycol 400, pluronic P85, and vitamin E d- $\alpha$ -tocopheryl polyethylene glycol 1000 succinate on P-glycoprotein efflux and enterocyte-based metabolism in excised rat intestine. *AAPS PharmSci* 2002 Dec 1;4(4):193-205.
- (88) Butt U, ElShaer A, Snyder LAS, Al-Kinani AA, Le Gresley A, Alany RG. Fatty Acid Based Microemulsions to Combat Ophthalmia Neonatorum Caused by *Neisseria gonorrhoeae* and *Staphylococcus aureus*. *Nanomaterials* 2018 Jan 19;8(1):51.
- (89) Bergsson G, Arnfinnsson J, Steingrimsson O, Thormar H. In Vitro Killing of *Candida albicans* by Fatty Acids and Monoglycerides. *Antimicrob Agents Chemother* 2001 Nov 1;45(11):3209-3212.
- (90) Yoon BK, Jackman JA, Valle-González ER, Cho N. Antibacterial Free Fatty Acids and Monoglycerides: Biological Activities, Experimental Testing, and Therapeutic Applications. *International Journal of Molecular Sciences* 2018 Apr 8;19(4):1114.
- (91) Kabara JJ, Swieczkowski DM, Conley AJ, Truant JP. Fatty Acids and Derivatives as Antimicrobial Agents. *Antimicrobial Agents and Chemotherapy* 1972 Jul 1;2(1):23-28.
- (92) Kabara JJ, Vrable R, Lie Ken Jie MSF. Antimicrobial lipids: Natural and synthetic fatty acids and monoglycerides. *Lipids* 1977 Sep;12(9):753-759.
- (93) Kabara JJ. Antimicrobial agents derived from fatty acids. *Journal of the American Oil Chemists' Society* 1984 Feb;61(2):397-403.
- (94) Kabara JJ, Conley AJ, Truant JP. Relationship of Chemical Structure and Antimicrobial Activity of Alkyl Amides and Amines. *Antimicrobial Agents and Chemotherapy* 1972 Dec 1;2(6):492-498.

- (95) Inhibition of cytochrome P450 enzymes by saturated and unsaturated fatty acids in human liver microsomes, characterization of enzyme kinetics in the presence of bovine serum albumin (0.1 and 1.0% w/v) and in vitro—in vivo extrapolation of hepatic clearance. .
- (96) Schoch GA, Yano JK, Wester MR, Griffin KJ, Stout CD, Johnson EF. Structure of Human Microsomal Cytochrome P450 2C8. *The Journal of biological chemistry* 2004 Mar 2,;279(10):9497-9503.
- (97) Backman JT, Filppula AM, Niemi M, Neuvonen PJ. Role of Cytochrome P450 2C8 in Drug Metabolism and Interactions. *Pharmacological reviews* 2016 Jan;68(1):168-241.
- (98) Yao H, Chang Y, Lan S, Chen C, Hsu JTA, Yeh T. The inhibitory effect of polyunsaturated fatty acids on human CYP enzymes. *Life sciences* (1973) 2006;79(26):2432-2440.
- (99) Rifkind AB, Lee C, Chang TKH, Waxman DJ. Arachidonic acid metabolism by human cytochrome P450s 2C8, 2C9, 2E1, and 1A2: Regioselective oxygenation and evidence for a role for CYP2C enzymes in arachidonic acid epoxygenation in human liver microsomes. *Archives of biochemistry and biophysics* 1995;320(2):380-389.
- (100) Yamazaki H. Effects of arachidonic acid, prostaglandins, retinol, retinoic acid and cholecalciferol on xenobiotic oxidations catalysed by human cytochrome P450 enzymes. *Xenobiotica* 1999;29(3):231-241.
- (101) Iwase M, Kurata N, Ehana R, Nishimura Y, Masamoto T, Yasuhara H. Evaluation of the effects of hydrophilic organic solvents on CYP3A-mediated drug-drug interaction in vitro. *Human & experimental toxicology* 2006 Dec;25(12):715-721.
- (102) Cotreau-Bibbo MM, Von Moltke LL, Greenblatt DJ. Influence of Polyethylene Glycol and Acetone on the in Vitro Biotransformation of Tamoxifen and Alprazolam by Human Liver Microsomes. *Journal of pharmaceutical sciences* 1996 Nov;85(11):1180-1185.
- (103) Draper AJ, Madan A, Parkinson A. Inhibition of Coumarin 7-Hydroxylase Activity in Human Liver Microsomes. *Archives of biochemistry and biophysics* 1997 May 1,;341(1):47-61.
- (104) Chauret N, Gauthier A, Nicoll-griffith DA. Effect of common organic solvents on in vitro cytochrome P450-mediated metabolic activities in human liver microsomes. *Drug metabolism and disposition* 1998;26(1):1-4.
- (105) Hickman D, Wang J, Wang YI, Unadkat JD. Evaluation of the Selectivity of In Vitro Probes and Suitability of Organic Solvents for the Measurement of Human Cytochrome P450 Monooxygenase Activities. *Drug metabolism and disposition* 1998 Mar 1,;26(3):207-215.
- (106) Busby WF, Ackermann JM, Crespi CL. Effect of methanol, ethanol, dimethyl sulfoxide, and acetonitrile on in vitro activities of cDNA-expressed human cytochromes P-450. *Drug metabolism and disposition* 1999;27(2):246-249.

- (107) Collier JK, Somogyi AA, Bochner F. Flunitrazepam oxidative metabolism in human liver microsomes: involvement of CYP2C19 and CYP3A4. *Xenobiotica* 1999;29(10):973-986.
- (108) Palamanda J, Feng W-, Lin C-, Nomeir AA. Stimulation of Tolbutamide Hydroxylation by Acetone and Acetonitrile in Human Liver Microsomes and in a Cytochrome P-450 2C9-Reconstituted System. *Drug metabolism and disposition* 2000 Jan 1;28(1):38-43.
- (109) Tolonen A, Petsalo A, Turpeinen M, Uusitalo J, Pelkonen O. In vitro interaction cocktail assay for nine major cytochrome P450 enzymes with 13 probe reactions and a single LC/MSMS run: analytical validation and testing with monoclonal anti-CYP antibodies. *Journal of mass spectrometry*. 2007 Jul;42(7):960-966.
- (110) Youdim KA, Lyons R, Payne L, Jones BC, Saunders K. An automated, high-throughput, 384 well Cytochrome P450 cocktail IC50 assay using a rapid resolution LC-MS/MS end-point. *Journal of pharmaceutical and biomedical analysis* 2008;48(1):92-99.
- (111) Jennifer N. Otten, Gary P. Hingorani, Dylan P. Hartley, Scott D. Kragerud, Ronald B. Franklin. An In Vitro, High Throughput, Seven CYP Cocktail Inhibition Assay for the Evaluation of New Chemical Entities Using LC-MS/MS. *Drug metabolism letters* 2011 Jan;5(1):17-24.
- (112) Kozakai K, Yamada Y, Oshikata M, Kawase T, Suzuki E, Haramaki Y, et al. Reliable High-throughput Method for Inhibition Assay of 8 Cytochrome P450 Isoforms Using Cocktail of Probe Substrates and Stable Isotope-labeled Internal Standards. *Drug metabolism and pharmacokinetics* 2012;27(5):520-529.
- (113) Chen Z, Zhang S, Long N, Lin L, Chen T, Zhang F, et al. An improved substrate cocktail for assessing direct inhibition and time-dependent inhibition of multiple cytochrome P450s. *Acta pharmacologica Sinica* 2016;37(5):708-718.
- (114) Li D, Han Y, Meng X, Sun X, Yu Q, Li Y, et al. Effect of Regular Organic Solvents on Cytochrome P450-Mediated Metabolic Activities in Rat Liver Microsomes: Fig. 1. *Drug metabolism and disposition* 2010 Nov;38(11):1922-1925.
- (115) Nishiya Y, Nakamura K, Okudaira N, Abe K, Kobayashi N, Okazaki O. Effects of organic solvents on the time-dependent inhibition of CYP3A4 by diazepam. *Xenobiotica* 2010 Jan;40(1):1-8.
- (116) Tatsumi A, Ikegami Y, Morii R, Sugiyama M, Kadobayashi M, Iwakawa S. Effect of Ethanol on S-Warfarin and Diclofenac Metabolism by Recombinant Human CYP2C9.1. *Biological & pharmaceutical bulletin* 2009 Mar 1;32(3):517-519.
- (117) Tompkins L, Lynch C, Haidar S, Polli J, Wang H. Effects of Commonly Used Excipients on the Expression of CYP3A4 in Colon and Liver Cells. *Pharm Res* 2010;27(8):1703-1712.
- (118) Klaassen CD, Slitt AL. Regulation of Hepatic Transporters by Xenobiotic Receptors. *Current drug metabolism* 2005 Aug;6(4):309-328.
- (119) Meyer UA. Overview of enzymes of drug metabolism. *Journal of pharmacokinetics and biopharmaceutics* 1996 Oct;24(5):449-459.

- (120) Lin JH. Sense and Nonsense in the Prediction of Drug-Drug Interactions. *Current drug metabolism* 2000 Dec;1(4):305-331.
- (121) Wang H, LeCluyse EL. Role of Orphan Nuclear Receptors in the Regulation of Drug-Metabolising Enzymes. *Clinical Pharmacokinetics* 2003;42(15):1331-1357.
- (122) Kliewer SA, Moore JT, Wade L, Staudinger JL, Watson MA, Jones SA, et al. An Orphan Nuclear Receptor Activated by Pregnanes Defines a Novel Steroid Signaling Pathway. *Cell* 1998;92(1):73-82.
- (123) Lehmann JM, McKee DD, Watson MA, Willson TM, Moore JT, Kliewer SA. The human orphan nuclear receptor PXR is activated by compounds that regulate CYP3A4 gene expression and cause drug interactions. *The Journal of clinical investigation* 1998 Sep 1;102(5):1016-1023.
- (124) Takeshita A, Igarashi-Migitaka J, Nishiyama K, Takahashi H, Takeuchi Y, Koibuchi N. Acetyl Tributyl Citrate, the Most Widely Used Phthalate Substitute Plasticizer, Induces Cytochrome P450 3A through Steroid and Xenobiotic Receptor. *Toxicological sciences* 2011 Oct;123(2):460-470.
- (125) Shah P, Jogani V, Bagchi T, Misra A. Role of Caco-2 Cell Monolayers in Prediction of Intestinal Drug Absorption. *Biotechnology progress* 2006;22(1):186-198.
- (126) Shono Y, Nishihara H, Matsuda Y, Furukawa S, Okada N, Fujita T, et al. Modulation of Intestinal P-Glycoprotein Function by Cremophor EL and Other Surfactants by an In Vitro Diffusion Chamber Method Using the Isolated Rat Intestinal Membranes. *Journal of pharmaceutical sciences* 2004 Apr;93(4):877-885.
- (127) Tayrouz Y, Ding R, Burhenne J, Riedel K, Weiss J, Hoppe-Tichy T, et al. Pharmacokinetic and pharmaceutic interaction between digoxin and Cremophor RH40. *Clinical pharmacology and therapeutics* 2003 May;73(5):397-405.
- (128) Rege BD, Kao JPY, Polli JE. Effects of nonionic surfactants on membrane transporters in Caco-2 cell monolayers. *European journal of pharmaceutical sciences* 2002 Sep 1;16(4):237-246.
- (129) Nerurkar MM, Ho NFH, Burton PS, Vidmar TJ, Borchardt RT. Mechanistic Roles of Neutral Surfactants on Concurrent Polarized and Passive Membrane Transport of a Model Peptide in Caco-2 Cells. *Journal of pharmaceutical sciences* 1997 Jul;86(7):813-821.
- (130) Peng Y, Wu H, Zhang X, Zhang F, Qi H, Zhong Y, et al. A comprehensive assay for nine major cytochrome P450 enzymes activities with 16 probe reactions on human liver microsomes by a single LC/MS/MS run to support reliable in vitro inhibitory drug–drug interaction evaluation. *Xenobiotica* 2015;45(11):961-977.
- (131) Zhang J, Thi Thanh Ha P, Lou Y, Hoogmartens J, Van Schepdael A. Kinetic study of CYP3A4 activity on verapamil by capillary electrophoresis. *J Pharm Biomed Anal* 2005;39(3):612-617.
- (132) International Conference on Harmonisation of Technical Requirements For Registration of Pharmaceuticals for Human Use ICH Harmonised Tripartite Guideline Validation of Analytical Procedures: Text and Methodology Q2(R1).

- (133) Gibhard L, Pravin K, Abay E, Wilhelm A, Swart K, Lawrence N, et al. In Vitro and In Vivo Pharmacokinetics of Aminoalkylated Diarylpropanes NP085 and NP102. *Antimicrob Agents Chemother* 2016 May 1,;60(5):3065-3069.
- (134) Becker Peres L, Becker Peres L, de Araújo PHH, Sayer C. Solid lipid nanoparticles for encapsulation of hydrophilic drugs by an organic solvent free double emulsion technique. *Colloids and surfaces, B, Biointerfaces* 2016 Apr 1,;140:317-323.
- (135) Souza VM, Shertzer HG, Menon AG, Pauletti GM. High glucose concentration in isotonic media alters Caco-2 cell permeability. *AAPS PharmSci* 2003 Sep 01,;5(3):E24-25.
- (136) Drug-like properties : concepts, structure design and methods : from ADME to toxicity optimization / Edward H. Kerns and Li Di. Amsterdam: Academic Press; 2008.
- (137) Prentis R, Lis Y, Walker S. Pharmaceutical innovation by the seven UK-owned pharmaceutical companies (1964-1985). *British journal of clinical pharmacology* 1988 Mar;25(3):387-396.
- (138) Di L, Kerns EH, Ma XJ, Huang Y, Carter GT. Applications of High Throughput Microsomal Stability Assay in Drug Discovery. *Combinatorial chemistry & high throughput screening* 2008 Jul;11(6):469-476.
- (139) Riley RJ, Martin IJ, Cooper AE. The Influence of DMPK as an Integrated Partner in Modern Drug Discovery. *Current drug metabolism* 2002 Oct;3(5):527-550.
- (140) Di L, Kerns EH, Hong Y, Kleintop TA, Mc Connell OJ, Huryn DM. Optimization of a Higher Throughput Microsomal Stability Screening Assay for Profiling Drug Discovery Candidates. *Journal of biomolecular screening* 2003 Aug;8(4):453-462.
- (141) Spaggiari D, Geiser L, Daali Y, Rudaz S. A cocktail approach for assessing the in vitro activity of human cytochrome P450s: An overview of current methodologies. *Journal of pharmaceutical and biomedical analysis* 2014 Dec;101:221-237.
- (142) Bu H, Magis L, Knuth K, Teitelbaum P. High-throughput cytochrome P450 (CYP) inhibition screening via a cassette probe-dosing strategy. VI. Simultaneous evaluation of inhibition potential of drugs on human hepatic isozymes CYP2A6, 3A4, 2C9, 2D6 and 2E1. *Rapid Commun Mass Spectrom* 2001;15(10):741-748.
- (143) Kim H, Lee H, Ji H, Lee T, Liu K. Screening of ten cytochrome P450 enzyme activities with 12 probe substrates in human liver microsomes using cocktail incubation and liquid chromatography–tandem mass spectrometry. *Biopharm Drug Dispos* 2019;40(3-4):101-111.
- (144) Lee T, Liu K. Screening of twelve cytochrome P450 enzyme activities with 12 probe substrates in human liver microsomes using cocktail incubation and liquid chromatography–tandem mass spectrometry. *Biopharm Drug Dispos* 2019;40(3-4):101.

- (145) Kavanagh P, Grigoryev A, Melnik A, Savchuk S, Simonov A, Rozhanets V. Detection and tentative identification of urinary phase I metabolites of phenylacetylindole cannabimimetics JWH-203 and JWH-251, by GC–MS and LC–MS/MS. *Journal of chromatography. B, Analytical technologies in the biomedical and life sciences* 2013 Sep 1,;934:102-108.
- (146) Matabosch X, Pozo OJ, Pérez-Mañá C, Farré M, Marcos J, Segura J, et al. Identification of budesonide metabolites in human urine after oral administration. *Anal Bioanal Chem* 2012 May 10,;404(2):325-340.
- (147) Li Q, Zhang G. Identification of n-hydroxy acid metabolites in electron impact ionization mass spectrometry. *Rapid communications in mass spectrometry* 2012 Jun 15,;26(11):1355-1362.
- (148) Korfmacher WA. Foundation review: Principles and applications of LC-MS in new drug discovery. *Drug discovery today* 2005 Oct 15,;10(20):1357-1367.
- (149) Lim C, Lord G. Current Developments in LC-MS for Pharmaceutical Analysis. *Biological & pharmaceutical bulletin* 2002;25(5):547-557.
- (150) Parasuraman S, Rao A, Balamurugan S, Muralidharan S, Kumar KJ, Vijayan V, et al. An Overview of Liquid Chromatography-Mass Spectroscopy Instrumentation. ;2.
- (151) Glish GL, Vachet RW. The basics of mass spectrometry in the twenty-first century. *Nature reviews. Drug discovery* 2003 Feb;2(2):140-150.
- (152) Chen R, Cheng X, Mitchell DW, Hofstadler SA, Wu Q, Rockwood AL, et al. Trapping, Detection, and Mass Determination of Coliphage T4 DNA Ions by Electrospray Ionization Fourier Transform Ion Cyclotron Resonance Mass Spectrometry. *Analytical chemistry (Washington)* 1995 Apr 1,;67(7):1159-1163.
- (153) Smith RD, Cheng X, Brace JE, Hofstadler SA, Anderson GA. Trapping, detection and reaction of very large single molecular ions by mass spectrometry. *Nature (London)* 1994 May 12,;369(6476):137-139.
- (154) Ho CS, Lam CWK, Chan MHM, Cheung RCK, Law LK, Lit LCW, et al. Electrospray ionisation mass spectrometry: principles and clinical applications. *Clinical biochemist reviews* 2003;24(1):3-12.
- (155) Busch D, Fritz A, Partecke LI, Heidecke C, Oswald S. LC–MS/MS method for the simultaneous quantification of intestinal CYP and UGT activity. *Journal of pharmaceutical and biomedical analysis* 2018 Jun 05,;155:194-201.
- (156) Jennifer N. Otten, Gary P. Hingorani, Dylan P. Hartley, Scott D. Kragerud, Ronald B. Franklin. An In Vitro, High Throughput, Seven CYP Cocktail Inhibition Assay for the Evaluation of New Chemical Entities Using LC-MS/MS. *Drug metabolism letters* 2011 Jan;5(1):17-24.
- (157) Liu L, Han Y, Zhu J, Yu Q, Yang Q, Lu J, et al. A sensitive and high-throughput LC-MS/MS method for inhibition assay of seven major cytochrome P450s in human liver microsomes using an in vitro cocktail of probe substrates. *Biomed Chromatogr* 2014 -08-06;29(3):437.

- (158) Jing-Jing Wang Jian-Jun Guo Jenny Zhan Hai-Zhi Bu Jiunn H. Lin. An in-vitro cocktail assay for assessing compound-mediated inhibition of six major cytochrome P450 enzymes. *Journal of pharmaceutical analysis* 2014;4(4):270-278.
- (159) Uchida S, Tanaka S, Namiki N. Simultaneous and comprehensive in vivo analysis of cytochrome P450 activity by using a cocktail approach in rats. *Biopharmaceutics & drug disposition* 2014 May;35(4):228-236.
- (160) Grangeon A, Gravel S, Gaudette F, Turgeon J, Michaud V. Highly sensitive LC–MS/MS methods for the determination of seven human CYP450 activities using small oral doses of probe-drugs in human. *Journal of chromatography. B, Analytical technologies in the biomedical and life sciences* 2017 Jan 01.;1040:144-158.
- (161) Srinivas-Shankar U, Wu FC. Drug Insight: testosterone preparations. *Nature clinical practice urology* 2006 Dec;3(12):653-665.
- (162) Ongkowijoyo. Proton Pump Inhibitors: Omeprazole. 2014;109.
- (163) Birkett DJ, Andersson T, Miners JO. [14] Assays of omeprazole metabolism as a substrate probe for human CYP isoforms. *Methods in Enzymology United States: Elsevier Science & Technology*; 1996. p. 132-139.
- (164) Taylor CP, Traynelis SF, Siffert J, Pope LE, Matsumoto RR. Pharmacology of dextromethorphan: Relevance to dextromethorphan/quinidine (Nuedexta®) clinical use. *Pharmacology & Therapeutics* 2016 Aug;164:170-182.
- (165) Al-Jenoobi FI, Al-Thukair AA, Alam MA, Abbas FA, Al-Mohizea AM, Alkharfy KM, et al. Modulation of CYP2D6 and CYP3A4 metabolic activities by Ferula asafetida resin. *Saudi Pharmaceutical Journal* 2014 Dec;22(6):564-569.
- (166) Thörn HA, Lundahl A, Schrickx JA, Dickinson PA, Lennernäs H. Drug metabolism of CYP3A4, CYP2C9 and CYP2D6 substrates in pigs and humans. *European journal of pharmaceutical sciences* 2011;43(3):89-98.
- (167) Chaturvedi, Saxena, Saxena, Singh, Agrawal, Chaturvedi. Lipid Excipients in Self Emulsifying Drug Delivery Systems Solubility and dissolution enhancement of domperidone View project Lipid Excipients in Self Emulsifying Drug Delivery Systems.
- (168) Bushee JL, Liang G, Dunne CE, Harriman SP, Argikar UA. Identification of saturated and unsaturated fatty acids released during microsomal incubations. *Xenobiotica* 2014 Aug;44(8):687-695.
- (169) Tsoutsikos P, Miners JO, Stapleton A, Thomas A, Sallustio BC, Knights KM. Evidence that unsaturated fatty acids are potent inhibitors of renal UDP-glucuronosyltransferases (UGT): kinetic studies using human kidney cortical microsomes and recombinant UGT1A9 and UGT2B7. *Biochemical pharmacology* 2004;67(1):191-199.
- (170) Ogilvie BW, Yerino P, Kazmi F, Buckley DB, Rostami-Hodjegan A, Paris BL, et al. The proton pump inhibitor, omeprazole, but not lansoprazole or pantoprazole, is a metabolism-dependent inhibitor of CYP2C19: implications for coadministration with clopidogrel. *Drug metabolism and disposition* 2011;39(11):2020-2033.



- (171) Di L, Kerns EH, Li SQ, Petusky SL. High throughput microsomal stability assay for insoluble compounds. *International journal of pharmaceutics* 2006 Jul 06;;317(1):54-60.
- (172) *In Vitro Metabolism- and Transporter-Mediated Drug-Drug Interaction Studies, and Clinical Drug Interaction Studies--Study Design, Data Analysis, and Clinical Implications; Draft Guidances for Industry; Availability.* *The Federal Register / FIND* 2017 Oct 25;;82(205):49371.
- (173) Usmani KA, Tang J. Human Cytochrome P450: Metabolism of Testosterone by CYP3A4 and Inhibition by Ketoconazole. *Current Protocols in Toxicology* 2004 May;20(1):4.13.1-4.13.9.
- (174) Youdim KA, Saunders KC. A review of LC–MS techniques and high-throughput approaches used to investigate drug metabolism by cytochrome P450s. *Journal of chromatography. B, Analytical technologies in the biomedical and life sciences* 2010;878(17):1326-1336.
- (175) Li Y, Yue XX, Pan Z, Liu Y, Shen M, Zhai Y, et al. Development and validation of an LC-MS/MS method for quantifying nine antimicrobials in human serum and its application to study the exposure of Chinese pregnant women to antimicrobials. *J Clin Lab Anal* 2021;35(3).
- (176) Wu J, Qian Y, Zhang C, Zheng T, Chen L, Lu Y, et al. Application of Graphene-based Solid-Phase Extraction Coupled with Ultra High-performance Liquid Chromatography-Tandem Mass Spectrometry for Determination of Macrolides in Fish Tissues. *Food Analytical Methods* 2013;6(5):1448-1457.
- (177) Kachingwe BH, Uang Y, Huang T, Wang L, Lin S. Development and validation of an LC–MS/MS method for quantification of NC-8 in rat plasma and its application to pharmacokinetic studies. *J Food Drug Anal* 2018;26(1):401-408.
- (178) Wang J, Guo J, Zhan J, Bu H, Lin JH. An in-vitro cocktail assay for assessing compound-mediated inhibition of six major cytochrome P450 enzymes. *Journal of Pharmaceutical Analysis* 2014;4(4):270-278.
- (179) Jia L, Liu X. The Conduct of Drug Metabolism Studies Considered Good Practice (II): In Vitro Experiments. *Current drug metabolism* 2007 Dec;8(8):822-829.
- (180) Peng Y, Wu H, Zhang X, Zhang F, Qi H, Zhong Y, et al. A comprehensive assay for nine major cytochrome P450 enzymes activities with 16 probe reactions on human liver microsomes by a single LC/MS/MS run to support reliable in vitro inhibitory drug–drug interaction evaluation. *Xenobiotica* 2015 Nov 02;;45(11):961-977.
- (181) Sun H, Veith H, Xia M, Austin CP, Huang R. Predictive Models for Cytochrome P450 Isozymes Based on Quantitative High Throughput Screening Data. *J Chem Inf Model* 2011;51(10):2474-2481.
- (182) Di L, Kerns EH, Li SQ, Petusky SL. High throughput microsomal stability assay for insoluble compounds. *International journal of pharmaceutics* 2006 Jul 06;;317(1):54-60.

- (183) Li D, Han Y, Meng X, Sun X, Yu Q, Li Y, et al. Effect of regular organic solvents on cytochrome P450-mediated metabolic activities in rat liver microsomes. *Drug Metab Dispos* 2010 Nov;38(11):1922-1925.
- (184) Chauret N, Gauthier A, Nicoll-Griffith D. Effect of Common Organic Solvents on *in Vitro* Cytochrome P450-Mediated Metabolic Activities in Human Liver Microsomes. *Drug Metab Disposition* 1998;26(1):1.
- (185) Williamson B, Wilson C, Dagnell G, Riley RJ. Harmonised high throughput microsomal stability assay. *J Pharmacol Toxicol Methods* 2017;84:31-36.
- (186) Di L, Kerns EH, Li SQ, Carter GT. Comparison of cytochrome P450 inhibition assays for drug discovery using human liver microsomes with LC–MS, rhCYP450 isozymes with fluorescence, and double cocktail with LC–MS. *Int J Pharm* 2007;335(1):1-11.
- (187) Äbelö A, Andersson TB, Antonsson M, Naudot AK, Skånberg I, Weidolf L. Stereoselective Metabolism of Omeprazole by Human Cytochrome P450 Enzymes. *Drug Metab Disposition* 2000;28(8):966.
- (188) Axelsson H, Granhall C, Flöby E, Jaksch Y, Svedling M, Sohlenius-Sternbeck A-. Rates of metabolism of chlorzoxazone, dextromethorphan, 7-ethoxycoumarin, imipramine, quinidine, testosterone and verapamil by fresh and cryopreserved rat liver slices, and some comparisons with microsomes. *Toxicology in vitro* 2003;17(4):481-488.
- (189) Lee E, Shon JC, Liu K. Simultaneous evaluation of substrate-dependent CYP3A inhibition using a CYP3A probe substrates cocktail. *Biopharmaceutics & drug disposition* 2016 Sep;37(6):366-372.
- (190) Yao H, Chang Y, Lan S, Chen C, Hsu JTA, Yeh T. The inhibitory effect of polyunsaturated fatty acids on human CYP enzymes. *Life sciences (1973)* 2006;79(26):2432-2440.
- (191) Palacharla RC, Uthukam V, Manoharan A, Ponnamaneni RK, Padala NP, Boggavarapu RK, et al. Inhibition of cytochrome P450 enzymes by saturated and unsaturated fatty acids in human liver microsomes, characterization of enzyme kinetics in the presence of bovine serum albumin (0.1 and 1.0% w/v) and in vitro – in vivo extrapolation of hepatic clearance. *European journal of pharmaceutical sciences* 2017 Apr 1;101:80-89.
- (192) Martin P, Gillen M, Millson D, Oliver S, Brealey C, Grossbard EB, et al. Effects of CYP3A4 Inhibitors Ketoconazole and Verapamil and the CYP3A4 Inducer Rifampicin on the Pharmacokinetic Parameters of Fostamatinib: Results from In Vitro and Phase I Clinical Studies. *Drugs R D* 2016;16(1):81-92.
- (193) Kandel SE, Han LW, Mao Q, Lampe JN. Digging Deeper into CYP3A Testosterone Metabolism: Kinetic, Regioselectivity, and Stereoselectivity Differences between CYP3A4/5 and CYP3A7. *Drug metabolism and disposition* 2017 Dec;45(12):1266-1275.
- (194) Saad F, Röhrig G, von Haehling S, Traish A. Testosterone Deficiency and Testosterone Treatment in Older Men. *Gerontology (Basel)* 2017;63(2):144-156.

- (195) El-Kamel AH, Al-Fagih IM, Alsarra IA. Testosterone solid lipid microparticles for transdermal drug delivery. Formulation and physicochemical characterization. *Journal of microencapsulation* 2007;24(5):457-475.
- (196) Swerdloff RS, Wang C, White WB, Kaminetsky J, Gittelman MC, Longstreth JA, et al. A New Oral Testosterone Undecanoate Formulation Restores Testosterone to Normal Concentrations in Hypogonadal Men. *The journal of clinical endocrinology and metabolism* 2020 Aug;105(8):2515-2531.
- (197) Yin AY, Htun M, Swerdloff RS, Diaz-Arjonilla M, Dudley RE, Faulkner S, et al. Reexamination of Pharmacokinetics of Oral Testosterone Undecanoate in Hypogonadal Men With a New Self-Emulsifying Formulation. *Journal of andrology* 2012 Mar;33(2):190-201.
- (198) Aungst BJ. Novel Formulation Strategies for Improving Oral Bioavailability of Drugs with Poor Membrane Permeation or Presystemic Metabolism. *Journal of pharmaceutical sciences* 1993 Oct;82(10):979-987.
- (199) Padhye S, Nagarsenker M. Simvastatin solid lipid nanoparticles for oral delivery: Formulation development and In vivo evaluation. *Indian Journal of Pharmaceutical Sciences* 2013 Feb 1,;75(5):591-598.
- (200) Müller RH, Mäder K, Gohla S. Solid lipid nanoparticles (SLN) for controlled drug delivery – a review of the state of the art. *European Journal of Pharmaceutics and Biopharmaceutics* 2000;50(1):161-177.
- (201) Zur Mühlen A, Mehnert W. Drug release and release mechanism of prednisolone loaded Solid Lipid Nanoparticles. *Pharmazie* 1998;53(8):552-555.
- (202) Grenha A, Remuñán-López C, Carvalho ELS, Seijo B. Microspheres containing lipid/chitosan nanoparticles complexes for pulmonary delivery of therapeutic proteins. *European journal of pharmaceutics and biopharmaceutics* 2008;69(1):83-93.
- (203) Chauhan H, Mohapatra S, Munt DJ, Chandratre S, Dash A. Physical-Chemical Characterization and Formulation Considerations for Solid Lipid Nanoparticles. *AAPS PharmSciTech* 2015 Aug 21,;17(3):640-651.
- (204) Xie S, Zhu L, Dong Z, Wang Y, Wang X, Zhou W. Preparation and evaluation of ofloxacin-loaded palmitic acid solid lipid nanoparticles. *International Journal of Nanomedicine* 2011;6:547-555.
- (205) Sznitowska M, Gajewska M, Janicki S, Radwanska A, Lukowski G. Bioavailability of diazepam from aqueous-organic solution, submicron emulsion and solid lipid nanoparticles after rectal administration in rabbits. *European journal of pharmaceutics and biopharmaceutics* 2001;52(2):159-163.
- (206) Uner M, Yener G. Importance of solid lipid nanoparticles (SLN) in various administration routes and future perspectives. *International Journal of Nanomedicine* 2007;2(3):289-300.
- (207) Shah R, Harding I, Palombo E, Eldridge D. *Lipid Nanoparticles: Production, Characterization and Stability*. Cham: Springer International Publishing; 2015.

- (208) Wissing SA, Müller RH. The influence of solid lipid nanoparticles on skin hydration and viscoelasticity – in vivo study. *European journal of pharmaceutics and biopharmaceutics* 2003;56(1):67-72.
- (209) AKS, . PA, . PC. Formulation of solid lipid nanoparticles and their applications. *Current pharma research* 2011 Feb 15,;1(2):197-203.
- (210) N Jawahar, S N Meyyanathan, Gowtham Reddy, Sumeet Sood. Solid lipid Nanoparticles for Oral delivery of Poorly Soluble Drugs. *Journal of pharmaceutical sciences and research* 2012 Jul 1,;4(7):1848.
- (211) Wissing SA, Kayser O, Müller RH. Solid lipid nanoparticles for parenteral drug delivery. *Advanced drug delivery reviews* 2004;56(9):1257-1272.
- (212) Vijayan V, Aafreen S, Sakthivel S, Reddy KR. Formulation and characterization of solid lipid nanoparticles loaded Neem oil for topical treatment of acne. *Journal of Acute Disease* 2013;2(4):282-286.
- (213) Faghihi S, Awadi MR, Mousavi SE, Rezayat Sorkhabadi SM, Karboni M, Azarmi S, et al. Diazepam Loaded Solid Lipid Nanoparticles: In Vitro and in Vivo Evaluations. *Advanced pharmaceutical bulletin* 2020 Sep 8,;12(1):86-92.
- (214) Xu Z, Zhang F, Sun F, Gu K, Dong S, He D, et al. Dimethyl fumarate for multiple sclerosis. *Cochrane database of systematic reviews* 2015 Apr 22,;2015(4):CD011076.
- (215) Blasi P, Giovagnoli S, Schoubben A, Ricci M, Rossi C. Solid lipid nanoparticles for targeted brain drug delivery. *Advanced drug delivery reviews* 2007;59(6):454-477.
- (216) Zur Mühlen A, Schwarz C, Mehnert W. Solid lipid nanoparticles (SLN) for controlled drug delivery – Drug release and release mechanism. *European journal of pharmaceutics and biopharmaceutics* 1998;45(2):149-155.
- (217) Wissing SA, Müller RH. Cosmetic applications for solid lipid nanoparticles (SLN). *International journal of pharmaceutics* 2003;254(1):65-68.
- (218) Kumar P, Sharma G, Kumar R, Malik R, Singh B, Katare OP, et al. Stearic acid based, systematically designed oral lipid nanoparticles for enhanced brain delivery of dimethyl fumarate. *Nanomedicine (London, England)* 2017 Dec 1,;12(23):2607-2621.
- (219) Mahajan A, Kaur S. Design, Formulation, and Characterization of Stearic Acid-Based Solid Lipid Nanoparticles of Candesartan Cilexetil to Augment its Oral Bioavailability. *Asian journal of pharmaceutical and clinical research* 2018 Apr 01,;11(4):344.
- (220) Shah RM, Malherbe F, Eldridge D, Palombo EA, Harding IH. Physicochemical characterization of solid lipid nanoparticles (SLNs) prepared by a novel microemulsion technique. *Journal of colloid and interface science* 2014 Aug 15,;428(428):286-294.

- (221) Kalepu S, Nekkanti V. Insoluble drug delivery strategies: review of recent advances and business prospects. *Acta Pharmaceutica Sinica B* 2015;5(5):442-453.
- (222) Muchow M, Maincent P, Müller RH, Keck CM. Production and characterization of testosterone undecanoate-loaded NLC for oral bioavailability enhancement. *Drug development and industrial pharmacy* 2011 Jan;37(1):8-14.
- (223) S V Shekade, S V Shirolkar, Yatesh Chaudhari. A Review on Microemulsion Drug Delivery System for Nasal Application. *Journal of pharmaceutical sciences and research* 2020 Jan 1,;12(1):63-73.
- (224) Pant A, Jha K, Singh M. Role of Excipient's HLB Values in Microemulsion System. *IOSR Journal Of Pharmacy And Biological Sciences* ;14(2).
- (225) Toth G, Madarasz A. Structure of BRIJ-35 Nonionic Surfactant in Water: A Reverse Monte Carlo Study. *Langmuir* 2006 Jan 17,;22(2):590-597.
- (226) Syed HK, Peh KK. Identification of phases of various oil, surfactant/ co-surfactants and water system by ternary phase diagram. *Acta Poloniae pharmaceutica* 2014 Mar;71(2):301-309.
- (227) Yong Yong ENG, Sharma VK, RAY AK. Photocatalytic degradation of nonionic surfactant, Brij 35 in aqueous TiO<sub>2</sub> suspensions. *Chemosphere (Oxford)* 2010;79(2):205-209.
- (228) Whitehead K, Karr N, Mitragotri S. Safe and Effective Permeation Enhancers for Oral Drug Delivery. *Pharm Res* 2007 Dec 5,;25(8):1782-1788.
- (229) Duong V, Nguyen T, Maeng H. Preparation of Solid Lipid Nanoparticles and Nanostructured Lipid Carriers for Drug Delivery and the Effects of Preparation Parameters of Solvent Injection Method. *Molecules (Basel, Switzerland)* 2020 Oct 18,;25(20):4781.
- (230) Vitorino C, Carvalho FA, Almeida AJ, Sousa JJ, Pais AACC. The size of solid lipid nanoparticles: An interpretation from experimental design. *Colloids and surfaces, B, Biointerfaces* 2011 May 1,;84(1):117-130.
- (231) Mehnert W, Mader K. Solid lipid nanoparticles Production, characterization and applications. *Advanced drug delivery reviews* 2012;64:83-101.
- (232) Reddy LH, Murthy RSR. Etoposide-loaded nanoparticles made from glyceride lipids: formulation, characterization, in vitro drug release, and stability evaluation. *AAPS PharmSciTech* 2005 Sep 30,;6(2):E158-E166.
- (233) Lim S, Kim C. Formulation parameters determining the physicochemical characteristics of solid lipid nanoparticles loaded with all-trans retinoic acid. *International journal of pharmaceutics* 2002;243(1):135-146.
- (234) Kaur IP, Bhandari R, Bhandari S, Kakkar V. Potential of solid lipid nanoparticles in brain targeting. *Journal of controlled release* 2008;127(2):97-109.
- (235) Das S, Ng WK, Tan RBH. Are nanostructured lipid carriers (NLCs) better than solid lipid nanoparticles (SLNs): Development, characterizations and comparative

evaluations of clotrimazole-loaded SLNs and NLCs? *European journal of pharmaceutical sciences* 2012 Aug 30;47(1):139-151.

(236) Li M, Zahi MR, Yuan Q, Tian F, Liang H. Preparation and stability of astaxanthin solid lipid nanoparticles based on stearic acid. *European journal of lipid science and technology* 2016 Apr;118(4):592-602.

(237) Parhi R, Suresh P. Preparation and Characterization of Solid Lipid Nanoparticles-A Review. *Current drug discovery technologies* 2012 Mar;9(1):2-16.

(238) Abdelbary G, Fahmy RH. Diazepam-Loaded Solid Lipid Nanoparticles: Design and Characterization. *AAPS PharmSciTech* 2009 Mar 10;10(1):211-219.

(239) Ekambaram P, Abdul HSA. Formulation and evaluation of solid lipid nanoparticles of ramipril. *Journal of Young Pharmacists : JYP* 2011 Jul;3(3):216-220.

(240) Westesen K, Bunjes H, Koch MHJ. Physicochemical characterization of lipid nanoparticles and evaluation of their drug loading capacity and sustained release potential. *Journal of controlled release* 1997;48(2):223-236.

(241) Kalkura SN, Devanarayanan S. Crystal growth of steroids in silica gel: Testosterone. *Journal of crystal growth* 1989;94(3):810-813.

(242) Interpreting DSC curves Part 1: Dynamic measurements.

(243) Shen J, Sun M, Ping Q, Ying Z, Liu W. Incorporation of liquid lipid in lipid nanoparticles for ocular drug delivery enhancement. *Nanotechnology* 2010 Jan 15;21(2):025101.

(244) Seyfoddin A, Shaw J, Al-Kassas R. Solid lipid nanoparticles for ocular drug delivery. *Drug delivery* 2010 Oct;17(7):467-489.

(245) Fang J, Fang C, Liu C, Su Y. Lipid nanoparticles as vehicles for topical psoralen delivery: Solid lipid nanoparticles (SLN) versus nanostructured lipid carriers (NLC). *European journal of pharmaceutics and biopharmaceutics* 2008;70(2):633-640.

(246) Patlolla RR, Chougule M, Patel AR, Jackson T, Tata PNV, Singh M. Formulation, characterization and pulmonary deposition of nebulized celecoxib encapsulated nanostructured lipid carriers. *Journal of controlled release* 2010;144(2):233-241.

(247) Hu L, Tang X, Cui F. Solid lipid nanoparticles (SLNs) to improve oral bioavailability of poorly soluble drugs. *Journal of pharmacy and pharmacology* 2004 Dec;56(12):1527-1535.

(248) Mahajan A, Kaur S. Design, Formulation, and Characterization of Stearic acid-Based Solid Lipid Nanoparticles of Candesartan Cilexetil to Augment its Oral Bioavailability. *Asian journal of pharmaceutical and clinical research* 2018 Apr 1;11(4):344.

(249) Das S, Ng WK, Tan RBH. Are nanostructured lipid carriers (NLCs) better than solid lipid nanoparticles (SLNs): Development, characterizations and comparative

evaluations of clotrimazole-loaded SLNs and NLCs? *European journal of pharmaceutical sciences* 2012 Aug 30,;47(1):139-151.

(250) Gaur PK, Mishra S, Bajpai M, Mishra A. Enhanced Oral Bioavailability of Efavirenz by Solid Lipid Nanoparticles: In Vitro Drug Release and Pharmacokinetics Studies. *BioMed Research International* 2014 May 21,;2014:363404-9.

(251) Abdelbary G, Fahmy RH. Diazepam-Loaded Solid Lipid Nanoparticles: Design and Characterization. *AAPS PharmSciTech* 2009 Mar 10,;10(1):211-219.

(252) zur Mühlen A, Schwarz C, Mehnert W. Solid lipid nanoparticles (SLN) for controlled drug delivery – Drug release and release mechanism. *European journal of pharmaceuticals and biopharmaceutics* 1998;45(2):149-155.

(253) Luo Y, Chen D, Ren L, Zhao X, Qin J. Solid lipid nanoparticles for enhancing vinpocetine's oral bioavailability. *Journal of controlled release* 2006;114(1):53-59.

(254) Gori M, Altomare A, Cocca S, Solida E, Ribolsi M, Carotti S, et al. Palmitic Acid Affects Intestinal Epithelial Barrier Integrity and Permeability In Vitro. *Antioxidants* 2020 May 13,;9(5):417.

(255) Patel M, Mundada V, Sawant K. Enhanced intestinal absorption of asenapine maleate by fabricating solid lipid nanoparticles using TPGS: elucidation of transport mechanism, permeability across Caco-2 cell line and in vivo pharmacokinetic studies. *Artificial cells, nanomedicine, and biotechnology* 2019 Dec 4,;47(1):144-153.

(256) Denizot F, Lang R. Rapid colorimetric assay for cell growth and survival: Modifications to the tetrazolium dye procedure giving improved sensitivity and reliability. *Journal of immunological methods* 1986;89(2):271-277.

(257) Bunjes H. Lipid nanoparticles for the delivery of poorly water-soluble drugs. *Journal of pharmacy and pharmacology* 2010 Nov;62(11):1637-1645.

(258) Shah M, Agrawal Y, Garala K, Ramkishan A. Solid lipid nanoparticles of a water soluble drug, ciprofloxacin hydrochloride. *Indian Journal of Pharmaceutical Sciences* 2012 Feb 1,;74(5):434-442.

(259) Mirchandani Y, Patravale VB, S. B. Solid lipid nanoparticles for hydrophilic drugs. *Journal of controlled release* 2021 Jul 10,;335:457-464.

(260) Alihosseini F, Ghaffari S, Dabirsiaghi AR, Haghghat S. Freeze-drying of ampicillin solid lipid nanoparticles using mannitol as cryoprotectant. *Brazilian Journal of Pharmaceutical Sciences* 2015 Dec;51(4):797-802.

(261) Varshosaz J, Ghaffari S, Khoshayand MR, Atyabi F, Azarmi S, Kobarfard F. Development and optimization of solid lipid nanoparticles of amikacin by central composite design. *Journal of liposome research* 2010 Jun;20(2):97-104.

(262) Güney G, Kutlu HM, Genç L. Preparation and characterization of ascorbic acid loaded solid lipid nanoparticles and investigation of their apoptotic effects. *Colloids and surfaces, B, Biointerfaces* 2014 Sep 1,;121:270-280.

- (263) Heiati H, Tawashi R, Phillips NC. Solid lipid nanoparticles as drug carriers: II. Plasma stability and biodistribution of solid lipid nanoparticles containing the lipophilic prodrug 3'-azido-3'-deoxythymidine palmitate in mice. *International journal of pharmaceutics* 1998;174(1):71-80.
- (264) Garcia-Fuentes M, Prego C, Torres D, Alonso MJ. A comparative study of the potential of solid triglyceride nanostructures coated with chitosan or poly(ethylene glycol) as carriers for oral calcitonin delivery. *European journal of pharmaceutical sciences* 2005;25(1):133-143.
- (265) Qi C, Chen Y, Jing Q, Wang X. Preparation and Characterization of Catalase-Loaded Solid Lipid Nanoparticles Protecting Enzyme against Proteolysis. *International Journal of Molecular Sciences* 2011;12(7):4282-4293.
- (266) Tian J, Pang X, Yu K, Liu L, Zhou J. Preparation, characterization and in vivo distribution of solid lipid nanoparticles loaded with cisplatin. *Pharmazie* 2008 Aug 1;63(8):593-597.
- (267) Gallarate M, Trotta M, Battaglia L, Chirio D. Cisplatin-loaded SLN produced by coacervation technique. *Journal of drug delivery science and technology* 2010;20(5):343-347.
- (268) Shazly GA. Corrigendum to "Ciprofloxacin Controlled-Solid Lipid Nanoparticles: Characterization, In Vitro Release, and Antibacterial Activity Assessment". *BioMed Research International* 2017 Aug 13;2017:6761452-1.
- (269) Pignatello R, Leonardi A, Fuochi V, Petronio G, Greco AS, Furneri PM. A Method for Efficient Loading of Ciprofloxacin Hydrochloride in Cationic Solid Lipid Nanoparticles: Formulation and Microbiological Evaluation. *Nanomaterials* 2018 May 6;8(5):304.
- (270) Muga JO, Gathirwa JW, Tukulula M, Jura WGZO. In vitro evaluation of chloroquine-loaded and heparin surface-functionalized solid lipid nanoparticles. *Malaria Journal* 2018 Apr 2;17(1):133.
- (271) Liu D, Ge Y, Tang Y, Yuan Y, Zhang Q, Li R, et al. Solid lipid nanoparticles for transdermal delivery of diclofenac sodium: preparation, characterization and in vitro studies. *Journal of microencapsulation* 2010 Dec;27(8):726-734.
- (272) Hosseini SM, Abbasalipourkabir R, Jalilian FA, Asl SS, Farmany A, Roshanaei G, et al. Doxycycline-encapsulated solid lipid nanoparticles as promising tool against *Brucella melitensis* enclosed in macrophage: a pharmacodynamics study on J774A.1 cell line. *Antimicrobial Resistance and Infection Control* 2019;8(1):62.
- (273) Battaglia L, Gallarate M, Peira E, Chirio D, Muntoni E, Biasibetti E, et al. Solid Lipid Nanoparticles for Potential Doxorubicin Delivery in Glioblastoma Treatment: Preliminary In Vitro Studies. *Journal of pharmaceutical sciences* 2014 Jul;103(7):2157-2165.
- (274) Stella B, Peira E, Dianzani C, Gallarate M, Battaglia L, Gigliotti CL, et al. Development and Characterization of Solid Lipid Nanoparticles Loaded with a Highly Active Doxorubicin Derivative. *Nanomaterials* 2018 Feb 16;8(2):110.



- (275) Chirio D, Peira E, Battaglia L, Ferrara B, Barge A, Sapino S, et al. Lipophilic Prodrug of Floxuridine Loaded into Solid Lipid Nanoparticles: In Vitro Cytotoxicity Studies on Different Human Cancer Cell Lines. *Journal of nanoscience and nanotechnology* 2018 Jan 1,;18(1):556-563.
- (276) Bhandari R, Kaur IP. Pharmacokinetics, tissue distribution and relative bioavailability of isoniazid-solid lipid nanoparticles. *International journal of pharmaceutics* 2013 Jan 30,;441(1-2):202-212.
- (277) Gallarate M, Trotta M, Battaglia L, Chirio D. Preparation of solid lipid nanoparticles from W/O/W emulsions: Preliminary studies on insulin encapsulation. *Journal of microencapsulation* 2009 Aug;26(5):394-402.
- (278) Gallarate M, Battaglia L, Peira E, Trotta M. Peptide-Loaded Solid Lipid Nanoparticles Prepared through Coacervation Technique. *International Journal of Chemical Engineering* 2011 Dec 1,;2011:1-6.
- (279) Almeida AJ, Runge S, Müller RH. Peptide-loaded solid lipid nanoparticles (SLN): Influence of production parameters. *International journal of pharmaceutics* 1997;149(2):255-265.
- (280) Battaglia L, Serpe L, Muntoni E, Zara G, Trotta M, Gallarate M. Methotrexate-loaded SLNs prepared by coacervation technique: in vitro cytotoxicity and in vivo pharmacokinetics and biodistribution. *Nanomedicine (London, England)* 2011 Nov;6(9):1561-1573.
- (281) Zhuang Y, Xu B, Huang F, Wu J, Chen S. Solid lipid nanoparticles of anticancer drugs against MCF-7 cell line and a murine breast cancer model. *Pharmazie* 2012 Nov 1,;67(11):925-929.
- (282) Vakilinezhad MA, Amini A, Akbari Javar H, Baha'addini Beigi Zarandi BF, Montaseri H, Dinarvand R. Nicotinamide loaded functionalized solid lipid nanoparticles improves cognition in Alzheimer's disease animal model by reducing Tau hyperphosphorylation. *DARU J Pharm Sci* 2018;26(2):165-177.
- (283) Prombutara P, Kulwatthanasal Y, Supaka N, Sramala I, Chareonpornwattana S. Production of nisin-loaded solid lipid nanoparticles for sustained antimicrobial activity. *Food control* 2012 Mar;24(1-2):184-190.
- (284) Severino P, Silveira EF, Loureiro K, Chaud MV, Antonini D, Lancellotti M, et al. Antimicrobial activity of polymyxin-loaded solid lipid nanoparticles (PLX-SLN): Characterization of physicochemical properties and in vitro efficacy. *European journal of pharmaceutical sciences* 2017 Aug 30,;106:177-184.
- (285) Shah RM, Malherbe F, Eldridge D, Palombo EA, Harding IH. Physicochemical characterization of solid lipid nanoparticles (SLNs) prepared by a novel microemulsion technique. *Journal of colloid and interface science* 2014 Aug 15,;428(428):286-294.
- (286) Cavalli R, Gasco MR, Chetoni P, Burgalassi S, Saettone MF. Solid lipid nanoparticles (SLN) as ocular delivery system for tobramycin. *International journal of pharmaceutics* 2002;238(1):241-245.

- (287) You J, Wan F, de Cui F, Sun Y, Du Y, Hu Fq. Preparation and characteristic of vinorelbine bitartrate-loaded solid lipid nanoparticles. *International journal of pharmaceutics* 2007;343(1):270-276.
- (288) Morel S, Terreno E, Ugazio E, Aime S, Gasco MR. NMR relaxometric investigations of solid lipid nanoparticles (SLN) containing gadolinium(III) complexes. *European journal of pharmaceutics and biopharmaceutics* 1998;45(2):157-163.
- (289) Trotta M, Debernardi F, Caputo O. Preparation of solid lipid nanoparticles by a solvent emulsification–diffusion technique. *International journal of pharmaceutics* 2003;257(1):153-160.
- (290) Arpicco S, Battaglia L, Brusa P, Cavalli R, Chirio D, Dosio F, et al. Recent studies on the delivery of hydrophilic drugs in nanoparticulate systems. *Journal of drug delivery science and technology* 2016 Apr;32:298-312.
- (291) Rassu G, Soddu E, Posadino AM, Pintus G, Sarmiento B, Giunchedi P, et al. Nose-to-brain delivery of BACE1 siRNA loaded in solid lipid nanoparticles for Alzheimer's therapy. *Colloids and surfaces, B, Biointerfaces* 2017 Apr 1;;152:296-301.
- (292) Kuo Y, Hsu C. Anti-melanotransferrin and apolipoprotein E on doxorubicin-loaded cationic solid lipid nanoparticles for pharmacotherapy of glioblastoma multiforme. *Journal of the Taiwan Institute of Chemical Engineers* 2017 Aug;77:10-20.
- (293) Müller RH, Mäder K, Gohla S. Solid lipid nanoparticles (SLN) for controlled drug delivery – a review of the state of the art. *European Journal of Pharmaceutics and Biopharmaceutics* 2000;50(1):161-177.
- (294) Article R, Sarangi MK, Padhi S. Solid Lipid Nanoparticles-A Review.
- (295) Li, Hui Zhou, Ping Xu. Ping Xu Z. Self-Nanoemulsifying Drug-Delivery System and Solidified Self-Nanoemulsifying Drug-Delivery System. *Nanocarriers for Drug Delivery* 2019:421.
- (296) Mahdi ES, Sakeena MHF, Abdulkarim MF, Abdullah GZ, Sattar MA, Noor AM. Effect of surfactant and surfactant blends on pseudoternary phase diagram behavior of newly synthesized palm kernel oil esters. *Drug Design, Development and Therapy* 2011;5:311-323.
- (297) Čerpnjak K, Zvonar A, Gašperlin M, Vrečer F. Lipid-based systems as a promising approach for enhancing the bioavailability of poorly water-soluble drugs. *Acta pharmaceutica (Zagreb, Croatia)* 2013 Dec 1;;63(4):427-445.
- (298) Elsheikh MA, Elnaggar YSR, Gohar EY, Abdallah OY. Nanoemulsion liquid preconcentrates for raloxifene hydrochloride: optimization and in vivo appraisal. *International Journal of Nanomedicine* 2012;7:3787-3802.
- (299) Singh S, Dobhal AK, Jain A, Pandit JK, Chakraborty S. Formulation and Evaluation of Solid Lipid Nanoparticles of a Water Soluble Drug: Zidovudine. *Chemical & pharmaceutical bulletin* 2010;58(5):650-655.

- (300) Wang X, Zhang Q. pH-sensitive polymeric nanoparticles to improve oral bioavailability of peptide/protein drugs and poorly water-soluble drugs. *European journal of pharmaceutics and biopharmaceutics* 2012 Oct;82(2):219-229.
- (301) Hetal T, Bindesh P, Sneha T. A Review on Techniques for Oral Bioavailability Enhancement of Drugs. *International Journal of Pharmaceutical Sciences Review and Research* ;4(3).
- (302) Vikas K, Arvind S, Ashish S, Gourav J, Vipasha D, Vikas K, et al. Recent Advances In Ndds (Novel Drug Delivery System) For Delivery Of Anti-Hypertensive Drugs.
- (303) Prisant LM, Elliott WJ. Drug Delivery Systems for Treatment of Systemic Hypertension. *Clinical pharmacokinetics* 2003;42(11):931-940.
- (304) Prisant LM, Bottini B, DiPiro JT, Carr AA. Novel drug-delivery systems for hypertension. *The American journal of medicine* 1992;93(2):S45-S55.
- (305) Mohanraj VJ, Chen Y. Nanoparticles - A review. *Tropical Journal of Pharmaceutical Research* 2007 Jul 31,;5(1):561.
- (306) Quan P, Xia D, Piao H, Piao H, Shi K, Jia Y, et al. Nitrendipine Nanocrystals: Its Preparation, Characterization, and In Vitro–In Vivo Evaluation. *AAPS PharmSciTech* 2011;12(4):1136-1143.
- (307) Gorain B, Choudhury H, Kundu A, Sarkar L, Karmakar S, Jaisankar P, et al. Nanoemulsion strategy for olmesartan medoxomil improves oral absorption and extended antihypertensive activity in hypertensive rats. *Colloids and surfaces, B, Biointerfaces* 2014 Mar 1,;115:286-294.
- (308) Dwivedi DK, Singh AK. Dendrimers: A Novel Carrier System For Drug Delivery. *Journal of drug delivery and therapeutics* 2014 Sep 15,;4(5).
- (309) Sisinthy SP, Rao NK, Sarah CYL. Design, Optimization and In Vitro Characterization of Self Nano Emulsifying Drug Delivery System of Olmesartan Medoxomil. *International journal of pharmacy and pharmaceutical sciences* 2016 Dec 31,;9(1):94.
- (310) Satturwar P, Eddine MN, Ravenelle F, Leroux J. pH-responsive polymeric micelles of poly(ethylene glycol)- b-poly(alkyl(meth)acrylate- co-methacrylic acid): Influence of the copolymer composition on self-assembling properties and release of candesartan cilexetil. *European journal of pharmaceutics and biopharmaceutics* 2007;65(3):379-387.
- (311) Xu W, Ling P, Zhang T. Polymeric Micelles, a Promising Drug Delivery System to Enhance Bioavailability of Poorly Water-Soluble Drugs. *Journal of Drug Delivery* 2013 Dec 1,;2013:340315-15.
- (312) Ge H, Hu Y, Jiang X, Cheng D, Yuan Y, Bi H, et al. Preparation, characterization, and drug release behaviors of drug nimodipine-loaded poly( $\epsilon$ -caprolactone)-poly(ethylene oxide)-poly( $\epsilon$ -caprolactone) amphiphilic triblock copolymer micelles. *Journal of pharmaceutical sciences* 2002 Jun,;91(6):1463-1473.

- (313) Bharti C, Nagaich U, Pal A, Gulati N. Mesoporous silica nanoparticles in target drug delivery system: A review. *International Journal of Pharmaceutical Investigation* 2015 Jul 1,;5(3):124-133.
- (314) Gutiérrez JM, González C, Maestro A, Solè I, Pey CM, Nolla J. Nano-emulsions: New applications and optimization of their preparation. *Current opinion in colloid & interface science* 2008;13(4):245-251.
- (315) Alexa IF, Ignat M, Popovici RF, Timpu D, Popovici E. In vitro controlled release of antihypertensive drugs intercalated into unmodified SBA-15 and MgO modified SBA-15 matrices. *INTERNATIONAL JOURNAL OF PHARMACEUTICS* 2012 Oct 15,;436(1-2):111-119.
- (316) Yu M, Jie X, Xu L, Chen C, Shen W, Cao Y, et al. Recent Advances in Dendrimer Research for Cardiovascular Diseases. *Biomacromolecules* 2015 Sep 14,;16(9):2588-2598.
- (317) Francis MF, Cristea M, Winnik FM. Polymeric micelles for oral drug delivery: Why and how. *Pure and applied chemistry* 2004 Jan 1,;76(7):1321-1335.
- (318) Sharma M, Sharma R, Jain DK. Nanotechnology Based Approaches for Enhancing Oral Bioavailability of Poorly Water Soluble Antihypertensive Drugs. *Scientifica* 2016 Apr 30,;2016:8525679-11.
- (319) Ocheke NA, Olorunfemi PO, Ngwuluka NC. Nanotechnology and Drug Delivery Part 2: Nanostructures for Drug Delivery. *Tropical Journal of Pharmaceutical Research* 2009 Jul 30,;8(3).
- (320) Pilaniya U, Pilaniya K, Chandrawanshi HK, Gupta N, Rajput MS. Formulation and evaluation of verapamil hydrochloride loaded solid lipid microparticles. *Pharmazie* 2011 Jan 15,;66(1):24-30.
- (321) Agrawal YO, Husain M, Patil KD, Sodgir V, Patil TS, Agnihotri VV, et al. Verapamil hydrochloride loaded solid lipid nanoparticles: Preparation, optimization, characterisation, and assessment of cardioprotective effect in experimental model of myocardial infarcted rats. *Biomedicine & pharmacotherapy* 2022 Oct;154:113429.
- (322) Havanoor S, Manjunath K, Bhagawati S, Veerapur V. Isradipine Loaded Solid Lipid Nanoparticles for Better Treatment of Hypertension – Preparation, Characterization and In Vivo Evaluation. *International Journal of Biopharmaceutics* 2014;5.
- (323) Chalikwar SS, Belgamwar VS, Talele VR, Surana SJ, Patil MU. Formulation and evaluation of Nimodipine-loaded solid lipid nanoparticles delivered via lymphatic transport system. *Colloids and surfaces, B, Biointerfaces* 2012 Sep 1,;97:109-116.
- (324) Dudhipala N, Veerabrahma K. Candesartan cilexetil loaded solid lipid nanoparticles for oral delivery: characterization, pharmacokinetic and pharmacodynamic evaluation. *Drug delivery* 2016 Feb 12,;23(2):395-404.

- (325) Bhalekar M, Upadhaya P, Madgulkar A. Formulation and characterization of solid lipid nanoparticles for an anti-retroviral drug darunavir. *Appl Nanosci* 2017 Feb 01,;7(1-2):47-57.
- (326) Ji H, Tang J, Li M, Ren J, Zheng N, Wu L. Curcumin-loaded solid lipid nanoparticles with Brij78 and TPGS improved in vivo oral bioavailability and in situ intestinal absorption of curcumin. *Drug delivery* 2016 Feb 12,;23(2):459-470.
- (327) Kushwaha AK, Vuddanda PR, Karunanidhi P, Singh SK, Singh S. Development and Evaluation of Solid Lipid Nanoparticles of Raloxifene Hydrochloride for Enhanced Bioavailability. *BioMed Research International* 2013 Jan 01,;2013:584549-9.
- (328) Martins S, Silva AC, Ferreira DC, Souto EB. Improving Oral Absorption of Samon Calcitonin by Trimyristin Lipid Nanoparticles. *Journal of biomedical nanotechnology* 2009 Feb;5(1):76-83.
- (329) Bhalekar MR, Madgulkar AR, Desale PS, Marium G. Formulation of piperine solid lipid nanoparticles (SLN) for treatment of rheumatoid arthritis. *Drug development and industrial pharmacy* 2017 Jun 3,;43(6):1003-1010.
- (330) Van Breemen RB, Li Y. Caco-2 cell permeability assays to measure drug absorption. *Expert Opinion on Drug Metabolism and Toxicology* 2005 Aug 1,;1(2):175-185.
- (331) Hilgendorf C, Spahn-Langguth H, Regårdh CG, Lipka E, Amidon GL, Langguth P. Caco-2 versus Caco-2/HT29-MTX Co-cultured Cell Lines: Permeabilities Via Diffusion, Inside- and Outside-Directed Carrier-Mediated Transport. *Journal of pharmaceutical sciences* 2000 Jan;89(1):63-75.
- (332) Salah E, Abouelfetouh MM, Pan Y, Chen D, Xie S. Solid lipid nanoparticles for enhanced oral absorption: A review. *Colloids and surfaces, B, Biointerfaces* 2020 Dec;196:111305.

# 8. Appendices

## 8.1 Appendix A

TSQ MS Method Settings:

Method Type: Regular Method  
MS Run Time (min): 10.00  
Segment 1  
Duration (min) 10.00  
Scan Events 5

Segment 1:

Tune Method C:\Xcalibur\methods\Rahul\rahul-tune.TSQTune

Chrom filter: Not used

Q2 Gas Pressure: 1.5

Syringe Pump: Off

Scan Events:

1: + p SRM Skimmer Offset 10, Micro Scans 1,

Parent	Center	Width	Time	CE	Q1 PW	Q3 PW	Tube Lens
260.076	116.156	0.010	0.100	19	0.70	0.70	65
260.076	155.103	0.010	0.100	26	0.70	0.70	65
260.076	157.060	0.010	0.100	20	0.70	0.70	65
260.076	183.040	0.010	0.100	18	0.70	0.70	65

2: + p SRM Skimmer Offset 10, Micro Scans 1,

Parent	Center	Width	Time	CE	Q1 PW	Q3 PW	Tube Lens
346.000	136.097	0.010	0.100	32	0.70	0.70	100
346.000	150.093	0.010	0.100	35	0.70	0.70	100
346.000	180.039	0.010	0.100	27	0.70	0.70	100
346.000	197.911	0.010	0.100	13	0.70	0.70	100

3: + p SRM Skimmer Offset 10, Micro Scans 1,

Parent	Center	Width	Time	CE	Q1 PW	Q3 PW	Tube Lens
272.086	147.081	0.010	0.100	29	0.70	0.70	89
272.086	171.040	0.010	0.100	38	0.70	0.70	89
272.086	213.079	0.010	0.100	27	0.70	0.70	89
272.086	215.065	0.010	0.100	23	0.70	0.70	89

4: + c SRM Skimmer Offset 10, Micro Scans 1,

Parent	Center	Width	Time	CE	Q1 PW	Q3 PW	Tube Lens
455.205	149.975	0.010	0.100	33	0.70	0.70	123
455.205	165.041	0.010	0.100	27	0.70	0.70	123
455.205	260.088	0.010	0.100	33	0.70	0.70	123
455.205	303.067	0.010	0.100	24	0.70	0.70	123

**Figure 8.1** Mass spectrometry parameters optimised for individual analytes where, 260.07, 346.00, 272.09, and 455.05 m/z represents propranolol (IS), omeprazole, dextromethorphan, and verapamil, respectively.

## 8.2 Appendix B

TSQ MS Method Settings:

Method Type: Regular Method  
MS Run Time (min): 5.00  
Segment 1  
Duration (min) 5.00  
Scan Events 1

Segment 1:

Tune Method C:\Xcalibur\methods\Rahul\rahul-tune.TSQTune

Chrom filter: Not used

Q2 Gas Pressure: 1.5

Syringe Pump: Off

Scan Events:

1: + p SRM Skimmer Offset 10, Micro Scans 1,

Parent	Center	Width	Time	CE	Q1 PW	Q3 PW	Tube Lens
289.000	79.241	0.010	0.100	33	0.70	0.70	Tuned Value
289.000	91.187	0.010	0.100	41	0.70	0.70	Tuned Value
289.000	97.150	0.010	0.100	26	0.70	0.70	Tuned Value
289.000	109.118	0.010	0.100	24	0.70	0.70	Tuned Value

**Figure 8.2** Mass spectrometry parameters optimised for testosterone where 289.00 m/z represents parent ion testosterone.